

Stochastic Image Reconstruction as Ground State of Hamiltonian Operators

Inauguraldissertation
zur Erlangung des akademischen Grades eines
Doktors der Naturwissenschaften
der Universität Mannheim

vorgelegt von
Diplom-Mathematiker Alexander Dejon
aus Simmern/Hunsrück

Mannheim, 2006

Dekan: Prof. Dr. Matthias Krause, Universität Mannheim
Referent: Prof. Dr. Jürgen Potthoff, Universität Mannheim
Korreferent: Prof. Dr. Christoph Schnörr, Universität Mannheim

Tag der mündlichen Prüfung: 08. Februar 2007

To Sandra and my family

Abstract

A new image processing method is introduced. This method (called stochastic image reconstruction) is based on a well known phenomenon from quantum theory. Accordingly every physical system with a non-degenerated ground state will reach this ground state for times growing to infinity. Moreover this behaviour is independent of the initial state of the system at the beginning. Using the stochastic image reconstruction new methods for edge enhancement, inhomogeneous image smoothing and for noise reduction are exemplarily given.

Kurzdarstellung

Es wird eine neue Bildverarbeitungsmethode vorgestellt. Diese Methode (als stochastische Bildrekonstruktion bezeichnet) basiert auf einem bekannten Phänomen aus der Quantentheorie. Danach erreicht jedes physikalische System dessen Grundzustand nicht-entartet ist diesen Grundzustand im Grenzwert für unbeschränkt wachsende Zeiten. Außerdem ist dieses Grenzwertverhalten unabhängig von dem Startzustand, in dem sich das System zu Beginn befindet. Exemplarisch werden neue Verfahren zur Hervorhebung von Kanten, inhomogenen Bildglättung und Rauschreduktion jeweils unter Verwendung der stochastischen Bildrekonstruktion vorgestellt.

Acknowledgements

First of all I owe gratitude to Professor Jürgen Potthoff. His suggestions initiated this work and he was my adviser. Moreover we had interesting discussions on mathematics and beyond. Overall I am grateful to all the members of the Chair of Mathematics V for a warm atmosphere. I am greatly indebted to Dr. Thomas Deck for many lively discussions concerning L^2 -Theory, and to Professor Martin Schmidt for his useful hints on operator calculus. Also I thank Dr. Thomas Deck, Moritz Martens and Christoph Minnameier for reading some revisions and for their linguistical improvements. Finally I wish to express my gratitude to Professor Christoph Schnörr for his willingness to undertake the work of a referee.

In addition the support of my family was very important for me. Especially I wish to thank my father who always inspired me. Finally I owe deep gratitude to Sandra Müller for her mental support during the last years. She endured the process of writing this thesis with me, always listened to my problems and gave me a lot of strength.

Table of Contents

Introduction	1
1 Theoretical Approach	7
1.1 Operators in $L^2(\mathbb{R}^d, \lambda^d)$	7
1.2 Semigroups of operators	11
1.3 Reproducing property in $L^2(\mathbb{R}^d, \lambda^d)$	14
1.4 The corresponding Cauchy problem	15
1.5 Itô Diffusion and its generator	16
1.6 Solutions with the Feynman-Kac-Formula	20
1.7 Operators mapped to $L^2(\mathbb{R}^d, f_\infty^2 \lambda^d)$	21
1.8 Review of some statements using the map to $L^2(\mathbb{R}^d, f_\infty^2 \lambda^d)$	23
1.9 Solutions with the Kolmogorov backward equation	27
2 Reformulation for Bounded Regions	29
2.1 Restrictions coming from potentials	30
2.2 Boundary conditions	32
2.3 Reproducing operators in $L^2(D, \lambda^d)$	34
2.3.1 Regions with smooth boundary	35
2.3.2 Bounded, convex regions	37
2.4 Itô Diffusion on bounded regions	44
2.4.1 Exit time	45
2.4.2 Reflection	47
2.5 Feynman-Kac Formula for domains with smooth boundary	50
2.5.1 Dirichlet boundary condition	51
2.5.2 Neumann boundary condition	52

2.6	Solutions on bounded convex domains	54
2.7	Reproducing property in $L^2(D, \lambda^d)$	63
3	Implementation	69
3.1	Approximation of Itô diffusion in convex regions	69
3.2	Monte Carlo integration	75
3.3	Continuous images	77
3.3.1	Smoothing piecewise constant functions	79
3.3.2	Spline interpolation	87
3.4	Approximation of the derivative	91
3.5	Error considerations	94
3.5.1	Distance from the limit	94
3.5.2	Error from Monte Carlo integration	95
3.5.3	Convergence rate of the projection scheme	96
4	Applications	99
4.1	Time dependent scale factor	102
4.2	Image reconstruction	104
4.3	Reconstruction without spline interpolation	131
4.4	Image smoothing	136
4.5	Remark on colour images	155
5	Results and Perspectives	161
	Notation	167
	Appendices	170
A	Friedrichs' Extension of Semi-Bounded Operators	171
B	Skorokhod's Problem	175
C	Multidimensional Stochastic Taylor Expansion	181
	Zusammenfassung	193

Abbildungsverzeichnis

2.1	Vector ν orthogonal to the boundary of a convex domain D	32
2.2	Set of normal vectors \mathcal{N}_x at the corner point $x \in \partial D$	33
2.3	Example path of an Itô diffusion on \overline{D} reflected at ∂D	49
3.1	Schematic representation of a typical CCD-Array	78
3.2	Image enlargement mechanism	80
3.3	Convolution of piecewise constant functions	82
3.4	Sinc function in \mathbb{R}^2	83
3.5	Example for bilinear interpolation	84
3.6	Cubic B-spline	84
3.7	B-Spline centred at a sample point	86
3.8	B-Spline at the boundary of a pixel	87
3.9	Cubic spline interpolation of a test pattern	89
3.10	Derivative of the interpolating spline	92
3.11	Partition of a pixel into sub-pixels	93
3.12	Comparison of discrete derivatives on sub-pixels	93
4.1	Generic image pair – Experiments 1-5, 7, 9	104
4.2	Example for image reconstruction – Experiment 1/1	105
4.3	Average error and maximum error – Experiment 1/1	106
4.4	Difference between \mathbb{I}_{400} and \mathbb{I}_{∞} – Experiment 1/1	107
4.5	Image reconstruction using average scale – Experiment 1/3	108
4.6	Comparison of the time dependent scale values – Ex. 1/2-3	109
4.7	Overview of the parameter setup – Experiments 2-4	110
4.8	Two sets of selected pixels $M1, M2$ – Experiments 2-4	111
4.9	Average error – Experiments 2/1-3	112

4.10	Average error – Experiments 3/1-3	114
4.11	Average error – Experiments 4/1-3	116
4.12	Three generic start images – Experiment 5	118
4.13	Image reconstruction sequence – Experiment 5/1	120
4.14	Image reconstruction sequence – Experiment 5/2	121
4.15	Image reconstruction sequence – Experiment 5/3	122
4.16	Average error for different start images – Experiment 5	123
4.17	Three images showing real scenes – Experiments 6, 12, 13	125
4.18	Image reconstruction at time $t_1 = 10$ – Experiment 6	126
4.19	Image reconstruction at time $t_2 = 50$ – Experiment 6	127
4.20	Image reconstruction at time $t_3 = 1000$ – Experiment 6	128
4.21	Image reconstruction at time $t_4 = 10000$ – Experiment 6	129
4.22	Average error for different stop images – Experiment 6	130
4.23	Average error using the fast transformation – Experiment 7	132
4.24	Edge enhancing illustrated on a fingerprint – Experiment 8	134
4.26	Example for image smoothing – Experiment 9/1	137
4.27	Generic image with 70% noise and rescaled versions – Ex. 10	139
4.28	Image smoothing sequence – Experiment 10/1	141
4.29	Image smoothing sequence – Experiment 10/2	142
4.30	Image smoothing sequence – Experiment 10/3	143
4.31	Example for partial image smoothing – Experiment 11	144
4.32	Image smoothing at time $t_1 = 1$ – Experiment 12	146
4.33	Image smoothing at time $t_2 = 10$ – Experiment 12	147
4.34	Image smoothing at time $t_3 = 50$ – Experiment 12	148
4.35	Image smoothing at time $t_4 = 100$ – Experiment 12	149
4.36	Stop images for advanced image smoothing – Experiment 13	150
4.37	Advanced image smoothing at time $t_1 = 0.1$ – Experiment 13	151
4.38	Advanced image smoothing at time $t_2 = 1$ – Experiment 13	152
4.39	Advanced image smoothing at time $t_3 = 5$ – Experiment 13	153
4.40	Advanced image smoothing at time $t_4 = 10$ – Experiment 13	154
4.41	Generic test image pair – Experiment 14	156
4.42	Example for image smoothing – Experiment 14/1	156
4.43	Example for advanced image smoothing – Experiment 14/2	157

Ἡ δ' αἰσθητὴ οὐσία μεταβλητή.
Das sinnlich wahrnehmbare Sein
ist des Wechsels fähig.
Aristoteles, Metaphysik XII

Introduction

This thesis describes the mathematical basis for a new procedure applicable to different image processing problems and gives examples of applications to the problem of edge enhancement, image smoothing and de-noising. The main idea of our new method is based on the fact that the operator $\exp(-tH)$ where H is the Hamilton operator $H := -\frac{1}{2}\Delta + V$ maps every function $f_0 : \mathbb{R}^2 \rightarrow \mathbb{R}$ in the domain of H (under certain circumstances) for $t \rightarrow \infty$ up to a constant factor to the ground state of H . If we define $V := \frac{\Delta f_\infty}{2f_\infty}$ for some function $f_\infty : \mathbb{R}^2 \rightarrow \mathbb{R}_{>0}$ then f_∞ is the ground state of H . Thus for every $t \geq 0$ we get a function $f_t := \exp(-tH)f_0$ (corresponding to a transformed image at time t) which is equal to some given function f_0 at time $t = 0$ and converges pointwisely to a multiple of f_∞ for t approaching infinity. Moreover the function f_t obeys the diffusion equation

$$\frac{df}{dt} = \frac{1}{2}\Delta f - Vf.$$

So we obtain a transformation algorithm depending on f_0 and f_∞ (as well as on the step size Δt) which allows us to observe the state of transformation by the function f_t . At the end of this work we show that we can derive different algorithms from our transformation algorithm which are applicable to the problems of image processing mentioned above. These algorithms correspond to special choices of the parameters f_0, f_∞ . Indeed we can imagine an application of our method to other problems (e.g. super resolution, image restoration, face recognition) but a discussion is left open.

In Chapter 1 we consider functions $f_0, f_\infty \in L^2(\mathbb{R}^d, \lambda^d)$ in order to present the main idea of our transformation algorithm. We choose $f_\infty > 0$ such that $V(x)$ grows unboundedly whenever $\|x\|$ goes to infinity. Then we can use a result from [61] for the Hamilton operator H to show that H is semi-bounded

and has a pure point spectrum consisting of its eigenvalues. The corresponding eigenfunctions constitute an orthonormal basis of $L^2(\mathbb{R}^d, \lambda^d)$. Moreover the eigenspace corresponding to the smallest eigenvalue 0 has dimension one (which means the ground state is non-degenerated). After that we define and discuss the representation $f(t) = \exp(-tH)f_0$. Using this representation we prove the convergence of $f(t)$ to f_∞ (up to a constant). Then in Section 1.4 we introduce the Cauchy problem

$$\frac{du}{dt} = \frac{1}{2}\Delta u - Vu \quad \text{with} \quad u(0) = f_0$$

and show that $f(t)$ is the unique solution. Using the Feynman-Kac formula in Section 1.6 this leads to the representation

$$f(t)(x) = \mathbb{E} \left[\exp \left(- \int_0^t V(B_s^x) ds \right) f_0(B_t^x) \right] \quad \text{for} \quad t \geq 0, \quad (1)$$

where $(B_t^x | t \geq 0)$ is a Brownian motion starting in $x \in \mathbb{R}^d$. Possibly the exponential term in Equation 1 takes large values and therefore may cause difficulties during computer experiments. For this reason we eliminate this term using the unitary map $f \mapsto f \cdot (f_\infty)^{-1}$ from $L^2(\mathbb{R}^d, \lambda^d)$ to the space $L^2(\mathbb{R}^d, f_\infty^2 \lambda^d)$. In Section 1.8 we use the commutative diagram

$$\begin{array}{ccc} L^2(\mathbb{R}^d, \lambda^d) & \xleftarrow{\cdot f_\infty} & L^2(\mathbb{R}^d, f_\infty^2 \lambda^d) \\ \downarrow H & & \downarrow L \\ L^2(\mathbb{R}^d, \lambda^d) & \xrightarrow{\cdot (f_\infty)^{-1}} & L^2(\mathbb{R}^d, f_\infty^2 \lambda^d) \end{array}$$

and find that the operator $L = -\frac{1}{2}\Delta - (\nabla \ln f_\infty) \nabla$ and formulate the Cauchy problem

$$\frac{d\tilde{u}}{dt} = -L\tilde{u} \quad \text{with} \quad \tilde{u}(0) = f_0 \cdot (f_\infty)^{-1}. \quad (2)$$

Finally in Section 1.9 using the Cauchy problem 2 we obtain the representation

$$\exp(-tL) \frac{f_0}{f_\infty}(x) = \mathbb{E} \left[\frac{f_0}{f_\infty}(X_t^x) \right] \quad \text{for} \quad x \in \mathbb{R}^d, t \geq 0, \quad (3)$$

of Equation 1 now in $L^2(\mathbb{R}^d, f_\infty^2 \lambda^d)$. Here $(X_t^x | t \geq 0)$ is a d -dimensional Itô diffusion with diffusion coefficient $\sigma = -I_d$ and drift $b = -\nabla \ln f_\infty$.

For the computation of the function $f(t)$ we would have to compute its representation as in Equation 3 for every x in \mathbb{R}^d . Actually it is sufficient to know the value of $f(t)$ for every x in its support D because outside the function is 0. Obviously in the case of applications in image processing D is always bounded. Thus we could approximate the right side of Equation 3 by a Monte-Carlo simulation. But in the following we do not want to extend given images to functions on \mathbb{R}^2 which are congruent 0 outside their bounded support D because we would like to consider strictly positive functions f_∞ . Instead we use a spline interpolation to get functions defined only on the subset D of \mathbb{R}^2 (a rectangle). Additionally we arrange the interpolation of the discrete image data such that the resulting function fulfils a Dirichlet or Neumann boundary condition (both with constant 0). Therefore in the following we consider two times continously differentiable functions $f_0, f_\infty : D \rightarrow \mathbb{R}$ with Dirichlet or Neumann null boundary condition and additionally assume f_∞ to be strictly positive as before.

Because of the fact that the boundary ∂D is possibly non-smooth we have to prove several statements which are well known in the case of smooth boundaries and extend some definitions. For example we have to replace the usual definition of the Neumann boundary condition because at those points of the boundary of D where ∂D is non-smooth the normal is not unique. Hence we say that the function f_∞ fulfils the strong Neumann boundary condition with constant 0 if the derivative of f_∞ restricted to the boundary of D (excluding the corner points) vanishes in the direction of the normal to the boundary as in the usual definition of the Neumann null boundary condition. Additionally at the corner points the derivative of f_∞ has to vanish for all directions $\nu \in \mathcal{N}_x$ where we define \mathcal{N}_x as a set of normals for the point $x \in \partial D$. That way in Chapter 2 we are able to consider functions f_0, f_∞ defined on a bounded, open and convex set $D \subset \mathbb{R}^d$ with Dirichlet or Neumann null boundary conditions. This means in our theoretical discussion we consider a more general case than needed in the view of applications in image processing.

As before we take f_∞ to be strictly positive and demand f_0, f_∞ to be two

times continuously differentiable. Then we prove that the operator H defined on functions in $\overline{C_2}(D)$ with Dirichlet or Neumann boundary condition has a purely discrete point spectrum and is non-negative. Moreover we prove that the eigenspace corresponding to the smallest eigenvalue 0 is 1-dimensional (which means that the ground state is non-degenerated). Using some existing results for solutions of differential equations of second order this will lead to the point-wise convergence of $\exp(-tH)f_0$ to f_∞ . First we show these attributes of H for regions D with sufficiently smooth boundary. Then in Section 2.3.2 we give a proof for the case of a possibly non-smooth boundary. After this we give a detailed construction of an Itô diffusion reflected at ∂D for the case of a smooth boundary. In the non-smooth case this construction is replaced by solutions of Skorokhod problems (see Appendix B and [66]) to avoid the construction of a reflection at a non-smooth boundary. This enables us to give representations of $f(t)$ in terms of the reflected Itô diffusion $(X_t^x | t \geq 0)$ equivalent to Equation 1 and Equation 3. For this purpose we use a Cauchy problem and the Feynman-Kac formula as before. Once more we treat the case of smooth and non-smooth boundaries separately. First we resume existing results for regions D with smooth boundaries. Then in Section 2.6 we prove a version of the Itô formula for solutions (X_t, φ_t) of Skorokhod problems. This result is known in the more general context of locally square integrable, continuous martingales (cp. [42]). We give a new, easy proof for our special situation. With this formula we are able to determine the infinitesimal generator of (X_t, φ_t) . Then we state a Cauchy problem as in Equation 2 (now for functions in $\overline{C_2}(D)$) and once more use our version of the Itô formula to get a solution of the Cauchy problem.

Up to now we know that the function $f(t) = \mathbb{E}[\frac{f_0}{f_\infty}(X_t)]f_\infty$ converges in $L^2(D, \lambda^d)$ to f_∞ for t growing to infinity. This is a similar result as in Chapter 1 where we treated functions in $L^2(\mathbb{R}^d, \lambda^d)$. At this point we have this result for f_0, f_∞ in $L^2(D, \lambda^d)$ with Dirichlet or Neumann boundary condition. Then we show that the convergence of $f(t)$ to f_∞ is actually point-wise. Nevertheless if we are concerned with applications in image processing it is impossible to compute $f(t)$ for all $x \in D \subset \mathbb{R}^2$ where D is a rectangle (it is an uncountable set of points). Therefore in Chapter 3 we discuss everything that belongs to the discrete aspects of computer experiments. We start with the approximation

of Itô diffusions in convex regions. We give the Euler approximation scheme (cp. [72, 73]) and extend it according to the existing approximation schemes for Itô diffusions on \mathbb{R}^d as in [39] to get approximation schemes for Itô diffusions with reflection of higher approximation order¹. Then in Section 3.2 we present the algorithm for the approximative computation of $\mathbb{E}\left[\frac{f_0}{f_\infty}(X_t^x)\right]f_\infty(x)$ for one $x \in D$. After this we describe some possibilities to get functions in $\overline{C_2}(D)$ from digital images (defined on a finite set of points) and give approximations to the derivative of a spline interpolated function. Finally at the end of Chapter 3 we discuss the resulting approximation (simulation) error.

Chapter 4 is devoted to some computer experiments concerning the presentation of our transformation algorithm according to the behaviour of f_t in discrete time. We start with an illustration of the basic functionality of the transformation algorithm using some examples. During these experiments we clearly observe an edge enhancing effect in the transformed image. Then we formulate a version of our transformation algorithm which reduces the computation times by a factor of five compared with the original transformation algorithm. It is worth noting that the fast version of the transformation algorithm produces results with very small visual differences to the results from the original version. After that we show how to make use of the transformation algorithm in order to improve an image of a fingerprint. Then we give some examples for image smoothing, make a connection to image smoothing by convolution with a Gaussian, and illustrate the difference to our method. We finish with some examples which concern the problem of de-noising. Overall the experiments show that our method is applicable to the problems of image processing we considered here. Moreover the results of the experiments confirm our expectation given by the theoretical considerations.

¹The extensions of the approximation schemes will not be needed for the formulation of the transformation algorithm. They are an add-on of this work.

Chapter 1

Theoretical Approach

In this chapter we develop the basic theory for the reproduction of functions f_∞ in the space of square integrable functions with respect to Lebesgue measure. The class of reproduceable functions will be investigated as well as the class of reproducing Hamiltonians. The main interest of this work is to obtain representations of the evolution in time f_t . So we consider the exponential of operators and formulate a Cauchy problem related to this. After that we will see that solutions of the Cauchy problem can be represented in terms of stochastic processes and their expectation. Finally we give a second approach to the reproduction of functions by considering the space of square integrable functions with respect to a weighted Lebesgue measure. Again we formulate this approach in terms of a Cauchy problem. We give a solution for this problem which enables us to represent the time evolution we are interested in. As before we will use the expectation value of a stochastic process for this representation.

1.1 Operators in $L^2(\mathbb{R}^d, \lambda^d)$

As usual we denote by \mathbb{R} the set of real numbers. In the whole text we make use of the notation $\mathbb{R}_{\geq 0}$ and $\mathbb{R}_{> 0}$ for the set of positive respectively strictly positive real numbers. For every natural number $d \in \mathbb{N}$ we write \mathbb{R}^d for the d -dimensional Euclidian space with the norm $|x| := \sqrt{x_1^2 + \cdots + x_d^2}$. We further denote the d -dimensional Lebesgue measure by λ^d and frequently omit

the superscript d . Then $\mathcal{L}^2(\mathbb{R}^d, \lambda^d)$ denotes the set of all real, square integrable functions with respect to λ^d . It is equipped with the usual inner product

$$(f, g) := \int f g d\lambda$$

and the norm $\|f\| := \sqrt{(f, f)}$. With the equivalence relation \sim defined by $f \sim g :\Leftrightarrow \|f - g\| = 0$ we obtain the quotient space $L^2(\mathbb{R}^d, \lambda^d)$ with the same inner product and norm as in $\mathcal{L}^2(\mathbb{R}^d, \lambda^d)$. As usual we simply call the elements of the *real Hilbert space* $L^2(\mathbb{R}^d, \lambda^d)$ functions. A sequence $(f_n | n \in \mathbb{N})$ of elements in $L^2(\mathbb{R}^d, \lambda^d)$ is called *convergent to* $f \in L^2(\mathbb{R}^d, \lambda^d)$, iff

$$\lim_{n \rightarrow \infty} \|f_n - f\| = 0,$$

and we write

$$L^2\text{-}\lim_{n \rightarrow \infty} f_n = f \quad \text{or} \quad f_n \xrightarrow{L^2} f.$$

For families $(f_t | t \in I)$ of elements in $L^2(\mathbb{R}^d, \lambda^d)$ with an uncountable set I this convergence generalises in the usual way. Further information about general Hilbert spaces can be found e.g. in [62, 78]. This also holds for the following two definitions. We give these definitions in an general context in order to apply them to different situations later.

Definition 1.1.1. We call the elements v_0, v_1, \dots of a Hilbert space \mathcal{H} an *orthonormal basis (ONB) of \mathcal{H}* , iff

- a) $(v_i, v_j) = 0$ for all $i, j \in \mathbb{N}_0$ with $i \neq j$,
- b) $\|v_i\| = 1$ for all $i \in \mathbb{N}_0$ and
- c) for all $h \in \mathcal{H}$ there exist unique $\alpha_0, \alpha_1, \dots$ in \mathbb{R} , such that

$$h = L^2\text{-}\lim_{n \rightarrow \infty} \sum_{k=0}^n \alpha_k v_k \tag{1.1}$$

$$= \sum_{k \in \mathbb{N}_0} \alpha_k v_k. \tag{1.2}$$

Remark. It is well known that $h \in \mathcal{H}$, iff the sum over $\alpha_k^2 = (h, v_k)^2$ for all $k \in \mathbb{N}_0$ is finite. So the limit in 1.1 does not depend on the summation order

which justifies 1.2. Moreover the first two conditions in Definition 1.1.1 are often abbreviated as $(v_i, v_j) = \delta_{i,j}$. Here $\delta_{i,j}$ is equal to 1 for $i = j$ and defined as 0 in all other cases.

Definition 1.1.2. Let the operator $H : \mathcal{D}_H \rightarrow \mathcal{H}$ be densely defined on some Hilbert space \mathcal{H} . We call H an *operator with purely discrete spectrum*, iff there exist *eigenvalues* $\lambda_0 \leq \lambda_1 \leq \lambda_2 \dots$ in \mathbb{R} and *eigenvectors* v_0, v_1, v_2, \dots in \mathcal{D}_H such that

$$Hv_k = \lambda_k v_k, \quad \text{for all } k \in \mathbb{N}_0, \quad (1.3)$$

and $(v_k | k \in \mathbb{N}_0)$ is an ONB of \mathcal{H} . If we denote by Id the identity map $f \mapsto f$ we call the dimension of $\ker(H - \lambda_k \text{Id})$ the *multiplicity* of the eigenvalue λ_k . There $\ker(H)$ is the *null space* of H , that is the set $\{f | Hf = 0\}$. The operator H is *symmetric*, iff for all $f, g \in \mathcal{D}_H$ we have $(Hf, g) = (f, Hg)$.

To be more explicite we consider $\mathcal{H} = L^2(\mathbb{R}^d, \lambda^d)$. For every symmetric operator H Equation 1.3 leads to the *spectral representation*

$$Hf = \sum_{k \in \mathbb{N}_0} \lambda_k (f, v_k) v_k. \quad (1.4)$$

This representation shows, that the *natural (maximal) domain* of an symmetric operator as above is defined by

$$\mathcal{D}_H := \left\{ f \in L^2(\mathbb{R}^d, \lambda^d) \mid f = \sum_{k \in \mathbb{N}_0} \alpha_k v_k, \sum_{k \in \mathbb{N}_0} \alpha_k^2 \lambda_k^2 < \infty \right\}. \quad (1.5)$$

If H is explicitly given it might be necessary to restrict its domain to a dense subset in order to guaranty existence of derivatives and then to enlarge it by taking limits. So if we want to define

$$\begin{aligned} H : \mathcal{D}_H &\rightarrow L^2(\mathbb{R}^d, \lambda^d) \\ f &\mapsto -\frac{1}{2}\Delta f + Vf \end{aligned} \quad (1.6)$$

for some $V : \mathbb{R}^d \rightarrow \mathbb{R}$, where Δ is the d -dimensional Laplace-Operator, then it is convenient to take f as a two times differentiable function. Actually $C^2(\mathbb{R}^d)$ the set of all two times continuously differentiable functions can be restricted to a dense subset in $L^2(\mathbb{R}^d, \lambda^d)$. That means every function in $L^2(\mathbb{R}^d, \lambda^d)$ can

be expressed as limit of functions in $C^2(\mathbb{R}^d) \cap L^2(\mathbb{R}^d, \lambda^d)$. So the domain \mathcal{D}_H of H can be taken as in Equation 1.5 for appropriate V .

Indeed we are interested in symmetric operators with purely discrete spectrum of the form 1.6 where the potential V is given by $\frac{\Delta f_\infty}{2f_\infty}$, so we define

$$Hf := \left(-\frac{\Delta}{2} + V\right)f = -\frac{\Delta f}{2} + \frac{\Delta f_\infty}{2f_\infty} \cdot f \quad (1.7)$$

for all $f \in \mathcal{D}_H$. If we choose f_∞ as strictly positive function in $L^2(\mathbb{R}^d, \lambda^d)$ then V might not be in $L^2(\mathbb{R}^d, \lambda^d)$. Moreover the derivative has to be interpreted in the sense of distributions (see Appendix A) or as L^2 -limit like we will do in this chapter. Nevertheless we are interested in such potentials so we give the following definition.

Definition. A function f is called *locally square integrable*, iff for every compact set $K \subset \mathbb{R}^d$ the integral of f^2 over K is finite. The real vector space of all locally square integrable functions is denoted by $L^2_{\text{loc}}(\mathbb{R}^d, \lambda^d)$.

Now we apply Theorem XIII.47 from [61] to our situation. For simplicity we assume f_∞ to be chosen such that V is non-negative (in Chapter 2 we give a different argument without this additional assumption). In Theorem XIII.47 from [61] it is not mentioned that the spectrum of H is purely discrete, but it is used and explained in the proof of the theorem. So we resume as follows.

Theorem 1.1.3. *If $V \in L^2_{\text{loc}}(\mathbb{R}^d, \lambda^d)$ is positive and $V(x)$ grows unboundedly whenever $|x|$ goes to infinity then H as defined in Equation 1.7 with domain \mathcal{D}_H has non-negative, purely discrete spectrum. The smallest eigenvalue has multiplicity one.*

Finally we want to know what the smallest eigenvalue and its corresponding eigenfunction is.

Lemma 1.1.4. *The function $f_\infty \in L^2(\mathbb{R}^d, \lambda^d)$ is an eigenvector of the operator H as defined in Equation 1.7 with domain \mathcal{D}_H to the eigenvalue 0.*

Proof. We have

$$Hf_\infty = -\frac{\Delta f_\infty}{2} + \frac{\Delta f_\infty}{2f_\infty} \cdot f_\infty = -\frac{\Delta f_\infty}{2} + \frac{\Delta f_\infty}{2}. \quad \blacksquare$$

From Theorem 1.1.3 it follows, that f_∞ is the only solution of $Hf = 0$ with $f \in L^2(\mathbb{R}^d, \lambda^d)$. Also the theorem implies that there is no eigenvalue below 0.

1.2 Semigroups of operators

As mentioned at the beginning we are mainly interested in functions f_t converging for $t \rightarrow \infty$ to a given function f_∞ . Later we will see that $\exp(-tH)f$ with H defined in Equations 1.6, 1.7 are such functions. So our aim in this section is to define $\exp(-tH)$ for the special class of operators H we consider in this work and give some of its properties.

A definition for the exponential of operators in a general sense can be found in the book of Kato [38], but we consider special operators which make an easier approach possible. Therefore for the class of operators discussed in Section 1.1 we take

$$T_t f := \exp(-tH)f := \sum_{k \in \mathbb{N}_0} \exp(-t\lambda_k) \alpha_k v_k \quad (1.8)$$

for every f in its domain

$$\mathcal{D}_{T_t} := \{f \in L^2(\mathbb{R}^d, \lambda^d) \mid f = \sum_{k \in \mathbb{N}_0} \alpha_k v_k \text{ with } \sum_{k \in \mathbb{N}_0} \alpha_k^2 \exp(-t\lambda_k)^2 < \infty\} \quad (1.9)$$

and notice that $\exp(-t\lambda_k) \leq 1$ for every $\lambda_k \geq 0$ and every $t \geq 0$. So we are able to conclude $\mathcal{D}_H \subset \mathcal{D}_{T_t} = L^2(\mathbb{R}^d, \lambda^d)$ and define $\exp(-tH)f$ for all $f \in L^2(\mathbb{R}^d, \lambda^d)$ as in 1.8.

Definition. We call $(T_t \mid t \geq 0)$ a *strongly continuous semigroup*, iff the operator T_t acting on $L^2(\mathbb{R}^d, \lambda^d)$ satisfies $(T_s \circ T_t) = T_{s+t}$ for all $0 \leq s, t \leq \infty$ and $T_t \rightarrow T_0$ for t decreasing to 0. Here the operator T_t converges to the operator T_0 , iff for every $f \in \mathcal{D}_T$ the norm $\|T_t f - T_0 f\|$ vanishes for $t \searrow 0$.

Remark. The semigroup is continuous for every $t \in \mathbb{R}_{\geq 0}$ because for every function $f \in L^2(\mathbb{R}^d, \lambda^d)$ we have $\tilde{f} = T_t f$ as an element of $L^2(\mathbb{R}^d, \lambda^d)$ and so $\|T_{t+h} f - T_t f\| = \|T_h \tilde{f} - T_0 \tilde{f}\|$ vanishes for $h \geq 0$ converging to 0.

Before we show that T_t from Equation 1.8 defines a strongly continuous semigroup we give a useful lemma. It will allow us to interchange limits.

Lemma 1.2.1. *Let $(v_k | k \in \mathbb{N}_0)$ denote an ONB of $L^2(\mathbb{R}^d, \lambda^d)$. For every $k \in \mathbb{N}_0$ we consider $\alpha_k(t)$, $\beta_k \in \mathbb{R}$ such that for every $t \in \mathbb{R}_{\geq 0}$ the function α_k is continuous and we have $\alpha_k(t)^2 \leq \beta_k$. The sum of all β_k for $k \in \mathbb{N}_0$ is assumed to be finite. Then for $t \in \mathbb{R}_{\geq 0}$ the function $f(t) := \sum_{k \in \mathbb{N}_0} \alpha_k(t) v_k$ is an element of $L^2(\mathbb{R}^d, \lambda^d)$. Furthermore f is continuous with respect to t .*

Proof. For every $t \geq 0$ we have

$$\sum_{k=0}^{\infty} \alpha_k(t)^2 \leq \sum_{k=0}^{\infty} \beta_k < \infty$$

because of $\alpha_k(t)^2 \leq \beta_k$. Hence $f(t)$ is in $L^2(\mathbb{R}^d, \lambda^d)$ and $\sum_{k=0}^m \|\alpha_k(t) v_k\|^2$ converges. Now we prove the continuity property. For this we note that the partial sums $\sum_{k=0}^n \beta_k$ form a Cauchy sequence. But then for every $\epsilon > 0$ there exists $n_0 \in \mathbb{N}_0$ such that for all $n_1, n_2 \geq n_0$ with $n_2 \geq n_1$ we have

$$\left\| \sum_{k=0}^{n_2} \alpha_k(t) v_k - \sum_{k=0}^{n_1} \alpha_k(t) v_k \right\|^2 = \left\| \sum_{k=n_1}^{n_2} \alpha_k(t) v_k \right\|^2 \leq \sum_{k=n_1}^{n_2} \beta_k < \tilde{\epsilon} < \epsilon$$

independent of $t \geq 0$. If we take $n_2 \rightarrow \infty$ and use the continuity of the norm it follows

$$\left\| f_t - \sum_{k=0}^n \alpha_k(t) v_k \right\|^2 < \epsilon$$

for all $n \geq n_0$. This shows that $\sum_{k=0}^n \alpha_k(t) v_k$ converges *uniformly* in t to the function f_t as n goes to infinity. Finally we get

$$L^2\text{-}\lim_{t \rightarrow t_0} f_t = \sum_{k=0}^{\infty} \lim_{t \rightarrow t_0} \alpha_k(t) v_k = f(t_0).$$

■

Theorem 1.2.2. *Denote by $T_t = \exp(-tH)$ the operator defined in 1.8. Then $(T_t | t \geq 0)$ is a strongly continuous semigroup on \mathcal{D}_T with $T_0 = \text{Id}$.*

Proof. First we prove the semigroup property. Let $0 \leq s, t \leq \infty$ and $f \in \mathcal{D}_T$

with $f = \sum_{k \in \mathbb{N}_0} \alpha_k v_k$ then we have

$$(T_s \circ T_t)f = \exp(-sH) \sum_{k \in \mathbb{N}_0} \exp(-t\lambda_k) \alpha_k v_k. \quad (1.10)$$

Using the definition of $\exp(-sH)$ we rewrite the right side of 1.10 as

$$\sum_{k \in \mathbb{N}_0} \exp(-s\lambda_k) \exp(-t\lambda_k) \alpha_k v_k.$$

Hence we find $(T_s \circ T_t)f = \exp(-(s+t)H)f = T_{s+t}f$. From Equation 1.8 it follows for $t = 0$

$$\begin{aligned} T_0 f &= \exp(0 \cdot H)f \\ &= \sum_{k \in \mathbb{N}_0} \exp(0) \alpha_k v_k = f \end{aligned}$$

which means that $T_0 = \text{Id}$.

Now we show that the semigroup is strongly continuous. To do this we have to prove

$$\lim_{\substack{t \rightarrow 0 \\ t > 0}} \|T_t f - f\| = 0. \quad (1.11)$$

One more time we use Equation 1.8 and the fact that f is in $L^2(\mathbb{R}^d, \lambda^d)$ to write

$$\begin{aligned} \|T_t f - f\|^2 &= \|\exp(-tH)f - f\|^2 \\ &= \sum_{k \in \mathbb{N}_0} ((\exp(-t\lambda_k) - 1)\alpha_k)^2 \\ &\leq \sum_{k \in \mathbb{N}_0} \alpha_k^2 < \infty. \end{aligned} \quad (1.12)$$

So the series 1.12 is absolutely convergent. Moreover $(\exp(-t\lambda_k) - 1)^2 \leq 1$ so we can apply Lemma 1.2.1. Using this and the continuity of the norm we see that Equation 1.11 is equivalent to

$$\sum_{k \in \mathbb{N}_0} \left(\lim_{\substack{t \rightarrow 0 \\ t > 0}} (\exp(-t\lambda_k) - 1) \alpha_k \right)^2 = 0. \quad \blacksquare$$

Definition 1.2.3. The (infinitesimal) generator H of a semigroup $(U_t|t \geq 0)$ is defined by

$$Hf := L^2\text{-}\lim_{t \searrow 0} \frac{U_t f - f}{t} \quad (1.13)$$

for every f in \mathcal{D}_H . The domain \mathcal{D}_H is the set of all $f \in L^2(\mathbb{R}^d, \lambda^d)$ for which the limit 1.13 exists.

Here we used U_t to denote the semigroup, because the generator of T_t defined in Equation 1.8 is $-H$ as we will see later.

Remark. Let \mathcal{D}_H denote the domain of the generator H defined above. If U_t is acting on $L^2(\mathbb{R}^d, \lambda^d)$ then we know from [16] Lemma 1.1 that \mathcal{D}_H is a dense subset of $L^2(\mathbb{R}^d, \lambda^d)$.

1.3 Reproducing property in $L^2(\mathbb{R}^d, \lambda^d)$

In this section we will give the theorem which plays the central role in the development of applications later on. Again we consider the semigroup $(T_t|t \geq 0)$ from the section above. But here we are interested in the limit

$$L^2\text{-}\lim_{t \rightarrow \infty} T_t f = L^2\text{-}\lim_{t \rightarrow \infty} \exp(-tH)f.$$

Theorem 1.3.1. Let $(T_t|t \geq 0)$ denote the semigroup defined in Equation 1.8. Then for $f \in L^2(\mathbb{R}^d, \lambda^d)$ the function $T_t f$ converges for $t \rightarrow \infty$ to $(v_0, f)v_0$.

Proof. Let f be in \mathcal{D}_H then using Equation 1.8 we have

$$\begin{aligned} \|T_t f - \alpha_0 v_0\|^2 &= \left\| \sum_{k \in \mathbb{N}_0} \exp(-t\lambda_k) \alpha_k v_k - \alpha_0 v_0 \right\|^2 \\ &= \sum_{k \in \mathbb{N}} \left(\exp(-t\lambda_k) \alpha_k \right)^2 \end{aligned} \quad (1.14)$$

because $(v_i, v_j) = \delta_{i,j}$ and $\exp(-t\lambda_0)^2 \alpha_0^2 = \alpha_0^2$ which is simply a consequence of Lemma 1.1.4. The limit $t \rightarrow \infty$ of 1.14 gives 0 by dominated convergence. ■

This shows that up to the constant $(v_0, f) = \int v_0 f d\lambda$ the limit of $T_t f$ is independent of the function f . That means the limit operator T_∞ projects

every $f \in \mathcal{D}_T$ onto the *ground state* f_∞ (the eigenfunction corresponding to the smallest eigenvalue 0). We call this the *reproducing property* of the semigroup $(T_t|t \geq 0)$. As mentioned before this is the property which will be used for applications later on.

1.4 The corresponding Cauchy problem

In order to state a Cauchy problem related to the semigroup $(T_t|t \geq 0)$ considered in Sections 1.2, 1.3 we define the derivative of $f : \mathbb{R}_{\geq 0} \rightarrow L^2(\mathbb{R}^d, \lambda^d)$ by

$$\frac{df}{dt}(t) = L^2\text{-}\lim_{h \rightarrow 0} \frac{f(t+h) - f(t)}{h},$$

where the limit is taken such that $t+h \geq 0$.

Definition 1.4.1. Let H denote the operator defined in Equation 1.4 and u_s an element of $L^2(\mathbb{R}^d, \lambda^d)$. The problem of finding a continuous function $u : [s, T] \rightarrow L^2(\mathbb{R}^d, \lambda^d)$ which satisfies

$$\frac{du}{dt} = -Hu \tag{1.15a}$$

for every $t \in (s, T]$ and fulfils the *initial condition*

$$u(s) = u_s \tag{1.15b}$$

is called a *Cauchy problem*. Then the function u is called a *solution of the Cauchy problem*.

Now we show that we can get solutions of the Cauchy problem from the semigroup $(T_t|t \geq 0)$ defined in Section 1.2.

Theorem 1.4.2. Given $f \in L^2(\mathbb{R}^d, \lambda^d)$ the function $u(t) := \exp(-tH)f$ is a solution for 1.15a with initial condition $u(0) = f$.

Proof. For every $f \in \mathcal{D}_H$ and $t_0 > 0$ we use Equation 1.8 to derive

$$\left. \frac{d \exp(-tH)f}{dt} \right|_{t=t_0} = L^2\text{-}\lim_{t \rightarrow t_0} \frac{\sum_{k \in \mathbb{N}_0} \exp(-t\lambda_k) \alpha_k v_k - \sum_{k \in \mathbb{N}_0} \exp(-t_0\lambda_k) \alpha_k v_k}{t - t_0}.$$

But the absolute value of $(\exp(-(t - t_0)\lambda_k) - 1)(t - t_0)^{-1}$ is dominated by λ_k for $|t - t_0|$ sufficiently small. So if we take

$$\gamma_k(t) := \frac{\exp(-t\lambda_k) - \exp(-t_0\lambda_k)}{t - t_0} \alpha_k$$

it follows $\gamma^2 \leq \lambda_k^2 \alpha_k^2$ where the sum $\sum_{k \in \mathbb{N}_0} \lambda_k^2 \alpha_k^2$ is finite as we know from the definition of the domain (see Equation 1.5). Moreover $\gamma_k(t)$ converges to $-\lambda_k \alpha_k$ for t to 0. As a consequence of Lemma 1.2.1 it is permitted to interchange the derivative and the sum. This leads to

$$\frac{d \exp(-t_0 H) f}{dt} = - \sum_{k \in \mathbb{N}_0} \lambda_k \exp(-t_0 \lambda_k) \alpha_k v_k. \quad (1.16)$$

Finally $\exp(-t\lambda_k) \alpha_k = (u, v_k)$ is the k -th coefficient of the spectral representation of $\exp(-tH)f$. So the right side of 1.16 is equal to $-H \exp(-t_0 H) f$.

From Theorem 1.2.2 we know that the semigroup $(T_t | t \geq 0)$ defined by $T_t = \exp(-tH)$ is strongly continuous. This implies $u(0) = f$ for every function $f \in \mathcal{D}_H$. ■

1.5 Itô Diffusion and its generator

This section is devoted to the introduction of a (time homogeneous) Itô diffusion as the solution of a stochastic differential equation (SDE) and the definition of the generator of an Itô diffusion. For this we give some basic definitions and resume available existing and uniqueness results for SDEs. Finally we state the relation between the generator of the Itô diffusion and the coefficients of the defining SDE. In the next chapter this relation will be used to find solutions of the Cauchy Problem 1.15a, 1.15b. But first of all we give some statements about Itô diffusions in general.

If we want to describe the motion of a small particle in a moving liquid, subject to random bombardments and $b(t, x) \in \mathbb{R}^3$ is the velocity of the liquid at point x at time t , then the solution of the stochastic differential equation of the form

$$dX_t = b(t, X_t)dt + \sigma(t, X_t)dB_t \quad (1.17)$$

is a frequently used mathematical model for the position X_t of the particle at time t . There B_t is an m -dimensional Brownian motion and $\sigma(t, x) \in \mathbb{R}^{3 \times m}$. Also solutions of Equation 1.17 are popular in mathematical finance to model the behaviour of asset prices. Many more applications have been considered in the past. However in this work we are not interested in modelling issues concerning X_t , but we will use X_t to give a representation for the semigroup $(T_t | t > 0)$.

Remark. We leave it as an open question to give a substantiated interpretation of the (transformation) reconstruction mechanism presented in this work in terms of particle transport. That means if f_t is the solution of the Cauchy problem we do not go into a detailed discussion concerning the change of $f_t(x)$ for fixed $x \in \mathbb{R}^d$ and growing t . Nevertheless such a discussion seems interesting because it may lead to further applications.

Now we turn to the formal definition of an Itô diffusion. We restrict ourself to the time homogeneous case. That is b and σ are constant in time. As usual we denote the underlying probability space by (Ω, \mathcal{A}, P) . Moreover we consider $\mathcal{B}(\mathbb{R}^d)$ the Borel σ -algebra defined on \mathbb{R}^d . A function $X : \Omega \rightarrow \mathbb{R}^d$ is called *random variable*, iff for every $B \in \mathcal{B}(\mathbb{R}^d)$ we have $X^{-1}(B) \in \mathcal{A}$. In this case we call X an \mathcal{A} - $\mathcal{B}(\mathbb{R}^d)$ -measurable function. We say a statement A depending on ω is *almost surely (a.s.)* true, iff there exists a set $N \in \mathcal{A}$ with $P(N) = 0$ such that for all $\omega \in N^c$ the statement $A(\omega)$ is true. Here N^c is the complement of N in Ω .

Definition. Let $\mathbb{R}_{\geq 0}$ denote the *time parameter set*. We call a family of random variables $(X_t | t \in \mathbb{R}_{\geq 0})$ with values in \mathbb{R}^d a *stochastic process*, iff all random variables X_t are defined on the same probability space (Ω, \mathcal{A}, P) . The function $X(\omega) : \mathbb{R}_{\geq 0} \rightarrow \mathbb{R}^d$ defined by $t \mapsto X_t(\omega)$ is the *path of X_t for the realization ω* . A family $(\mathcal{F}_t | t \in \mathbb{R})$ of σ -algebras defined on Ω is a *filtration in Ω* , iff $s \leq t$ implies $\mathcal{F}_s \subset \mathcal{F}_t$. Then the quadruple $(\Omega, \mathcal{A}, P, (\mathcal{F}_t | t \geq 0))$ is called *filtered probability space*. The stochastic process $(X_t | t \geq 0)$ is *adapted to the filtration $(\mathcal{F}_t | t \geq 0)$* , iff for every $t \geq 0$ the random variable X_t is \mathcal{F}_t - $\mathcal{B}(\mathbb{R}^d)$ -measurable.

As suggested before we are interested in stochastic processes satisfying a

stochastic differential equation

$$dX_t = b(X_t)dt + \sigma(X_t)dB_t \quad (1.18)$$

where $X_t \in \mathbb{R}^d$, $b(x) \in \mathbb{R}^d$, $\sigma(x) \in \mathbb{R}^{d \times m}$. Here the m -dimensional Brownian motion $(B_t|t \geq 0)$ generates a natural filtration $(\mathcal{F}_t^B = \sigma(B_s|s \leq t)|t \geq 0)$. To be more precise we give the following definition with Equation 1.18 rewritten in integral form.

Definition. Let us denote by B_t a m -dimensional Brownian motion defined for $t \in [0, T]$ generating the filtration $(\mathcal{F}_t^B|t \geq 0)$. We consider a stochastic process

$$\begin{aligned} X^x : [0, T] \times \Omega &\rightarrow \mathbb{R}^d \\ (t, \omega) &\mapsto X^x(t, \omega) := X_t^x(\omega) \end{aligned}$$

defined on the filtered probability space $(\Omega, \mathcal{A}, P, \mathcal{F}_t^B)$ such that X_t^x is a.s. satisfying the stochastic integral equation

$$X_t^x(\omega) = x + \int_0^t b(X_s^x(\omega)) ds + \int_0^t \sigma(X_s^x(\omega)) dB_s(\omega) \quad \text{for all } t \in [0, T]. \quad (1.19)$$

Then we call X_t a *(time-homogeneous) Itô diffusion* with *initial condition* $x \in \mathbb{R}^d$, iff almost every path $X(\omega)$ is a continuous function and $(X_t|t \geq 0)$ is adapted to $(\mathcal{F}_t^B|t \geq 0)$. We call b the *drift coefficient* and σ the *diffusion coefficient*.

There exists a lot of literature [10, 18, 26, 27, 29, 51, 55, 79, 81] about probability theory, stochastic processes and stochastic integration providing much information about these subjects. For instance the definition of the integral $\int dB_t$ has to be taken from one of these references. Now we give Theorem 5.2.1 from [55] which is an existence and uniqueness result for the solution of Equation 1.18.

Theorem 1.5.1. *Let $b : \mathbb{R}^d \rightarrow \mathbb{R}^d$, $\sigma : \mathbb{R}^d \rightarrow \mathbb{R}^{d \times m}$ be measurable functions. Further for some constant $C \in \mathbb{R}$ b, σ satisfy the Lipschitz continuity condition*

$$|b(x) - b(y)| + |\sigma(x) - \sigma(y)| \leq C|x - y| \quad \text{for all } x, y \in \mathbb{R}^d$$

where $|\sigma|^2 := \sum |\sigma_{ij}|^2$. Then Equation 1.19 has a unique solution in $C^0([0, T])$ for every $T > 0$. Here uniqueness means path-wise unique (i.e. in the strong sense). That is if a second stochastic process $(Y_t | t \geq 0)$ satisfying Equation 1.19 is given then almost surely we have $X_t(\omega) = Y_t(\omega)$ for every $t \in [0, T]$.

As mentioned a proof of this can be found in [55] also in [26, 27, 51, 84] so we skip it here. To investigate solutions of the Cauchy problem defined in Equations 1.15a, 1.15b we introduce the generator of an Itô diffusion similar to Definition 1.2.3 as follows.

Definition 1.5.2. For every (time-homogeneous) Itô diffusion $(X_t^x | t \in \mathbb{R}_{\geq 0})$ in \mathbb{R}^d we define the (infinitesimal) generator A of the process X_t^x by

$$Af(x) := \lim_{t \searrow 0} \frac{\mathbb{E}[f(X_t^x)] - f(x)}{t} \quad \text{for all } x \in \mathbb{R}^d,$$

where $\tilde{\mathcal{D}}_A(x) := \{f \in \mathcal{L}^2(\mathbb{R}^d, \lambda^d) | Af(x) \text{ exists}\}$ and $\tilde{\mathcal{D}}_A := \bigcap_{x \in \mathbb{R}^d} \tilde{\mathcal{D}}_A(x)$ is called the *domain of the generator*. (We denote by $\mathbb{E}[X]$ the expectation of X respective P .)

Remark. This definition is also valid for a more general class of stochastic processes (see [27]).

Now we are prepared to give relations between A and the coefficients b, σ in the stochastic differential Equation 1.18 defining X_t . Therefore we use the following theorem which can be found in [55] and is a consequence of Itô's formula. For this we denote by $C^2(\mathbb{R}^d)$ the set of all twice continuous differentiable functions and define

$$C_0^2(\mathbb{R}^d) := \{f \in C^2(\mathbb{R}^d) | f \text{ has compact support}\}$$

which is naturally embedded in $L^2(\mathbb{R}^d, \lambda^d)$ by $f \mapsto [f]$. Here $[f]$ is the set of all functions $g \in \mathcal{L}^2(\mathbb{R}^d, \lambda^d)$ equivalent to f (i.e. the class of f). Using the same embedding we define $\mathcal{D}_A := \{[f] | f \in \tilde{\mathcal{D}}_A\}$.

Theorem 1.5.3. Let $(X_t | t \in \mathbb{R}_{\geq 0})$ be a (time-homogeneous) Itô diffusion and

$f \in C_0^2(\mathbb{R}^d)$, then we have $f \in \mathcal{D}_A$ and Af is a.e. given by

$$Af(x) = \sum_{i=1}^d b_i(x) \frac{\partial f}{\partial x_i} + \frac{1}{2} \sum_{i,j=1}^d (\sigma \sigma^\top)_{i,j}(x) \frac{\partial^2 f}{\partial x_i \partial x_j} \quad (1.20)$$

where σ^\top denotes the transpose of σ .

Remark. The operator A acts on $L^2(\mathbb{R}^d, \lambda^d)$ because the embedding of $C_0^2(\mathbb{R}^d)$ is a dense subset.

1.6 Solutions with the Feynman-Kac-Formula

In this section we give a solution of the Cauchy problem 1.15a with initial condition 1.15b which was found by *Feynman* and *Kac*. A simple proof of Theorem 1.6.1 can be found in [55].

Theorem 1.6.1. *Let $(X_t^x | t \in \mathbb{R}_{\geq 0})$ be an Itô diffusion with generator A . Further we take $f \in C_0^2(\mathbb{R}^d)$ and assume $V \in C(\mathbb{R}^d)$ is bounded from below.*

a) Define

$$u(t, x) := \mathbb{E} \left[\exp \left(- \int_0^t V(X_s^x) ds \right) f(X_t^x) \right], \quad (1.21)$$

then $u(t, \cdot) \in \mathcal{L}^2(\mathbb{R}^d, \lambda^d)$ for all $t \geq 0$, and its class $u_t := [u(t, \cdot)]$ in $L^2(\mathbb{R}^d, \lambda^d)$ satisfies

$$\frac{du_t}{dt} = Au_t - Vu_t, \quad \text{for all } t > 0, x \in \mathbb{R}^d \quad (1.22a)$$

and

$$u(0, x) = f(x), \quad \text{for all } x \in \mathbb{R}^d. \quad (1.22b)$$

b) The solution is unique in the sense that, if $\tilde{u}(t, x) \in C^{1,2}(\mathbb{R} \times \mathbb{R}^d)$ is bounded on $K \times \mathbb{R}^d$ for each compact $K \subset \mathbb{R}$ and \tilde{u} solves 1.22a, 1.22b, then we have $u = \tilde{u}$ and 1.21 holds.

Remark 1.6.2. In Equation 1.22a the derivative $\frac{du_t}{dt}$ is in the $L^2(\mathbb{R}^d, \lambda^d)$ -sense, and we use the “generator-definition 1.5.2” for A . Equation 1.22a is also correct

in the sense of ordinary partial derivatives (see [19]). For our approach (i.e. using spectral theory) it is more appropriate to use the $L^2(\mathbb{R}^d, \lambda^d)$ -definition.

Now we consider the generator $A := \frac{1}{2}\Delta$ of an Itô diffusion $(X_t^x | t \in \mathbb{R}_{\geq 0})$ with drift equal to 0 and diffusion equal to the d -dimensional unit matrix I_d . (In this case the Itô diffusion is simply a Brownian motion.) As in Equation 1.7 we take $V := \frac{\Delta f_\infty}{2f_\infty}$ and $H = -A + V$. Then $T_t f = \exp(-tH)f$ as defined in Theorem 1.2.2 is a solution of the Cauchy problem 1.15a with initial condition 1.15b. Hence we know $T_t f(x) = u(t, x)$ which enables us to compute the solution explicitly as given in Equation 1.21.

One possibility to do this is to perform a Monte Carlo simulation for the Expression 1.21. But then we have to compute $\exp(x)$ where x can take large values. Even if V is bounded from below, $\exp(x)$ may become smaller than the precision of the computer system which will be used for the simulation. Hence we have to apply a special mechanism (e.g. algebraic computing theory as described in [47] and implemented in the **GMP** library) to handle very large (resp. small) numbers during the computer experiments. But we do not simulate Expression 1.21 because of the inconvenience which possibly occurs. Instead we are going to avoid the term $\exp(x)$ by transforming the problem to another space as mentioned at the beginning.

1.7 Operators mapped to $L^2(\mathbb{R}^d, f_\infty^2 \lambda^d)$

In this section we consider the space $L^2(\mathbb{R}^d, f_\infty^2 \lambda^d)$ which is the set of functions $f : \mathbb{R}^d \rightarrow \mathbb{R}$ with $\|f\|_{f_\infty^2} < \infty$ where

$$\|f\|_{f_\infty^2}^2 := (f, f)_{f_\infty^2} := \int f^2 f_\infty^2 d\lambda. \quad (1.23)$$

We recall, that we have taken $f_\infty : \mathbb{R}^d \rightarrow \mathbb{R}_{>0}$ as a strictly positive function and from now on we suppose

$$\int f_\infty^2 d\lambda = 1.$$

In order to formulate equivalent statements to the statements given (in the chapters before) for the operator H acting on $L^2(\mathbb{R}^d, \lambda^d)$ and the semigroup $(T_t | t \geq 0)$ we need an identification between $L^2(\mathbb{R}^d, \lambda^d)$ and $L^2(\mathbb{R}^d, f_\infty^2 \lambda^d)$. Therefore we give the following connection.

Definition 1.7.1. For every strictly positive function $f_\infty : \mathbb{R}^d \rightarrow \mathbb{R}_{>0}$ we define

$$\begin{aligned} U_{f_\infty} : L^2(\mathbb{R}^d, \lambda^d) &\rightarrow L^2(\mathbb{R}^d, f_\infty^2 \lambda^d) \\ \psi &\mapsto \frac{\psi}{f_\infty}. \end{aligned}$$

So with the next proposition we state that this gives the desired identification between the two spaces.

Proposition 1.7.2. U_{f_∞} as in the definition above is a unitary map between the spaces $L^2(\mathbb{R}^d, \lambda^d)$ and $L^2(\mathbb{R}^d, f_\infty^2 \lambda^d)$.

Proof. For every function $\psi \in L^2(\mathbb{R}^d, f_\infty^2 \lambda^d)$ we have $U_{f_\infty}(\psi \cdot f_\infty) = \psi$ and $\psi \cdot f_\infty \in L^2(\mathbb{R}^d, \lambda^d)$ because of

$$\begin{aligned} \|\psi \cdot f_\infty\|^2 &= \int \psi^2 f_\infty^2 d\lambda \\ &= \|\psi\|_{f_\infty^2}^2 < \infty. \end{aligned}$$

So U_{f_∞} is a surjective map and we go ahead to prove injectivity which is easy to see. For arbitrary functions $\psi_1, \psi_2 \in L^2(\mathbb{R}^d, \lambda^d)$ we have

$$\psi_1 \neq \psi_2 \Leftrightarrow U_{f_\infty}(\psi_1) \neq U_{f_\infty}(\psi_2)$$

if $f_\infty > 0$, which is one of our assumptions. Moreover for $a_1, a_2 \in \mathbb{R}$ we have

$$U_{f_\infty}(a_1 \psi_1 + a_2 \psi_2) = a_1 U_{f_\infty}(\psi_1) + a_2 U_{f_\infty}(\psi_2)$$

and

$$(\psi_1, \psi_2) = (U_{f_\infty}(\psi_1), U_{f_\infty}(\psi_2))_{f_\infty}$$

which makes the proof complete. ■

Remark. In the space $L^2(\mathbb{R}^d, f_\infty^2 \lambda^d)$ we consider convergence as induced by the norm coming from the inner product in $L^2(\mathbb{R}^d, \lambda^d)$. To be precise we use $(f, g)_{f_\infty^2} = (U_{f_\infty}^{-1} f, U_{f_\infty}^{-1} g)$ to get the norm in $L^2(\mathbb{R}^d, f_\infty^2 \lambda^d)$ as defined in 1.23.

Obviously we have the inverse map

$$\begin{aligned} U_{f_\infty}^{-1} : L^2(\mathbb{R}^d, f_\infty^2 \lambda^d) &\rightarrow L^2(\mathbb{R}^d, \lambda^d) \\ \psi &\mapsto \psi \cdot f_\infty \end{aligned}$$

which makes the identification between $L^2(\mathbb{R}^d, \lambda^d)$ and $L^2(\mathbb{R}^d, f_\infty^2 \lambda^d)$ complete.

Remark. If $(v_k | k \in \mathbb{N})$ is an ONB of $L^2(\mathbb{R}^d, \lambda^d)$, then $(\frac{v_k}{f_\infty} | k \in \mathbb{N})$ is an ONB of its counterpart $L^2(\mathbb{R}^d, f_\infty^2 \lambda^d)$.

1.8 Review of some statements using the map to $L^2(\mathbb{R}^d, f_\infty^2 \lambda^d)$

Here we use the isomorphism from Definition 1.7.1 to define operators L acting on the space $L^2(\mathbb{R}^d, f_\infty^2 \lambda^d)$ starting from operators H acting on $L^2(\mathbb{R}^d, \lambda^d)$ as shown below.

$$\begin{array}{ccc} L^2(\mathbb{R}^d, \lambda^d) & \xleftarrow{U_{f_\infty}^{-1}} & L^2(\mathbb{R}^d, f_\infty^2 \lambda^d) \\ \downarrow H & & \downarrow L \\ L^2(\mathbb{R}^d, \lambda^d) & \xrightarrow{U_{f_\infty}} & L^2(\mathbb{R}^d, f_\infty^2 \lambda^d) \end{array}$$

Then we define a semigroup according to Section 1.2 using the operator L . This leads to solutions of a Cauchy problem which is formulated at the end of the section (similar to Definition 1.4).

Once again we consider the operator H acting on $L^2(\mathbb{R}^d, \lambda^d)$ as defined in Section 1.1 Equation 1.7. Then naturally we have the operator $L := U_{f_\infty} H U_{f_\infty}^{-1}$ acting on $L^2(\mathbb{R}^d, f_\infty^2 \lambda^d)$ (as shown in the diagram above). As before we denote by $(\lambda_k | k \in \mathbb{N}_0)$ the eigenvalues of H and by $(v_k | k \in \mathbb{N}_0)$ the corresponding normalised eigenvectors. If ψ is an element of $\mathcal{D}_L = U_{f_\infty}(\mathcal{D}_H)$ represented as

$$\psi = \sum_{k \in \mathbb{N}_0} (U_{f_\infty}(v_k), \psi)_{f_\infty^2} U_{f_\infty}(v_k)$$

we easily calculate the spectral representation

$$L\psi = \sum_{k \in \mathbb{N}_0} \lambda_k(U_{f_\infty}(v_k), \psi)_{f_\infty^2} U_{f_\infty}(v_k)$$

analogous to Equation 1.4. This is because for every $k \in \mathbb{N}_0$ we have

$$\begin{aligned} LU_{f_\infty}(v_k) &= U_{f_\infty} H v_k \\ &= \lambda_k(v_k, v_k) U_{f_\infty} v_k \\ &= \lambda_k(U_{f_\infty}(v_k), U_{f_\infty}(v_k))_{f_\infty^2} U_{f_\infty}(v_k). \end{aligned}$$

So we are able to define $\exp(-tL)\psi$ for all $t \in \mathbb{R}_{\geq 0}$ and all $\psi \in \mathcal{D}_L$ analogous to Equation 1.8 as an element of \mathcal{D}_L . On the other hand we defined a strongly continuous semigroup T_t acting on $L^2(\mathbb{R}^d, \lambda^d)$. In the same natural way this leads to a semigroup \hat{T}_t acting on $L^2(\mathbb{R}^d, f_\infty^2 \lambda^d)$.

Theorem 1.8.1. *If $\hat{T}_t := U_{f_\infty} \exp(-tH) U_{f_\infty}^{-1}$ for $t \geq 0$, then $(\hat{T}_t | t \geq 0)$ is a strongly continuous semigroup with domain $\mathcal{D}_{\hat{T}} = L^2(\mathbb{R}^d, f_\infty^2 \lambda^d)$.*

Proof. The proof uses the semigroup property for $T_t := e^{-tH}$ and the fact that every inner product is a continuous function. We calculate

$$\begin{aligned} \hat{T}_t \circ \hat{T}_s &= U_{f_\infty} e^{-tH} U_{f_\infty}^{-1} \circ U_{f_\infty} e^{-sH} U_{f_\infty}^{-1} \\ &= U_{f_\infty} e^{-tH} \circ e^{-sH} U_{f_\infty}^{-1} \\ &= U_{f_\infty} e^{-(t+s)H} U_{f_\infty}^{-1} \\ &= \hat{T}_{t+s} \end{aligned}$$

which shows the semigroup property for \hat{T} . In order to prove strong continuity of the semigroup we have to show that for every $\psi \in L^2(\mathbb{R}^d, f_\infty^2 \lambda^d)$ we have

$$(U_{f_\infty} e^{-tH} U_{f_\infty}^{-1}) \psi \xrightarrow{L^2 f_\infty^2} (U_{f_\infty} e^{-t_0 H} U_{f_\infty}^{-1}) \psi$$

whenever $t \rightarrow t_0$ in $\mathbb{R}_{\geq 0}$. Now let f be an element in $L^2(\mathbb{R}^d, \lambda^d)$ then

$$\begin{aligned} (U_{f_\infty} e^{-tH} U_{f_\infty}^{-1})_{f_\infty^2} f &= U_{f_\infty} e^{-tH} f \xrightarrow{L^2 f_\infty^2} U_{f_\infty} e^{-t_0 H} f \\ &= (U_{f_\infty} e^{-t_0 H} U_{f_\infty}^{-1})_{f_\infty^2} f. \end{aligned}$$

■

Certainly one may ask for the connection between the two naturally arising objects which can be guessed easily. We formulate it as follows.

Theorem 1.8.2. *Let $(T_t|t \geq 0)$ denote the semigroup defined in Section 1.2 and $(\hat{T}_t|t \geq 0)$ the semigroup defined in Theorem 1.8.1. If H is the generator of T_t and L is the generator of \hat{T}_t it follows $L = U_{f_\infty} \circ H \circ U_{f_\infty}^{-1}$.*

Proof. Let $\psi \in \mathcal{D}_L$ and $f := U_{f_\infty}^{-1}\psi$ then we know

$$\frac{e^{-tL} - 1}{t}\psi = \frac{U_{f_\infty}e^{-tH}U_{f_\infty}^{-1}\psi - U_{f_\infty}U_{f_\infty}^{-1}\psi}{t} = U_{f_\infty}\left(\frac{e^{-tH}f - f}{t}\right).$$

So if we take the L^2 -limit $t \searrow 0$ and use the continuity of U_{f_∞} we find

$$\begin{aligned} -L\psi &= U_{f_\infty}(-H)f \\ &= [U_{f_\infty} \circ (-H) \circ U_{f_\infty}^{-1}]\psi. \end{aligned} \quad \blacksquare$$

Now we turn to the investigation of \mathcal{D}_L . Independent from its formal definition we give the connection to \mathcal{D}_H .

Theorem 1.8.3. *In the notation used above the equation $\mathcal{D}_L = U_{f_\infty}(\mathcal{D}_H)$ holds true.*

Proof. According to Definition 1.2.3 we have

$$\mathcal{D}_L = \left\{ \psi \in L^2(\mathbb{R}^d, f_\infty^2 \lambda^d) \left| \frac{\hat{T}_t\psi - \psi}{t} \text{ converges for } t \searrow 0 \right. \right\}$$

where the limit has to be taken in $L^2(\mathbb{R}^d, f_\infty^2 \lambda^d)$. The convergence condition is equivalent to the fact, that there is an $f \in L^2(\mathbb{R}^d, \lambda^d)$ namely $f := \psi U_{f_\infty}^{-1}$ such that the limit of $(\hat{T}_t U_{f_\infty} f - U_{f_\infty} f)t^{-1}$ exists in $L^2(\mathbb{R}^d, f_\infty^2 \lambda^d)$ for $t \searrow 0$. On account of Proposition 1.7.2 we know that this means also

$$U_{f_\infty}^{-1}\left(\frac{\hat{T}_t U_{f_\infty} f - U_{f_\infty} f}{t}\right) = \frac{T_t f - f}{t}$$

converges in $L^2(\mathbb{R}^d, \lambda^d)$ for $t \searrow 0$. Then the function f is an element of \mathcal{D}_H . This shows the equivalence of $f \in \mathcal{D}_H$ and $\frac{f}{f_\infty} \in \mathcal{D}_L$. \blacksquare

Remark 1.8.4. Just as in Theorem 1.3.1 for all $\psi \in \mathcal{D}_L$ we know that the function $\hat{T}_t\psi$ converges to $(1, \psi)_{f_\infty}1$ for $t \rightarrow \infty$. So up to the constant $(1, \psi)_{f_\infty}$ the semigroup \hat{T}_t projects $\psi \in \mathcal{D}_L$ to $1 \in L^2(\mathbb{R}^d, f_\infty^2 \lambda^d)$. Here we once again just point to the similarity of the arguments given in the proof of Theorem 1.3.1 which let us expect this statement. Nevertheless we will prove this in the next chapter in detail.

Proposition 1.8.5. *If we set $H := -\frac{1}{2}\Delta + \frac{\Delta f_\infty}{2f_\infty}$ then $L = -\frac{1}{2}\Delta - (\nabla \ln f_\infty)\nabla$ in the above notation.*

Proof. First we transform the Laplacian:

$$\begin{aligned}
 U_{f_\infty} \Delta U_{f_\infty}^{-1} \psi &= U_{f_\infty} \Delta f_\infty \psi \\
 &= U_{f_\infty} \nabla ((\nabla f_\infty) \psi + f_\infty \nabla \psi) \\
 &= U_{f_\infty} ((\Delta f_\infty) \psi + (\nabla f_\infty)(\nabla \psi) + (\nabla f_\infty)(\nabla \psi) + f_\infty \Delta \psi) \\
 &= \frac{\Delta f_\infty}{f_\infty} \psi + 2 \frac{\nabla f_\infty}{f_\infty} \nabla \psi + \Delta \psi \\
 &= \frac{\Delta f_\infty}{f_\infty} \psi + 2(\nabla \ln f_\infty) \nabla \psi + \Delta \psi
 \end{aligned}$$

The transformed Hamiltonian H will be called L calculated as follows:

$$\begin{aligned}
 L\psi &= U_{f_\infty} H U_{f_\infty}^{-1} \psi \\
 &= U_{f_\infty} \left(-\frac{1}{2}\Delta + \frac{1}{2} \frac{\Delta f_\infty}{f_\infty} \right) U_{f_\infty}^{-1} \psi \\
 &= U_{f_\infty} \left(-\frac{1}{2}\Delta \right) U_{f_\infty}^{-1} \psi + U_{f_\infty} \left(\frac{1}{2} \frac{\Delta f_\infty}{f_\infty} \right) U_{f_\infty}^{-1} \psi \\
 &= -\frac{1}{2} \frac{\Delta f_\infty}{f_\infty} \psi - (\nabla \ln f_\infty) \nabla \psi - \frac{1}{2} \Delta \psi + \frac{1}{2} \frac{\Delta f_\infty}{f_\infty} \psi \\
 &= -\frac{1}{2} \Delta \psi - (\nabla \ln f_\infty) \nabla \psi
 \end{aligned}$$

■

According to Definition 1.4.1 we formulate the Cauchy problem in the space $L^2(\mathbb{R}^d, f_\infty^2 \lambda^d)$ as follows. Given a function \hat{u}_s in $L^2(\mathbb{R}^d, f_\infty^2 \lambda^d)$, we search a continuous function $\hat{u} : [s, T] \rightarrow L^2(\mathbb{R}^d, f_\infty^2 \lambda^d)$ satisfying

$$\frac{d\hat{u}}{dt} = -L\hat{u} \quad \text{for all } t \in (s, T] \quad (1.24a)$$

and satisfying the initial condition

$$\hat{u}(s) = \hat{u}_s. \quad (1.24b)$$

Proposition 1.8.6. *Given $\psi \in \mathcal{D}_L$ the function $\hat{u}(t) := \exp(-tL)\psi$ is a solution of 1.24a with initial condition $\hat{u}(0) = \psi$.*

We omit the proof, because it is the same as the proof given in Section 1.4 equipped with the necessary transformation terms U_{f_∞} .

1.9 Solutions with the Kolmogorov backward equation

Now we give a solution of the Cauchy problem 1.24a with initial condition 1.24b in terms of a stochastic process $(X_t | t \in \mathbb{R}_{\geq 0})$ and its expectation. For this we use Kolmogorov's backward equation which can be found in [55]. Similarly to Section 1.6 we consider an Itô diffusion $(X_t | t \in \mathbb{R}^d)$, but here we choose another generator denoted by \hat{A} . From Theorem 1.5.3 we know that the generator of an Itô diffusion is of the form

$$\hat{A}\psi(x) = \sum_i \hat{b}_i(x) \frac{\partial \psi}{\partial x_i} + \frac{1}{2} \sum_{i,j} (\hat{\sigma} \hat{\sigma}^T)_{i,j}(x) \frac{\partial^2 \psi}{\partial x_i \partial x_j}$$

where $\hat{b} : \mathbb{R}^d \rightarrow \mathbb{R}^d$ is the drift coefficient of the process and $\hat{\sigma} : \mathbb{R}^d \rightarrow \mathbb{R}^{d \times d}$ is the diffusion coefficient, compare to formula 1.20. But then we are able to identify the operator $L = -\frac{1}{2}\Delta - (\nabla \ln f_\infty) \nabla$ (see Prop. 1.8.5) directly as a generator of an Itô diffusion with drift coefficient $\hat{b} = -\nabla \ln f_\infty$ and diffusion coefficient $\hat{\sigma} = -I_d$.

Theorem 1.9.1. *Let $\psi \in C_0^2(\mathbb{R}^d)$ and define $\hat{u}(t, x) := \mathbb{E}[\psi(X_t^x)]$ then the function $\hat{u}(t, \cdot)$ is an element of $\mathcal{D}_{\hat{A}}$. Further we have*

$$\frac{d\hat{u}}{dt} = -\hat{A}\hat{u} \quad \text{for all } t > 0, x \in \mathbb{R}^d$$

and $\hat{u}(0, x) = \psi(x), x \in \mathbb{R}^d$. The solution is unique in the sense of Theo. 1.6.1.

Chapter 2

Reformulation for Bounded Regions

In this chapter we will review the arguments from the chapter above. Instead of functions defined on \mathbb{R}^d we consider functions $f : D \rightarrow \mathbb{R}$ where $D \subset \mathbb{R}^d$ is open, bounded and convex. We do this because we want to give applications in image processing later on. In image processing we have to deal with such functions f as we will see in Chapter 3. In this view the natural candidates for D are a rectangle as subset of \mathbb{R}^2 with a boundary ∂D which is just piecewise smooth or an approximation of this with a sufficiently smooth boundary. In the following we'll keep both possibilities in mind and generalise them to the cases of bounded, convex subsets of \mathbb{R}^d with smooth and non-smooth boundary. Actually we restrict the non-smooth case to boundaries which are smooth except for a finite set of points. Before we introduce boundary conditions we start with some remarks about the extension of f to a function defined on \mathbb{R}^2 . Later on we will not use this approach. We give the remarks just to be complete at this point. As mentioned then in Section 2.2 we introduce boundary conditions. After that we define operators as in Section 1.1 now acting on functions $f : D \rightarrow \mathbb{R}$ which fulfil those boundary conditions. In Section 2.3 we show that the resulting operators have discrete point spectrum whose lowest eigenvalue $\lambda_0 = 0$ has multiplicity one. This guarantees the projection property (see Theorem 1.3.1) which will be important for the application in image processing. Then in Section 2.4 we make some necessary remarks concerning

Itô diffusion processes defined on \overline{D} , and we construct Itô diffusions on \overline{D} with sufficiently smooth boundary. In the non-smooth case we replace this construction by solutions of the Skorokhod problem (see Appendix B). Then we give a reformulation of the Cauchy problem introduced in Section 1.4. Now the solutions to this reformulated problem can be given using the Itô diffusion on \overline{D} . Finally the applications in image processing will make use of the projection property of the operators. It leads to a mechanism for transforming one image into another by means of grey value transport: The solution of the reformulated Cauchy problem is a time dependent function which represents one given image at time $t = 0$ (which will be called *start image*) and reproduces another image at time $t = \infty$ (we call it the *stop image*). In order to prove this at the end of this chapter we formulate a theorem, which tells us that the solution of the reformulated Cauchy problem converges for $t \rightarrow \infty$ point-wise (up to a constant) to the function associated to the stop image. Moreover this behaviour is independent of the start image.

2.1 Restrictions coming from potentials

As mentioned above here we consider the possibility to extend a given function $f : D \rightarrow \mathbb{R}$ to a function \tilde{f} defined on \mathbb{R}^d . For this we do not distinguish the cases of smooth or non-smooth region D , because we simply assume f and its derivatives to be continuously extendable to \overline{D} the closure of D in the euclidian metric. Now if we take $H := -\frac{1}{2}\Delta + V$ with $V := \frac{\Delta \tilde{f}}{2\tilde{f}}$ as usual we know from Theorem 1.1.3 that \tilde{f} has to fulfil some additional condition in order to guarantee $V(x) \rightarrow \infty$ for $|x| \rightarrow \infty$. We recall that this leads to H with discrete point spectrum and a lowest eigenvalue with multiplicity one as stated in [61] Theorem XIII.46 for $V \in L^2_{\text{loc}}(\mathbb{R}^d, \lambda^d)$.

Definition 2.1.1. Let (M, μ) be a finite measure space. Then a function $f \in L^2(M, \mu)$ is called positive iff $f \geq 0$ a.e. and is not the zero function. It is called strictly positive iff $f > 0$ a.e..

Definition 2.1.2. A bounded operator A on $L^2(M, \mu)$ is called positivity preserving iff Af is positive whenever $f \in L^2(M, \mu)$ is positive. The operator

A is called positivity improving if Af is strictly positive whenever f is positive. Finally, we call the operator A ergodic iff it is positivity preserving and for any two functions $f, g \in L^2(M, \mu)$ that are both positive there is some $n \in \mathbb{N}$ such that we have $(f, A^n g) \neq 0$.

Now we are prepared to formulate Theorem XIII.44 from [61].

Theorem 2.1.3. *Let H be a self-adjoint operator that is bounded from below on $L^2(M, \mu)$ and $\sigma(H)$ its spectrum. Suppose e^{-tH} is positivity preserving for all $T > 0$ and that $E = \inf \sigma(H)$ is an eigenvalue. Then the following assertions are equivalent:*

- a) *The eigenvalue E has multiplicity one and the corresponding eigenfunction is strictly positive.*
- b) *$(H - \lambda)^{-1}$ is ergodic for some $\lambda < E$.*
- c) *e^{-tH} is ergodic for some $t > 0$.*
- d) *$(H - \lambda)^{-1}$ is positivity improving for all $\lambda < E$.*
- e) *e^{-tH} is positivity improving for all $t > 0$.*

Starting with an explicitly given \tilde{f} we could proceed to investigate one of the conditions above. Further information concerning operators of type $-\frac{1}{2}\Delta + V$ could be found e.g. in [61, 38] whereas for the theory of semigroups we refer to [16]. We do not go into detail here. We just remark that for $|x| \rightarrow \infty$ the potential V grows unboundedly if $\Delta \tilde{f}$ converges slower to 0 than \tilde{f} as in the following example.

Example. In this example we restrict ourself to the 1-dimensional case. We consider an extension of f denoted by \hat{f} with $\hat{f}(x) = \exp(x^{2n})$ for $|x|$ sufficiently large. By elementary analysis it follows $V(x) = (2n - 1)nx^{2n-2} + 2n^2x^{4n-2}$, which is an element of $L^2_{\text{loc}}(\mathbb{R}, \lambda)$, and $V(x) \rightarrow \infty$ for $|x| \rightarrow \infty$ as wanted.

Later on we want to verify our theoretical results through computer experiments and use them for some applications in image processing. Therefore it is not convenient to handle processes on unbounded domains as \mathbb{R}^d . Even though it is possible to overcome the difficulties arising from the use of \mathbb{R}^d we

take another approach. In the following we consider bounded subsets of \mathbb{R}^d and introduce boundary conditions as mentioned before.

2.2 Boundary conditions

In Section 1.9 we described solutions $u : \mathbb{R}_{\geq 0} \rightarrow L^2(\mathbb{R}^d, \lambda^d)$ of the Cauchy problem 1.24a in terms of stochastic processes defined on \mathbb{R}^d and their expectation. Later on we are interested in solutions u with values in the space $\overline{C}_2(D)$ and again we give a representation of $u(x, t)$ in terms of stochastic processes $(X_t | t \in \mathbb{R}_{\geq 0})$ and their expectation. Now X_t is a random variable with values in $\overline{D} = D \cup \partial D$ where D is an open, bounded, convex subset of \mathbb{R}^d . In order to describe the behaviour of X_t at the boundary of D we introduce boundary conditions. In the following we assume $f \in \overline{C}_2(D)$ to be uniquely extendable to \overline{D} with one of the following boundary conditions:

- Dirichlet for $c \in \mathbb{R}$ $\forall x \in \partial D, y \in D : \lim_{y \rightarrow x} f(y) = c$
- Neumann for $c \in \mathbb{R}$ $\forall x \in \partial D, y \in D : \lim_{y \rightarrow x} \frac{\partial f(y)}{\partial \nu(x)} = c$

There the boundary of D is denoted by ∂D and ν is a vector field defined on ∂D orthogonal to the boundary. So $\frac{\partial f(y)}{\partial \nu(x)}$ is the derivative of f in direction $\nu(x)$ evaluated at y . If the boundary is sufficiently smooth, then for every $x \in \partial D$ the vector $\nu(x)$ is uniquely determined (Fig. 2.1). If D is only assumed to

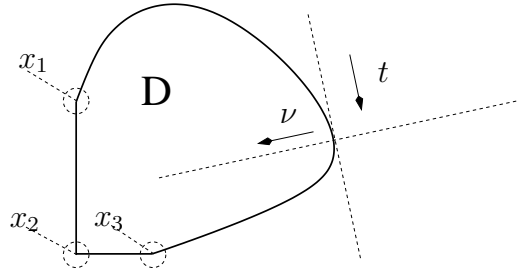


Figure 2.1. The area $D \subset \mathbb{R}^2$ is an open, convex set with non-smooth boundary ∂D which defines a vector field $\nu : \partial D \rightarrow \mathbb{R}^2$ on almost all points. If $t(x)$ is the direction of the tangent of the boundary at the point $x \in \partial D$ then we have $\nu(x) \perp t(x)$. The points x_1, x_2, x_3 will be treated separately.

be convex in general the normal $\nu(x)$ for $x \in \partial D$ is not uniquely determined. Then we define

$$\mathcal{N}_x := \bigcup_{r>0} \{ \nu \in \mathbb{R}^d \mid |\nu| = 1, \mathcal{B}(x - r\nu, r) \cap D = \emptyset \} \quad (2.1)$$

where $\mathcal{B}(x, r) := \{y \in \mathbb{R}^d \mid |x - y| < r\}$ and take the *strong Neumann condition*:

- Neumann for $c \in \mathbb{R} \quad \forall x \in \partial D, \nu(x) \in \mathcal{N}_x, y \in D : \lim_{y \rightarrow x} \frac{\partial f(y)}{\partial \nu(x)} = c$

The name is justified, because the usual Neumann condition is automatically included and our condition is stronger.

Remark. For every boundary point $x \in \partial D$ we are able to describe the set \mathcal{N}_x by the union of all (inward) unit normal vectors ν of all hyperplanes H that contain x and do not intersect with D .

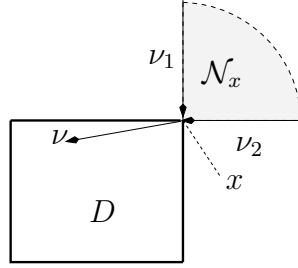


Figure 2.2. All vectors ν between ν_1 and ν_2 with length 1 belong to the normal set \mathcal{N}_x at the point $x \in \partial D$. The vectors ν_1, ν_2 are included.

Example. For $D = \{(x, y) \in \mathbb{R}^2 \mid 0 < x < x_0, 0 < y < y_0\}$ we naturally define

$$\nu(x, y) = \begin{cases} (1, 0) & x = 0 \wedge y \neq 0 \wedge y \neq y_0 \\ (0, -1) & y = y_0 \wedge x \neq 0 \wedge x \neq x_0 \\ (-1, 0) & x = x_0 \wedge y \neq 0 \wedge y \neq y_0 \\ (0, 1) & y = 0 \wedge x \neq 0 \wedge x \neq x_0 \end{cases} \text{ if } (x, y) \in \partial D$$

as the only element in the corresponding normal set. If (x, y) is one of the corner points e.g. $(x, y) = (x_0, y_0)$ we have

$$\mathcal{N}_{(x_0, y_0)} = \left\{ \frac{(x_0, y_0) - (x, y)}{|(x_0, y_0) - (x, y)|} \mid x \geq x_0, y \geq y_0, (x, y) \neq (x_0, y_0) \right\}$$

as shown in Figure 2.2. The definition of the sets $\mathcal{N}_{(0,0)}$, $\mathcal{N}_{(x_0,0)}$ and $\mathcal{N}_{(0,y_0)}$ is analogous.

Other boundary conditions exist but they are out of the scope of this work.

2.3 Reproducing operators in $L^2(D, \lambda^d)$

We proceed with the reformulation of the statements given in $L^2(\mathbb{R}^d, \lambda^d)$ now for the space $L^2(D, \lambda^d)$. This is the space of all square integrable functions $f : D \rightarrow \mathbb{R}^d$. As we know $\overline{C_2}(D)$ can be imbedded into $L^2(D, \lambda^d)$. (Here the bar indicates that f can be extended to \overline{D} such that f and its derivatives of order one and two are continuous.)

Remark.

- If $f \in \overline{C_2}(D)$ then the extension \tilde{f} of f to \overline{D} at every boundary point x is defined by the limit of $f(x_n)$ where $(x_n | n \in \mathbb{N})$ converges in D to x . The same holds true for the derivatives of \tilde{f} . In general continuous extensions do not always exist even for functions which are continuous on D , but they are unique.
- The set of all k -times continuously differentiable functions on D is denoted by $C^k(D)$. So the symbol $\overline{C^k(D)}$ is typically used for the closure of the topological space $C^k(D)$ with sup-norm. To avoid confusion we choose $\overline{C_k}(D)$ to denote the set of all k -times continuously differentiable functions. As before the bar indicates that the functions in $\overline{C_k}(D)$ and their derivatives are continuously extendable to \overline{D} . Depending on D we have $\overline{C_k}(D) \neq \overline{C^k(D)}$ and $\overline{C_k}(D) \neq C^k(\overline{D})$.

In the following we consider functions with Neumann boundary condition because we will use it in the implementation (see Chapter 3). Additionally we give remarks to the Dirichlet case because it is very similar. Unfortunately in both cases we can not apply Theorem 1.1.3. This told us that the operator $H := -\frac{1}{2}\Delta + V$ with $V := \frac{\Delta f_\infty}{2f_\infty}$ has a purely discrete point spectrum and its smallest eigenvalue is non-negative and has multiplicity one. So in the next two sections we will give a different argument leading to the same result.

2.3.1 Regions with smooth boundary

This section is mostly a resume of the results taken from [78] with some slight modifications. For this we consider a bounded area $D \subset \mathbb{R}^d$ with smooth boundary $\partial D \in \mathcal{C}^1$ and denote the normal to the boundary at the boundary point $x \in \partial D$ by $\nu(x) = (\nu_1(x), \dots, \nu_d(x))$.

Definition 2.3.1. For $m \in \mathbb{N}_0$ we say that *the boundary ∂D belongs to the class \mathcal{C}^m* , iff the following statements hold:

- It exists a finite set of balls $\{\mathcal{B}_i | i = 1, \dots, k\}$ such that for $1 \leq i \leq k$ we have $\mathcal{B}_i \cap \partial D \neq \emptyset$ and

$$\bigcup_{i=1}^k \mathcal{B}_i \supset \partial D.$$

- It exists an injective function $f^i(x) = (f_1^i(x), \dots, f_d^i(x))$ with $f_j^i \in \overline{C_m}(\mathcal{B}_i)$ for $j = 1, \dots, d$ such that

$$f^i(\partial D \cap \overline{\mathcal{B}_i}) \subset \{f^i(x) = (y_1, \dots, y_d) \in \mathbb{R}^d | y_d = 0\}.$$

- The image of $D \cap \mathcal{B}_i$, which is denoted by $E_i := f^i(D \cap \mathcal{B}_i)$, is a simply connected subset (see [68]) of $\{y \in \mathbb{R}^d | y_d > 0\}$.
- There exist bounds $d_1, d_2 \in \mathbb{R}_{>0}$ such that

$$0 < d_1 < \det \begin{pmatrix} \frac{\partial f_1^{i-1}}{\partial x_1} & \cdots & \frac{\partial f_d^{i-1}}{\partial x_1} \\ \vdots & & \vdots \\ \frac{\partial f_1^{i-1}}{\partial x_d} & \cdots & \frac{\partial f_d^{i-1}}{\partial x_d} \end{pmatrix} < d_2 < \infty$$

for the determinant of the Jacobi matrix of $f^{i-1} : S_i \rightarrow D \cap \mathcal{B}_i$ (i.e. the inverse function of f^i for $i = 1, \dots, k$).

Recall that $\partial D \in \mathcal{C}^1$ implies that we have a unique normal at the boundary.

But then we are able to define the operator A_N by

$$A_N f := - \sum_{i=1}^d \frac{\partial^2 f}{2 \partial x_i^2} + V f \quad (2.2)$$

where $V \in \overline{C_2}(D)$ with the domain

$$\mathcal{D}_{A_N} := \left\{ f \in \overline{C_2}(D) \left| \frac{\partial f}{\partial \nu} \Big|_{\partial D} = 0 \right. \right\}. \quad (2.3)$$

For the main result concerning the operator A_N we make use of the *Friedrichs' extension* A_F of an operator A as defined in Appendix A.

Theorem 2.3.2. *If $V \geq 0$ the operator A_N with domain \mathcal{D}_{A_N} is symmetric on $L^2(D, \lambda^d)$ and for all $f \in L^2(D, \lambda^d)$ we have $(A_N f, f) \geq \text{const.}$ (i.e. A_N is semi-bounded). Moreover its Friedrichs' extension $(A_N)_F$ is an operator with pure point spectrum. The smallest eigenvalue is non-negative and has multiplicity one. The set of normalised eigenvectors is an ONB of $L^2(D, \lambda^d)$.*

The statement is a consequence of Theorem 29.2 and Remark 29.11 from [78]. There the functions are taken from $\overline{C_\infty}(D) \subset \overline{C_2}(D)$ but the proof holds true without modification for the set $\overline{C_2}(D)$ too.

Remark. The operator A_N is also an operator with a pure point spectrum, because the spectrum of A_N is a subset of the spectrum of its extension $(A_N)_F$.

In fact we are interested in operators of the form 2.2 where c is not necessarily positive but bounded. As D is bounded \overline{D} is compact and so

$$V_{\min} := \min_{x \in \overline{D}} V(x)$$

exists in \mathbb{R} . But then we are able to apply Theorem 2.3.2 to the operator $A_N - V_{\min}$ because $V - V_{\min} \geq 0$. From this it follows that the operator A_N with bounded V has a pure point spectrum, because we know from operator theory (see [38, 61]) that the spectrum of the operator A_N is a translation of the spectrum of $A_N - V_{\min}$.

Now if we define the operator A_D as in Equation 2.2 with an arbitrary

$V \in \overline{C_2}(D)$ and with domain

$$\mathcal{D}_{A_D} := \left\{ f \in \overline{C_2}(D) \mid f|_{\partial D} = 0 \right\}$$

we get an equivalent to Theorem 2.3.2.

Theorem 2.3.3. *The operator A_D with domain \mathcal{D}_{A_D} is symmetric on the space $L^2(D, \lambda^d)$ and there exists one $b \in \mathbb{R}$ such that $(A_D f, f) \geq b$ for all f in $L^2(D, \lambda^d)$. Moreover its Friedrichs' extension $(A_D)_F$ is an operator with pure point spectrum. The smallest eigenvalue is strictly positive and has multiplicity one. The set of normalised eigenvalues is an ONB of $L^2(D, \lambda^d)$.*

For a proof of this theorem we refer again to [78], Theorem 29.1, and Remark 29.6 also with generalisation to the space \mathcal{D}_{A_D} .

2.3.2 Bounded, convex regions

Let D denote an open, bounded, convex subset of \mathbb{R}^d . Because the boundary ∂D is possibly non-smooth we can not apply Theorem 2.3.2 in this situation. Nevertheless we will use the parts of the proof which do not make use of the smoothness of ∂D and replace those which use it. Therefore we need the statement of the well known *Gauss theorem*. It allows one to replace the volume integral of the divergence of a vector field by a surface integral and is proven under different smoothness conditions to the boundary [21, 40, 41]. For example if $D \subset \mathbb{R}^2$ (we have the application in image processing in mind) it is actually sufficient that ∂D is a rectifiable Jordan curve. A proof of this and the theory of orientation of Jordan curves given by Apostol can be found in [9]. For the treatment of a more general case we refer to [86]. There the Gauss theorem is proven for sets $\tilde{D} \subset \mathbb{R}^d$ of finite perimeter (see [86] Theorem 5.8.2). Actually every open, bounded, convex set is of finite perimeter because it is a Lipschitz domain. Moreover there is a proof of the Gauss theorem given by Hadwiger (see [30]) for bounded, convex subsets of \mathbb{R}^d . Hence we can use the Gauss theorem in our situation. But we want to keep the notation simple so we do not state the Gauss theorem in one of those general forms as mentioned above. Instead we restrict ourself to the case of regions $D \subset \mathbb{R}^d$ where the

normal to the boundary is not defined for at most a countable set of points. Because in this case one could easily give a formal definition of a measure σ defined on ∂D as in the well known case of a smooth boundary. For the definition of σ and a proof of (the following version of) the Gauss theorem we refer to [49].

Gauss Theorem 2.3.1. *Let D denote an open, bounded, convex subset of \mathbb{R}^d . Further the outer normal ν of the boundary ∂D is assumed to be σ almost everywhere defined. Then for every continuous differentiable vector field $F : \overline{D} \rightarrow \mathbb{R}^d$ where $F = (F_1, \dots, F_d)$ with $F_i \in \overline{C}_1(D)$ for $i = 1, \dots, d$ the equality*

$$\int_D \nabla(F) d\lambda = \int_{\partial D} F \cdot \nu d\sigma$$

holds true.

We note that the following method of proof carries over to arbitrary open, bounded, convex domains because Theorem 2.3.1 is valid in this case too.

As in Section 2.3.1 we are interested in the operator

$$A_N := - \sum_{i=1}^d \frac{\partial^2}{2\partial x_i^2} + V$$

(equal to the operator defined in Equation 2.2) with domain

$$\mathcal{D}_{A_N} := \left\{ f \in \overline{C}_2(D) \mid \forall x \in \partial D, \nu \in \mathcal{N}_x : \frac{\partial f}{\partial \nu} \Big|_{\partial D} = 0 \right\}.$$

In difference to the domain given in Equation 2.3 here we take the strong Neumann boundary condition because the boundary ∂D may be non-smooth.

Theorem 2.3.4. *The operator A_N is symmetric and semi-bounded in the space $L^2(D, \lambda^d)$. So the Friedrichs' extension $(A_N)_F$ of the operator A_N exists.*

Proof. First we show the symmetry. For every $f, g \in \mathcal{D}_{A_N}$ we have

$$(A_N f, g)_{L^2} = - \int_D \left\{ \sum_{i=1}^d \frac{\partial}{2\partial x_i} \left(\frac{\partial f}{\partial x_i} \right) \cdot g \right\} d\lambda + \int_D V f g d\lambda. \quad (2.4)$$

So we can apply Theorem 2.3.1 to the right side of Equation 2.4. As an auxilliary calculation we have

$$-\int_D \sum_{i=1}^d \frac{\partial}{2\partial x_i} \left(\frac{\partial f}{\partial x_i} \right) \cdot g \, d\lambda = \int_D \sum_{i=1}^d \frac{\partial f}{2\partial x_i} \cdot \frac{\partial g}{\partial x_i} \, d\lambda - \int_{\partial D} \sum_{i=1}^d \frac{\partial f}{2\partial x_i} \cdot \nu_i \cdot g \, d\sigma$$

and on the other hand

$$\begin{aligned} & -\int_D \left\{ \sum_{i=1}^d \frac{\partial}{2\partial x_i} \left(\frac{\partial g}{\partial x_i} \right) \cdot f \right\} d\lambda \\ &= \int_D \left\{ \sum_{i=1}^d \frac{\partial g}{2\partial x_i} \cdot \frac{\partial f}{\partial x_i} \right\} d\lambda - \int_{\partial D} \sum_{i=1}^d \frac{\partial g}{2\partial x_i} \cdot \nu_i \cdot f \, d\sigma. \end{aligned} \tag{2.5}$$

Because of $f \in \mathcal{D}_{A_N}$ it follows

$$\int_{\partial D} \sum_{i=1}^d \frac{\partial f}{2\partial x_i} \cdot \nu_i \cdot g \, d\sigma = \int_{\partial D} \frac{\partial f}{2\partial \nu} \cdot g \, d\sigma = 0$$

and the same is true for the last term in Equation 2.5 as $g \in \mathcal{D}_{A_N}$. Hence we have

$$(A_N f, g) = -\int_D \left\{ \sum_{i=1}^d \frac{\partial}{2\partial x_i} \left(\frac{\partial g}{\partial x_i} \right) \cdot f \right\} d\lambda + \int_D V g f \, d\lambda = (A_N g, f) = (f, A_N g).$$

Moreover from the arguments above we see that

$$(A_N f, f) = \int_D \left\{ \sum_{i=1}^d \frac{1}{2} \left(\frac{\partial f}{\partial x_i} \right)^2 \right\} d\lambda + \int_D V f^2 \, d\lambda$$

and so we deduce that the operator is semi-bounded by using

$$(A_N f, f) \geq V_{\min} \cdot \|f\|^2 + \frac{1}{2} \|\nabla f\|^2.$$

Now we have verified the conditions which guarantee the existence of the Friedrichs' extension. At least we can extend this argument because the domain of the operator is dense in $L^2(D, \lambda^d)$. That means the operator is semi-bounded in $L^2(D, \lambda^d)$. ■

One more time we consider the operator A_D defined as

$$A_D f := - \sum_{i=1}^d \frac{\partial^2 f}{2 \partial x_i^2} + V f$$

for every f in the domain $\mathcal{D}_{A_D} := \{f \in \overline{C_2(D)} \mid f|_{\partial D} = 0\}$ and get a similar statement as in Theorem 2.3.4.

Theorem 2.3.5. *The operator A_D is symmetric and semi-bounded on the space $L^2(D, \lambda^d)$. So the Friedrichs' extension $(A_D)_F$ of the operator A_D exists.*

Proof. We can use the same argument as in the proof of Theorem 2.3.4, because \mathcal{D}_{A_D} is dense in $L^2(D, \lambda^d)$. The only thing we have to note is

$$\int_{\partial D} \frac{\partial f}{2 \partial \nu} \cdot g \, d\sigma = 0$$

in this case too, because the derivative is bounded and $g|_{\partial D} = 0$. ■

In order to investigate the spectrum of the operator A_N (respectively A_D) for our purpose it will be adequate to have a closer look at the spectrum of its Friedrichs' extension. To prepare this we give the following lemmas where we refer to Appendix A for precise definitions of the involved objects.

Lemma 2.3.6. *The norms $\|\cdot\|_{W_2^1}$ and $\|\cdot\|_{A_N}$ are equivalent.*

Proof. It is sufficient to show the existence of constants $c_1, c_2 \in \mathbb{R}$ such that we have $c_1 \|f\|_{W_2^1}^2 \geq 2 \|f\|_{A_N}^2 \geq c_2 \|f\|_{W_2^1}^2$ for all $f \in \mathcal{D}_{A_N}$. Because of

$$\begin{aligned} \|f\|_{W_2^1}^2 &= \int_D \sum_{i=1}^d \frac{\partial f^2}{\partial x_i} + f^2 \, d\lambda \\ 2 \|f\|_{A_N}^2 &= \int_D \sum_{i=1}^d \frac{\partial f^2}{\partial x_i} + (2V + 2) f^2 \, d\lambda \end{aligned}$$

we can choose

$$c_1 := \max\{\max_{x \in \overline{D}} 2V(x) + 2, 1\} \quad \text{and} \quad c_2 := \min\{\min_{x \in \overline{D}} 2V(x) + 2, 1\}. \quad \blacksquare$$

Lemma 2.3.7. *The energetic space H_{A_N} of the operator A_N is a subset of the Sobolev space $W_2^1(D)$.*

Proof. The set H_{A_N} is the closure of $\mathcal{D}_{A_N} \subset \overline{C_2}(D)$ in the norm $\|\cdot\|_{A_N}$ which is equivalent to the norm $\|\cdot\|_{W_2^1}$. Then H_{A_N} is likewise the closure of \mathcal{D}_{A_N} in the norm $\|\cdot\|_{W_2^1}$. But W_2^1 is the closure of the whole space $\overline{C_2}(D)$ in that norm. So the lemma follows. ■

Theorem 2.3.8. *The Friedrichs' extension of the operator A_N (resp. A_D) is an operator with pure point spectrum.*

Proof. By the theory of distributions (see [78, 76, 1]) we know that the imbedding of $W_2^1(D)$ in $L^2(D, \lambda^d)$ is compact. Moreover from the lemma above we have $H_{A_N} \subset W_2^1(D)$ with equivalent norms, so the imbedding of H_{A_N} in $L^2(D, \lambda^d)$ is compact. This is the assumption of the *Criterion of Rellich* (see [78]) so the theorem follows for A_N . The proof of the statement for the operator A_D can be given with the same argument. A shorter version is given in [78]. ■

Remark. This shows that the operators A_N and A_D are also operators with pure point spectra, because their spectra are subsets of the spectra of their extensions.

In order to achieve the situation described in Chapter 1 now for the operator A_N where V is bounded it remains to prove that the smallest eigenvalue vanishes and has multiplicity one. To do this, we modify a proof of the *Allegretto-Piepenbrink Theorem* [3, 4, 5, 53, 58, 59], which can be found in the book of Cycon, Froese, Kirsch and Simon [14] and is given under weak regularity condition to the potential V . Roughly speaking the theorem states that eigenvalues below the spectrum have positive eigenfunctions. But the potential is defined on \mathbb{R}^d so the theorem is not usable in the case of operators with boundary condition. We do not repeat the original proof here. Nevertheless we make use of the argument given there adapted to the special form of potentials we are interested in.

Theorem 2.3.9. *Let f_∞ denote an element of $\overline{C_2}(D)$ which can be extended to a strictly positive function defined on \overline{D} such that $V := \frac{\Delta f_\infty}{2f_\infty} \in \overline{C_0}(D)$.*

Moreover let the operator

$$A_N f := - \sum_{i=1}^d \frac{\partial^2 f}{2 \partial x_i^2} + V f$$

be defined on

$$\mathcal{D}_{A_N} := \left\{ f \in \overline{C_2(D)} \mid \forall x \in \partial D, \nu \in \mathcal{N}_x : \frac{\partial f}{\partial \nu} \Big|_{\partial D} = 0 \right\}.$$

If $f \in \mathcal{D}_{A_N}$ is a positive solution (extendable to a strictly positive function on \overline{D}) of $(A_N - c)f = 0$ for some constant c then this constant is below the spectrum of A_N denoted by $\sigma(A_N)$ (i.e. $\inf \sigma(A_N) \geq c$).

We prove the theorem in several steps and start with the following preliminary lemma.

Lemma 2.3.10. *Let the operator A_N with domain \mathcal{D}_{A_N} be defined as in Theorem 2.3.9. Further let $f \in \mathcal{D}_{A_N}$ be a positive solution (extendable to a strictly positive function on \overline{D}) of $(A_N - c)f = 0$. If*

$$\int_{\partial D} \varphi f \nabla(f^{-1} \varphi) \cdot \nu \, d\sigma = 0 \tag{2.6}$$

for every $\varphi \in \mathcal{D}_{A_N}$, then

$$(\varphi, (A_N - c)\varphi) = \frac{1}{2} \|f \nabla(f^{-1} \varphi)\|^2.$$

As above, in the following the gradient of a function f will be denoted by $\nabla(f)$ with brackets to be clear which argument we take.

Proof. First we note that

$$-2(A_N - c) = \Delta - \frac{\Delta f_\infty}{f_\infty} + 2c \quad \text{with} \quad -\frac{\Delta f_\infty}{f_\infty} + 2c \in \overline{C_0(D)}.$$

We assumed f to be a strictly positive solution of $(A_N - c)f = 0$ so we write $-2(A_N - c) = \Delta - f^{-1} \Delta f$. Using the product rule for every $\varphi \in \mathcal{D}_{A_N}$ we find

$$\Delta(f f^{-1} \varphi) = \nabla(f \nabla(f^{-1} \varphi)) + f^{-1} \varphi \Delta f + \nabla(f^{-1} \varphi) \nabla(f).$$

Hence we established

$$-2(A_N - c)\varphi = f^{-1}[f\nabla(f\nabla(f^{-1}\varphi)) + \nabla(f)f\nabla(f^{-1}\varphi)]$$

and it follows

$$-2(A_N - c)\varphi = f^{-1}\nabla(f^2\nabla(f^{-1}\varphi)). \quad (2.7)$$

As we know from Theorem 2.3.1 we have

$$\int_{\partial D} \varphi f \nabla(f^{-1}\varphi) \cdot \nu \, d\sigma = \int_D \nabla(\varphi f \nabla(f^{-1}\varphi)) \, d\lambda. \quad (2.8)$$

By application of the product rule to the right side of Equation 2.8 we find

$$\int_D \nabla(f^{-1}\varphi) f^2 \nabla(f^{-1}\varphi) \, d\lambda = - \int_D \varphi f^{-1} \nabla(f^2 \nabla(f^{-1}\varphi)) \, d\lambda$$

because of Assumption 2.6. With this and Equation 2.7 we have

$$\int_D \varphi 2(A_N + c)\varphi \, d\lambda = \int_D \nabla(f^{-1}\varphi) f^2 \nabla(f^{-1}\varphi) \, d\lambda = \|f\nabla(f^{-1}\varphi)\|^2. \quad \blacksquare$$

Obviously condition 2.6 holds true if

$$\left. \frac{\nu f \nabla(\varphi)}{f^2} \right|_{\partial D} = 0 \quad \text{and} \quad \left. \frac{\nu \varphi \nabla(f)}{f^2} \right|_{\partial D} = 0, \quad (2.9)$$

because $\varphi, f \in \overline{C_2}(D)$ are extendable to \overline{D} . But the extensions are bounded on ∂D so $\varphi \cdot f$ is. Finally the conditions 2.9 are true if $f, \varphi \in D_{A_N}$ and the extension of f is strictly positive for every boundary point as we assumed.

One of the consequences of the lemma above is that $\lambda_0 = 0$ is the lowest eigenvalue of A_N . This is true because we know that the strictly positive eigenfunction $v_0 = f_\infty$ is a solution of $(A_N - c)\varphi = 0$ with $c = 0$. So from Theorem 2.3.9 follows, that c is below the spectrum. Now we show that the dimension of the eigenspace corresponding to the eigenvalue 0 is one (that is λ_0 has multiplicity one).

Theorem 2.3.11. *Let the operator A_N with domain \mathcal{D}_{A_N} be defined as in Theorem 2.3.9 with $f_\infty \in \mathcal{D}_{A_N}$. Further let φ denote an element of \mathcal{D}_{A_N} such that $A_N\varphi = 0$. Then up to a constant φ is equal to f_∞ .*

Proof. From Lemma 2.3.10 we have

$$\begin{aligned}
(\varphi, A_N \varphi) = 0 &\Rightarrow \|f_\infty \nabla(f_\infty^{-1} \varphi)\|^2 = 0 && \|\cdot\| \text{ is a norm} \\
&\Rightarrow f_\infty \nabla(f_\infty^{-1} \varphi) = 0 && f_\infty \text{ is strictly positive} \\
&\Rightarrow \nabla(f_\infty^{-1} \varphi) = 0 && [78] \text{ Remark 28.6} \\
&\Rightarrow f_\infty^{-1} \varphi = \text{const.} && \blacksquare
\end{aligned}$$

Remark. It is easy to see that the same statements are true if we replace the domain \mathcal{D}_{A_N} by $\mathcal{D}_{A_D} := \{f \in \overline{\mathcal{C}_2(D)} | f|_{\partial D} = 0\}$ and take $f_\infty \in \overline{\mathcal{C}_2(D)}$ with the same additional condition that the extension of f_∞ is strictly positive for every boundary point.

As mentioned before we are mainly interested in the operator with Neumann boundary condition and treat the Dirichlet case just by the way because of its similarity. Because of this we summarise only the results for the first one.

Theorem 2.3.12. *Let $D \subset \mathbb{R}^d$ denote an open, bounded, convex set and $\nu(x)$ the normal to the boundary ∂D of D at $x \in \partial D \setminus S$ where S is a finite set of boundary points. Further let $f_\infty \in \mathcal{D}_{A_N}$ denote a strictly positive extendable function such that $(2f_\infty)^{-1} \Delta f_\infty \in \overline{\mathcal{C}_2(D)}$. Then the operator A_N with domain \mathcal{D}_{A_N} defined in Theorem 2.3.9 is symmetric in $L^2(D, \lambda^d)$ and positive definite. The Friedrichs' extension $(A_N)_F$ is an operator with purely discrete point spectrum where the smallest eigenvalue vanishes and has multiplicity one. The corresponding eigenfunction is f_∞ .*

2.4 Itô Diffusion on bounded regions

As described in Section 1.6 and Section 1.9 under certain circumstances the solution of a given Cauchy problem on \mathbb{R}^d can be expressed in terms of functions of an Itô diffusion on \mathbb{R}^d . In Sections 2.5, 2.6 we will give an equivalent expression for Cauchy problems on bounded, convex sets $D \subset \mathbb{R}^d$. Therefore we need a formulation of Itô diffusions on D , depending on the type of boundary condition we take. First we consider Itô diffusions that stop moving

after they have reached any point of the boundary ∂D of D , which will lead to solutions of Cauchy problems with boundary condition of Dirichlet type. After that we give a short overview about Itô diffusions that are reflected at the boundary of D which will lead to solutions corresponding to boundary conditions of Neumann type.

2.4.1 Exit time

Let $\mathcal{X} = (X_t^x | t \in \mathbb{R}_{\geq 0})$ denote an Itô diffusion as defined in Section 1.5 on the filtered probability space $(\Omega, \mathcal{A}, P, (\mathcal{F}_t | t \geq 0))$. Then for every $\omega \in \Omega$ and every $x \in \mathbb{R}^d$ we have $X_t^x(\omega) \in \mathbb{R}^d$. If we choose the start value X_0^x of \mathcal{X} in D the question arises what happens when the process leaves the domain D . Because of the continuity of each path of the process this question is equivalent to the question of what happens when the process enters the boundary of D , denoted by ∂D as usual.

Definition 2.4.1. For every bounded, open set $D \subset \mathbb{R}^d$ and every $x \in \overline{D}$ the random variable

$$\tau_D^x := \inf\{t | X_t^x \in \partial D\}$$

is defined on the same filtered probability space $(\Omega, \mathcal{A}, P, (\mathcal{F}_t | t \geq 0))$ as we defined $(X_t^x | t \in \mathbb{R}_{\geq 0})$. Furthermore let $\tau_D^x = \infty$ iff $X_t^x \in D$ for all $t \in \mathbb{R}_{\geq 0}$ and naturally $\tau_D^x = 0$ iff X_0^x is an element of ∂D . Then τ_D^x is called the *exit time* of the random function X_t^x from the domain D .

Now let us denote the set of all continuous functions $f : [0, \infty) \rightarrow \mathbb{R}^d$ by $C([0, \infty), \mathbb{R}^d)$. On this space we consider the σ -algebra \mathcal{E} generated by the cylinder sets Z_t^B where we set

$$Z_t^B := \{f \in C([0, \infty), \mathbb{R}^d) | (f_{t_1}, \dots, f_{t_d}) \in B\}$$

for $t = (t_1, \dots, t_d)$ and $B \in \mathcal{B}(\mathbb{R}^d)$. Finally on this σ -algebra we define the probability measure $P_{\mathcal{X}}^x(E) := P(X^x \in E)$ for $E \in \mathcal{E}$ and $x \in \overline{D}$.

Definition 2.4.2. Once again we consider a bounded, open set $D \subset \mathbb{R}^d$. Then

the set of limit points of the trajectories $X_t^x(\omega)$ is denoted by

$$\gamma_D^x(\omega) := \{y \in D \mid y = \lim_{\substack{t \rightarrow \tau_D^x \\ 0 \leq t \leq \tau_D^x}} X_t^x(\omega)\}, \quad x \in D.$$

We say that *condition \mathfrak{A} holds* iff $P_X^x(\gamma_D^x \neq \emptyset, \gamma_D^x \subset \partial D) = 1$ for every $x \in D$.

For verifying condition \mathfrak{A} we will use the following Lemma, which is proven in a wider sense in [24] Lemma III.3.1. Therefore we recall the representation of the generator

$$Af(x) = \sum_i b_i(x) \frac{\partial f}{\partial x_i} + \frac{1}{2} \sum_{i,j} a_{i,j}(x) \frac{\partial^2 f}{\partial x_i \partial x_j}, \quad f \in \mathcal{D}_A,$$

of an Itô diffusion with drift coefficient $b = (b_1, \dots, b_d) \in \mathbb{R}^d$ and diffusion coefficient $\sigma = (\sigma_{i,j}) \in \mathbb{R}^{d \times d}$, which was given in Theorem 1.5.3 and where we have taken $a_{i,j} = (\sigma \sigma^\top)_{i,j}$.

Lemma 2.4.3. *Assume there exists at least one $i \in \{1, \dots, d\}$ and a positive constant $a \in \mathbb{R}_{\geq 0}$ and $R_1, R_2 \in \mathbb{R}$ such that*

$$D \subset \{x = (x_1, \dots, x_d) \in \mathbb{R}^d \mid R_1 \leq x_i \leq R_2\}$$

and, either $a_{i,i} \geq a > 0$ for all $x \in D$, or $b_i(x)$ preserves its sign in D (i.e. for all $x \in D$ we have $b_i(x) \geq 0$ or $b_i(x) \leq 0$) and $|b_i(x)| \geq a > 0$ for $x \in D$. Then condition \mathfrak{A} holds and the set γ_D^x consists of one point P_X^x a.s. for $x \in D$. Further $P_X^x(\tau_D^x > t)$ converges to 0 for $t \rightarrow \infty$, the convergence is uniform in $x \in D$ so it is possible to estimate $P_X^x(\tau_D^x > t)$ only depending on $t \in [0, \infty)$ and independently of x . For some positive constant $c \in \mathbb{R}_{\geq 0}$ it follows $\mathbb{E}_{P_X^x}[\tau_D^x] \leq c < \infty$.

Remark. In consequence of the last lemma it can be shown, that the process leaves the area D uniformly exponentially fast. That means

$$\lim_{t \rightarrow \infty} \frac{1}{t} \ln \gamma(t) < 0, \quad \text{where } \gamma(t) := \sup_{x \in D} P_X^x(\tau_D^x > t).$$

Remark. Lemma 2.4.3 holds also true, if there exists $T, \delta > 0$ such that $P_X(\tau_D < T) > \delta$ for all $x \in D$.

2.4.2 Reflection

In this section we give a brief construction of an Itô diffusion on a bounded, convex set $D \subset \mathbb{R}^d$ which will be reflected at the smooth boundary ∂D of D . That means for a.e. $\omega \in \Omega$ and all $t \geq 0$ and $x \in D$ we have $X_t^x(\omega) \in \overline{D}$.

Remark. The terminus *reflected* can be split into different types of behaviour of the process reaching the boundary. At least we have *instantaneous reflection* [71], *oblique reflection* [20], *sticky reflection* and *non-sticky reflection* [81, 54], but we do not go into detail here. Our topic is the instantaneous reflection.

Now after a general definition of what we understand by a reflected diffusion we start with the construction of an Itô diffusion on state space $\mathbb{R}_{\geq 0}^d$ (i.e. the set $\{x = (x_1, \dots, x_d) \in \mathbb{R}^d | x_1 \geq 0\}$) with reflection at the hyper plane $x_1 = 0$.

Definition 2.4.4. Let $D \subset \mathbb{R}^d$ denote a bounded, convex region with boundary $\partial D \in \mathcal{C}^2$ and $\nu(x) = (\nu_1(x), \dots, \nu_d(x))$ for all $x \in \partial D$ the inward normal vector to the boundary. (It is supposed that every coordinate of ν is a two times differentiable function on ∂D then.) Further $\gamma(x) = (\gamma_1(x), \dots, \gamma_d(x))$ is a vector field on ∂D of vectors directed into D where the derivatives up to order three of the functions γ_i , $i = 1, \dots, d$ are continuous and the angle between $\gamma(x)$ and the tangential plane at $x \in \partial D$ is strictly positive, $(\gamma(x), n(x)) > 0$. We consider the following stochastic differential equation

$$\begin{aligned} dX_t^x &= \sigma(X_t^x)dB_t + b(X_t^x)dt + 1_{\partial D}(X_t^x)\gamma(X_t^x)d\xi_t^x, \\ X_0^x &= x, \xi_0^x = 0, \end{aligned} \tag{2.10}$$

where $1_{\partial D}(x)$ is the characteristic function of the set ∂D . By $(B_t | t \geq 0)$ we denoted a Brownian motion adapted to the increasing family of σ -fields \mathcal{F}_t and $\sigma(x)$, $b(x)$ are Lipschitz continuous and bounded. The pair X_t^x, ξ_t^x of a.s. continuous processes adapted to \mathcal{F}_t and satisfying the Equation 2.10 is designated as a solution of 2.10 iff $X_t^x \in \overline{D}$ for every $t \geq 0$ and $(\xi_t^x | t \geq 0)$ is a non-decreasing process, which can increase only if $t \in \{s \in \mathbb{R}_+ | X_s^x \in \partial D\} =: S$ (i.e. if for all $\epsilon > 0$, sufficiently small, it is $|\xi_{t+\epsilon}^x - \xi_t^x| > 0$ then we have $t \in S$) and a.s. S has Lebesgue measure 0. Then we call $(X_t^x, t \geq 0)$ an *Itô diffusion*

in D with (instantaneous) reflection on the boundary and $(\xi_t^x | t \geq 0)$ the local time on the boundary.

Remark. With slight modifications this is nothing else than the description of Skorokhod's Problem (see Appendix B) and its solution.

Now we follow the argument of [7] in order to construct a process X_t^x on $\mathbb{R}_{\geq 0}^d$. Other constructions can be found in [71, 81]. For this we consider the function $\Gamma : C([0, \infty), \mathbb{R}^d) \rightarrow C([0, \infty), \mathbb{R}^d)$ which is defined for every element $\zeta = (\zeta_1, \dots, \zeta_d)$ in $C([0, \infty), \mathbb{R}^d)$ by $\Gamma(\zeta) = \eta$ with coordinates

$$\eta_i(t) := \begin{cases} \zeta_1(t) - \min_{0 \leq s \leq t} \{\min(\zeta_1(s), 0)\} & \text{for } i=1 \\ \zeta_i(t) & \text{for } i = 2, \dots, d. \end{cases}$$

Further by $\sigma(x)$, $b(x)$ we denote some bounded, Lipschitz continuous coefficients defined on $\mathbb{R}_{\geq 0}^d$. Then the coefficients $\sigma(\Gamma(x))$, $b(\Gamma(x))$ are defined for $x \in \mathbb{R}^d$. Moreover it follows for $i, j = 1, \dots, d$, $t \geq 0$, some constant $K < \infty$ and all $\zeta, \tilde{\zeta} \in C([0, \infty), \mathbb{R}^d)$ that

$$\begin{aligned} \sup_{0 \leq s \leq 0} |\sigma_{i,j}(\Gamma(\zeta)(s)) - \sigma_{i,j}(\Gamma(\tilde{\zeta})(s))| &\leq K \cdot \sup_{0 \leq s \leq 0} |\zeta(s) - \tilde{\zeta}(s)| \\ \sup_{0 \leq s \leq 0} |b_i(\Gamma(\zeta)(s)) - b_i(\Gamma(\tilde{\zeta})(s))| &\leq K \cdot \sup_{0 \leq s \leq 0} |\zeta(s) - \tilde{\zeta}(s)|. \end{aligned} \quad (2.11)$$

Then it can be shown similarly to the proof of Theorem 1.5.1, that the stochastic integral equation

$$Y_t^x = x + \int_0^t \sigma(\Gamma(Y_s^x)) dB_t + \int_0^t b(\Gamma(Y_s^x)) ds \quad (2.12)$$

has a unique solution $(Y_t^x | t \geq 0)$ which is a.s. continuous in the variables (t, x) and for every $t \geq 0$ measurable with respect to the filtration \mathcal{F}_t . The process Y_t^x takes values in \mathbb{R}^d .

Theorem 2.4.5. Assume Equation 2.12 for $(Y_t^x | t \geq 0)$ and Equation 2.11 for its coefficients $\sigma(x)$, $b(x)$. Further let the matrix $\sigma \sigma^\top(x)$ be non-degenerate for all $x \in \mathbb{R}_{\geq 0}^d$ and define $\xi : C([0, \infty), \mathbb{R}^d) \rightarrow C([0, \infty), \mathbb{R})$ by $\xi(\zeta) = \Gamma_1(\zeta) - \zeta_1$. Then the pair $(X_t^x := \Gamma(Y_t^x), \xi_t^x := \xi(Y_t^x))$ is a solution of Equation 2.10 with

$\overline{D} := \mathbb{R}_{\geq 0}^d$ and $\gamma(x) := (1, 0, \dots, 0)$ for $x \in \partial D$ defining the vector field on ∂D .

Remark. Let \mathcal{D}_A denote the set of all two times continuously differentiable function f defined on $\mathbb{R}_{\geq 0}^d$ with

$$\left. \frac{\partial f}{\partial x_1}(x) \right|_{x_1=0} = 0.$$

One can show, that the infinitesimal generator of the reflected diffusion process $X_t^x + \xi_t^x$ in $\mathbb{R}_{\geq 0}^d$ is given by

$$Af(x) = \sum_i b_i(x) \frac{\partial f}{\partial x_i} + \frac{1}{2} \sum_{i,j} a_{i,j}(x) \frac{\partial^2 f}{\partial x_i \partial x_j}, \quad f \in \mathcal{D}_A.$$

A proof of this statement and Theorem 2.4.5 is given in [24] so we do not repeat it here. According to Anderson and Orey [7] we proceed to construct a reflected process in an arbitrary bounded set $D \subset \mathbb{R}^d$ which has a boundary that satisfies the conditions mentioned in Definition 2.4.4 as follows.

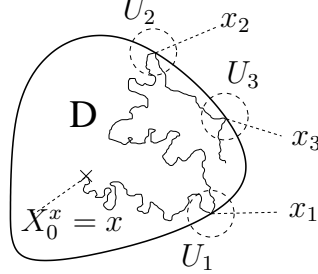


Figure 2.3. The area $D \subset \mathbb{R}^2$ is an open, convex set with smooth boundary ∂D and an approximation of the area D as shown in Figure 2.1. The process X_t^x is hitting ∂D at the points x_1, x_2, x_3 inside the neighbourhoods U_1, U_2, U_3 .

For every point $x \in \partial D$ there exists a neighbourhood $U(x)$ and a local transformation of the coordinate system, such that the vectors $\gamma(y)$ have the form $(1, 0, \dots, 0)$ for every $y \in \partial D \cap U(x)$ and the boundary ∂D is represented by $\{z = (z_1, \dots, z_d) \in \mathbb{R}^d | z_1 = 0\}$. Because $\overline{D} = D \cup \partial D$ is compact and the boundary ∂D is smooth in the sense of Definition 2.4.4 there exists $n \in \mathbb{N}$ and $x_1, \dots, x_n \in \partial D$ such that we can find neighbourhoods U_i of x_i , $i = 1, \dots, n$

covering the whole boundary. But then from Theorem 2.4.5 we are able to construct solutions of Equation 2.10 with initial condition $X_0^x = x \in U_i$ up to time $\tau_{U_i}^x$, the first exit time from U_i where we set $U_0 = D$ and for this special case denote the entry of $(X_t^x | t \geq 0)$ into one of the neighbourhoods U_i by τ_{U_0} . Now $(X_t^x | 0 \leq t \leq \tau_{U_i})$ is a process with reflection for $1 \leq i \leq n$ and without reflection for $i = 0$. Finally we repeat this construction for the new starting point $X_{\tau_{U_i}}^x$ and proceed until $\tau_{U_i} = T$. Due to smoothness of the vector fields $n(x)$, $\gamma(x)$ and the existence of a bound for the coefficients $\sigma(x)$, $b(x)$ this procedure will take just a finite number of steps with probability one. (For details see [7].) In Figure 2.3 we have shown the result of this strategy for an example sample path and three hitting points.

Remark. By the construction described above we obtain a pair of processes following Definition 2.4.4. Thus it is a Itô diffusion reflected at ∂D . The functions $X^x : [0, \infty) \times \Omega \rightarrow D$ and $\xi_t^x : [0, \infty) \times \Omega \rightarrow \mathbb{R}$ are progressively measurable and continuous with probability one. Moreover the process $(\xi_t^x | t \geq 0)$ is non-decreasing and increases only for t in the set $\{s \geq 0 | X_s^x \in \partial D\}$, which is a null-set with probability one if

$$\sum_{1 \leq i, j \leq d} (\sigma \sigma^T)_{i,j} \gamma_i(x) \gamma_j(x) > 0.$$

2.5 Feynman-Kac Formula for domains with smooth boundary

This section corresponds to Section 1.6 where we gave a solution of the Cauchy problem 1.15a, 1.15b defined in Section 1.4 for functions on \mathbb{R}^d . As before we now assume $D \subset \mathbb{R}^d$ to be open, bounded and convex and reformulate for this the statements given in the case of \mathbb{R}^d . In the next two sections we additionally assume the boundary ∂D of D to be smooth as formulated in Definition 2.4.4. We briefly discuss existing results taken from [24]. The case of non-smooth boundaries not included there will be discussed thereafter. As before we treat the Dirichlet and the Neumann case, but we do this just for smooth boundaries. Processes used to solve Dirichlet problems on non-smooth

areas just stop if they reach the boundary so there is no difference between the behaviour of the process at smooth boundaries and at non-smooth boundaries.

2.5.1 Dirichlet boundary condition

Let $(X_t^x | t \geq 0)$ denote an Itô diffusion on \overline{D} with Lipschitz continuous coefficients $\sigma(x)$, $b(x)$ and generator

$$A_D f(x) = \sum_{i=1}^d b_i(x) \frac{\partial f}{\partial x_i} + \frac{1}{2} \sum_{i,j=1}^d a_{i,j}(x) \frac{\partial^2 f}{\partial x_i \partial x_j}, \quad f \in \mathcal{D}_{A_D}, x \in D.$$

We assume $a_{i,j} := (\sigma \sigma^T)_{i,j}$ to be a non-negative definite matrix. Further $c : D \rightarrow \mathbb{R}$, $g : [0, \infty) \times D \rightarrow \mathbb{R}$ and $f : D \rightarrow \mathbb{R}$ are supposed to be bounded and continuous functions in the domains of their definition and $g(0, x) = f(x)$ for $x \in \partial D$. Then we consider the mixed Cauchy problem

$$\frac{\partial u(t, x)}{\partial t} = -A_D u(t, x) + c(x)u(t, x), \quad t > 0, x \in D, \quad (2.13a)$$

with the initial condition

$$u(0, x) = f(x) \quad (2.13b)$$

and Dirichlet boundary condition

$$u(t, x)|_{x \in \partial D} = g(t, x). \quad (2.13c)$$

Definition 2.5.1. Let $(D_n | n \in \mathbb{N})$ denote an increasing sequence of subsets of D with smooth boundaries (according to Def. 2.4.4) such that $\bigcup_{n=1}^{\infty} D_n = D$. Further suppose, that for every $n \in \mathbb{N}$ it is $\mathbb{E}[\tau_{D_n}^x] < \infty$. If $u_n(x)$ for $x \in D_n$ is a solution of the mixed Cauchy problem 2.13a, 2.13b, 2.13c and $u(t, x) := \lim_{n \rightarrow \infty} u_n(t, x)$ exists for all (t, x) , then u is called a *generalised solution in the Wiener sense*.

As usual we are interested in conditions which guaranty the existence and uniqueness of the solution. For this we define for all $x \in \mathbb{R}^d$ the distance to the boundary of D by $\text{dist}(x, \partial D) := \inf_{y \in \partial D} |x - y|$. Further we denote the set $\{\omega | \tau_D^x(\omega) = t\}$ by $A(t)$ and of course the complementary event $\{\omega | \tau_D^x(\omega) \neq t\}$

by $A(t)^c$ as the complement in Ω .

Theorem 2.5.2. *If $u(t, x)$ is a bounded, continuous solution of the mixed Cauchy problem 2.13a, 2.13b, 2.13c on $[0, T] \times (D \cup \partial D)$ where D fulfils condition \mathfrak{A} (see Definition 2.4.2) and the first-order derivative of $u(x, t)$ with respect to t and second-order derivatives with respect to x are bounded and continuous in the domain*

$$\{t | s < t < T\} \times \{x \in D | \text{dist}(x, \partial D) > s\}$$

for any $s \in (0, T)$ and $T > 0$. Then the representation

$$\begin{aligned} u(t, x) = & \mathbb{E} \left[f(X_t^x) 1_{A(t)} \exp \left(\int_0^t c(X_s^x) ds \right) \right] \\ & + \mathbb{E} \left[f(X_{\tau_D^x}^x) 1_{A(t)^c} \exp \left(\int_0^{\tau_D^x} c(X_s^x) ds \right) \right] \end{aligned} \quad (2.14)$$

is valid.

A proof of this theorem (in a more general case) can be found in [24] Chapter II Theorem 2.3. There it is supposed that $\mathbb{E}[\tau_D^x]$ is finite for all $x \in D$. We ensure this by condition \mathfrak{A} .

Remark. It can be shown, that $u(t, x)$ given in equation (2.14) is a unique solution (see [24] Theorem III.5.2) if D has a regular boundary and fulfils the condition \mathfrak{A} . The regularity of the boundary guarantees, that $u(t, x)$ is a generalised solution in the Wiener sense (see [24] Chapter III Section 3.5).

2.5.2 Neumann boundary condition

Here we will use Itô diffusions with reflection¹ in order to give solutions to Cauchy problems with Neumann boundary conditions. So we take $D \subset \mathbb{R}^d$ open, bounded, convex with a sufficiently smooth boundary ∂D and denote by $\gamma(x)$ a vector field on ∂D with components $\gamma_i(x)$. Further we denote by $(X_t^x | t \geq 0)$ an Itô diffusion on \overline{D} with reflection at ∂D in direction γ whose

¹See Definition 2.4.4. The conditions on the boundary and the vector field γ are specified there too.

generator on D is given by

$$A_N f(x) = \sum_{i=1}^d b_i(x) \frac{\partial f}{\partial x_i} + \frac{1}{2} \sum_{i,j=1}^d a_{i,j}(x) \frac{\partial^2 f}{\partial x_i \partial x_j}, \quad f \in \mathcal{D}_{A_N}$$

and which is an non-degenerate operator such that for all $x \in \partial D$ we have $\sum_{i,j=1}^d a_{i,j}(x) \gamma_i(x) \gamma_j(x) > a > 0$. We consider the mixed Cauchy problem

$$\frac{\partial u(t, x)}{\partial t} = A_N u(t, x) + c(x) u(t, x), \quad t > 0, x \in D, \quad (2.15a)$$

with the initial condition

$$u(0, x) = f(x) \quad (2.15b)$$

and Neumann boundary condition

$$(\nabla u(t, x), \gamma(x))|_{x \in \partial D} = h(x), \quad (2.15c)$$

with continuous, bounded functions $c : D \rightarrow \mathbb{R}^d$, $f : D \rightarrow \mathbb{R}^d$, $h : \partial D \rightarrow \mathbb{R}$. Then we have the following existence result (see [24] Theorem III.5.1).

Theorem 2.5.3. *If $u : [0, T] \times D \cup \partial D \rightarrow \mathbb{R}^d$ is a solution of the mixed Cauchy problem with Neumann boundary condition 2.15a, 2.15b, 2.15c and the derivatives $\frac{\partial u}{\partial t}(t, x)$, $\frac{\partial u}{\partial x_i}(t, x)$, $\frac{\partial^2 u}{\partial x_i \partial x_j}(t, x)$ for $i, j = 1, \dots, d$ are continuous and bounded on the domain of definition, then the representation*

$$\begin{aligned} u(t, x) = & \mathbb{E} \left[f(X_t^x) \exp \left(\int_0^t c(X_s^x) ds \right) \right] \\ & + \mathbb{E} \left[\int_0^t h(X_s^x) \exp \left(\int_0^s c(X_r^x) dr \right) d\xi_s^x \right] \end{aligned} \quad (2.16)$$

is valid.

We remind, that the process $(\xi_t^x | t \geq 0)$ was defined in 2.4.4 as the local time on the boundary.

Remark. The solution $u(t, x)$ given in the theorem above may be understood as a generalised solution in the Wiener sense (see [24] Remark III.5.1).

2.6 Solutions on bounded convex domains

In Section 2.4.2 we saw how to construct Itô diffusions on regions with smooth boundary and additionally got constructions on regions which could be approximated through series of those. Now we do not discuss these approximations. Instead we choose the approach introduced by [71] (see Appendix B) to questions of reflected processes. We do this because it is also valid in the case of arbitrary (unbounded) convex domains as it was shown in [77]. So we are interested in statements corresponding to those in Section 2.5.2.

In the following let $X_t = (X_t^1, \dots, X_t^d)$ denote an Itô diffusion on \mathbb{R}^d as before with

$$dX_t = b(X_t)dt + \sigma(X_t)dB_t.$$

Further we consider a continuous process $(\varphi_t | t \geq 0)$ with $\varphi_t = (\varphi_t^1, \dots, \varphi_t^d)$ of bounded variation (that means for every $\omega \in \Omega$ the function $\varphi_\cdot(\omega) : [0, T) \rightarrow \mathbb{R}^d$ is continuous and of bounded variation). Then we define $\hat{X}_t = X_t + \varphi_t$ and assume for all $t \geq 0$ that $\hat{X}_t = (\hat{X}_t^1, \dots, \hat{X}_t^d) \in \overline{D}$, where $D \subset \mathbb{R}^d$ is open, bounded and convex. We will provide an Itô formula for the process \hat{X}_t similar to the formulas given in [42, 27]. In fact the authors of [42, 27] formulated their statements for locally square integrable martingales and used integration by the variation of those martingales. So the proofs in [42, 27] are written in this context. Here we are in a special case of this so we reformulate the proofs and simplify them if possible due to absence of generality. Then we will use this Itô formula to derive a Feynman-Kac formula and finally investigate the generator of \hat{X}_t on \overline{D} .

Definition. Let $\alpha, \alpha_0, \alpha_1, \dots, \alpha_{n-1}$ denote n random variables defined on the probability space (Ω, \mathcal{A}, P) with filtration $(\mathcal{F}_t | t \geq 0)$, where α is \mathcal{F}_0 -measurable and α_i is \mathcal{F}_{t_i} -measurable for $i = 0, 1, \dots, n-1$ and a subdivision of the interval $[0, T]$. Then we call

$$\alpha(\omega)1_{\{0\}}(t) + \sum_{i=0}^{n-1} \alpha_i(\omega)1_{(t_i, t_{i+1}]}(t), \quad t \in [0, T]$$

a simple function.

Theorem 2.6.1. *Let f be an element of $\overline{C}_2(D)$ and \hat{X}_t be defined as above then we have*

$$\begin{aligned} f(\hat{X}_t) - f(\hat{X}_0) &= \sum_{i=1}^d \int_0^t \frac{\partial f}{\partial x_i}(\hat{X}_s) dX_s^i \\ &\quad + \sum_{i=1}^d \int_0^t \frac{\partial f}{\partial x_i}(\hat{X}_s) d\varphi_s^i \\ &\quad + \frac{1}{2} \sum_{i,j=1}^d \int_0^t \frac{\partial^2 f}{\partial x_i \partial x_j}(\hat{X}_s) (\sigma(\hat{X}_s) \sigma(\hat{X}_s)^\top)_{i,j} ds \end{aligned}$$

for every $t \geq 0$.

Proof. The proof will be given in two steps. According to the argument given in [48] part I, first we assume that the diffusion coefficient $\sigma(t, \omega) := \sigma(X_t(\omega))$ and the drift coefficient $b(t, \omega) := b(X_t(\omega))$ of the Itô diffusion are simple functions. In the second step we approximate the given coefficients by a sequence of simple functions.

For all $0 = t_0 \leq t_1 \leq \dots \leq t_N = t$ we have

$$f(\hat{X}_t) - f(\hat{X}_0) = \sum_{n=1}^N f(\hat{X}_{t_n}) - f(\hat{X}_{t_{n-1}})$$

and for $1 \leq i, j \leq d$ we have

$$\begin{aligned} \int_0^t \frac{\partial f}{\partial x_i}(\hat{X}_s) dX_s^i &= \sum_{n=1}^N \int_{t_{n-1}}^{t_n} \frac{\partial f}{\partial x_i}(\hat{X}_s) dX_s^i, \\ \int_0^t \frac{\partial^2 f}{\partial x_i \partial x_j}(\hat{X}_s) (\sigma \sigma^\top)_{i,j} ds &= \sum_{n=1}^N \int_{t_{n-1}}^{t_n} \frac{\partial^2 f}{\partial x_i \partial x_j}(\hat{X}_s) (\sigma \sigma^\top)_{i,j} ds, \\ \int_0^t \frac{\partial f}{\partial x_i}(\hat{X}_s) d\varphi_s^i &= \sum_{n=1}^N \int_{t_{n-1}}^{t_n} \frac{\partial f}{\partial x_i}(\hat{X}_s) d\varphi_s^i. \end{aligned}$$

So in the first step of the proof it is sufficient that we restrict ourself to constant diffusion $\hat{\sigma}$ and constant drift \hat{b} . Now we choose $0 \leq s \leq t \leq T$. Then for every $k \in \mathbb{N}$ we consider a set of times $\{t_0^k, \dots, t_{N_k}^k\}$ with $t_0^k = 0$ and $t_{N_k}^k = t$ such that for every $1 \leq n \leq N_k$ we have $|t_n^k - t_{n-1}^k| \leq \frac{1}{2^k}$. Using this sequence

for $k \in \mathbb{N}$ we write

$$f(\hat{X}_t) - f(\hat{X}_s) = \sum_{n=1}^{N_k} (f(\hat{X}_{t_n^k}) - f(\hat{X}_{t_{n-1}^k})).$$

Then as consequence of Taylor's formula (see [23]) for every $1 \leq n \leq N_k$ there exists $\xi_{n-1}^k \in [\min(\hat{X}_{t_{n-1}^k}, \hat{X}_{t_n^k}), \max(\hat{X}_{t_{n-1}^k}, \hat{X}_{t_n^k})]$ such that

$$\begin{aligned} f(\hat{X}_t) - f(\hat{X}_s) &= \sum_{n=1}^{N_k} \left(\sum_{i=1}^d \frac{\partial f}{\partial x_i}(\hat{X}_{t_{n-1}^k})(\hat{X}_{t_n^k}^i - \hat{X}_{t_{n-1}^k}^i) \right) \\ &\quad + \sum_{n=1}^{N_k} \left(\frac{1}{2} \sum_{i,j=1}^d \frac{\partial^2 f}{\partial x_i \partial x_j}(\xi_{n-1}^k)(\hat{X}_{t_n^k}^i - \hat{X}_{t_{n-1}^k}^i)(\hat{X}_{t_n^k}^j - \hat{X}_{t_{n-1}^k}^j) \right). \end{aligned} \quad (2.17)$$

Moreover we note

$$\frac{\partial f}{\partial x_i}(\hat{X}_{t_{n-1}^k})(\hat{X}_{t_n^k}^i - \hat{X}_{t_{n-1}^k}^i) = \frac{\partial f}{\partial x_i}(\hat{X}_{t_{n-1}^k})((X_{t_n^k}^i - X_{t_{n-1}^k}^i) + (\varphi_{t_n^k}^i - \varphi_{t_{n-1}^k}^i))$$

because of $\hat{X}_t = X_t + \varphi_t$. But then from the definition of stochastic integrals (see [18, 55]) we can derive the stochastic convergence

$$\sum_{n=1}^{N_k} \left(\sum_{i=1}^d \frac{\partial f}{\partial x_i}(\hat{X}_{t_{n-1}^k})(X_{t_n^k}^i - X_{t_{n-1}^k}^i) \right) \xrightarrow{k \rightarrow \infty} \sum_{i=1}^d \int_s^t \frac{\partial f}{\partial x_i}(\hat{X}_s) dX_s^i$$

and by definition of Stieltjes integrals (see [29, 79]) we have

$$\sum_{n=1}^{N_k} \left(\sum_{i=1}^d \frac{\partial f}{\partial x_i}(\hat{X}_{t_{n-1}^k})(\varphi_{t_n^k}^i - \varphi_{t_{n-1}^k}^i) \right) \xrightarrow{k \rightarrow \infty} \sum_{i=1}^d \int_s^t \frac{\partial f}{\partial x_i}(\hat{X}_s) d\varphi_s^i.$$

With the second term in Equation 2.17 we proceed in the same manner and get

$$\sum_{n=1}^{N_k} \left(\sum_{i,j=1}^d \frac{\partial^2 f}{\partial x_i \partial x_j}(\xi_{n-1}^k)(\hat{X}_{t_n^k}^i - \hat{X}_{t_{n-1}^k}^i)(\hat{X}_{t_n^k}^j - \hat{X}_{t_{n-1}^k}^j) \right) = T_1 + T_2 + T_3$$

where

$$\begin{aligned} T_1 &= \sum_{n=1}^{N_k} \left(\sum_{i,j=1}^d \frac{\partial^2 f}{\partial x_i \partial x_j}(\xi_{n-1}^k) (X_{t_n^k}^i - X_{t_{n-1}^k}^i) (X_{t_n^k}^j - X_{t_{n-1}^k}^j) \right), \\ T_2 &= 2 \sum_{n=1}^{N_k} \left(\sum_{i,j=1}^d \frac{\partial^2 f}{\partial x_i \partial x_j}(\xi_{n-1}^k) (X_{t_n^k}^i - X_{t_{n-1}^k}^i) (\varphi_{t_n^k}^j - \varphi_{t_{n-1}^k}^j) \right), \\ T_3 &= \sum_{n=1}^{N_k} \left(\sum_{i,j=1}^d \frac{\partial^2 f}{\partial x_i \partial x_j}(\xi_{n-1}^k) (\varphi_{t_n^k}^i - \varphi_{t_{n-1}^k}^i) (\varphi_{t_n^k}^j - \varphi_{t_{n-1}^k}^j) \right). \end{aligned}$$

For $k \rightarrow \infty$ the term T_2 converges to 0 almost sure because

$$|T_2| \leq 2 \sum_{i,j=1}^d \left(\max_{0 \leq n \leq N_k} |X_{t_n^k}^i - X_{t_{n-1}^k}^i| \max_{x \in \overline{D}} \left| \frac{\partial^2 f}{\partial x_i \partial x_j}(x) \right| \sum_{n=1}^{N_k} |\varphi_{t_n^k}^j - \varphi_{t_{n-1}^k}^j| \right)$$

and $\sum_{n=1}^{N_k} |\varphi_{t_n^k}^j - \varphi_{t_{n-1}^k}^j|$ is smaller than the variation of φ_t which is finite. The maximum over the increments $|X_{t_n^k}^i - X_{t_{n-1}^k}^i|$ converges a.s. to 0 because the sample paths of X_t are a.s. continuous in t . The same is true for the process φ_t and so the same argument holds for T_3 because $\max_{1 \leq n \leq N_k} |\varphi_{t_n^k}^j - \varphi_{t_{n-1}^k}^j|$ converges to 0 for $k \rightarrow \infty$ too.

Once more we expand the remaining term. If we denote the i -th coordinate of the drift vector by \hat{b}_i and i, j -th entry of the diffusion matrix by $\hat{\sigma}_{i,j}$ we note

$$(X_{t_n^k}^i - X_{t_{n-1}^k}^i) = \hat{b}_i(t_n^k - t_{n-1}^k) + \sum_{l=1}^m \hat{\sigma}_{i,l}(B_{t_n^k}^l - B_{t_{n-1}^k}^l).$$

Hence for $1 \leq i, j \leq d$ and $1 \leq n \leq N_k$ we get

$$\begin{aligned} & \frac{\partial^2 f}{\partial x_i \partial x_j}(\xi_{n-1}^k) (X_{t_n^k}^i - X_{t_{n-1}^k}^i) (X_{t_n^k}^j - X_{t_{n-1}^k}^j) \\ &= \frac{\partial^2 f}{\partial x_i \partial x_j}(\xi_{n-1}^k) \sum_{l_1=1}^m \hat{\sigma}_{i,l_1} (B_{t_n^k}^{l_1} - B_{t_{n-1}^k}^{l_1}) \sum_{l_2=1}^m \hat{\sigma}_{j,l_2} (B_{t_n^k}^{l_2} - B_{t_{n-1}^k}^{l_2}) \\ & \quad + 2 \frac{\partial^2 f}{\partial x_i \partial x_j}(\xi_{n-1}^k) \sum_{l=1}^m \hat{\sigma}_{i,l} (B_{t_n^k}^l - B_{t_{n-1}^k}^l) \hat{b}_i(t_n^k - t_{n-1}^k) \\ & \quad + \frac{\partial^2 f}{\partial x_i \partial x_j}(\xi_{n-1}^k) \hat{b}_i \hat{b}_j (t_n^k - t_{n-1}^k)^2. \end{aligned}$$

Moreover for $1 \leq l \leq m$ we have

$$\left| \frac{\partial^2 f}{\partial x_i \partial x_j}(\xi_{n-1}^k) \hat{\sigma}_{i,l}(B_{t_n^k}^l - B_{t_{n-1}^k}^l) \right| \leq \max_{x \in \overline{D}} \left| \frac{\partial^2 f}{\partial x_i \partial x_j}(x) \hat{\sigma}_{i,l} \right| \max_{1 \leq n \leq N_k} |B_{t_n^k}^l - B_{t_{n-1}^k}^l|$$

where the second maximum converges a.s. to 0 for $k \rightarrow \infty$. Furthermore the inequality

$$\left| \frac{\partial^2 f}{\partial x_i \partial x_j}(\xi_{n-1}^k) \hat{b}_i(t_n^k - t_{n-1}^k) \right| \leq \max_{x \in \overline{D}} \left| \frac{\partial^2 f}{\partial x_i \partial x_j}(x) \hat{b}_i \right| \frac{1}{2^k}$$

shows that again in the limit $k \rightarrow \infty$ there is just one term

$$\frac{\partial^2 f}{\partial x_i \partial x_j}(\xi_{n-1}^k) \sum_{l_1, l_2=1}^m \hat{\sigma}_{i,l_1}(B_{t_n^k}^{l_1} - B_{t_{n-1}^k}^{l_1}) \hat{\sigma}_{j,l_2}(B_{t_n^k}^{l_2} - B_{t_{n-1}^k}^{l_2})$$

not vanishing. From [29] Example 4.26 we know that we have

$$\sum_{n=1}^{N_k} \frac{\partial^2 f}{\partial x_i \partial x_j}(\hat{X}_{n-1}^k) \sum_{l=1}^m \hat{\sigma}_{i,l} \hat{\sigma}_{j,l} (B_{t_n^k}^l - B_{t_{n-1}^k}^l)^2 \xrightarrow{k \rightarrow \infty} \int_s^t \frac{\partial^2 f}{\partial x_i \partial x_j}(\hat{X}_s) (\hat{\sigma} \hat{\sigma}^\top)_{i,j} ds,$$

$$\text{and } \sum_{n=1}^{N_k} \frac{\partial^2 f}{\partial x_i \partial x_j}(\xi_{n-1}^k) \sum_{\substack{l_1, l_2=1 \\ l_1 \neq l_2}}^m \hat{\sigma}_{i,l_1}(B_{t_n^k}^{l_1} - B_{t_{n-1}^k}^{l_1}) \hat{\sigma}_{j,l_2}(B_{t_n^k}^{l_2} - B_{t_{n-1}^k}^{l_2}) \xrightarrow{k \rightarrow \infty} 0$$

almost surely. So the theorem is proven for step functions $\hat{b}(x)$, $\hat{\sigma}(x)$ if we can show that

$$\sum_{n=1}^{N_k} \sum_{l=1}^m \left| \hat{\sigma}_{i,l} \hat{\sigma}_{j,l} \frac{\partial^2 f}{\partial x_i \partial x_j}(\hat{X}_{n-1}^k) - \hat{\sigma}_{i,l} \hat{\sigma}_{j,l} \frac{\partial^2 f}{\partial x_i \partial x_j}(\xi_{n-1}^k) \right| (B_{t_n^k}^l - B_{t_{n-1}^k}^l)^2$$

converges almost everywhere to 0. For this (and the remaining part of the proof) we apply the argument given in [18] to our case. We choose $N \in \mathcal{A}$ with $P(N) = 0$ such that $\sum_{n=1}^{N_k} (B_{t_n^k}^l(\omega) - B_{t_{n-1}^k}^l(\omega))^2$ converges to $t - s$ for all $\omega \in N^C$ and remark that

$$\left| \hat{\sigma}_{i,l} \hat{\sigma}_{j,l}(\hat{X}_{n-1}^k) \frac{\partial^2 f}{\partial x_i \partial x_j}(\hat{X}_{n-1}^k) - \hat{\sigma}_{i,l} \hat{\sigma}_{j,l}(\xi_{n-1}^k) \frac{\partial^2 f}{\partial x_i \partial x_j}(\xi_{n-1}^k) \right|$$

converges a.s., uniformly in k to 0.

Now we will finish the proof by approximation of continuous $b(x)$ and $\sigma(x)$ through sequences of step functions $(b_n(x)|n \in \mathbb{N})$ and $(\sigma_n(x)|n \in \mathbb{N})$. We define

$$X_{t,n} := X_0 + \int_0^t b_n(X_{s,n}) ds + \int_0^t \sigma_n(X_{s,n}) dB_s$$

as a.s., uniformly convergent approximation of X_t (using the uniqueness of the limit of $X_{t,n}$ for $n \rightarrow \infty$ as strong solution [48] I 4.4) and denote the components of $X_{t,n}$ by $X_{t,n}^i$. Moreover from [77] lemma 2.2 (or [8] lemma 3) we know that the corresponding sequence $(\varphi_{t,n}|t \geq 0)$ converges uniformly a.s. to φ_t (for the case of non-smooth boundary see appendix of [73]). Here $\varphi_{t,n}$ is a stochastic process of bounded variation such that for all $t \geq 0$ we have $\hat{X}_{t,n} := X_{t,n} + \varphi_{t,n} \in \overline{D}$. It follows from step one

$$\begin{aligned} f(\hat{X}_{t,n}) - f(\hat{X}_{0,n}) = & \sum_{i=1}^d \int_0^t \frac{\partial f}{\partial x_i}(\hat{X}_{s,n}) b_n^i(\hat{X}_{s,n}) ds + \sum_{i=1}^d \sum_{j=1}^m \int_0^t \frac{\partial f}{\partial x_i}(\hat{X}_{s,n}) \sigma_n(\hat{X}_{s,n})_{i,j} dB_s^j \\ & + \frac{1}{2} \sum_{i,j=1}^d \int_0^t \frac{\partial^2 f}{\partial x_i \partial x_j}(\hat{X}_{s,n}) (\sigma(\hat{X}_{s,n}) \sigma(\hat{X}_{s,n})^\top)_{i,j} ds + \sum_{i=1}^d \int_0^t \frac{\partial f}{\partial x_i}(\hat{X}_{s,n}) d\varphi_{s,n}^i \end{aligned}$$

and we know $f(\hat{X}_{t,n}) - f(\hat{X}_{0,n})$ converges (uniformly) a.s. to $f(\hat{X}_t) - f(\hat{X}_0)$. Furthermore following the argument of [18] given in the proof of theorem 5.9 we know that

$$\int_0^t \frac{\partial f}{\partial x_i}(\hat{X}_{s,n}) b_n^i(\hat{X}_{s,n}) ds \xrightarrow{a.s.} \int_0^t \frac{\partial f}{\partial x_i}(\hat{X}_s) b_n^i(\hat{X}_s) ds$$

and

$$\int_0^t \frac{\partial^2 f}{\partial x_i \partial x_j}(\hat{X}_{s,n}) (\sigma \sigma^\top(\hat{X}_{s,n}))_{i,j} ds \xrightarrow{a.s.} \int_0^t \frac{\partial^2 f}{\partial x_i \partial x_j}(\hat{X}_s) (\sigma \sigma^\top(\hat{X}_s))_{i,j} ds$$

for every $1 \leq i, j \leq d$. So finishing the proof we remark the convergence

$$\int_0^t \frac{\partial f}{\partial x_i}(\hat{X}_{s,n}) d\varphi_{s,n}^i \xrightarrow{a.s.} \int_0^t \frac{\partial f}{\partial x_i}(\hat{X}_s) d\varphi_s^i$$

which holds true because of the inequality

$$\begin{aligned} \left| \int_0^t \frac{\partial f}{\partial x_i}(\hat{X}_{s,n}) d\varphi_{s,n}^i - \int_0^t \frac{\partial f}{\partial x_i}(\hat{X}_s) d\varphi_s^i \right| \\ \leq \left| \int_0^t \frac{\partial f}{\partial x_i}(\hat{X}_s) d\varphi_{s,n}^i - \int_0^t \frac{\partial f}{\partial x_i}(\hat{X}_s) d\varphi_s^i \right| \\ + \left| \int_0^t \frac{\partial f}{\partial x_i}(\hat{X}_{s,n}) d\varphi_{s,n}^i - \int_0^t \frac{\partial f}{\partial x_i}(\hat{X}_s) d\varphi_{s,n}^i \right| \end{aligned}$$

and the fact that both terms at the right side converge a.s. to 0. \blacksquare

This formula enables us to give the following statement about the generator (cp. Definition 1.5.2) of the reflected process \hat{X}_t . As mentioned before here we use the formalism for reflected processes introduced by Skorokhod (see [71]).

Theorem 2.6.2. *Let $(X_t|t \geq 0)$ denote an Itô diffusion on \mathbb{R}^d satisfying*

$$dX_t = b(X_t)dt + \sigma(X_t)dB_t, \quad t > 0,$$

where σ, b obey the Lipschitz condition (see Theorem 1.5.1). Further suppose $(\varphi_t|t \geq 0)$ is a process of bounded variation growing only if $X_t \in \partial D$ with $\varphi_0 = 0$ such that (X_t, φ_t) is a solution of the Skorokhod problem associated to (X_t, \overline{D}) . If $\hat{X}_t^x := X_t + \varphi_t$ then the (infinitesimal) generator of the process $(\hat{X}_t|t \geq 0)$ is an extension of the operator

$$A_N f := \sum_{i=1}^d b_i \frac{\partial f}{\partial x_i} + \frac{1}{2} \sum_{i,j=1}^d (\sigma \sigma^\top)_{i,j} \frac{\partial^2 f}{\partial x_i \partial x_j}$$

with domain

$$\mathcal{D}_{A_N} := \left\{ f \in \overline{C}_2(D) \left| \forall x \in \partial D : \forall n \in \mathcal{N}_x : \frac{\partial f}{\partial n}(x) = 0 \right. \right\}$$

where \mathcal{N}_x is the set of all normal vectors at the point $x \in \partial D$ (see Section 2.2).

Proof. First we note that

$$\mathbb{E} \left[\int_0^t \frac{\partial f}{\partial x_i}(\hat{X}_s) \sigma_n(\hat{X}_s)_{i,j} dB_s^j \right] = 0$$

but then from Theorem 2.6.1 we know that for every $f \in \mathcal{D}_{A_N}$ we have

$$\frac{\mathbb{E}[f(\hat{X}_t^x) - f(x)]}{t} = \frac{1}{t} \mathbb{E} \left[\int_0^t A_N f(\hat{X}_s) ds + \sum_{i=1}^d \int_0^t \frac{\partial f}{\partial x_i}(\hat{X}_s) d\varphi_s^i \right].$$

From Appendix B we know that φ_t grows only for $t \in \{s \geq 0 | \hat{X}_s \in \partial D\}$ and the direction of the growths is an element of $\mathcal{N}_{\hat{X}_t}$ (see Equation B.4). This shows that the second term is equal to 0. So we deduce

$$\lim_{t \searrow 0} \frac{\mathbb{E}[f(\hat{X}_t^x) - f(x)]}{t} = A_N f(x)$$

because of the continuity of the derivatives of f and we get the statement of the theorem. \blacksquare

In order to give a representation of solutions of the Cauchy problem as defined in Section 2.5.2 we reformulate Theorem 2.6.1 for functions which are additionally continuously differentiable in t for $t \in [0, \infty)$.

Proposition 2.6.3. *Let $f : [0, \infty) \times D \rightarrow \mathbb{R}$ be continuously differentiable with respect to t and $f(t, \cdot) \in \overline{C_2}(D)$. For \hat{X}_t defined as above the equation*

$$\begin{aligned} f(t, \hat{X}_t) - f(0, \hat{X}_0) &= \int_0^t \frac{\partial f}{\partial t}(s, \hat{X}_s) ds \\ &+ \sum_{i=1}^d \int_0^t \frac{\partial f}{\partial x_i}(s, \hat{X}_s) dX_s^i \\ &+ \frac{1}{2} \sum_{i,j=1}^d \int_0^t \frac{\partial^2 f}{\partial x_i \partial x_j}(s, \hat{X}_s) (\sigma(\hat{X}_s) \sigma(\hat{X}_s)^\top)_{i,j} ds \\ &+ \sum_{i=1}^d \int_0^t \frac{\partial f}{\partial x_i}(s, \hat{X}_s) d\varphi_s^i \end{aligned} \tag{2.18}$$

holds for every $t \geq 0$.

Proof. Consider an $d + 1$ -dimensional process $Y_t := (\hat{X}_t, t)$ and use Theorem 2.6.1. \blacksquare

Now it is easy to see that we have a very similar situation as in the case of an area D with smooth boundary. Of course we do not define a vector field

at ∂D . Nevertheless we would like to compare the following theorem with Theorem 2.5.3 if we suggest a zero vector field $\gamma \equiv 0$. But then differentiation in the direction of γ does not make sense. This makes clear why we are in a different situation. However the resulting statement is very similar again.

As before we consider an Itô diffusion $(X_t | t \geq 0)$ on \mathbb{R}^d as continuous solution of the stochastic differential equation

$$\begin{aligned} dX_t &= b(X_t)dt + \sigma(X_t)dB_t \\ X_0 &= x \in \mathbb{R}^d \end{aligned}$$

where $\sigma, b \in \overline{C}_2(D)$ fulfil the Lipschitz condition. Further let $D \subset \mathbb{R}^d$ be a bounded convex open set and $(\varphi_t | t \geq 0)$ a process of bounded variation such that $\hat{X}_t^x := X_t + \varphi_t$ solves the Skorokhod problem corresponding to (X_t, D) . Then for every boundary point $x \in \partial D$ the set of normal vectors (see Section 2.2) is denoted by \mathcal{N}_x and for every $u \in \mathcal{D}_A$ where

$$\mathcal{D}_A := \{f \in \overline{C}_2(D) | \forall x \in \partial D : \forall \nu \in \mathcal{N}_x : \frac{\partial f}{\partial \nu}(x) = 0\}$$

we define the operator

$$Au := \sum_{i=1}^d b_i \frac{\partial u}{\partial x_i} - \frac{1}{2} \sum_{i,j=1}^d (\sigma \sigma^\top)_{i,j} \frac{\partial^2 u}{\partial x_i \partial x_j}.$$

Theorem 2.6.4. *Let $u : [0, \infty) \times D \rightarrow \mathbb{R}$ be continuous differentiable with respect to the first variable and $u(t, \cdot) \in \overline{C}_2(D)$. If u is a solution of the Cauchy problem*

$$\begin{aligned} \frac{\partial u}{\partial t}(t, x) &= -Au(t, x) & t > 0, x \in D \\ u(0, x) &= f_0(x) & x \in D, f_0 \in \overline{C}_2(D) \end{aligned}$$

with Neumann boundary condition then $u(t, x) = \mathbb{E}[f_0(\hat{X}_t^x)]$ for all $x \in D$.

Proof. We apply formula 2.18 to the function $f(s, x) := u(t - s, x)$ and obtain

$$\begin{aligned} u(0, \hat{X}_t^x) - u(t, x) &= \int_0^t \left[\frac{\partial u}{\partial t} + Af \right](t - s, \hat{X}_s^x) ds \\ &\quad + \sum_{i=1}^d \int_0^t \frac{\partial u}{\partial x_i}(t - s, \hat{X}_s^x) dB_s^i \\ &\quad + \sum_{i=1}^d \int_0^t \frac{\partial u}{\partial x_i}(t - s, \hat{X}_s^x) d\varphi_s^i \end{aligned} \quad (2.19)$$

which implies that $\mathbb{E}[u(0, \hat{X}_t^x) - u(t, x)] = 0$ because the expectation of the second term of Equation 2.19 is equal to 0 and the first term vanishes because u is solution of the Cauchy problem and so

$$\frac{\partial u}{\partial t}(t - s, x) = -Au(t - s, x).$$

Finally the paths of \hat{X}_t^x are continuous and $\hat{X}_0^x \in D$. So there exists an $\epsilon > 0$ (depending on ω) such that for all $t \in [0, \epsilon]$ we have $\hat{X}_t^x \in D$. But this implies

$$\int_0^t \frac{\partial u}{\partial x_i}(t - s, \hat{X}_s^x) d\varphi_s^i = 0$$

because φ_t grows only for such $t \geq 0$ with $\hat{X}_t^x \in \partial D$. ■

2.7 Reproducing property in $L^2(D, \lambda^d)$

In Theorem 1.3.1 we have shown that for every $f \in L^2(\mathbb{R}^d, \lambda^d)$ the function $T_t f := \exp(-tH)f$ with $H := -\frac{1}{2}\Delta + \frac{\Delta f_\infty}{2f_\infty}$ converges for $t \rightarrow \infty$ to $(f, f_\infty)f_\infty$ in the L^2 -norm. As a consequence of Theorem 2.3.12 we have the same result in the space $L^2(D, \lambda^d)$. For this let f_∞ denote an element of $\overline{C_2}(D)$ which can be extended to a strictly positive function defined on \overline{D} such that $V := \frac{\Delta f_\infty}{2f_\infty}$ is in $\overline{C_0}(D)$. As in Theorem 2.3.9 we consider the operator

$$A_N f := - \sum_{i=1}^d \frac{\partial^2 f}{2\partial x_i^2} + V f \quad (2.20a)$$

defined for f in

$$\mathcal{D}_{A_N} := \left\{ f \in \overline{C_2}(D) \mid \forall x \in \partial D, \nu \in \mathcal{N}_x : \frac{\partial f}{\partial \nu} \Big|_{\partial D} = 0 \right\} \quad (2.20b)$$

where \mathcal{N}_x is the set of normal vectors at $x \in \partial D$ (see Eqn. 2.1). The Friedrichs' extension $(A_N)_F$ of A_N is an operator with purely discrete point spectrum and its domain H_{A_N} (the energetic space of A_N , cp. Definition A.4) is a dense subset of the Sobolev space W_2^1 which in turn is dense in $L^2(D, \lambda^d)$. Moreover the eigenfunctions $(v_k | k \in \mathbb{N}_0)$ of $(A_N)_F$ form an orthogonal basis of the Hilbert space $(H_{A_N}, (\cdot, \cdot)_{A_N})$. We denote the eigenvalues of $(A_N)_F$ by $(\lambda_k | k \in \mathbb{N}_0)$ and assume $(A_N)_F v_k = \lambda_k v_k$. So for every $f = \sum_{k \in \mathbb{N}_0} \alpha_k v_k$ in H_{A_N} we have the representation

$$\begin{aligned} T_t f &= \exp(-tA_N) f \\ &= \sum_{k \in \mathbb{N}_0} \exp(-t\lambda_k) \alpha_k v_k \end{aligned} \quad (2.21)$$

equivalent to Equation 1.8. From this we are enabled to follow the argument given in Section 1.3. Hence $T_t f$ converges for $t \rightarrow \infty$ to $\alpha_0 f_\infty$ in the norm $\|\cdot\|_{A_N}$. But this norm is equivalent to the norm $\|\cdot\|_{W_2^1}$ as we have shown in Lemma 2.3.6. So for all $f \in H_{A_N}$ the convergence of $T_t f$ to $\alpha_0 f_\infty$ in the norm of $L^2(D, \lambda^d)$ is implied by the inequality $\|\cdot\|_{L^2(D, \lambda^d)} \leq \|\cdot\|_{W_2^1}$. If we take into account that H_{A_N} is dense in $L^2(D, \lambda^d)$ and that the norms are continuous we have the following theorem.

Theorem 2.7.1. *For every $f \in L^2(D, \lambda^d)$ the function $T_t f = \exp(-tA_N) f$ converges in W_2^1 and in $L^2(D, \lambda^d)$ for t to infinity to $(f, f_\infty)_{L^2(D, \lambda^d)} f_\infty$.*

Now every v_k is a solution of a second order differential equation

$$A_N f = -\frac{1}{2} \Delta f + \frac{\Delta f_\infty}{2 f_\infty} f = \lambda_k f \quad \text{for } f \in W_2^1. \quad (2.22)$$

Furthermore for every vector field $\nu : \partial D \rightarrow \mathbb{R}^d$ with $\nu(x) \in \mathcal{N}_x$ for every $x \in \partial D$ this solution has to fulfil the additional condition

$$\int_{\partial D} \frac{dv_k}{d\nu} f \, d\sigma = 0, \quad \text{for all } f \in W_2^1$$

because it is an element of H_{A_N} which is the closure of \mathcal{D}_{A_N} in the norm $\|\cdot\|_{A_N}$. (For a detailed deduction of *generalised boundary conditions* for functions in W_m^n we refer to [44].) In our case $V \in \overline{C_0}(D)$ where D is bounded and either convex or possesses a sufficiently smooth boundary. So it can be shown that solutions of 2.22 are already in W_2^2 (see [44] Lemma 8.1 for the estimate $\|f\|_{W_2^2(D)}^2 \leq c(\|(A_N)_F f\|_{L^2(D, \lambda^d)}^2 + \|f\|_{L^2(D, \lambda^d)}^2)$ and [43] Remark 6.2 for the adaption to the boundary condition). But then it is an immediate consequence of Sobolev's inequality (cp. [2] Theorem 3.9) and the Sobolev imbedding theorem (cp. [1] Theorem 5.4) that for every $f \in W_2^2$ there exists a unique $\tilde{f} \in C^0(D)$ with $\|f - \tilde{f}\|_{L^2(D, \lambda^d)} = 0$.

Theorem 2.7.2. *For every $f \in \mathcal{D}_{A_N}$ the function*

$$T_t f := \exp(-tA_N)f := \sum_{k=0}^{\infty} \exp(-t\lambda_k)(f, v_k)_{L^2(D, \lambda^d)} v_k$$

converges point-wise for t to infinity to the two times continuous differentiable function $(f, f_\infty)_{L^2(D, \lambda^d)} f_\infty$.

Proof. Since A_N is an operator with a purely discrete point spectrum, it exists an orthonormal system $(v_k | k \in \mathbb{N}_0)$ consisting of eigenfunctions of A_N such that for every $f \in \mathcal{D}_{A_N} \subset \overline{C_2}(D)$ we have

$$\int_D |f - \sum_{k=0}^{\infty} (f, v_k)_{L^2(D, \lambda^d)} v_k| d\lambda^d = 0.$$

But then it follows

$$\left\| \sum_{k=0}^{\infty} (f, v_k)_{L^2(D, \lambda^d)} v_k \right\|_{L^2(D, \lambda^d)} < \infty$$

and because of $f \in \overline{C_2}(D)$ and the natural imbedding $\overline{C_2}(D) \hookrightarrow W_2^2(D)$ it is

$$\|D^\alpha \sum_{k=0}^{\infty} (f, v_k)_{L^2(D, \lambda^d)} v_k\|_{L^2(D, \lambda^d)} < \infty \quad \text{for } 1 \leq |\alpha| \leq 2,$$

where D^α is the distributional derivative to the multiindex α (as given in Definition A.8). Consequently, $(\sum_{k=0}^n (f, v_k)_{L^2(D, \lambda^d)} v_k | n \in \mathbb{N})$ is a Cauchy sequence

in $W_2^2(D)$ converging to $[f]$ (the class of f in $L^2(D, \lambda^d)$). Let $(\lambda_k | k \in \mathbb{N})$ denote the eigenvalues of A_N , then it is $0 = \lambda_0 < \lambda_1 < \dots$ and we get

$$\left\| \sum_{k=n}^m \exp(-t\lambda_k) (f, v_k)_{L^2(D, \lambda^d)} v_k \right\|_{W_2^2(D)} \leq \exp(-t\lambda_n) \left\| \sum_{k=n}^m (f, v_k)_{L^2(D, \lambda^d)} v_k \right\|_{W_2^2(D)}$$

for all $n \leq m$. So $(\sum_{k=0}^n \exp(-t\lambda_k) (f, v_k)_{L^2(D, \lambda^d)} v_k | n \in \mathbb{N})$ is a Cauchy sequence in $W_2^2(D)$ too. As we know $W_2^2(D)$ is complete with respect to its norm, so the limit of the Cauchy sequence

$$\left(\sum_{k=0}^n \exp(-t\lambda_k) (f, v_k)_{L^2(D, \lambda^d)} v_k | n \in \mathbb{N} \right)$$

is an element of $W_2^2(D)$. Furthermore $\|f_\infty - v_0\|_{W_2^2(D)} = 0$ so it follows for every $t \geq 0$

$$\begin{aligned} & \left\| \sum_{k=0}^{\infty} \exp(-t\lambda_k) (f, v_k)_{L^2(D, \lambda^d)} v_k - (f, f_\infty)_{L^2(D, \lambda^d)} f_\infty \right\|_{W_2^2(D)} \\ & \leq \left\| \sum_{k=1}^{\infty} \exp(-t\lambda_k) (f, v_k)_{L^2(D, \lambda^d)} v_k \right\|_{W_2^2(D)} \\ & \leq \exp(-t\lambda_1) \|f - (f, f_\infty)_{L^2(D, \lambda^d)} f_\infty\|_{W_2^2(D)} < \infty. \end{aligned}$$

Using Sobolev's imbedding theorem taken from [1] we conclude

$$\sup_{x \in D} |T_t f(x) - (f_\infty, f)_{L^2(D, \lambda^d)} f_\infty(x)| \rightarrow 0$$

for $t \rightarrow \infty$. ■

Remark 2.7.3. For every $n \in \mathbb{N}_0$ we have the inclusion $W_2^{2+n}(D) \subset W_2^2(D)$ and the Hilbert space $W_2^{2+n}(D)$ can be imbedded in $C^n(D)$. So we could easily repeat the argument above to improve the smoothness of $T_t f$ by choosing f in $C^n(D)$. Easier we simply take the limit of

$$\frac{T_t f(x_0 + hx) - T_t f(x_0)}{h} = \frac{T_t(f(x_0 + hx) - f(x_0))}{h} \quad (2.23)$$

for $h \rightarrow 0$ to find $T_t f \in C^n(D)$ whenever $f \in C^n(D)$. The validity of Equ-

tion 2.23 is simply a consequence of the definition of $\exp(-tA_N)f$ as linear combination of basis elements.

Following the argumentation given in Section 1.7 the function

$$\begin{aligned} U_{f_\infty} : L^2(D, \lambda^d) &\rightarrow L^2(D, f_\infty^2 \lambda^d) \\ f &\mapsto \frac{f}{f_\infty} \end{aligned}$$

is a unitary map with inverse $U_{f_\infty}^{-1} = U_{1/f_\infty}$. As in Section 1.8 using U_{f_∞} this leads to the operator $L_N = U_{f_\infty} H U_{f_\infty}^{-1} = -\frac{1}{2}\Delta - \frac{\nabla f_\infty}{f_\infty} \nabla$ with domain $\mathcal{D}_{L_N} = \mathcal{D}_{A_N}$. Furthermore for every $t \geq 0$ we define $S_t f := \exp(-tL_N)f$ for $f \in \mathcal{D}_{L_N} \subset C^2(D)$. Then $S_t f$ is a solution of the Cauchy problem

$$\begin{aligned} \frac{\partial u}{\partial t}(t, x) &= -L_N u(t, x) & t > 0, x \in D \\ u(0, x) &= f(x) & x \in D, f \in \overline{C_2}(D) \end{aligned}$$

with Neumann boundary condition. So using Theorem 2.7.2 together with Remark 2.7.3 and taking into account that S_t is the image of T_t under the unitary map U_{f_∞} it follows $S_t f(\cdot) \in \overline{C_2}(D)$. Finally $S_t f$ is continuous differentiable in t so Theorem 2.6.4 implies $S_t f(x) = \mathbb{E}[f(\hat{X}_t^x)]$ for all $x \in D$ where \hat{X}_t^x is a reflected Itô diffusion on \overline{D} with diffusion coefficient I_d and drift $-\frac{\nabla f_\infty}{f_\infty}$. We resume as follows.

Theorem 2.7.4. *Given the operator A_N with domain \mathcal{D}_{A_N} (Eqns. 2.20a, 2.20b) for every $f \in \overline{C_2}(D)$ the function $S_t f := \exp(-tA_N)f$ is continuous differentiable with respect to $t \geq 0$. Further let $(\hat{X}|t \geq 0)$ denote a reflected Itô diffusion on \overline{D} with diffusion coefficient I_d and drift $-\frac{\nabla f_\infty}{f_\infty}$ then it is $S_t f(x) = \mathbb{E}[f(\hat{X}_t^x)]$ for every $x \in D, t \geq 0$ and $S_t f(\cdot) \in C^2(D)$.*

Chapter 3

Implementation

The last step leading to a mechanism applicable to image processing is a collection of statements concerning problems which arise from computer experiments and their discrete nature. We start with the discrete approximation of Itô diffusions in convex regions. Then we discuss the time and space discrete simulation algorithm for transforming a start image into a stop image. Afterwards we investigate several possibilities to get sufficiently smooth images from discrete image points and of course determine their derivatives. Both are needed for the implementation of the transformation algorithm. Finally we give a short discussion concerning the resulting approximation error.

3.1 Approximation of Itô diffusion in convex regions

In this section we will describe Euler's approximation of solutions of Skorohod's problem, which can be found e.g. in [8, 72, 73]. Later we need this in order to compute such solutions. Then we will improve the rate of convergence of the approximation by simple application of a stochastic Taylor expansion (as described in Appendix C), similar to the argument leading to schemes of higher approximation order corresponding to Itô diffusions in unbounded regions (see [39]). Frequently, these approximations are formulated for non-equidistant discretisations in time and space sometimes even with random time discretisation. This seems to be possible in our case too, but we

renounce this in order to keep the notation simple and restrict ourselves to the case of equidistant approximations in time.

As before, we consider D as an open, bounded, convex subset of \mathbb{R}^d . Further let $b : \mathbb{R}^d \rightarrow \mathbb{R}$ and $\sigma : \mathbb{R}^d \rightarrow \mathbb{R}^{m \times d}$ denote the drift, respectively the diffusion coefficient of the Itô diffusion $(X_t | t \geq 0)$ in \mathbb{R}^d . We remind that the process X_t is defined as solution of the stochastic differential equation

$$\begin{aligned} dX_t &= b(X_t)dt + \sigma(X_t)dB_t, \\ X_0 &= x \in \overline{D}. \end{aligned} \tag{3.1}$$

In order to get a unique solution of Equation 3.1 in the strong sense we suppose b and σ to be Lipschitz continuous (see Eqn. 2.11) as before. Then we can apply a result from [77] to the Skorokhod problem corresponding to (X_t, \overline{D}) as defined in Appendix B. This result guarantees the uniqueness of the solution (X_t, φ_t) of the Skorokhod problem (X_t, \overline{D}) in the strong sense¹. Now it is possible to define different sequences of stochastic processes $(\hat{X}_{t,n}^x := X_{t,n}^x + \varphi_t^n | t \geq 0)$ (piecewise constant in time) converging a.s. to the unique solution $\hat{X}_t := X_t + \varphi_t$. Here we just mention the penalisation scheme discussed in [13, 72, 73] and use the projection scheme (e.g. see [57, 72, 73]). Therefore we consider for every $n \in \mathbb{N}$ the sequence $(k/n | k \in \mathbb{N}_0)$ and define the function

$$p_n(t) := \max\left\{\frac{k}{n} | k \in \mathbb{N}_0, \frac{k}{n} \leq t\right\}, \quad \text{for } t \geq 0.$$

Then we obtain a discretisation of the Brownian motion B_t by $B_t^{p_n} := B_{k/n}$ for $t \in [k/n, (k+1)/n)$. In the following we denote by $X_{t-}(\omega)$ the limit of $X_s(\omega)$ for $s \nearrow t$.

Definition 3.1.1. In the notation above a discrete projection scheme as a solution of the stochastic differential equation

$$\overline{X}_t^n = \overline{X}_0^n + \int_0^t \sigma(\overline{X}_{s-}^n) dB_s^{p_n} + \int_0^t b(\overline{X}_{s-}^n) dp_n(s) + \varphi_t^n \tag{3.2}$$

is defined, where $\overline{X}_0^n = \hat{X}_0^x$ and $(\varphi_t^n | t \geq 0)$ is a process of bounded variation with $\varphi_0^n = 0$ growing only if $\overline{X}_t^n \in \partial D$.

¹The process $(\hat{X}_t := X_t + \varphi_t | t \geq 0)$ only takes values in \overline{D} .

To be precise, if $\mathcal{N}_{\overline{X}_s^n}$ is the set of normals to the boundary at the point $\overline{X}_s^n \in \partial D$ and $n_s \in \mathcal{N}_{\overline{X}_s^n}$, then we have

$$\varphi_t^n = \int_0^t n_s d[\varphi_s^n], \quad [\varphi_s^n] = \int_0^s 1_{\{\overline{X}_s^n \in \partial D\}} d[\varphi_s^n], \quad t \geq 0,$$

where we used the notation $[\varphi_t^n]$ for the variation of φ_t^n on $[0, t]$ as given in Definition B.2.

In the following theorem we present a recursive procedure for a discrete projection scheme which can be computed easily. Therefore we denote by $\Pi(x)$ for every $x \in \mathbb{R}^d$ the unique $y \in \partial D$ with $|x - y| \leq |x - z|$ for all $z \in \overline{D}$. Obviously we have $\Pi(x) = x$ for every $x \in \overline{D}$ and for every $x \in \mathbb{R}^d \setminus \overline{D}$ the point $\Pi(x)$ is nothing else than the unique projection of x to the boundary ∂D of D .

Theorem 3.1.2. *The process $\overline{Y}_t^n := \overline{Y}_{k/n}^n$ for $t \in [k/n, (k+1)/n)$ with*

$$\begin{aligned} \overline{Y}_{(k+1)/n}^n &:= \Pi(\overline{Y}_{k/n}^n + \sigma(\overline{Y}_{k/n}^n)(B_{(k+1)/n} - B_{k/n}) + b(\overline{Y}_{k/n}^n)\frac{1}{n}), \\ \overline{Y}_0^n &:= \hat{X}_0^x \end{aligned} \quad (3.3)$$

solves Equation 3.2 for all $t \geq 0$.

Proof. Because of $\overline{Y}_0^n := \hat{X}_0^x$ it is sufficient to prove

$$\overline{Y}_{(k+1)/n}^n = \overline{Y}_{k/n}^n + \sigma(\overline{Y}_{k/n}^n)(B_{(k+1)/n} - B_{k/n}) + b(\overline{Y}_{k/n}^n)\frac{1}{n} + \varphi_{(k+1)/n}^n.$$

Then the statement of the theorem follows by induction. But the equation above is obviously true if we define $\varphi_{(k+1)/n}^n := \Pi(Z_{(k+1)/n}^n) - Z_{(k+1)/n}^n$ with

$$Z_{(k+1)/n}^n := \overline{Y}_{k/n}^n + \sigma(\overline{Y}_{k/n}^n)(B_{(k+1)/n} - B_{k/n}) + b(\overline{Y}_{k/n}^n)\frac{1}{n} \quad (3.4)$$

and $\varphi_0^n = 0$. Moreover from the definition of $\varphi_{k/n}^n$ it follows that its increments are elements of $\mathcal{N}_{\overline{Y}_{(k+1)/n}^n}$ and the process grows only if $\overline{Y}_{(k+1)/n}^n$ is at the boundary of D . ■

Remark. In the proof above we have shown that for $t \in [k/n, (k+1)/n)$ the function $\varphi_t^n := \varphi_{k/n}^n$ possesses the properties claimed in Definition 3.1.1. Hence

we call the process defined by Equation 3.3 a projection scheme.

Now we give Theorem 3.1 from [73]. This shows that the projection scheme defined above converges to the process we are interested in.

Theorem 3.1.3. *Assume the solution of Skorokhod's problem associated with (X_t, \overline{D}) to be path-wise unique and let \overline{Y}_t^n be defined as in Theorem 3.1.2. Then for every $p \in \mathbb{N}$ and $q \in \mathbb{R}_{\geq 0}$ the term*

$$\mathbb{E} \left[\sup_{t \leq q} |\overline{Y}_t^n - X_t|^{2p} \right]$$

converges for $n \rightarrow \infty$ to 0.

As mentioned at the beginning of the section we use the projection scheme as a starting point for the development of another approximation scheme. Precisely, we extend the approximation scheme defined in Theorem 3.1.2 to an approximation scheme of higher order. Therefore we use a *multidimensional stochastic Taylor expansion* as described in Appendix C. This Taylor expansion provides the equation $dX_t^i = O_1 + O_2$ with

$$\begin{aligned} O_1 &= \left(b_i(X_0) + \int_0^t L^0 b_i(X_s) ds \right) dt + \sum_{k=1}^m \int_0^t L^k b_i(X_s) dB_s^k dt \\ &\quad + \sum_{j=1}^m \left(\sigma_{i,j}(X_0) + \int_0^t L^0 \sigma_{i,j}(X_s) ds \right) dB_t^j \end{aligned}$$

and

$$\begin{aligned} O_2 &= \sum_{j,k=1}^m \int_0^t L^k \sigma_{i,j}(X_0) dB_r^k dB_t^j + \sum_{j,k=1}^m \int_0^t \int_0^s L^0 L^k \sigma_{i,j}(X_r) dr dB_s^k dB_t^j \\ &\quad + \sum_{j,k,l=1}^m \int_0^t \int_0^s L^l L^k \sigma_{i,j}(X_r) dB_r^l dB_s^k dB_t^j \end{aligned}$$

for every $0 \leq i \leq d$ where

$$L^0 := \sum_{i=1}^d b_i \frac{\partial}{\partial x_i} + \sum_{i_1, i_2=1}^d \sum_{j=1}^m \sigma_{i_1, j} \sigma_{i_2, j} \frac{\partial^2}{\partial x_{i_1} \partial x_{i_2}} \quad \text{and} \quad L^k := \sum_{i=1}^d \sigma_{i, k} \frac{\partial}{\partial x_i}.$$

Now we define $\Delta t := 1/n$ and $\Delta B_{t_0}^j := B_{t_0+\Delta t}^j - B_{t_0}^j$ for $j = 1, \dots, m$. As we know $\Delta B_{t_0}^j \sim \mathcal{N}(0, \Delta t)$. That means $\Delta B_{t_0}^j$ is a normally distributed random variable with zero mean and variance $\text{Var}(\Delta B_{t_0}^j) = (\Delta t)$. In the following we assume $n \in \mathbb{N}$ to be chosen sufficiently large. Obviously we have the approximation

$$\int_{t_0}^{t_0+\Delta t} \sigma_{i,j}(X_t) dB_t^j \approx \sigma_{i,j}(X_{t_0}) \int_{t_0}^{t_0+\Delta t} dB_t^j = \sigma_{i,j}(X_{t_0}) \Delta B_{t_0}^j.$$

This is consistent with the Itô calculus because we evaluate the integrand at the lower end point of the interval $[t_0, t_0 + \Delta t]$. An application of the Itô formula gives

$$\int_{t_0}^{t_0+\Delta t} \int_{t_0}^t dB_s^j dB_t^j = \frac{1}{2}((\Delta B_{t_0}^j)^2 - \Delta t)$$

and

$$\int_{t_0}^{t_0+\Delta t} \int_{t_0}^t \int_{t_0}^s dB_r^j dB_s^j dB_t^j = \frac{1}{3!}((\Delta B_{t_0}^j)^3 - \Delta B_{t_0}^j \Delta t).$$

Finally from the deterministic approximation calculus we know

$$\int_{t_0}^{t_0+\Delta t} dt = \Delta t \quad \text{and} \quad \int_{t_0}^{t_0+\Delta t} \int_{t_0}^t L^0 b_i(X_s) ds dt \approx \frac{1}{2} L^0 b_i(X_{t_0}) (\Delta t)^2.$$

Then it follows the approximation

$$X_{t_0+\Delta t}^i - X_{t_0}^i \approx S_1 + S_2 + R$$

for the increments of the Itô diffusion, where

$$\begin{aligned} S_1 &= b_i(X_{t_0}) \Delta t + L^0 b_i(X_{t_0}) (\Delta t)^2 + \sum_{k=1}^m L^k b_i(X_s) \int_{t_0}^{t_0+\Delta t} \int_{t_0}^t dB_s^k dt \\ &\quad + \sum_{j=1}^m \sigma_{i,j}(X_{t_0}) \Delta B_{t_0}^j + \sum_{j=1}^m L^0 \sigma_{i,j}(X_{t_0}) \int_{t_0}^{t_0+\Delta t} \int_{t_0}^t ds dB_t^j, \end{aligned}$$

$$\begin{aligned}
S_2 &= \sum_{j=1}^m L^j \sigma_{i,j}(X_{t_0}) \frac{1}{2} ((\Delta B_{t_0}^j)^2 - \Delta t) \\
&\quad + \sum_{j=1}^m L^j L^j \sigma_{i,j}(X_{t_0}) \frac{1}{6} ((\Delta B_{t_0}^j)^3 - \Delta t \Delta B_{t_0}^j) \\
&\quad + \sum_{j,k=1}^m L^0 L^k \sigma_{i,j}(X_{t_0}) \int_{t_0}^{t_0+\Delta t} \int_{t_0}^t \int_{t_0}^s dr dB_s^k dB_t^j
\end{aligned}$$

and

$$\begin{aligned}
R &= \sum_{\substack{j,k=1 \\ j \neq k}}^m L^k \sigma_{i,j}(X_{t_0}) \int_{t_0}^{t_0+\Delta t} \int_{t_0}^t dB_s^k dB_t^j \\
&\quad + \sum_{\substack{j,k,l=1 \\ \neg(j=k=l)}}^m L^l L^k \sigma_{i,j}(X_{t_0}) \int_{t_0}^{t_0+\Delta t} \int_{t_0}^t \int_{t_0}^s dB_r^l dB_s^k dB_t^j.
\end{aligned}$$

The approximation above and the argument in the proof of Theorem 3.1.2 enables us to derive an approximation scheme equivalent to the *multidimensional order 1.5 strong Taylor scheme* (cp. [39] 10.5). This involves multiple Itô integrals with respect to different components of the Brownian motion, which is not very convenient for implementations in computer experiments. For this reason we avoid these terms and just deduce the following theorem.

Theorem 3.1.4. *Let $\bar{Y}_t^{n,i}$ denote the i -th component of \bar{Y}_t^n and define the process $\bar{Y}_t^n := \bar{Y}_{k/n}^n$ for $t \in [k/n, (k+1)/n)$ by the recursive equation*

$$\begin{aligned}
\bar{Y}_{(k+1)/n}^{n,i} &:= \Pi \left(\bar{Y}_{k/n}^n + b_i(\bar{Y}_{k/n}^n) \Delta t + L^0 b_i(\bar{Y}_{k/n}^n) (\Delta t)^2 \right. \\
&\quad + \sum_{j=1}^m \sigma_{i,j}(\bar{Y}_{k/n}^n) \Delta B_{k/n}^j + \sum_{j=1}^m L^j \sigma_{i,j}(\bar{Y}_{k/n}^n) \frac{1}{2} ((\Delta B_{k/n}^j)^2 - \Delta t) \\
&\quad \left. + \sum_{j=1}^m L^j L^j \sigma_{i,j}(\bar{Y}_{k/n}^n) \frac{1}{6} ((\Delta B_{k/n}^j)^3 - \Delta t \Delta B_{k/n}^j) \right)
\end{aligned}$$

with $\bar{Y}_0^n := \hat{X}_0^x$, then \bar{Y}_t^n solves Equation 3.2 for all $t \geq 0$.

For completeness and in view of the applications in Chapter 4 we mention

that the equivalent of the multidimensional Milstein scheme would be defined by

$$\begin{aligned} \bar{Y}_{(k+1)/n}^{n,i} := & \Pi \left(\bar{Y}_{k/n}^n + b_i(\bar{Y}_{k/n}^n) \Delta t + \sum_{j=1}^m \sigma_{i,j}(\bar{Y}_{k/n}^n) \Delta B_{k/n}^j \right. \\ & \left. + \sum_{j,k=1}^m L^k \sigma_{i,j}(\bar{Y}_{k/n}^n) \frac{1}{2} ((\Delta B_{k/n}^j)^2 - \Delta t) \right). \end{aligned} \quad (3.5)$$

Remark. If we assume $d = m$ and suppose that σ is the d -dimensional unit matrix, as it will be the case in our applications, then Equation 3.5 reduces to

$$\bar{Y}_{(k+1)/n}^{n,i} := \Pi \left(\bar{Y}_{k/n}^n + b_i(\bar{Y}_{k/n}^n) \Delta t + \Delta B_{k/n}^i \right),$$

which is nothing else than the known Euler projection scheme. Hence our main result of this section (i.e. the extension of the existing projection schemes in Theorem 3.1.4) is an add-on to the main work.

3.2 Monte Carlo integration

In this section we denote by D an open, bounded, convex subset of \mathbb{R}^d as before. In Theorem 2.6.4 we saw that $u(t, x) = E[\frac{f_0}{f_\infty}(X_t^x)]$ gives a representation of the solution of the Cauchy problem

$$\frac{du}{dt} = -Au \quad \text{with} \quad u(0) = \frac{f_0}{f_\infty},$$

we are interested in (see Chapter 2). There $f_0, f_\infty : D \rightarrow \mathbb{R}_{>0}$ are elements of $\overline{C}_2(D)$ and $(X_t|t \in \mathbb{R}_{\leq 0})$ denotes a d -dimensional Itô diffusion with reflection defined as solution of the differential equation

$$dX_t = b(X_t)dt + \sigma(X_t)dB_t + \varphi_t$$

starting at $X_0 = x \in D$ with generator $-A$. As before $(\varphi_t|t \geq 0)$ is a process of bounded variation starting at $\varphi_0 = 0$ and growing only if $X_t \in \partial D$. Algorithm 3.2.1 follows a simple Monte Carlo approach to approximate the

expectation of the random variable $\frac{f_0}{f_\infty}(X_{t,\Delta t}^x)$ for fixed $t \in \mathbb{R}_{>0}$ and x in D . Here $X_{t,\Delta t}^x$ is an approximation of X_t^x with step size Δt equidistant in time as presented in Section 3.1. For convenience we always assume $t = s\Delta t$ for some s in \mathbb{N}_0 . As we can see, Algorithm 3.2.1 uses Algorithm 3.2.2 for the com-

Algorithm 3.2.1 Computation of $u_k(t = s\Delta t, x)$, $t > 0$, $x \in D$

Require:

number of simulations = k
 $\frac{f_0}{f_\infty}({}_1X_{t,\Delta t}^x), \dots, \frac{f_0}{f_\infty}({}_kX_{t,\Delta t}^x)$
 /* using Algorithm 3.2.2 */

```

1:   $u \leftarrow 0$ 
2:  for  $l = 1$  to  $k$  do
3:       $u \leftarrow u + \frac{f_0({}_lX_{t,\Delta t}^x)}{f_\infty({}_lX_{t,\Delta t}^x)}$ 
4:  end for
5:   $u_k(t, x) \leftarrow \frac{u}{k}$ 

```

Ensure:

$u_k(t, x)$

putation of k paths ${}_lX_{t,\Delta t}^x$ of $X_{t,\Delta t}^x$ according to the multidimensional Milstein projection scheme. In this notation the index l indicates that we use independent random increments ${}_l\Delta B_i = ({}_l\Delta B_i^1, \dots, {}_l\Delta B_i^m)$ every time we compute a path of $X_{t,\Delta t}^x$. We use the notation $\Pi(x)$ for the projection of $x \in \mathbb{R}^d$ to the boundary ∂D of the region D as described in the section above.

Remark. In order to avoid stochastic integrals of the form $\int_{t_1}^{t_2} \int_{t_1}^{s_1} dB_{s_2}^i dB_{s_1}^j$ we assume commutative noise. Precisely, we consider a diffusion coefficient with

$$\sum_{k=1}^d \sigma_{k,i}(x) \frac{\partial \sigma_{j,l}}{\partial x_k} = \sum_{k=1}^d \sigma_{k,l}(x) \frac{\partial \sigma_{j,i}}{\partial x_k}.$$

This is at least true for additive, linear and diagonal noise (see [39]). So it does not seem to be a hard restriction to applications and their models. Moreover, in the applications we consider in Chapter 4, $(\sigma_{i,j})_{1 \leq i,j \leq d} = -I_d$ holds. Therefore the lines 3 to 8 of Algorithm 3.2.2 reduce to

$$\begin{aligned} X_1 &= X_1 + b_1(X)\Delta t + \Delta B_i^1 \\ X_2 &= X_2 + b_2(X)\Delta t + \Delta B_i^2. \end{aligned}$$

Algorithm 3.2.2 Computation of $X_{s\Delta t, \Delta t}^x$, $s \in \mathbb{N}$, $\Delta t > 0$, $x \in D$

Require: number of steps = s , step size = Δt , x , ΔB_i

```

1:   $X \leftarrow x$ 
2:  for  $i = 0$  to  $s$  do                                /* compute  $s$  steps of the process */
3:      for  $k = 1$  to  $d$  do
4:           $T_1 \leftarrow b_k(X)\Delta t$ 
5:           $T_2 \leftarrow \sum_{j=1}^m \sigma_{k,j}(X)\Delta B_i^j$ 
6:           $T_3 \leftarrow \sum_{j_1, j_2=1}^m \sum_{j_3=1}^d \sigma_{j_3, j_1}(X) \frac{\partial \sigma_{k, j_2}}{\partial x_{j_3}}(X) \Delta B_i^{j_1} \Delta B_i^{j_2}$ 
7:           $X_k \leftarrow X_k + T_1 + T_2 + T_3$ 
8:      end for
9:       $X \leftarrow \Pi(X)$                                 /*  $\Pi(X) = X$  if  $X \in \overline{D}$  */
10: end for
11:  $X_{t, \Delta t}^x \leftarrow X$ 

```

Ensure: $X_{t, \Delta t}^x$, $s\Delta t = t$

We note that the function $u_k(t = s\Delta t, x)$ resulting from Algorithm 3.2.1 is indeed an approximation of $\mathbb{E}[\frac{f_0}{f_\infty}(X_t^x)]$ for $x \in D$, because

$$\frac{1}{n} \sum_{l=1}^n \frac{f_0}{f_\infty}(X_{t, \Delta t}^x) \xrightarrow[n \rightarrow \infty]{a.s.} \mathbb{E} \left[\frac{f_0}{f_\infty}(X_{t, \Delta t}^x) \right]$$

and

$$\mathbb{E} \left[\frac{f_0}{f_\infty}(X_{t, \Delta t}^x) \right] \xrightarrow{\Delta t \rightarrow 0} \mathbb{E} \left[\frac{f_0}{f_\infty}(X_t^x) \right].$$

3.3 Continuous images

In computer vision, one of the common ways to produce images is by using sensors which consist of *Charged Coupled Devices* CCDs or *Active Pixel Sensors* APSs (often called CMOS sensors), arranged in two-dimensional arrays. This is also the predominant arrangement found in digital cameras and other light sensing instruments. The response of a single sensor is proportional to the integral of the light energy projected onto the surface of the sensor (up to a

threshold). Nevertheless, in computer vision, usually the continuous values produced by the sensing pixels or its discrete data representation have been taken as spatially sampled representation of the continuous scene. But there exist other approaches too. We just refer to the common literature [28, 35, 37]. For further information about the signal processing chain inside the detector see [36, 60]. All these arrangements have in common that they produce discrete quantisations

$$\mathbb{I}f : \{1, \dots, n\} \times \{1, \dots, m\} \rightarrow \{0, \dots, \text{gray}_{\max}\},$$

which we call *images* or *image functions*. There, $\mathbb{I}f(i, j)$ is the quantisation of the continuous signal of the sensor at position (i, j) and gray_{\max} is its maximum value. The maximum of the sensor response exists because the well capacities of the used sensing devices are bounded [35, 36]. Obviously every image can be assumed to be strictly positive by a translation of the function values to $\{1, \dots, \text{gray}_{\max} + 1\}$.

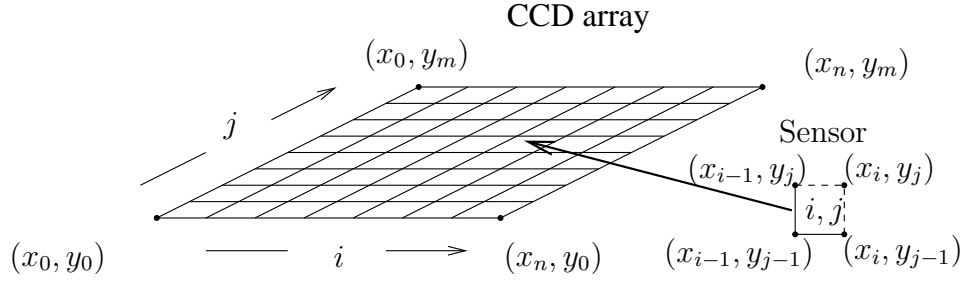


Figure 3.1. Correspondence between the position of the CCD sensors and the resulting image points.

Now we introduce the point sets $\{x_0, \dots, x_n\}$ and $\{y_0, \dots, y_m\}$ in order to denote the corner points of a single CCD sensor at position (i, j) by the tuples (x_{i-1}, y_{j-1}) , (x_i, y_{j-1}) , (x_i, y_j) and (x_{i-1}, y_j) . In this notation we started at the lower left corner and progressed counterclockwise direction (Figure 3.1). Obviously the centre (x_i^c, y_j^c) of the sensor at position (i, j) is located at $(\frac{x_{i-1}+x_i}{2}, \frac{y_{j-1}+y_j}{2})$ because each sensor well is taken as a square. In the following we will take D as the open rectangle $(0, x_n) \times (0, y_m)$.

3.3.1 Smoothing piecewise constant functions

As we have seen in the last section, because of the sensor layout, one natural interpretation of a given image function \mathbb{f} is as a piecewise constant function $\hat{\mathbb{f}}$. Furthermore the arrangement of the sensors tells us that we can not expect a natural definition of $\hat{\mathbb{f}}(x, y)$ where either $x \in \{x_0, \dots, x_n\}$ or $y \in \{y_0, \dots, y_m\}$. This is because the sensing device has gaps. In fact we do not want to leave these values undefined, so we simply associate the lower and left border of the sensor (i, j) to the image value $\mathbb{f}(i, j)$. Additionally the right border of the whole sensing device is associated to the last column of sensors ($i=n$) whereas the upper border of the sensing device is associated to the upper row of sensors ($j=m$).

Definition 3.3.1. We call a function $\hat{\mathbb{f}} : [0, n] \times [0, m] \rightarrow \{1, \dots, \mathbb{f}_{max} + 1\}$ a *piecewise constant version* of the given discrete image \mathbb{f} , iff the function $\hat{\mathbb{f}}$ satisfies

$$\hat{\mathbb{f}}(x, y) = \mathbb{f}(i, j) \quad \text{for} \quad (x, y) \in [x_{i-1}, x_i] \times [y_{j-1}, y_j] \quad (3.7a)$$

$$\hat{\mathbb{f}}(x, y_m) = \mathbb{f}(i, m) \quad \text{for} \quad x \in [x_{i-1}, x_i] \quad (3.7b)$$

$$\hat{\mathbb{f}}(x_n, y) = \mathbb{f}(n, j) \quad \text{for} \quad y \in [y_{j-1}, y_j] \quad (3.7c)$$

$$\hat{\mathbb{f}}(x_n, y_m) = \mathbb{f}(n, m) \quad (3.7d)$$

for every $1 \leq i \leq n$ and $1 \leq j \leq m$. The set of all piecewise constant versions of \mathbb{f} is called $\hat{\mathbb{f}}(\mathcal{D})$.

Before we produce a piecewise constant version $\hat{\mathbb{f}}$ of the given image function \mathbb{f} , we enlarge \mathbb{f} to adjust either Dirichlet or Neumann boundary conditions. For this purpose we put a frame of additional pixels (sensor areas) around the given image. The new image function \mathbb{f} is now defined on a bigger set of points as schematically shown in Figure 3.2. Now we can simply achieve Dirichlet boundary conditions by the redefinition of $\hat{\mathbb{f}}$ at the boundary as zero. This method has the advantage that we do not lose information at the boundary of the image. Furthermore for the Neumann boundary condition we

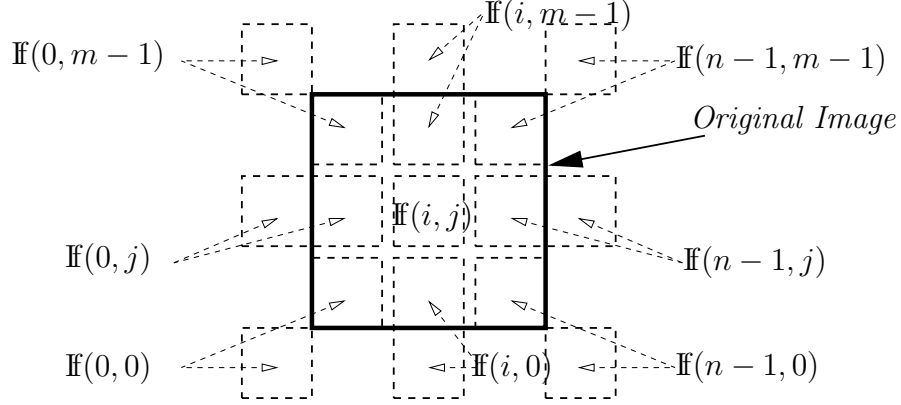


Figure 3.2. This presents a natural way to enlarge images in order to achieve Neumann boundary conditions. In the Dirichlet case the function values on the outer squares are set to zero.

define

$$\begin{aligned}
 & \mathbb{F}(-1, j) := \mathbb{F}(0, j) \\
 & \mathbb{F}(n+1, j) := \mathbb{F}(n, j) \\
 & \mathbb{F}(i, -1) := \mathbb{F}(i, 0) \\
 & \mathbb{F}(i, m+1) := \mathbb{F}(i, m)
 \end{aligned}
 \quad \begin{array}{l} j = 0, 1, \dots, m \\ \text{for} \\ i = -1, 0, 1, \dots, n+1 \end{array}$$

(cp. Fig. 3.2). Then for the computer experiments we use the resulting area just for the computation of the derivative of the piecewise constant function $\hat{\mathbb{F}}$. But we take the small originally given area as domain of $\hat{\mathbb{F}}$ (i.e. where $\hat{\mathbb{F}}$ is defined). For simplicity we use the same symbol \mathbb{F} (respectively $\hat{\mathbb{F}}$) and the point set $\{1, \dots, n\} \times \{1, \dots, m\}$ (resp. $[0, x_n] \times [0, y_m]$) as its domain in the Dirichlet case and the Neumann case as before.

Remark 3.3.2. We assume $x_i = i$ for $i = 0, \dots, n$ and $y_j = j$ for $j = 0, \dots, m$. In order to get a piecewise constant version of an image function \mathbb{F} it is natural to assign the function value $\mathbb{F}(i, j)$ to the square $[i-1, i) \times [j-1, j)$. To be precise we denote by $\lfloor x \rfloor$ the largest integer below or equal to $x \in \mathbb{R}$. Then the function $\hat{\mathbb{F}}$ defined by

$$\hat{\mathbb{F}}(x, y) := \begin{cases} \mathbb{F}(\lfloor x \rfloor + 1, \lfloor y \rfloor + 1) & \text{for } (x, y) \in [0, n) \times [0, m) \\ \mathbb{F}(\lfloor x \rfloor + 1, m) & \text{for } x \in [0, n), y = m \\ \mathbb{F}(n, \lfloor y \rfloor + 1) & \text{for } x = n, y \in [0, m) \\ \mathbb{F}(n, m) & \text{for } (x, y) = (n, m) \end{cases} \quad (3.8)$$

is an element of $\hat{\mathbb{F}}(D)$.

Now we define smooth functions with an interpolating property to establish a connection between image processing and the theory presented in Chapter 2.

Definition 3.3.3. For $k \in \mathbb{N}$ we call the function $\tilde{\mathbb{F}}$ defined on $[0, n] \times [0, m]$ with values in \mathbb{R} a *k-continuous version* of the given discrete image function \mathbb{F} , iff $\tilde{\mathbb{F}} \in \overline{C_k}(D)$ and for all $1 \leq i \leq n$, $1 \leq j \leq m$ we have $\tilde{\mathbb{F}}(i, j) = \mathbb{F}(i, j)$. The set of all *k-continuous versions* of \mathbb{F} is denoted by $\tilde{\mathbb{F}}^k(D)$.

In order to produce a smooth version of the given image \mathbb{F} , we introduce the convolution of two functions as in [83].

Definition 3.3.4. For $u, v \in L^2(\mathbb{R}^d, \lambda^d)$ we define the *convolution* by

$$(u * v)(x) := \int_{\mathbb{R}^d} u(x - y)v(y) dy \quad \text{for all } x \in \mathbb{R}^d$$

as element of $L^1(\mathbb{R}^d, \lambda^d)$. Then $u * v$ is also defined for $u, v \in L^2(D, \lambda^d)$ by the inclusion $L^2(D, \lambda^d) \rightarrow L^2(\mathbb{R}^d, \lambda^d)$. Therefore we simply assign zero function values to u and v outside \overline{D} .

Now it is easy to see that the convolution of $\hat{\mathbb{F}}$ and the square function W_0 defined by

$$W_0(x, y) = \begin{cases} 1 & -\frac{1}{2} \leq x, y < \frac{1}{2} \\ 0 & \text{otherwise} \end{cases} \quad (3.9)$$

leads to a continuous function. The most interesting case is shown in Figure 3.3 as 1-dimensional simplification. As we can see it is

$$|\hat{\mathbb{F}} * W_0(x + h) - \hat{\mathbb{F}} * W_0(x)| \leq h^2 (\max_{y \in D} \hat{\mathbb{F}}(y) - 1)^2 \quad \text{for all } h \in \mathbb{R}.$$

In the cases not shown in Figure 3.3 it is $|\hat{\mathbb{F}} * W_0(x + h) - \hat{\mathbb{F}} * W_0(x)| = 0$ for h sufficiently small. Up to here we got a continuous function $\tilde{\mathbb{F}} \in \mathbb{F}^0(D)$ from the given image function \mathbb{F} . Finally we get *k-times continuously differentiable functions* again by convolution of \mathbb{F} now with *k-times continuously differentiable functions*. This is the statement of the following lemma (see [12]).

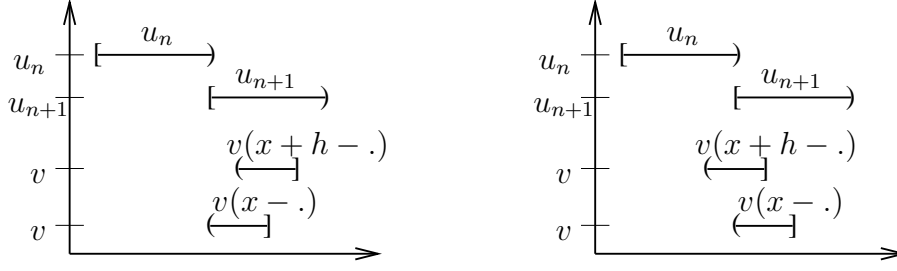


Figure 3.3. From this images we can derive the difference of the convolution of two 1-dimensional piecewise constant functions u, v at x and $x + h$. The left images shows the function $v(x + h - .)$ for $h < 0$ whereas in the right image $v(x + h - .)$ is shown for $h > 0$.

Lemma 3.3.5. *For $k \in \mathbb{N} \cup \{\infty\}$ we consider $C_0^k(\mathbb{R}^d)$ as the set of k -times continuous differentiable functions on \mathbb{R}^d with compact support. Then for every $u \in C_0^k(\mathbb{R}^d)$ and $v \in C_0^0(\mathbb{R}^d)$ it is $(u * v) \in C_0^k(\mathbb{R}^d)$.*

Later we want to reconstruct \mathbb{f} so we can not convolve $\tilde{\mathbb{f}}$ with every k -times continuous function (we may lose information). But we know from *Fourier analysis* (e.g. see [45]) that every real scene, which is interpreted as a 2π -periodic, differentiable function f , can be expressed as sum of frequencies. This is called the *Fourier series*. It is given by

$$f(x) = \frac{1}{2}a_0 + \sum_{n=1}^{\infty} (a_n \cos(nx) + b_n \sin(nx))$$

with coefficients

$$\begin{aligned} a_n &:= \frac{1}{\pi} \int_{-\infty}^{\infty} f(x) \cos(nx) dx, & n = 0, 1, \dots \\ b_n &:= \frac{1}{\pi} \int_{-\infty}^{\infty} f(x) \sin(nx) dx, & n = 1, 2, \dots \end{aligned}$$

If f is *band limited* (i.e. $\exists k \in \mathbb{N} : \forall n \geq k : a_n = b_n = 0$) and sampled at points with distance half of its highest frequency then it can be reconstructed exactly from the information given by the sample points. For this reason we have to convolve \mathbb{f} with an *ideal low-pass-filter* (see [69]). The most famous low-pass-filter for perfect reconstruction is the sinc function as shown in Figure 3.4.

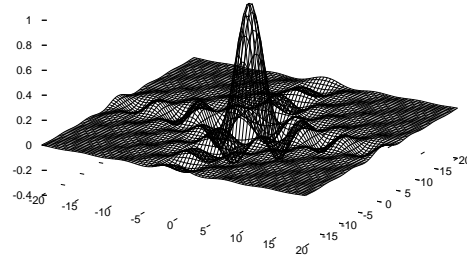


Figure 3.4. The graph of the sinc function (here defined on \mathbb{R}^2) is shown for values $(x, y) \in [-20, 20] \times [-20, 20]$.

In two dimensions it is defined by $\text{sinc}(0, 0) = 1$ and

$$\text{sinc}(x, y) := \frac{\sin(x) \sin(y)}{xy} \quad \text{for all } (x, y) \in \mathbb{R}^2 \setminus \{(0, 0)\}.$$

Because of its unbounded support this reconstruction filter can not be implemented. Hence it is natural to use filters similar to the sinc function but with bounded support. Also we want to preserve the orthogonal separability $W(x, y) = W(x)W(y)$. The following is a collection of suitable filters:

- a) One commonly used reconstruction filter is a truncation of the sinc function.
- b) The function W_0 as defined in Equation 3.9 is called *square function*. The convolution with W_0 leads to the simplest form of the so called *waveform interpolations*.
- c) The triangle function $W_1 := W_0 * W_0$ has pyramid shape. It can be shown (e.g. see [60]) that the interpolation with pyramid functions is equivalent to the bilinear spline interpolation (e.g. see Figure 3.5).
- d) The bell function W_2 is a convolution of W_0 and W_1 .
- e) We could easily enlarge this list by defining $W_{i+1} := W_0 * W_i$ for $i \geq 2$. The last example we mention in this context is the well known cubic

B-spline $W_3 := W_0 * W_2$ shown in Figure 3.6 (see [67] for more details).

f) We finish with the Gaussian function

$$\phi_\sigma(x, y) := \frac{1}{2\pi\sigma^2} \exp\left(-\frac{x^2 + y^2}{2\sigma^2}\right), \quad (3.10)$$

which is also used in a truncated version.

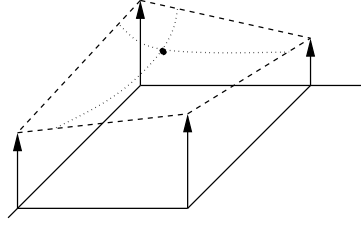


Figure 3.5. The Figure shows an example for a linear interpolation along separable orthogonal coordinates called bilinear interpolation. As we can see, the bilinear interpolation does not provide planar surfaces in general.

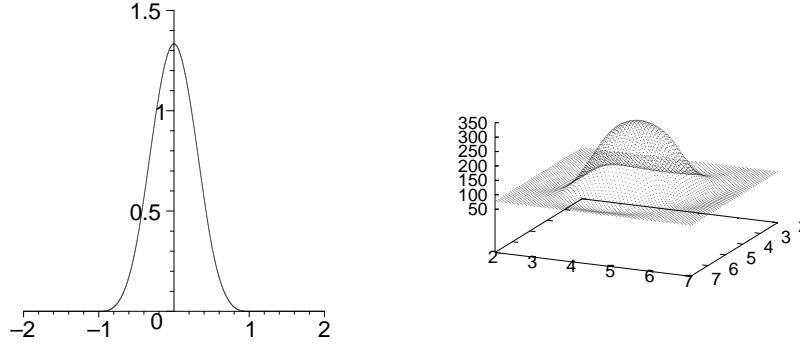


Figure 3.6. One- and two-dimensional cubic B-spline with equidistant node points $z_0 = -1, z_1 = -0.5, z_2 = 0, z_3 = 0.5, z_4 = 1$ in the one-dimensional case. The two-dimensional spline is just the tensor product of the one-dimensional with two orthogonal directions. The area between curve and x -axis respective xy -plane is normalised.

The functions W_i are strictly positive for (x, y) in the square $(-2^{-1}-i, 2^{-1}+i) \times (-2^{-1}-i, 2^{-1}+i)$ and equal to 0 outside, which is convenient for computations.

On the other hand this means that for sufficiently large $i \in \mathbb{N}$, depending on the distance between the sample points, the translated support of W_i contains more than one $(x, y) \in \mathbb{R}^2$ with $\mathbb{F}(x, y) \neq 0$. In other words, the convolution of W_i and \mathbb{F} depends not only on $\mathbb{F}(i, j)$ for one single sensor value (i, j) . By a closer look at the reconstruction mechanism presented in this work obviously this means that the reconstructed value at a given sample point is affected by its neighbour. In our case the distance between the sample points is one and so this holds for all $i \geq 1$ and is not true for $i = 0$. But we can easily avoid this effect by rescaling the functions W_i . Without loss of generality we suppose from now on

$$\{x_1^c, \dots, x_n^c\} \times \{y_1^c, \dots, y_m^c\} = \{(i, j) | i, j \in \{1, \dots, n\}\}.$$

The function was sampled at a square part of the 2-dimensional \mathbb{N} -grid. We set $i = 3$ and scale W_3 as follows. For every element $(x, y) \in \mathbb{R}^2$ and every $\epsilon > 0$ (sufficiently small) we define $w_3(x, y) := SW_3(sx, sy)$, where

$$s > \left(\frac{49n^2 \mathbb{F}_{\max}}{n^2 \mathbb{F}_{\max} - \epsilon} \right)^{\frac{1}{2}} \quad \text{and} \quad S^{-1} := \int_{\mathbb{R}} \int_{\mathbb{R}} W_3(sx, sy) dx dy.$$

Lemma 3.3.6. *In the notation used above it is $\int_{\mathbb{R}} \int_{\mathbb{R}} w_3(x, y) dx dy = 1$ and $\text{supp}(w_3) = \{(x, y) \in \mathbb{R}^2 | \|(x, y)\|_{\max} < 7(2s)^{-1}\}$.*

Both properties are obvious by the definition of w_3 and the scale factors s, S .

Lemma 3.3.7. *For all $1 \leq i, j \leq n$ it is $(\hat{\mathbb{F}} * w_3)(i, j) = \mathbb{F}(i, j)$.*

Proof. The statement follows from the fact that we scaled W_3 in order to decrease its support (see Figure 3.7). ■

Lemma 3.3.8. *Let $\hat{\mathbb{F}}$ be a piecewise constant version of an image. In the notation of this section, the difference*

$$d = \int_D |(\hat{\mathbb{F}} * w_3)(x, y) - \hat{\mathbb{F}}(x, y)| dx dy$$

is smaller than ϵ .

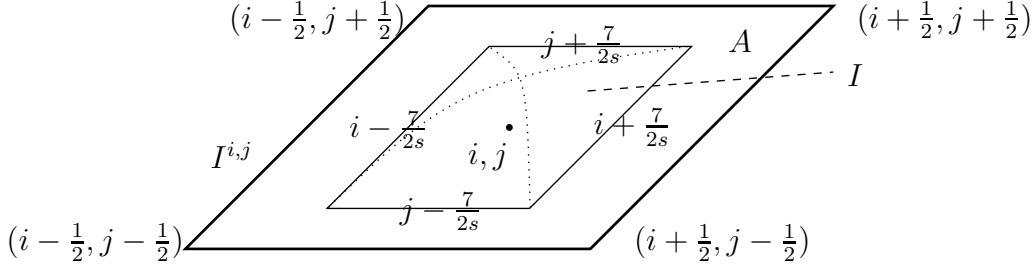


Figure 3.7. The function w_3 is centred on $[x_{i-1}, x_i] \times [y_{j-1}, y_j]$. As we can see, there is no interaction with sample points of neighbour squares.

Proof. First we note that

$$d = \sum_{i,j=1}^{n-1} \int_{I_{i,j}} |(\hat{\mathbb{F}} * w_3)(x, y) - \hat{\mathbb{F}}(x, y)| dx dy,$$

where $I_{i,j} := [i, i+1) \times [j, j+1)$. Hence it is sufficient to prove that each addend is smaller than $n^{-2}\epsilon$. For this purpose we define

$$\tilde{I}_{i,j} := (i + \frac{7}{2s}, i + 1 - \frac{7}{2s}) \times (j + \frac{7}{2s}, j + 1 - \frac{7}{2s})$$

as subset of \mathbb{R}^2 (shown in Figure 3.7). Because of

$$\int_{\tilde{I}_{i,j}} |(\hat{\mathbb{F}} * w_3)(x, y) - \hat{\mathbb{F}}(x, y)| dx dy = 0$$

we get an estimate for the difference $n^{-2}d$ by integration over $A_{i,j} := I_{i,j} \setminus \tilde{I}_{i,j}$ (see Figure 3.8). The area of $A_{i,j}$ is less or equal $1 - \frac{49}{s^2}$ and the maximum value the integrand can take is equal or less than \mathbb{F}_{\max} . It follows

$$d \leq n^2 \int_{A_{i,j}} |(\hat{\mathbb{F}} * w_3)(x, y) - \hat{\mathbb{F}}(x, y)| dx dy \leq (1 - \frac{49}{s^2}) \mathbb{F}_{\max} < \epsilon. \quad \blacksquare$$

Remark. If we interpret smooth versions produced by convolution of \mathbb{F} and w_3 , defined as above, as an digital image by integration over the pixel areas and quantisation of the integral values by rounding them to integer, we receive the image function \mathbb{F} .

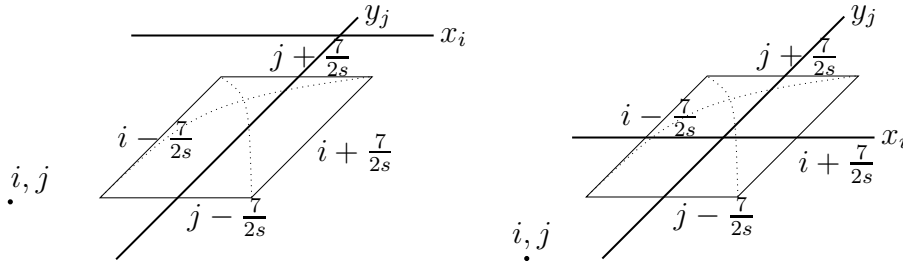


Figure 3.8. Here w_3 is centred on the borderline between two squares. The maximum of the integral can be reached if four pixels are involved as shown in the second case.

3.3.2 Spline interpolation

Another popular method providing smooth versions $\tilde{\mathbb{f}}$ of a given image \mathbb{f} is the *spline interpolation*. In Chapter 4 we will use this method so we give a short resume. For detailed informations see [17].

Definition 3.3.9. For $n \in \mathbb{N}$ we consider the points $x_0 < \dots < x_n$ in \mathbb{R} and take $K := \{x_i | i = 0, \dots, n\}$. Further we denote by

$$\Pi_m := \left\{ f : \mathbb{R} \rightarrow \mathbb{R} \mid \exists \alpha_i \in \mathbb{R}, i = 1, \dots, m : f(x) = \sum_{i=1}^m \alpha_i x^{i-1} \right\}$$

the set of *polynomials of order m* and define for $n > 1$, $m \geq 1$ the set

$$S_{m,n}(K) := \{f \in \overline{C_{m-1}}([x_0, x_n]) \mid \exists p_i \in \Pi_{m+1} : f|_{(x_{i-1}, x_i)} = p_i|_{(x_{i-1}, x_i)}, 1 \leq i \leq n\},$$

which is called *spline space of degree m with n - 1 inner nodes*.

In order to make explicite computations it is necessary to have a convenient basis of $S_{m,n}$. Therefore we give the next definition which (in a similar version) was introduced in [67] and is widely used today.

Definition 3.3.10. Let f denote a function defined at least at the $n + 1$ distinct points $\{x_0, \dots, x_n\}$ and k an element of $\{1, \dots, n\}$. Then for every $0 \leq i \leq n - k$ we define the *k-th divided difference* of the the function f at the

points x_i, \dots, x_{i+k} recursively by

$$\Delta[x_i, \dots, x_{i+k}; f] := \frac{\Delta[x_i, \dots, x_{i+k-1}; f] - \Delta[x_{i+1}, \dots, x_{i+k}; f]}{x_i - x_{i+k}}$$

with

$$\Delta[x_i; f] := f(x_i).$$

Furthermore for every $x \in \mathbb{R}$ we define the *truncated power function in x_i* by $(x - x_i)_+ := \max\{0, (x - x_i)\}$. Finally the i -th (normalised) B -spline of order k is defined by

$$B_{k,i}(x) := (-1)^{m+1} \Delta[x_i, \dots, x_{i+k}; (x - \cdot)_+^k], \quad \text{for } x \in \mathbb{R}. \quad (3.11)$$

As we know for every element $s \in S_{m,n}(K)$ there exist b_{-m}, \dots, b_{n-1} in \mathbb{R} such that $s(x) = \sum_{i=-m}^{n-1} b_i B_{m,i}(x)$ as shown in [17, 67]. For this representation one has to introduce the additional points $x_{-m}, \dots, x_{-1}, x_{n+1}, \dots, x_{n+m}$ and define the values of the function f at those points in an appropriate way (if they are not given). Note that neither the additional sample points have to be inside $[x_0, x_n]$ nor have they to be distinct. Again, for a detailed discussion how these additional sample points have to be chosen in order to reach a specific spline interpolation we refer to [17]. Here we just remark that the number of necessary nodes to reach an interpolation as element of $\overline{C_2}([x_0, x_n])$ is still $n+1$. To see this we remind that an element s of $S_{m,n}(K)$ consists of n polynomial pieces of order $m+1$. Hence s has $n(m+1)$ degrees of freedom. On the other hand the function s has to be $m-1$ times continuously differentiable so the polynomial pieces have to fulfil

$$\frac{d^k p_i}{dx^k}(x_i) = \frac{d^k p_{i+1}}{dx^k}(x_i) \quad \text{for } 0 \leq k \leq m-1, 1 \leq i \leq n-1.$$

These are $m(n-1)$ equations leading to $m+n$ degrees of freedom left for the determination of s . Now we simply choose $x_{-1} := x_0, x_{n+1} := x_n$ and claim

$$\frac{\partial f}{\partial x}(x_0) = \frac{\partial f}{\partial x}(x_n) = 0$$

leading to the *cubic spline interpolation for f on $[x_0, \dots, x_n]$ with Neumann*

boundary condition. To adjust the Dirichlet boundary condition we can choose $x_{-1} := 2x_0 - x_1$ and $x_{n+1} = 2x_n - x_{n-1}$. Then we define the function values $f(x_{-1}) = f(x_{n+1}) = 0$. We note that we end with two additional conditions naturally arising in both cases. This leads to $m + n - 2$ degrees of freedom for $s \in S_{m,n}$ with appropriate boundary conditions. Finally we set $m = 3$ therewith $s \in S_{m,n}$ is an element of $\overline{C}_2([x_0, x_n])$. So with the information given by the $n+1$ function values $f(x_i)$ we can provide $s \in \overline{C}_2([x_0, x_n])$ with Dirichlet or Neumann boundary conditions.

Remark. The additional nodes and the assignment of the function values described above is equivalent to the image enlargement procedure (p. 80) we apply to the image functions in order to reach either Dirichlet or Neumann boundary conditions.

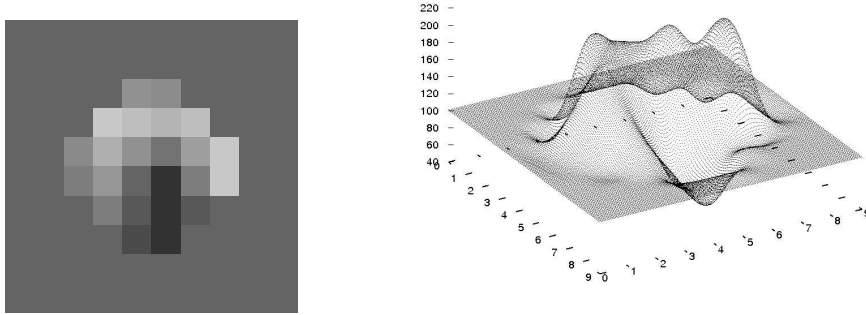


Figure 3.9. Given the test pattern f shown in the left image we built a 2-times continuously differentiable function \tilde{f} . The right image shows \tilde{f} sampled equidistant with 400 sample points per pixel.

Now we give some properties of spline interpolations in general, taken from [17].

Theorem 3.3.11. *Let $s \in \overline{C}_2(D)$ denote the cubic spline interpolation of f on K as introduced above. Then for every $g \in \overline{C}_2(D)$ with $g(x_i) = f(x_i)$ for $i = 0, \dots, n$ it is*

$$\int_{x_0}^{x_n} \left(\frac{\partial^2 f}{\partial x^2} \right)^2 dx \leq \int_{x_0}^{x_n} \left(\frac{\partial^2 g}{\partial x^2} \right)^2 dx.$$

So using cubic splines we are able to produce interpolations which minimise the L^2 -norm of its second derivative. Moreover we denote by $\Pi_2(K)$ the set of all functions p defined on $[x_0, x_n]$ where $p|_{[x_{i-1}, x_i]}$ is linear. Further we define the difference of some function h to the set $\Pi_2(K)$ by

$$\text{dist}(h, \Pi_2(K)) := \inf_{p \in \Pi_2(K)} \max_{x \in [x_0, x_n]} |h(x) - p(x)|.$$

Then we can give the following inequality

$$\max_{x \in [x_0, x_n]} |f(x) - s(x)| \leq \max_{i=1, \dots, n} |x_i - x_{i-1}|^2 \text{dist}\left(\frac{\partial^2 f}{\partial x^2}, \Pi_2(K)\right)$$

for the distance between f and s . We do not go into a detailed discussion of all known properties of s now. Instead we turn to the construction of two-dimensional interpolations from the one-dimensional ones.

For example, if we consider the points $\{(i, j) | 1 \leq i, j \leq n\}$ as the sample points of an image function \mathbb{F} , then for $(x_0, y_0) \in [0, n]^2$ we get an interpolated function value $\tilde{\mathbb{F}}(x_0, y_0)$ as follows. First we produce n one dimensional interpolations f_1, \dots, f_n using the function values

$$\{\mathbb{F}(1, 1), \dots, \mathbb{F}(1, n)\}, \{\mathbb{F}(2, 1), \dots, \mathbb{F}(2, n)\} \dots, \{\mathbb{F}(n, 1), \dots, \mathbb{F}(n, n)\}.$$

Then we get n new function values $f_1(y_0), \dots, f_n(y_0)$ sampled at $x = 1, \dots, n$. Finally we get the desired function value $\tilde{\mathbb{F}}(x_0, y_0)$ by an interpolation of $f_1(y_0), \dots, f_n(y_0)$ and evaluation of the resulting spline at the point $x = x_0$. An example for a spline interpolated function is shown in Figure 3.9.

Remark. We remind that the boundary conditions have to be adjusted before the interpolation. This has to be done in order to get the right amount of conditions. Dirichlet and Neumann boundary conditions are suitable for this. Moreover the spline interpolated function $\tilde{\mathbb{F}}$ may take negative function values even though $\hat{\mathbb{F}}$ is strictly positive. So after the interpolation we have to translate the function values by $-\min \tilde{\mathbb{F}} + 1$ to obtain a strictly positive function. (The minimum exists because $\tilde{\mathbb{F}}$ is continuously extendable to a compactum.)

Remark. The statements given for image functions defined on $\{1, \dots, n\}^2$ generalise straight forward to image functions defined on $\{1, \dots, n\} \times \{1, \dots, m\}$.

3.4 Approximation of the derivative

As we have seen in the previous section, for every image function \mathbb{f} we can construct a spline $s \in \overline{C}_2(D)$ with appropriate boundary condition. In Chapter 4 we make use of the derivatives of s , so the question arises how to compute them. Certainly it is easy to compute derivatives of all elements of the spline space $S_{m,n}$ if we know derivatives of the basis elements. But for this it is not very convenient to use the definition of B-splines as given in Equation 3.11. So in the notation used in the section before we give the following theorem.

Theorem 3.4.1. *Let K denote the set of points x_0, \dots, x_n . Then for $n \geq 2$ and $m \geq 1$ the functions in $s_{m,n} := \{1, x, \dots, x^m, (x - x_1)_+^m, \dots, (x - x_{n-1})_+^m\}$ constitute a basis of $S_{m,n}(K)$.*

We omit the proof of the statement above. Indeed it is very simple and can be done by direct calculation. We just remark that the statement above implies that for every $s \in S_{m,n}(K)$ exist uniquely determined values $\alpha_0, \dots, \alpha_{m+1}$ and $\beta_1, \dots, \beta_{n-1}$ such that

$$s(x) = \sum_{i=0}^{m+1} \alpha_i x^i + \sum_{j=1}^{n-1} \beta_j (x - x_j)_+^m.$$

From this equation we can easily compute the derivative of s . Unfortunately, after all, in the worst case this means evaluation of $m + n$ terms to get the derivative at one position. So we look for a possibility to approximate the derivative of s with less computation effort. Therefore we make use of the discrete image function \mathbb{f} from which we built the spline. If we define the discrete derivative in the usual way we get an approximation of the derivative of s as shown in Figure 3.10.

Definition 3.4.2. For every image function $\mathbb{f} : \{1, n\} \times \{1, n\} \rightarrow \mathbb{R}$ we define for all sample points (i, j) with $2 \leq i \leq n-1$, $1 \leq j \leq n$ the discrete derivative with respect to the first variable by

$$\frac{\partial \mathbb{f}}{\partial x}(i, j) := \frac{\mathbb{f}(i+1, j) - \mathbb{f}(i-1, j)}{2}.$$

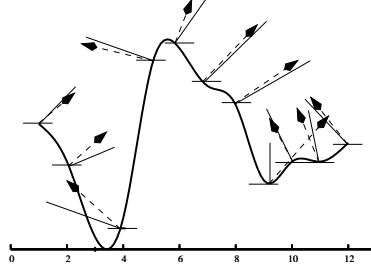


Figure 3.10. The image values given at 12 distinct sample points were interpolated using a cubic spline. The dashed arrows show the direction of the discrete derivative. The derivative of the cubic spline is indicated as a black line with now arrowhead, so we can compare it to the discrete derivative.

For $1 \leq i \leq n$, $2 \leq j \leq n - 1$ we define the derivative with respect to the second variable by

$$\frac{\partial \mathbb{F}}{\partial y}(i, j) := \frac{\mathbb{F}(i, j + 1) - \mathbb{F}(i, j - 1)}{2}.$$

At the left border we set

$$\frac{\partial \mathbb{F}}{\partial x}(1, j) := \mathbb{F}(2, j) - \mathbb{F}(1, j) \quad \text{for } j = 1, \dots, n$$

whereas we define the derivative at the right border as

$$\frac{\partial \mathbb{F}}{\partial x}(n, j) := \mathbb{F}(n, j) - \mathbb{F}(n - 1, j) \quad \text{for } j = 1, \dots, n.$$

Finally, for $i = 1, \dots, n$ on the lower border we take

$$\frac{\partial \mathbb{F}}{\partial y}(i, 1) := \mathbb{F}(i, 2) - \mathbb{F}(i, 1)$$

whereas on the upper border we set

$$\frac{\partial \mathbb{F}}{\partial y}(i, n) := \mathbb{F}(i, n) - \mathbb{F}(i, n - 1).$$

In order to get better approximations to the derivatives of s we do the same as we would do in order to get splines closer to the piecewise constant version

of \mathbb{f} , denoted by $\hat{\mathbb{f}}$ (see Definition 3.3.1). We simply divide the sensor square into n^2 squared pieces of equal size and introduce new sample points as shown in Figure 3.11. The function values at the sample points arising from sensor square (i, j) are set to $\mathbb{f}(i, j)$. Then we apply the discrete derivative to the new image function sampled in the x - and y -direction at

$$\{1, 1_1, \dots, 1_n, 2, 2_1, \dots, 2_n, 3, \dots, n-1, (n-1)_1, \dots, (n-1)_n, n\}.$$

In Figure 3.12 we have shown the result of this method which pays more respect to the structure of the image. Using more than three sub-pixels does

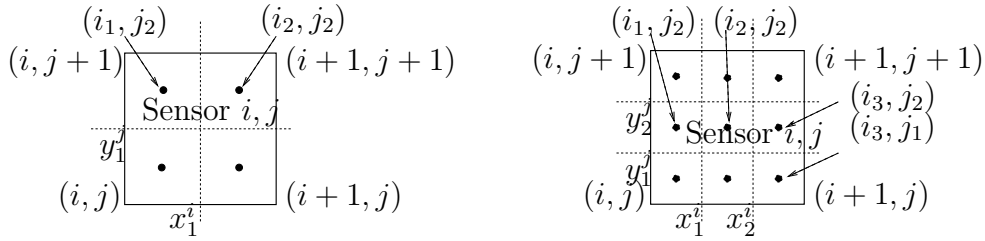


Figure 3.11. The pixel i, j is divided into four respectively nine sub-pixels. For each sub-pixel we get a new sample point associated to the midpoint of the sub-pixel. We denoted some examples of them. The function value associated to this is of course equal to $\mathbb{f}(i, j)$.

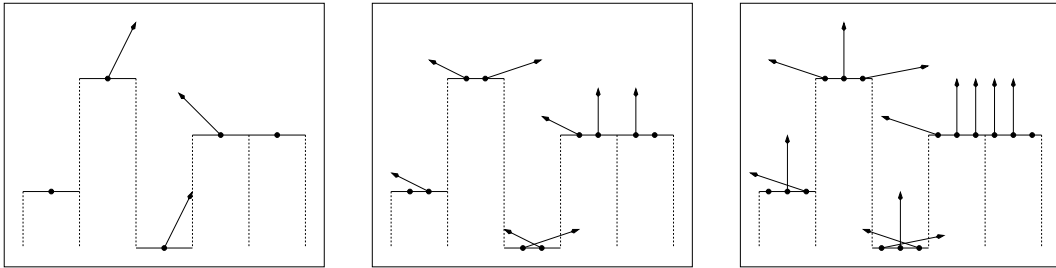


Figure 3.12. According to the division of one pixel into four respectively nine sub-pixels as shown in Figure 3.11 here we have an example for the resulting derivatives in one direction.

not improve the precision of the discrete derivative. It leads to a derivative which is zero on the main part of the original pixel, whereas the derivative at the border of each pixel remains constant.

3.5 Error considerations

Of course one part of every theoretical treatment of an algorithmic application should be the consideration of the error which is implied by the approximation of continuously defined objects or limits. We are interested in the solution $u(t, x)$ of a Cauchy problem as defined in Theorem 2.6.4. Actually we are interested in the limit of $u(t, x)$ for $t \rightarrow \infty$ but in the previous sections we discussed approximations of $u(T, x)$ for some fix $T \geq 0$. So in the following section we look at the distance between $u(T, x)$ and $u(\infty, x)$ which is one source of impreciseness. Another one arises from the fact that we represent u as the expectation of $\frac{f_0}{f_\infty}(X_t)$. Here $(X_t|t \geq 0)$ denotes an Itô diffusion on the bounded convex region $\overline{D} \subset \mathbb{R}^d$ and $\frac{f_0}{f_\infty} \in \overline{C_2}(D)$. In Section 3.5.2 we briefly resume some well known results about the approximation of the expectation and the resulting error. Finally the process X_t will be approximated as described in Section 3.1, which leads to the discrepancy we discuss in Section 3.5.3. After all it will be clear that we are theoretically able to adjust the approximation such that the resulting error is below a given threshold with a desired probability.

3.5.1 Distance from the limit

In this section we are interested in $\epsilon_T(x) := \lim_{t \rightarrow \infty} |u(T, x) - u(t, x)|$ where $u(t, x)$ is the solution of the Cauchy problem

$$\frac{\partial u}{\partial t}(t, x) = -Au(t, x) \quad \text{for } t \geq 0, x \in D, \quad (3.12)$$

with initial condition

$$u(0, \cdot) = \frac{f_0}{f_\infty} \in \overline{C_2}(D).$$

The operator A is defined by

$$Au := \sum_{i=1}^d b_i \frac{\partial u}{\partial x_i} - \frac{1}{2} \sum_{i,j=1}^d (\sigma \sigma^\top)_{i,j} \frac{\partial^2 u}{\partial x_i \partial x_j}$$

for every u in the domain $\mathcal{D}_A := \{f \in \overline{C_2}(D) | \forall x \in \partial D : \forall \nu \in \mathcal{N}_x : \frac{\partial f}{\partial \nu}(x) = 0\}$.

As usual we assume the coefficients b and σ to be chosen such that the solution

u is unique. Theorem 2.3.12 tells us that A has a purely discrete point spectrum and the smallest eigenvalue is 0. We denote the eigenvalues of A by $(\lambda_k | k \in \mathbb{N}_0)$ with $\lambda_k \in \mathbb{R}_{\geq 0}$ and the corresponding eigenfunctions by $(v_k | k \in \mathbb{N}_0)$, which is an ortho normal basis of $\overline{C_2}(D)$ as we know from the argument leading to Theorem 2.7.2. Thus for every $\frac{f_0}{f_\infty} \in \overline{C_2}(D)$ we can find a sequence $(\alpha_k | k \in \mathbb{N}_0)$ of values in \mathbb{R} such that

$$\exp(-tA) \frac{f_0}{f_\infty} = \sum_{k \in \mathbb{N}_0} \exp(-t\lambda_k) \alpha_k v_k.$$

Moreover the function $\exp(-tA) f_0 f_\infty^{-1}$ solves the Cauchy problem 3.12 and by uniqueness of the solution u follows

$$\epsilon_T = \lim_{t \rightarrow \infty} \left| \sum_{k \in \mathbb{N}_0} (\exp(-T\lambda_k) - \exp(-t\lambda_k)) \alpha_k v_k(x) \right|.$$

Finally we note that $\lim_{t \rightarrow \infty} \exp(-t\lambda_k) \alpha_k v_k(x) = \alpha_0 v_0(x)$ (as we know from Theorem 2.7.2), which leads to $\epsilon_T(x) \leq \sum_{k \in \mathbb{N}} |\exp(-T\lambda_k) \alpha_k v_k(x)|$ for every $x \in D$ as an error estimate for the distance to the limit.

3.5.2 Error from Monte Carlo integration

Today *Monte Carlo integration* is a frequently used approximation tool and many theoretical results exist (e.g. [22, 32]). We use a very simple approach derived from the strong law of large numbers (see [10]). This states that for every sequence $(Z_k | k \in \mathbb{N})$ of independent, identically distributed (i.i.d.), integrable, real random variables, the term

$$\frac{1}{n} \sum_{k=1}^n Z_k$$

converges for $n \rightarrow \infty$ a.s. to $\mathbb{E}[Z_1]$. In our case the random variable Z_k is given by the k -th simulation of an approximation of $f(X_T)$, denoted by $f(X_T^k)$, and its expectation is $\mathbb{E}[f(X_T)] = u(T, x)$. So if we define the random variable

$$\epsilon_M := \frac{1}{n} \sum_{k=1}^n f(X_T^k) - u(T, x)$$

it follows with Chebyshev's inequality for every $\epsilon > 0$ the estimate

$$p_\epsilon := P\left(\left|\frac{1}{n} \sum_{k=1}^n f_0(X_T^k) - u(T, x)\right| > \epsilon\right) \leq \frac{\sigma}{\epsilon^2}$$

where $\sigma := \mathbb{E}\left[\left(\frac{1}{n} \sum_{k=1}^n f_0(X_T^k)\right)^2\right] - u(T, x)^2$ is the variance of ϵ_M . Another possibility to estimate the probability p_ϵ is given by the well known *central limit theorem*, which is proven under different assumptions on the sequence of random variables. In the case of square integrable, i.i.d. random variables with strictly positive variance once more we refer to [10] for a proof of this theorem. If we apply the central limit theorem to our situation we can see, that ϵ_M converges in distribution to a $\mathcal{N}(0, \sigma)$ -distributed random variable. Thus we are able to approximate p_ϵ by

$$1 - \frac{1}{\sqrt{2\pi\sigma^2}} \int_{-\epsilon}^{\epsilon} \exp\left(\frac{-x^2}{2\sigma^2}\right) dx = \frac{2}{\sqrt{2\pi\sigma^2}} \int_{-\infty}^{-\epsilon} \exp\left(\frac{-x^2}{2\sigma^2}\right) dx$$

where the equality follows from the symmetry of $\exp(x^2/2\sigma^2)$. Finally in our case we can apply a theorem of Hoeffding (see [22]), because we just deal with bounded random variables. From this follows the estimate $p_\epsilon < 2\exp(-2n\epsilon^2)$.

3.5.3 Convergence rate of the projection scheme

The last approximation error we discuss in this chapter is the difference between the Itô diffusion process X_t at time $t = T > 0$ and its approximation $X_{T,n}$, denoted by

$$\epsilon_S := |X_{T,n} - X_T|.$$

Actually we introduced several different approximation schemes for Itô diffusions in a bounded region in Section 3.1. Hence we should give error estimates for each of them but we do not go into detail here. Instead we use a statement from [73] which tells us that one of these $X_{T,n}$ converges path-wise to X_T and is formulated as follows.

Theorem 3.5.1. *Let $X_{t,n}$ denote the projection scheme approximation of the Itô diffusion X_t as defined in Theorem 3.1.2. If the coefficient functions b and*

σ of X_t are Lipschitz continuous and the region D is convex then

$$n^{1/4-\epsilon} \sup_{t \leq q} |X_{t,n} - X_t|$$

converges for every $q \in \mathbb{R}_{\geq 0}$ a.s. to 0.

On the other hand we are just interested in $\mathbb{E}[f(X_t)]$, where f is continuous. Thus it is sufficient to use Theorem 3.2 from the same author. It states that for every $m \in \mathbb{N}$, $q \in \mathbb{R}_{\geq 0}$ there exists a constant $c > 0$ such that

$$\mathbb{E} \left[\sup_{t \leq q} |X_{t,n} - X_t|^{2m} \right] \leq c \left(\frac{\ln n}{n} \right)^{m/2}.$$

From this we derive the error bound $\epsilon_S \leq c \sqrt{n^{-1} \ln n}$.

Chapter 4

Applications

In this chapter we describe the *transformation algorithm* for the transformation of a start image \mathbb{F}_0 into a stop image \mathbb{F}_∞ , derived from the theory introduced in the chapters before. Afterwards we illustrate the basic functionality of our image transformation method and introduce a fast transformation algorithm. Then we apply the fast transformation algorithm to the problems of *edge enhancement*, *image smoothing* and *de-noising*. We start with a resume of our results, given from an image processing viewpoint. Therefore now and in the following we consider smooth versions of image functions $\tilde{\mathbb{F}} : D \rightarrow \mathbb{R}_{>0}$ which are two times continuous differentiable on $D := (0, x_n) \times (0, y_m) \subset \mathbb{R}^2$. Further the function $\tilde{\mathbb{F}}$ is assumed to fulfil the strong Neumann boundary condition with constant 0 as defined in Section 2.2. Moreover $\tilde{\mathbb{F}}$, its first derivative and second derivative are extendable to \overline{D} as continuous functions. In Section 3.3 we saw how to obtain such functions from the information \mathbb{F} , given on the discrete points

$$D_{\text{disc}} := \{(x_i, y_j) | 1 \leq i \leq n, 1 \leq j \leq m\} \subset D,$$

provided by usual sensors such as CCDs or APSs.

For two given images $\tilde{\mathbb{F}}_0, \tilde{\mathbb{F}}_\infty$ we define the operator $L := -\frac{1}{2}\Delta - \frac{\nabla \tilde{\mathbb{F}}_\infty}{2\tilde{\mathbb{F}}_\infty} \nabla$ and state the Cauchy problem

$$\frac{du}{dt} = -Lu \tag{4.1}$$

with initial condition $u(0) = \frac{\tilde{\mathbb{F}}_0}{\tilde{\mathbb{F}}_\infty} \in \overline{\mathcal{C}_2(D)}$, as described in Section 2.6 (p. 62). Now we denote by $X_t^{(x,y)}$ an Itô diffusion on \overline{D} starting at $(x, y) \in D$ with diffusion coefficient $\sigma = -I_2$ and drift coefficient

$$b(x, y) = -\frac{1}{\tilde{\mathbb{F}}_\infty(x, y)} \left(\frac{\partial \tilde{\mathbb{F}}_\infty}{\partial x}, \frac{\partial \tilde{\mathbb{F}}_\infty}{\partial y} \right)(x, y) \quad \text{for } (x, y) \in \overline{D}.$$

Then we know from Section 2.7 that for all $t \in \mathbb{R}_{\geq 0}$ the function

$$\begin{aligned} u(t, x, y) &:= \exp(-tL) \frac{\tilde{\mathbb{F}}_0}{\tilde{\mathbb{F}}_\infty}(x, y) \\ &= \mathbb{E} \left[\frac{\tilde{\mathbb{F}}_0}{\tilde{\mathbb{F}}_\infty}(X_t^{(x,y)}) \right] \end{aligned} \tag{4.2}$$

is a solution of the Cauchy Problem 4.1. Moreover we are able to approximate this solution by $u_k(t = s\Delta t, x, y)$ as we have seen in Section 3.2. Here $k \in \mathbb{N}$ is the number of Monte Carlo simulations we perform to approximate the expectation in Equation 4.2. The notation $t = s\Delta t$ indicates that the reflected Itô diffusion $X_t^{(x,y)}$ starting in $(x, y) \in D$ is approximated with equidistant step size $\Delta t \in \mathbb{R}_{>0}$ and $s \in \mathbb{N}$ number of steps. Now we define

$$\mathbb{F}_t^{\Delta t, k}(x, y) = u_k(t = s\Delta t, x, y) \mathbb{F}_\infty(x, y) \quad \text{for } (x, y) \in D_{\text{disc}} \tag{4.3}$$

as the *state of transformation* at time t . From Theorem 1.3.1 and the argument given in Section 3.2 we know that

$$\lim_{t \rightarrow \infty} \mathbb{F}_t^{\Delta t, k}(x, y) \approx \mathbb{F}_\infty(x, y) \quad \text{for } (x, y) \in D_{\text{disc}}$$

up to the multiplicative strictly positive constant

$$c := (\tilde{\mathbb{F}}_0, \tilde{\mathbb{F}}_\infty)_{L^2(D, \lambda^d)}.$$

Actually the image of D_{disc} under $\mathbb{F}_t^{\Delta t, k}$ may not only contain integers. This means $\mathbb{F}_t^{\Delta t, k}$ is not an image function. In order to obtain an image function we project the discrete image values of $\mathbb{F}_t^{\Delta t, k}$ to \mathbb{N}_0 by rounding them (u_k is non-negative). By $\text{int}(x)$ we denote this rounded value of $x \in \mathbb{R}$. Then we

$$\mathbb{F}_t(x, y) := \min\{256, \max\{1, \text{int}\left(\frac{\mathbb{F}_t^{\Delta t, k}(x, y)}{c}\right)\}\}. \quad (4.4)$$

As we know from Section 3.5, the approximation parameters s , Δt and k can be chosen such that the approximation error falls short of every given error bound with a designated probability p . So if we choose s , $(\Delta t)^{-1}$ and k sufficiently large it follows

$$\lim_{t \rightarrow \infty} \mathbb{F}_t(x, y) = \mathbb{F}_\infty(x, y) \quad \text{for every } (x, y) \in D_{\text{disc}}$$

with probability p . Hence we obtain a mechanism to transform one given image $\tilde{\mathbb{F}}_0$ into another given image $\tilde{\mathbb{F}}_\infty$ and represent the state of transformation at times $t = \Delta t, 2\Delta t, \dots, s\Delta t$ by the image \mathbb{F}_t . Algorithm 4.0.1 gives the

Algorithm 4.0.1
Computation of $\mathbb{F}_t(x_i, y_i)$, $t > 0$, $(x_i, y_i) \in D_{\text{disc}}$

Require: reconstruction time $t = s\Delta t$, $c = (\tilde{\mathbb{I}}_0, \tilde{\mathbb{I}}_\infty)$
 $\{u_k(t, x_1, y_1) | 1 \leq i \leq n, 1 \leq j \leq m\}$
 /* using Algorithm 3.2.1 */

$$u_k(t = s\Delta t, x, y) = \frac{1}{k} \sum_{l=1}^k \frac{\tilde{\mathbb{f}}_0}{\tilde{\mathbb{f}}_\infty} ({}_lX_{t,\Delta t}^{(x,y)})$$

$$\begin{array}{ll}
1: & \mathbb{F}_0 \leftarrow \mathbb{F}_0 \frac{256}{\mathbb{F}_0^{\max}}, \mathbb{F}_\infty \leftarrow \mathbb{F}_\infty \frac{256}{\mathbb{F}_\infty^{\max}} \quad /* \text{ 1st optional modification } */ \\
2: & \textbf{for } i = 1 \text{ to } n, j = 1 \text{ to } m \textbf{ do} \\
3: & \quad \mathbb{F}_t(x_i, y_j) \leftarrow \text{int}(u(t, x_i, y_j) \cdot \mathbb{F}_\infty(x_i, y_j) c^{-1}) \\
4: & \textbf{end for} \\
5: & \mathbb{F}_t \leftarrow \mathbb{F}_t \frac{\mathbb{F}_\infty^{\max}}{\mathbb{F}_t^{\max}} \quad /* \text{ 1st optional modification } */ \\
6: & \mathbb{F}_t \leftarrow \mathbb{F}_t \frac{\mathbb{F}_\infty^{\text{avr}}}{\mathbb{F}_t^{\text{avr}}} \quad /* \text{ 2th optional modification } */
\end{array}$$

Ensure: $\{\mathbb{I}_t(x_i, y_j) | 1 \leq i \leq n, 1 \leq j \leq m\}$

corresponding strategy to compute the function \mathbb{I}_t at the whole set D_{disc} and is called *transformation algorithm*. For its implementation we use the algorithms introduced in Section 3.2. Once more we remark that in our case the lines 3

to 8 of Algorithm 3.2.2 reduce to

$$\begin{aligned} X_1 &= X_1 + b_1(X)\Delta t + \Delta B_i^1 \\ X_2 &= X_2 + b_2(X)\Delta t + \Delta B_i^2. \end{aligned}$$

4.1 Time dependent scale factor

Again we consider the function

$$u(t, x, y) := \mathbb{E} \left[\frac{\tilde{\mathbb{F}}_0}{\tilde{\mathbb{F}}_\infty}(X_t^{(x,y)}) \right] \quad \text{for } (x, y) \in (0, x_n) \times (0, y_m), t \geq 0.$$

As we know from Section 2.7, the limit of $u(t, x, y) \mathbb{F}_\infty(x, y)c^{-1}$ for $t \rightarrow \infty$ is equal to \mathbb{F}_∞ where $c = (\tilde{\mathbb{F}}_0, \tilde{\mathbb{F}}_\infty)_{L^2(D, \lambda^d)}$ is strictly positive because both functions are strictly positive. Unfortunately it is not easy to compute c because $\tilde{\mathbb{F}}_0$ and $\tilde{\mathbb{F}}_\infty$ are spline interpolations. For this reason we introduce two different approaches avoiding the computation of $(\tilde{\mathbb{F}}_0, \tilde{\mathbb{F}}_\infty)_{L^2(D, \lambda^d)}$. Both approaches have in common that the constant c is substituted by a function $c : [0, \infty) \rightarrow \mathbb{R} \setminus \{0\}$ with $c(0) = 1$ (for some functions $\tilde{\mathbb{F}}_0$) and $\lim_{t \rightarrow \infty} c(t) = c$. For the first approach we choose

$$c(t) := \frac{\mathbb{F}_t^{\max}}{\mathbb{F}_\infty^{\max}} > 0, \quad t \geq 0, \quad (4.5)$$

where \mathbb{F}^{\max} is the maximum of $\mathbb{F}(x, y)$ for $(x, y) \in D_{\text{disc}}$. Then it is

$$\lim_{t \rightarrow \infty} c(t) = \frac{\max_{(x,y) \in D_{\text{disc}}} \lim_{t \rightarrow \infty} \mathbb{F}_t(x, y)}{\mathbb{F}_\infty^{\max}} = \frac{\max_{(x,y) \in D_{\text{disc}}} c \cdot \mathbb{F}_\infty(x, y)}{\mathbb{F}_\infty^{\max}} = c$$

and

$$\lim_{\substack{t \geq 0 \\ t \rightarrow 0}} c(t) = \frac{\mathbb{F}_0^{\max}}{\mathbb{F}_\infty^{\max}} = 1$$

if both functions reach the same maximum. This is not necessarily true but can be adjusted by rescaling (Alg. 4.0.1 Step 1). We obtain contrast spreaded images with $\mathbb{F}_0^{\max} = \mathbb{F}_\infty^{\max} = 256$. Now we modify Algorithm 4.0.1 by a final application of the factor $c(t)^{-1}$ to the transformed image function \mathbb{F}_t (Alg. 4.0.1 Step 5) and call it *transformation algorithm with maximum scale*.

Remark. If we replace the scale factor $(\tilde{\mathbb{F}}_0, \tilde{\mathbb{F}}_\infty)_{L^2(D, \lambda^d)}$ by $c(t)$ as defined in

Equation 4.5 then it is not necessary to take the minimum in the definition of the transformed image (see Equation 4.4) because $\mathbb{F}_\infty^{\max} \leq 256$. Moreover in Algorithm 4.0.1 we do not apply the int-function in Step 3. Instead we simply apply the definition of the transformed image in Step 5.

One disadvantage of this approach is that in special cases $c(t)$ and so \mathbb{F}_t depends only on a single pixel where the maximum is taken. Considering the uncertainty coming from the Monte Carlo integration, this has the potential to cause an additional approximation error. We do not go into detail here. Instead we turn to the second approach and define

$$\hat{c}(t) := \frac{\mathbb{F}_t^{\text{avr}}}{\mathbb{F}_\infty^{\text{avr}}} > 0 \quad \text{for } t \geq 0,$$

where \mathbb{F}^{avr} is the average of $\mathbb{F}(x, y)$ taken over all $(x, y) \in D_{\text{disc}}$. Similar to the first approach it is

$$\lim_{t \rightarrow \infty} \hat{c}(t) = \frac{n^{-1} \sum_{(x,y) \in D_{\text{disc}}} c \cdot \mathbb{F}_\infty(x, y)}{\mathbb{F}_\infty^{\text{avr}}} = c$$

and

$$\lim_{\substack{t \geq 0 \\ t \rightarrow 0}} \hat{c}(t) = \frac{\mathbb{F}_0^{\text{avr}}}{\mathbb{F}_\infty^{\text{avr}}} = 1$$

if both functions have the same average value. As before this is not necessarily true but can be adjusted by rescaling. Here we leave the images $\mathbb{F}_0, \mathbb{F}_\infty$ unchanged and apply $\hat{c}(t)$ in Algorithm 4.0.1 in Step 6. The resulting procedure is called *transformation algorithm with average scale*.

Remark. In Algorithm 4.0.1 we do not apply the int-function in Step 3. Instead we use the definition of the transformed image (see Equation 4.4) in Step 6.

Unlike $c(t)$ the function $\hat{c}(t)$ depends always on all values of \mathbb{F}_t . The disadvantage of this approach is that in special cases the values of the rescaled image function exceed 256. So we loose information by cutting off these values when we take the minimum of 256 and $\mathbb{F}_t \hat{c}(t)^{-1}$. On the other hand, we have more contrast because $[1, 256\hat{c}(t)]$ is spread to $[1, 256]$.

4.2 Image reconstruction

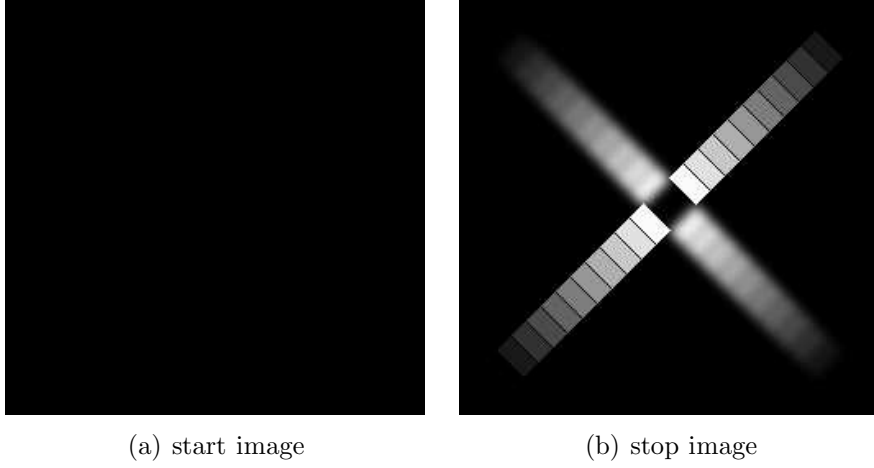


Figure 4.1. This is the first pair of images for transformation by application of the algorithm introduced in this work. The size of both has to be the same. In this case it is 256×256 Pixel.

The first thing which should be of interest (in our view) is whether we are able to reconstruct the given image \mathbb{F}_∞ . For example we consider the generic image shown in Figure 4.1(a) as the given image \mathbb{F}_0 which we call the start image and the one shown in Figure 4.1(b) as the given image \mathbb{F}_∞ we want to reconstruct. Then, according to Algorithm 4.0.1, for every $(x, y) \in D_{\text{disc}}$ we apply a Monte Carlo method to approximate $\mathbb{E}[\frac{\tilde{\mathbb{F}}_0}{\mathbb{F}_\infty}(X_{t,\Delta t}^{(x,y)})]$ by means of the average over 50 independent realisations of $X_{t,\Delta t}^{(x,y)}$. For this we use Algorithm 3.2.2 to give the independent approximations of $X_{t,\Delta t}^{(x,y)}$ we need. For **Experiment 1/1** we choose $\Delta t = 1$ (the step size of the approximating process) and use the transformation algorithm without modifications to produce six images $\mathbb{F}_{t_1}, \dots, \mathbb{F}_{t_6}$ shown in Figure 4.2. The image sequence gives a first impression of the behaviour of \mathbb{F}_t for increasing t . For simplicity we assumed $c = 1$, which is a good approximation as we will see later.

Now and in the following the average absolute value of the difference between $\mathbb{F}_t(x, y)$ and $\mathbb{F}_\infty(x, y)$ is denoted by

$$\epsilon_a := \frac{1}{|D_{\text{disc}}|} \sum_{(x,y) \in D_{\text{disc}}} |\mathbb{F}_t(x, y) - \mathbb{F}_\infty(x, y)|$$

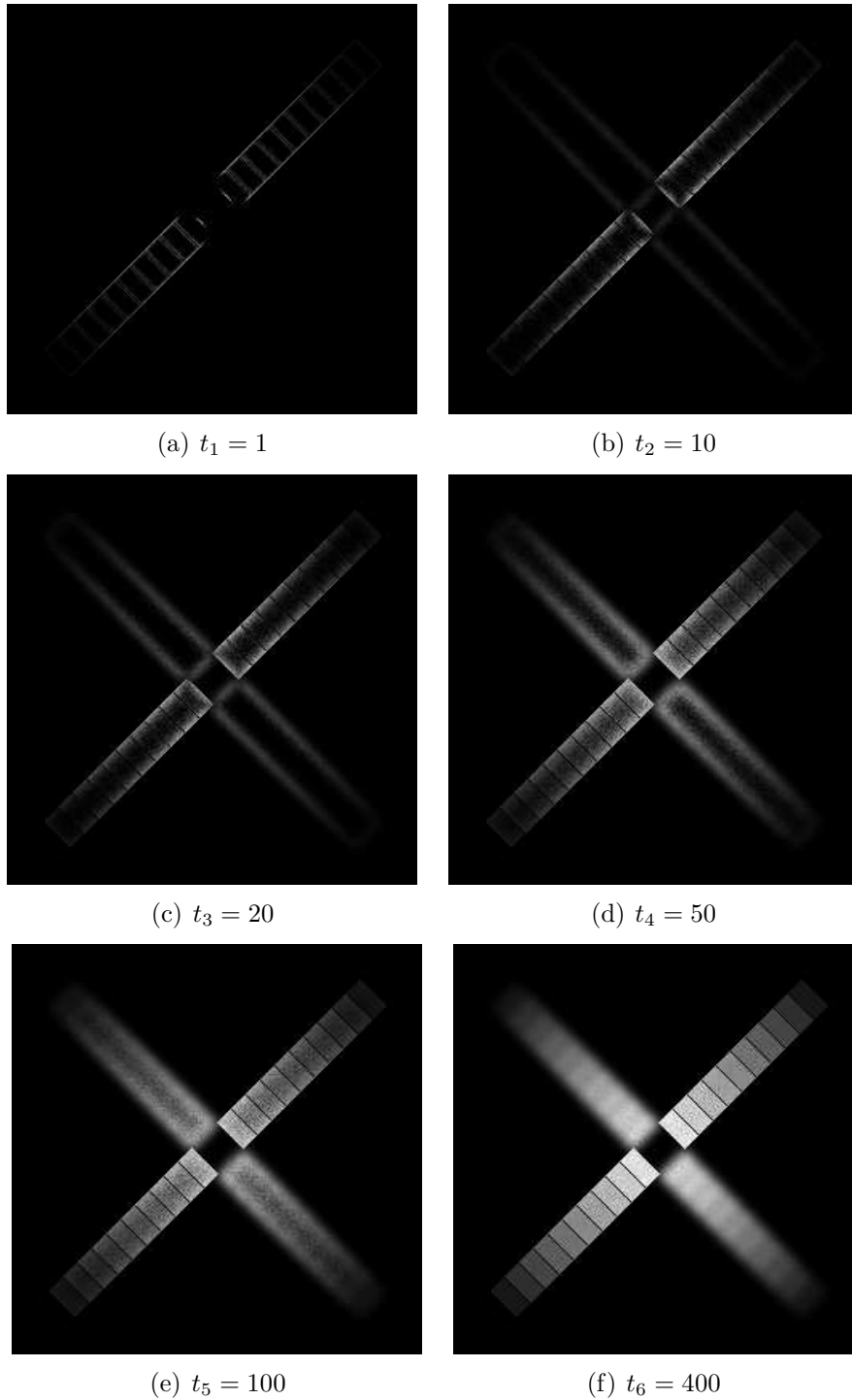


Figure 4.2. Reconstruction sequence for a simple generic image pair. We used the transformation Algorithm 4.0.1 without modifications and assumed $(\mathbb{I}_0, \mathbb{I}_\infty) = 1$ to produce these images (Experiment 1/1). All images are of size 256×256 Pixel as the start and stop image.

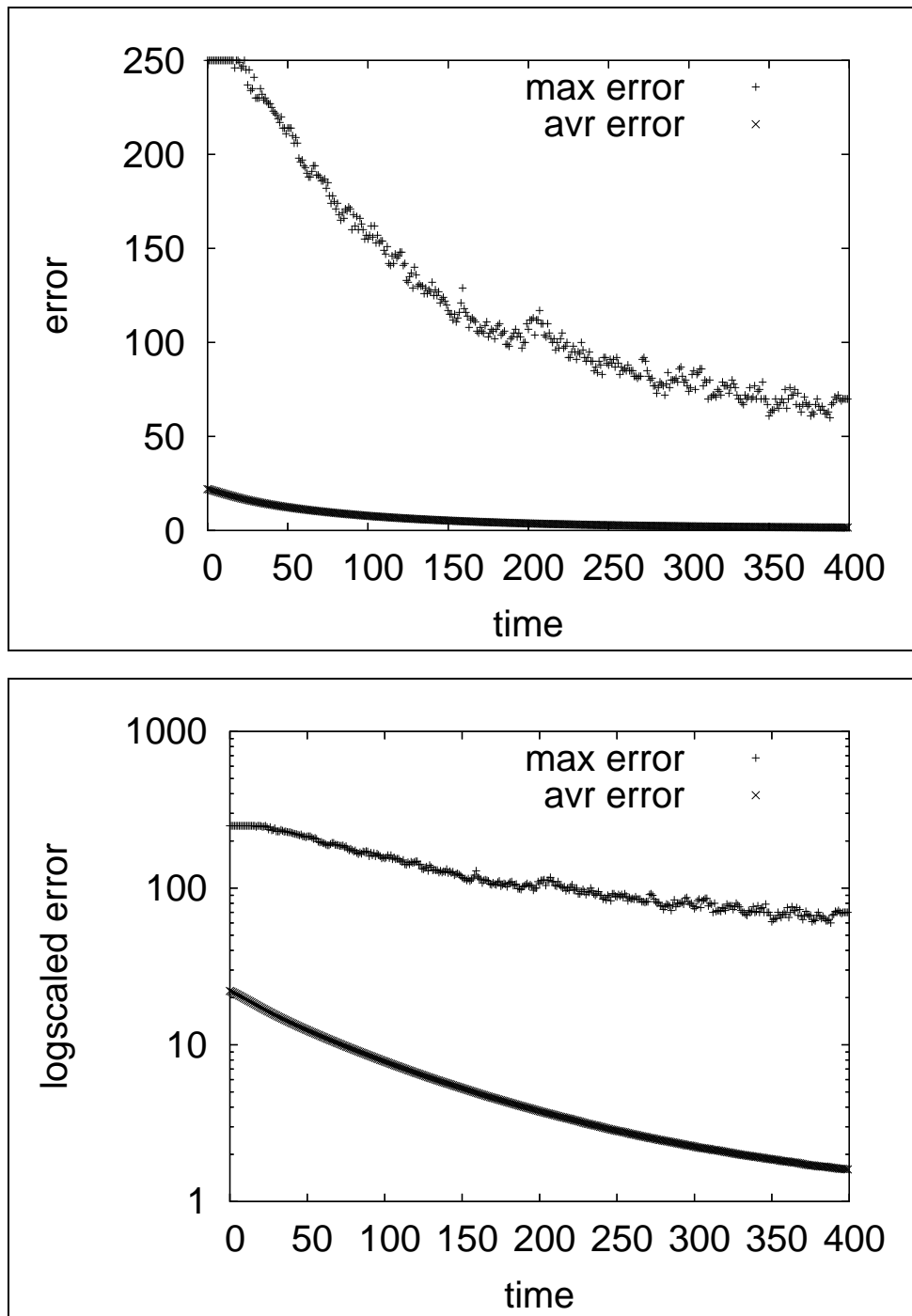


Figure 4.3. These two figures show the behaviour of the average error and the maximum error between \mathbb{F}_t and \mathbb{F}_∞ in time (Experiment 1/1). In the lower diagram we have logarithmic scaling on the y -axis.

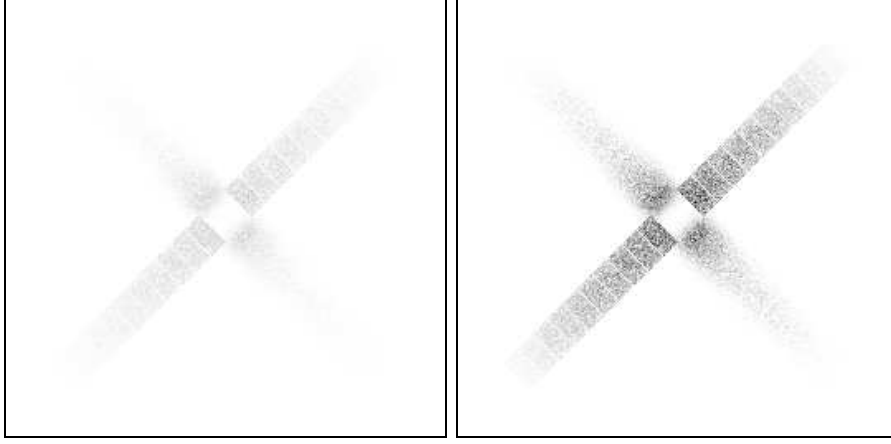


Figure 4.4. The inverted gray-values of the left image are equal to the absolute value of the difference between \mathbb{F}_{400} and \mathbb{F}_{∞} (see Experiment 1/1). The right image is rescaled such that the maximum gray-value of the left image becomes black.

where $|D_{\text{disc}}|$ is the number of elements in D_{disc} . (We call ϵ_a the \mathcal{L}^1 -distance of \mathbb{F}_t and \mathbb{F}_{∞} .) The value ϵ_a is obviously decreasing in time. In Figure 4.3 we show the development of the average error and the maximum error in time. At time $t_6 = 400$ we have $\epsilon_a \approx 1.6$ with a variance of 27.6 and a maximum difference of 70. So taking the low Monte Carlo iteration size and the big step size of the approximated Itô diffusion into account the result may be considered as satisfying. Moreover this will be confirmed by looking at Figure 4.4. There the left image is a representation of the visible difference between \mathbb{F}_{400} and \mathbb{F}_{∞} . The right image in Figure 4.4 shows the error rescaled to $[0, 255]$.

The reconstruction quality is even more surprising because we simply assumed $c = 1$. As we know from Section 4.1, the functions $c(t), \tilde{c}(t)$ converge for $t \rightarrow \infty$ to $c = (\tilde{\mathbb{F}}_0, \tilde{\mathbb{F}}_{\infty})_{L^2(D, \lambda^d)}$. So in **Experiments 1/2-3** we use the transformation algorithms with maximum scale and average scale to repeat the experiment. Once again we produce six images $\mathbb{F}_{t_1}, \dots, \mathbb{F}_{t_6}$. The images resulting from the use of average scale are shown in Figure 4.5. If we compare these images with the images shown in Figure 4.2 we can see that the application of the average scale value causes a stronger edge enhancing effect. The images resulting from the use of maximum scale do not show interesting differences to the images in Figure 4.2. This means the average scale value causes also a stronger edge enhancing effect than the use of the maximum

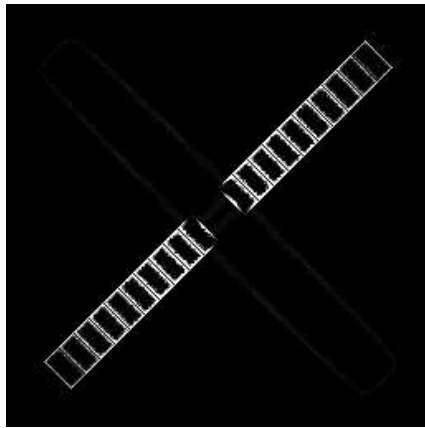
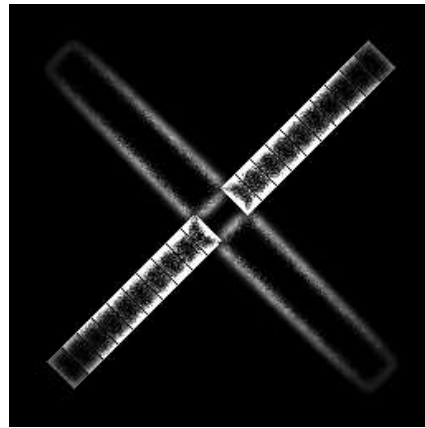
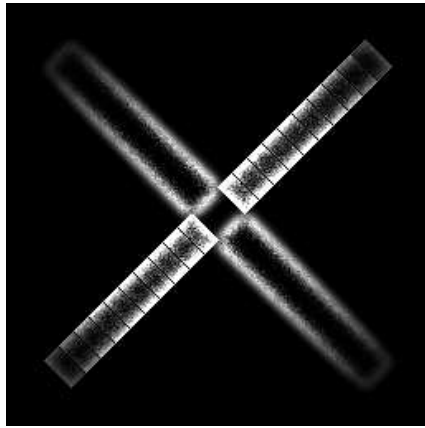
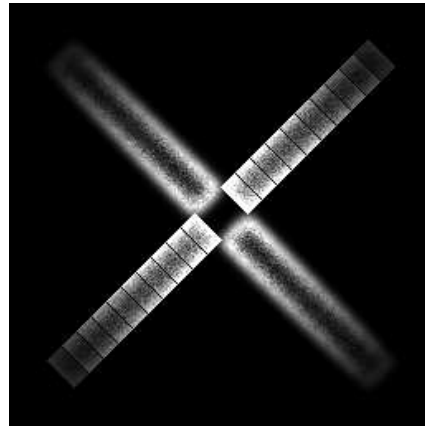
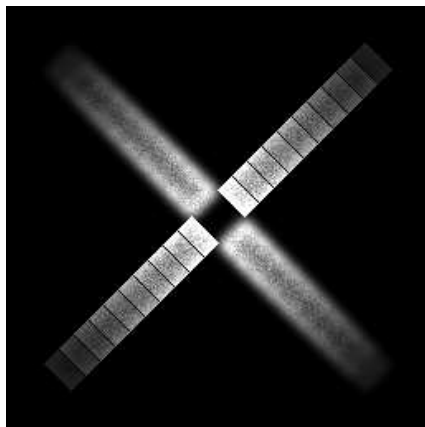
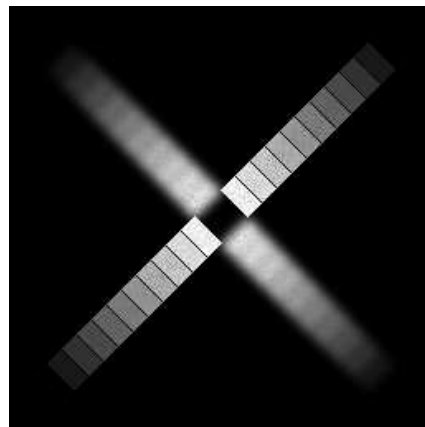
(a) $t_1 = 1$ (b) $t_2 = 10$ (c) $t_3 = 20$ (d) $t_4 = 50$ (e) $t_5 = 100$ (f) $t_6 = 400$

Figure 4.5. Reconstruction sequence for a simple generic image pair. We used the transformation algorithm with average scale to produce these images (Experiment 1/3).

scale value. Moreover the image sequence resulting from the use of average scale looks brighter than the sequence resulting from maximum scale. Hence there must be a difference in the behaviour of the scale values $c(t), \hat{c}(t)$. Therefore we observed all scale values during the corresponding experiments. Both functions are shown in Figure 4.6 (p. 109). Of course $c(t) \geq \hat{c}(t)$ holds for all $t \geq 0$. The observed scale values explain the different brightnesses of the resulting image sequences.

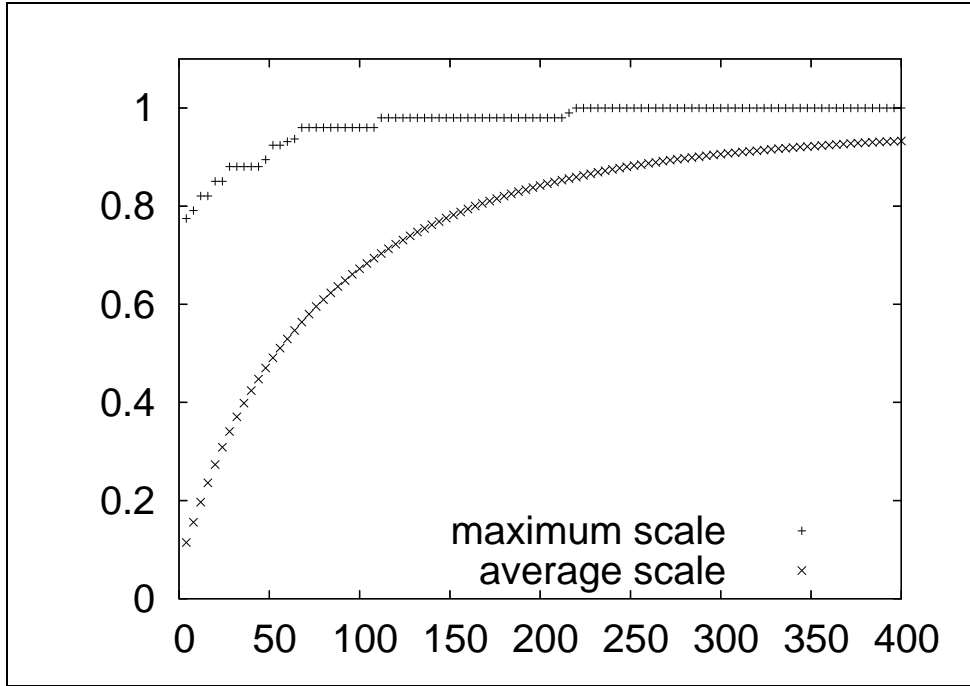


Figure 4.6. The diagram shows the behaviour of the scale values $c(t)$ (the upper graph) and $\hat{c}(t)$ in time (x -axis). They were observed during the application of the transformation algorithms with maximum and average scale to the image pair shown in Figure 4.1 (Experiments 1/2-3). For the plot we used one out of four values.

As we know from Section 3.5, the value of the absolute difference between \mathbb{I}_∞ and its approximation \mathbb{I}_t , denoted by ϵ_a , depends on the transformation time t , the step size Δt of the approximated Itô diffusion with reflection and the number of simulations k , used during the Monte Carlo approximation. Now we want to get an impression of the behaviour of ϵ_a depending on the approximation parameters Δt and k . For this purpose we use the image pair $\mathbb{I}_0, \mathbb{I}_\infty$ shown

in Figure 4.1 as before and compute \mathbb{f}_t for $t = 1000$ with the transformation Algorithm 4.0.1. We perform nine **Experiments 2/1-3, 3/1-3, 4/1-3** using the approximation parameters Δt and k as shown in Table 4.7.

No 2/1	No 2/2	No 2/3
$k = 10$ $\Delta t = 1$	$k = 10$ $\Delta t = 0.1$	$k = 10$ $\Delta t = 0.01$
No 3/1	No 3/2	No 3/3
$k = 100$ $\Delta t = 1$	$k = 100$ $\Delta t = 0.1$	$k = 100$ $\Delta t = 0.01$
No 4/1	No 4/2	No 4/3
$k = 1000$ $\Delta t = 1$	$k = 1000$ $\Delta t = 0.1$	$k = 1000$ $\Delta t = 0.01$

Table 4.7. Parameter setup for Experiments 2/1-3, 3/1-3, 4/1-3.

Obviously Experiment 4/3 takes the highest computation effort, so we will have a short look at the number of computations and the number of outcomes ${}_l\Delta B_i^j$ of the independent random increments $\Delta B_i^j \sim \mathcal{N}(0, \Delta t)$ needed. We remind that $s = t(\Delta t)^{-1} \in \mathbb{N}$ is assumed. If $nm \in \mathbb{N}$ is the number of pixels we are interested in and $k \in \mathbb{N}$ is the number of Monte Carlo simulations we perform, then the computation time depends linearly on $mnks$. The same holds for the number of outcomes of the random increments ΔB_i^j . We need two outcomes ${}_l\Delta B_i^j$ each time we compute one step of the approximated Itô diffusion $X_{t, \Delta t}^x$. Hence we need $2mnks$ outcomes overall. For Experiment 4/3 we set $\Delta t = 10^{-2}$ and $t = 10^3$. According to Algorithm 3.2.2 we have to compute 10^5 steps of each path of $X_{t, \Delta t}^x$. Therefore we need $2 \cdot 10^5$ outcomes ${}_l\Delta B_i^j$ for the computation of one path of the approximated Itô diffusion. The images \mathbb{f}_0 and \mathbb{f}_∞ consist of 256^2 pixels and we want to perform $k = 10^3$ Monte Carlo simulation runs. Thus approximatively we end with $6.6 \cdot 10^{12}$ computations and 10^{13} outcomes of ΔB_i^j needed for Experiment 4/3. We note that this experiment carried out on an Intel Celeron D 336, 2.8 GHz takes about 461 hours. To avoid this long computation time we perform two classes of experiments. In each class we focus on the image values corresponding to the pixels indicated black in Figure 4.8(a) respectively Figure 4.8(b). We denote these pixel sets by $M1$ and $M2$. Each of them contains 900 Pixels. Hence the

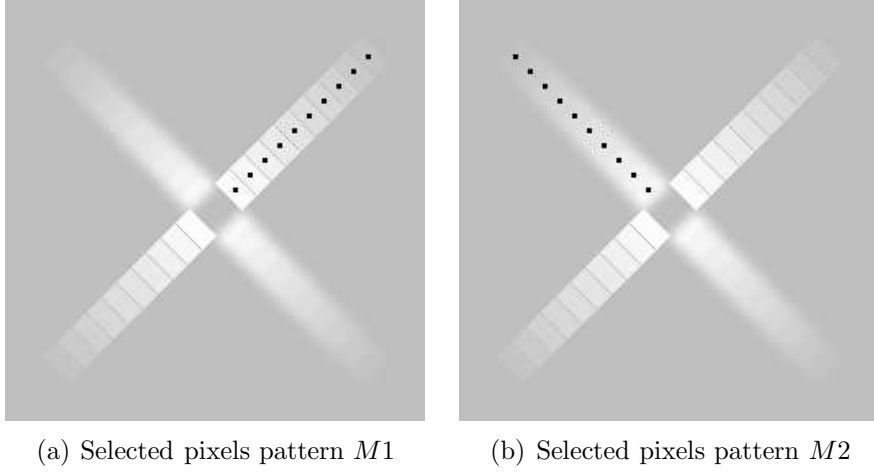
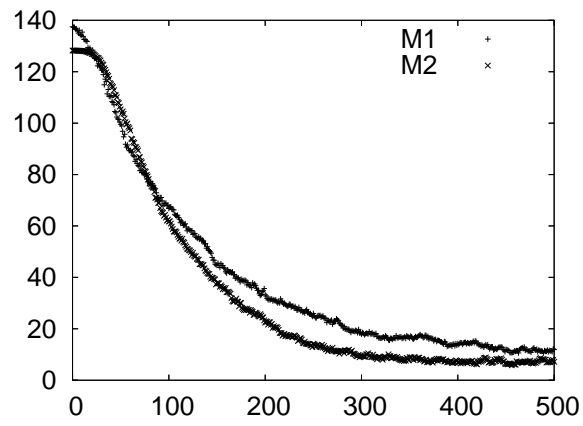
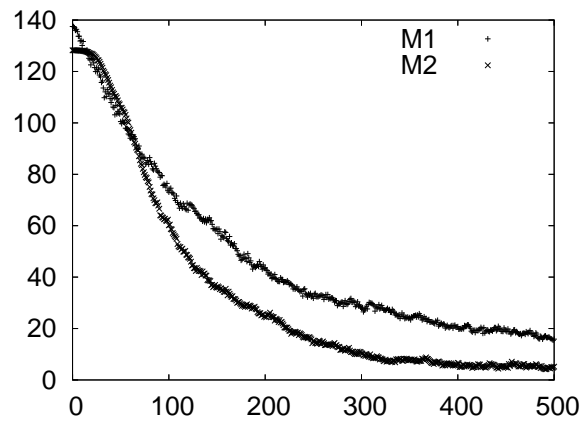


Figure 4.8. We perform nine Experiments 2/1-3,3/1-3,4/1-3 and each of them twice. The images show the two sets of pixels $M1, M2$ on which we focus our attention during these nine experiments. First we approximate \mathbb{F}_t for the pixels in $M1$. Then we repeat the experiments for the pixels in $M2$.

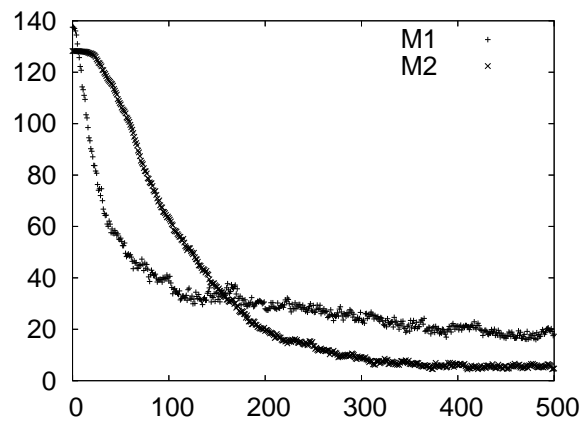
computation time reduces to approximatively 6 hours and 20 minutes in the case of Experiment 4/3 for each of the pixel sets. (Note that this is only true if there is enough RAM.) The computation time and number of outcomes of the random increments needed for the other experiments follows analogously. In Figures 4.9, 4.10, 4.11 the value of ϵ_a is shown at a time for both pixel sets $M1, M2$. There ϵ_a is computed using just the pixels in the corresponding set. As we have expected, the variance of ϵ_a is decreasing for a growing number k of Monte Carlo simulations. During the following experiments we will see that for our purpose it is sufficient to choose $k = 100$. If we decrease the step sizes Δt we do not observe changes of the variance of ϵ_a . Instead we see different shapes of the error graphs. Roughly speaking, we have a bigger difference in the reconstruction behaviour of pixels in $M1$ and $M2$ for small Δt . So for simple image reconstruction experiments, reaching large transformation times, we can choose big step sizes. In contrast to this, smaller step sizes become more important if we are interested in image smoothing or edge enhancement. The difference in the reconstruction behaviour of pixels in $M1$ and $M2$ gives a first hint that different values of Δt can be used to obtain different qualities of edge enhancing or smoothing effects.



(a) Experiment No 2/1

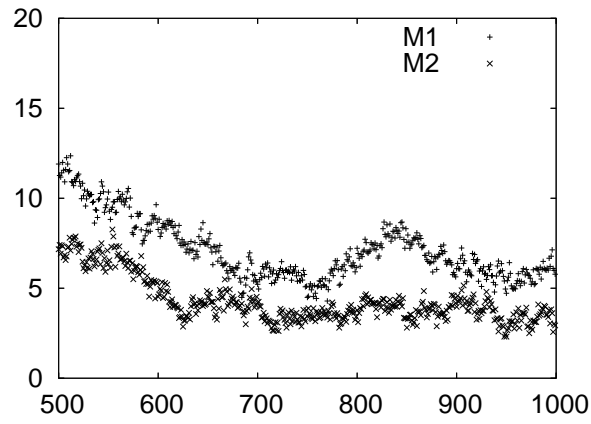


(b) Experiment No 2/2

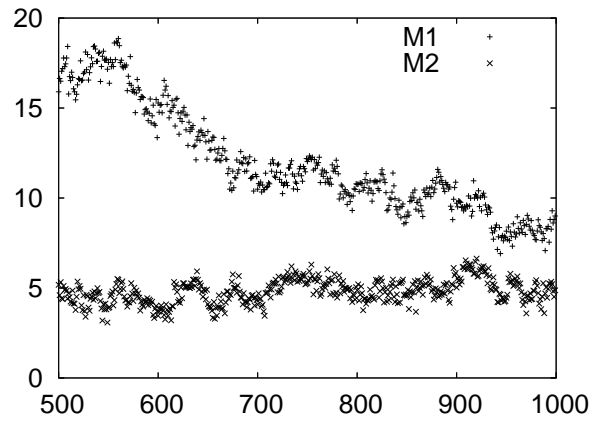


(c) Experiment No 2/3

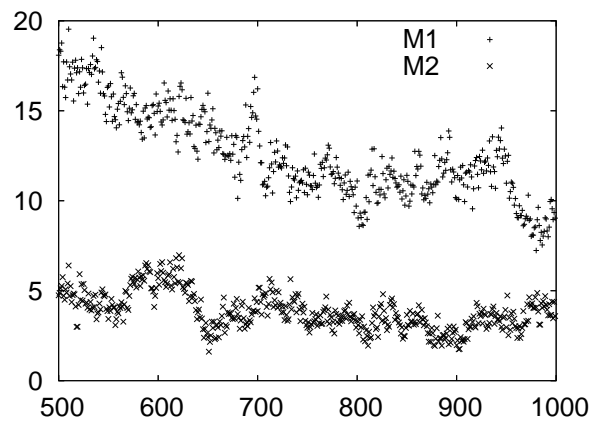
Figure 4.9. Error behaviour in Experiments 2/1-3 ($t \leq 500$).



(d) Experiment No 2/1

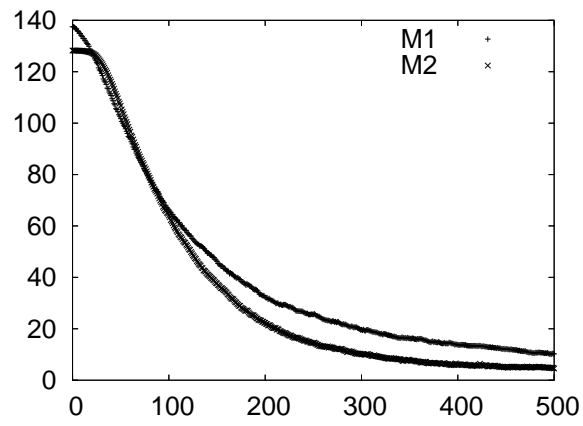


(e) Experiment No 2/2

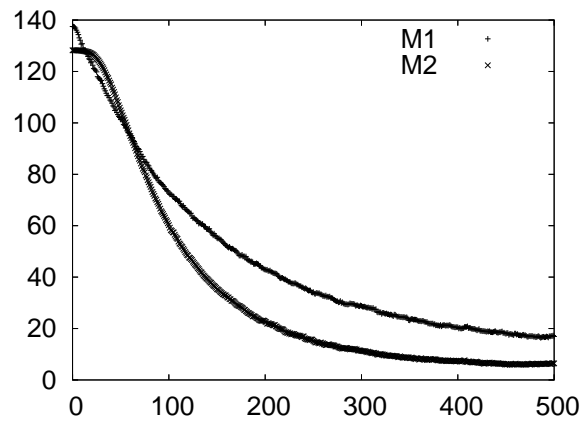


(f) Experiment No 2/3

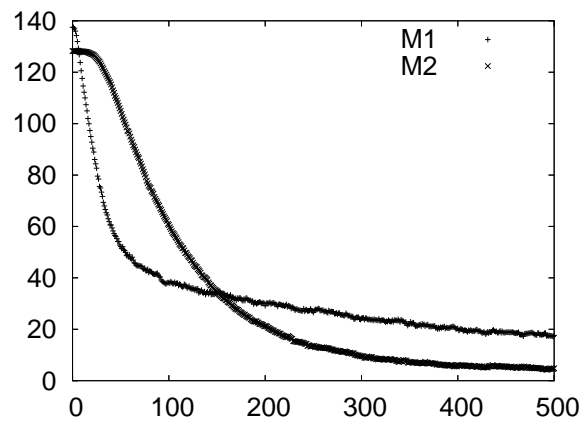
Figure 4.9. Error behaviour in Experiments 2/1-3 ($500 \leq t \leq 1000$).



(a) Experiment No 3/1

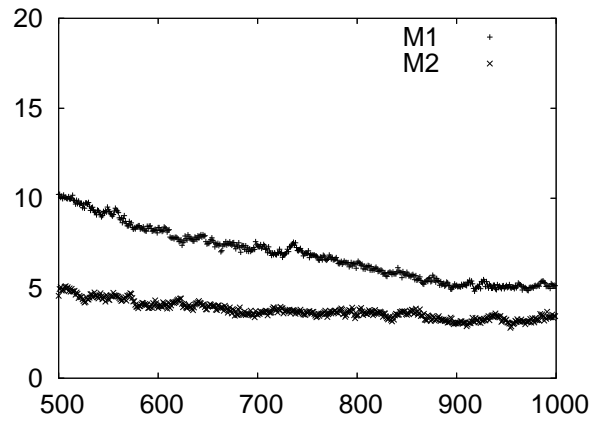


(b) Experiment No 3/2

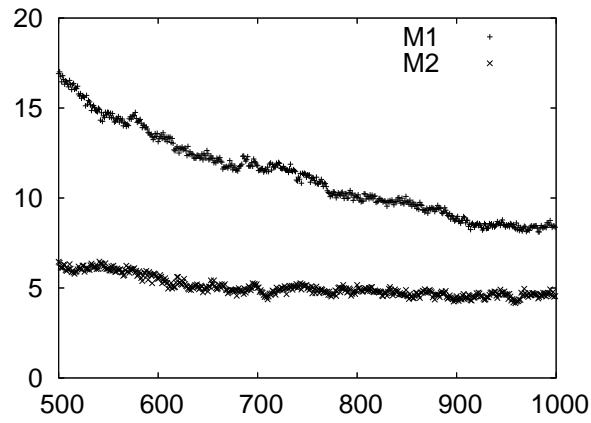


(c) Experiment No 3/3

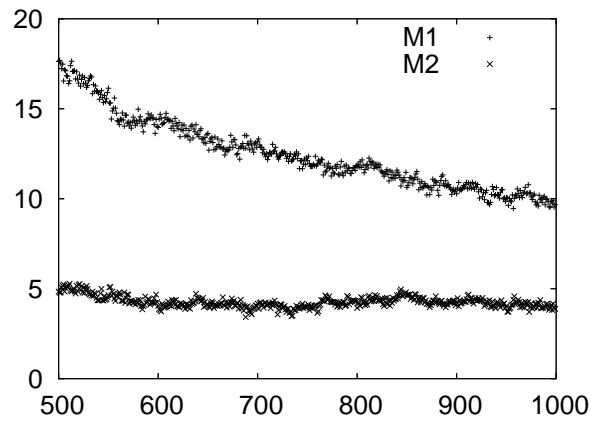
Figure 4.10. Error behaviour in Experiments 3/1-3 ($t \leq 500$).



(d) Experiment No 3/1

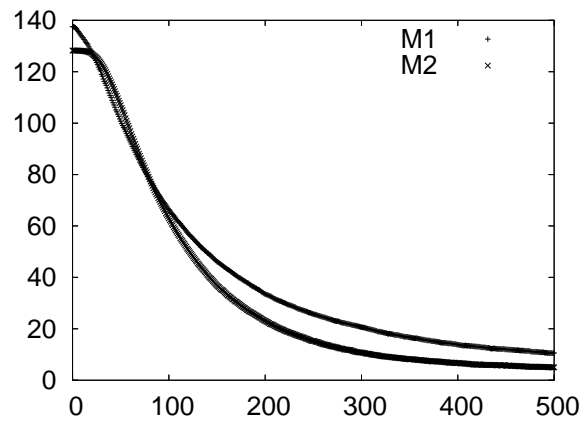


(e) Experiment No 3/2

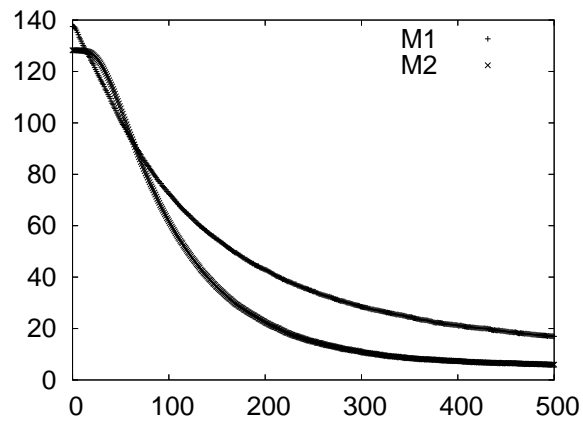


(f) Experiment No 3/3

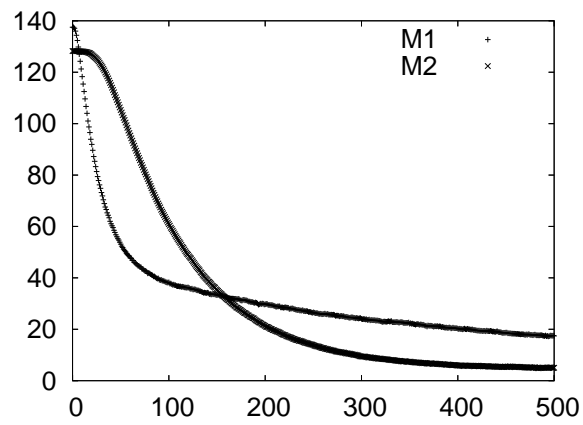
Figure 4.10. Error behaviour in Experiments 3/1-3 ($500 \leq t \leq 1000$).



(a) Experiment No 4/1

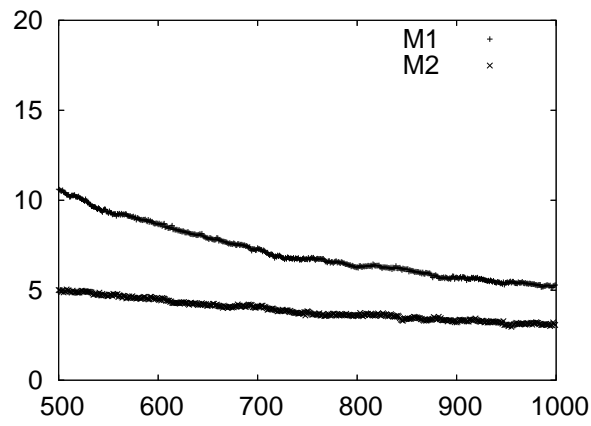


(b) Experiment No 4/2

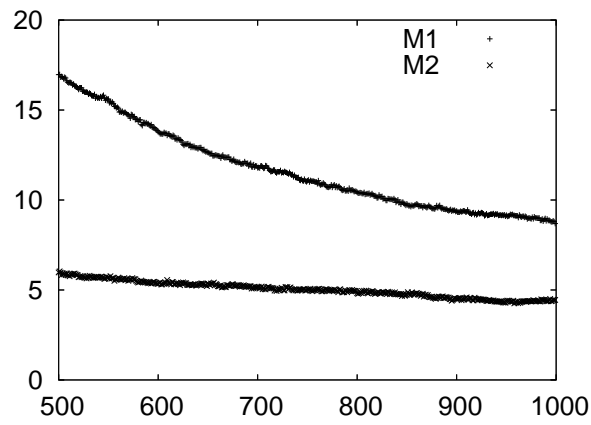


(c) Experiment No 4/3

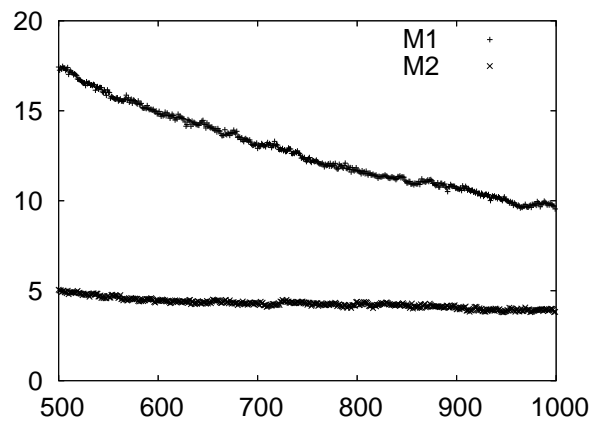
Figure 4.11. Error behaviour in Experiments 4/1-3 ($t \leq 500$).



(d) Experiment No 4/1



(e) Experiment No 4/2



(f) Experiment No 4/3

Figure 4.11. Error behaviour in Experiments 4/1-3 ($500 \leq t \leq 1000$).

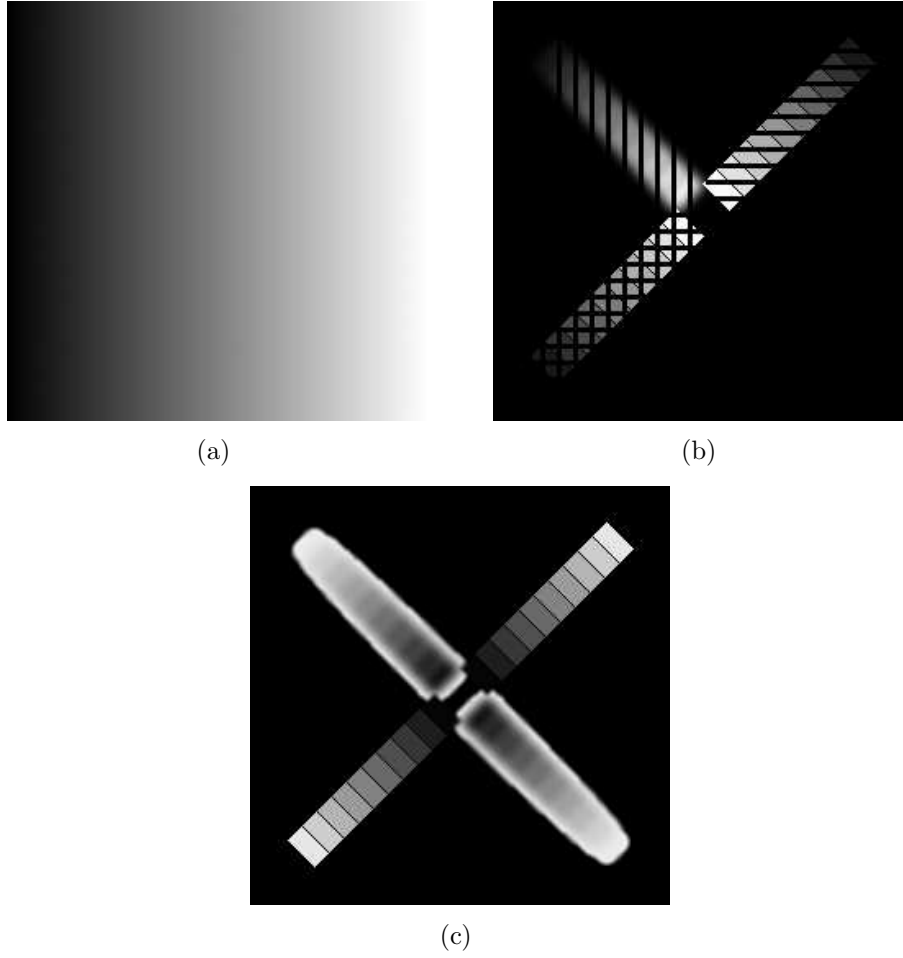


Figure 4.12. In order to show that the reconstruction works independent of the initial condition we choose these three start images. Each of them has to be of size 256×256 pixel.

Up to here we used the same start image in each experiment. Now we turn to the question whether we can reconstruct \mathbb{I}_∞ starting from some different image function. For this we perform **Experiments 5/1-3** where we apply the transformation algorithm with maximum scale to each of the images shown in Figure 4.12. For every experiment we choose the step size $\Delta t = 0.1$ and compute $s = 1000$ steps to reach the transformation time $t = 100$. We use a Monte Carlo approximation with $k = 100$ simulation runs. In Figures 4.13-4.15 the resulting image sequences are shown. As before we show the transformed image after one step. Additionally we have chosen the transformation times

t_2, \dots, t_6 to be comparable to the images (a)-(e) in Figures 4.2, 4.5. We can see that the transformed images in Experiments 5/1-3 are influenced by the different start images. For instance, the reconstruction shown in Figure 4.13 looks asymmetric. The right parts of the image \mathbb{F}_t underlie a faster reconstruction than the image values on the left side of the image (as expected). Next it is natural to ask for the behaviour of image values $\mathbb{F}_t(i, j)$ for (i, j) with $\mathbb{F}_0(i, j) = \mathbb{F}_\infty(i, j)$. So for Experiment 5/2 we have taken an appropriate start image. In Figure 4.14 we can see that, during the transformation, the equal parts of \mathbb{F}_0 and \mathbb{F}_∞ remain nearly constant (up to the scale value). Moreover we see that the black repainted stripes in the upper left diagonal half of the image are nearly reconstructed whereas the reconstruction of the missing lower right part of the \mathbf{X} is still at the beginning. Finally, in Experiment 5/3, we have chosen \mathbb{F}_0 as shown in Figure 4.12(c). This start image contains a (somehow) colour inverted version of the \mathbf{X} , whereas the background is black, too. We perform this experiment in order to get a first impression of the behaviour of different gray-values during the transformation. A closer look at the data computed during the transformation shows an interesting detail. The values of $\mathbb{F}_t^{\Delta t, k}$ (defined in Eqn. 4.3) exceed 500 (mainly at the edges of the \mathbf{X}). We remind that we obtain \mathbb{F}_t by rounding and cutting the values of $\mathbb{F}_t^{\Delta t, k}$ (see Eqn. 4.4). But we could also rescale the interval $[0, \max_{(i,j) \in D}(\text{int}(\mathbb{F}_t^{\Delta t, k}(i, j)))]$ to $[0, 256]$ instead taking the maximum of 256 and $\text{int}(\mathbb{F}_t^{\Delta t, k})$. In this case the result of Experiment 5/3 would show a very strong edge enhancing effect because nearly all values of \mathbb{F}_t would have been rescaled to values smaller than 60. So nearly all pixels of \mathbb{F}_t would appear very dark whereas those pixels where the values of $\mathbb{F}_t^{\Delta t, k}$ exceed 500 (mainly at edges of the \mathbf{X}) appear very bright.

As before we are interested in the behaviour of the \mathcal{L}^1 -distance between \mathbb{F}_t and \mathbb{F}_∞ , denoted by ϵ_a , for increasing transformation time. So in Figure 4.16 we present the \mathcal{L}^1 -distances ϵ_a corresponding to the three Experiments 5/1-3.

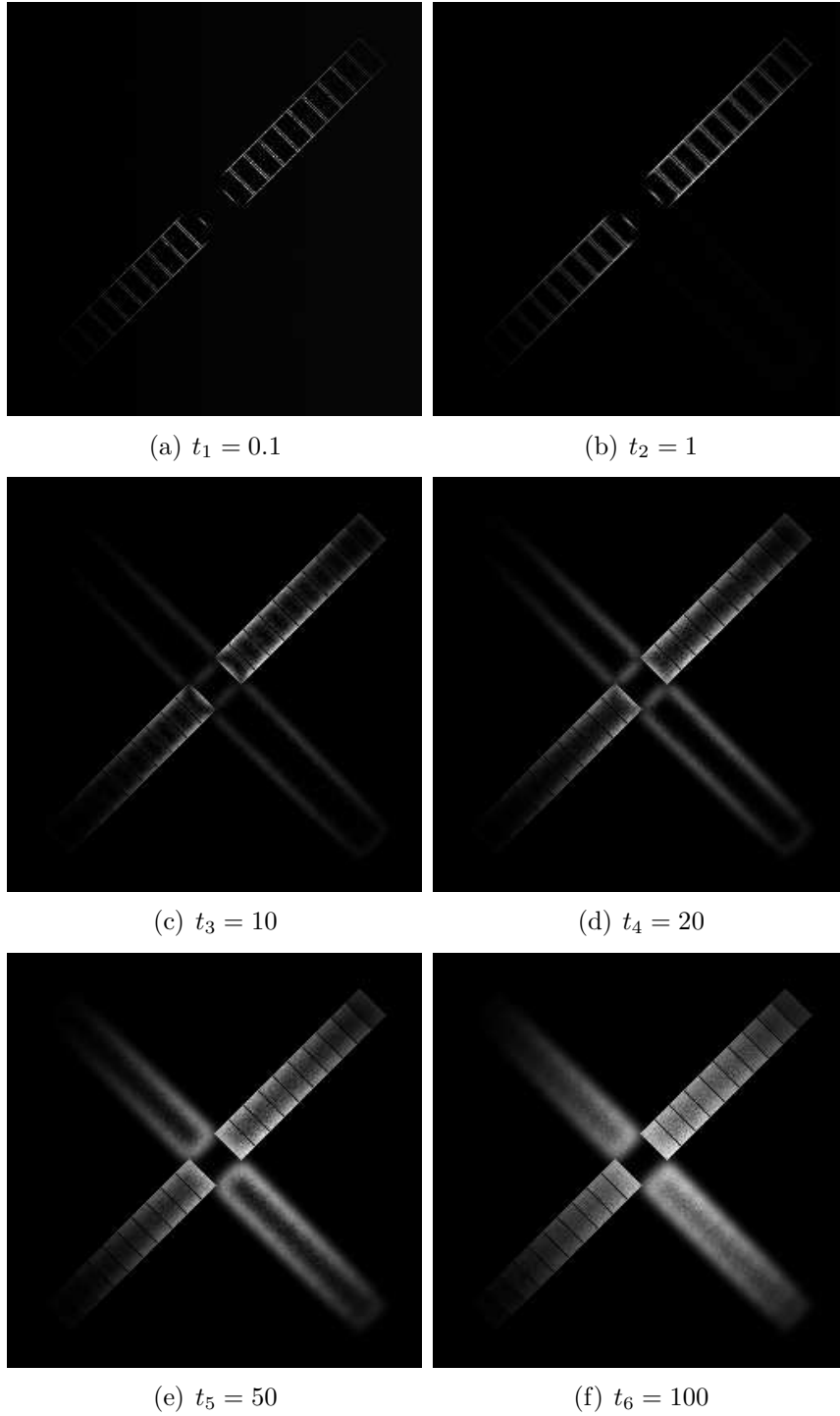


Figure 4.13. Image sequence according to Experiment 5/1. The start image is shown in Figure 4.12(a) and the stop image in Figure 4.1(b).

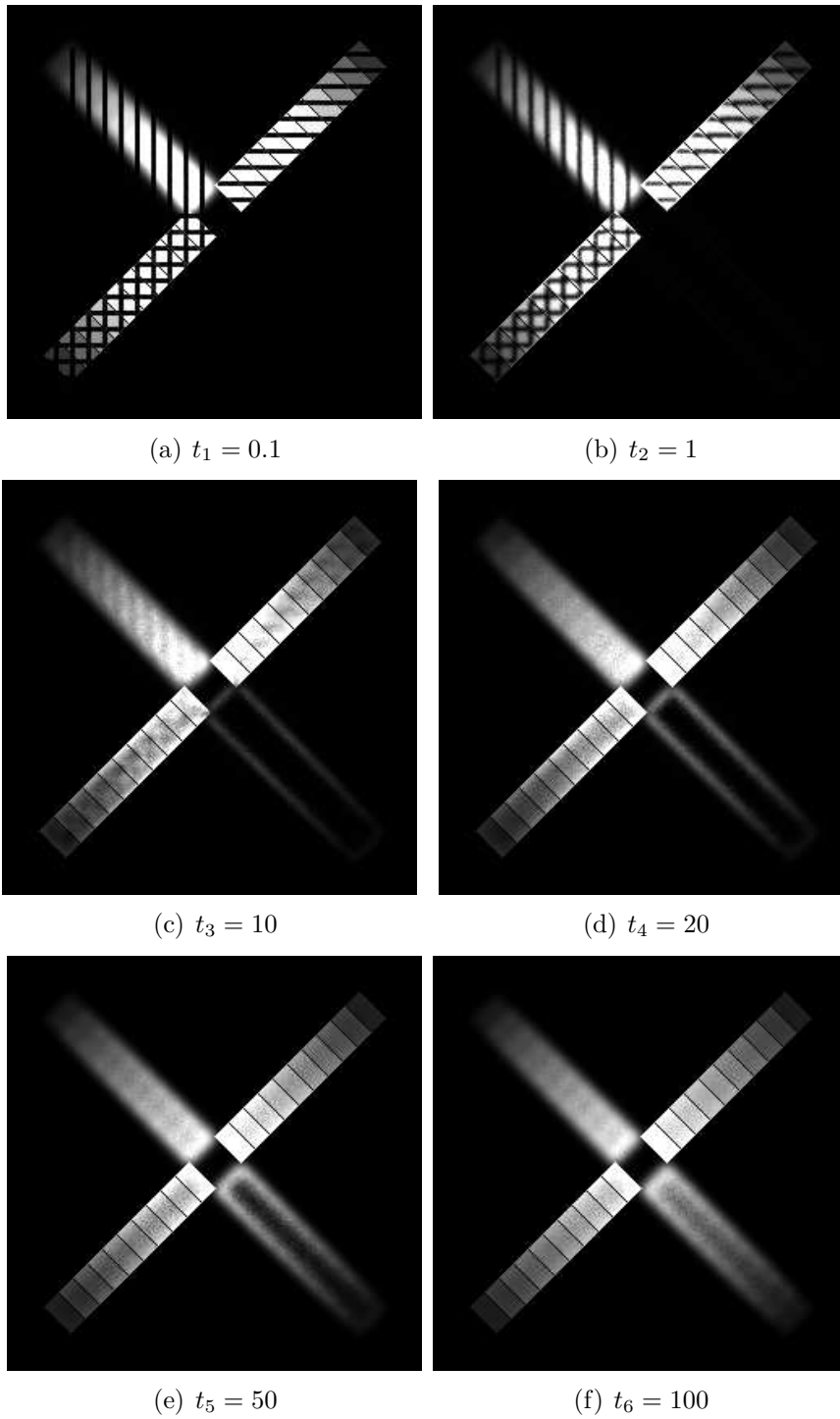


Figure 4.14. Image sequence according to Experiment 5/2. The start image is shown in Figure 4.12(b) and the stop image in Figure 4.1(b).

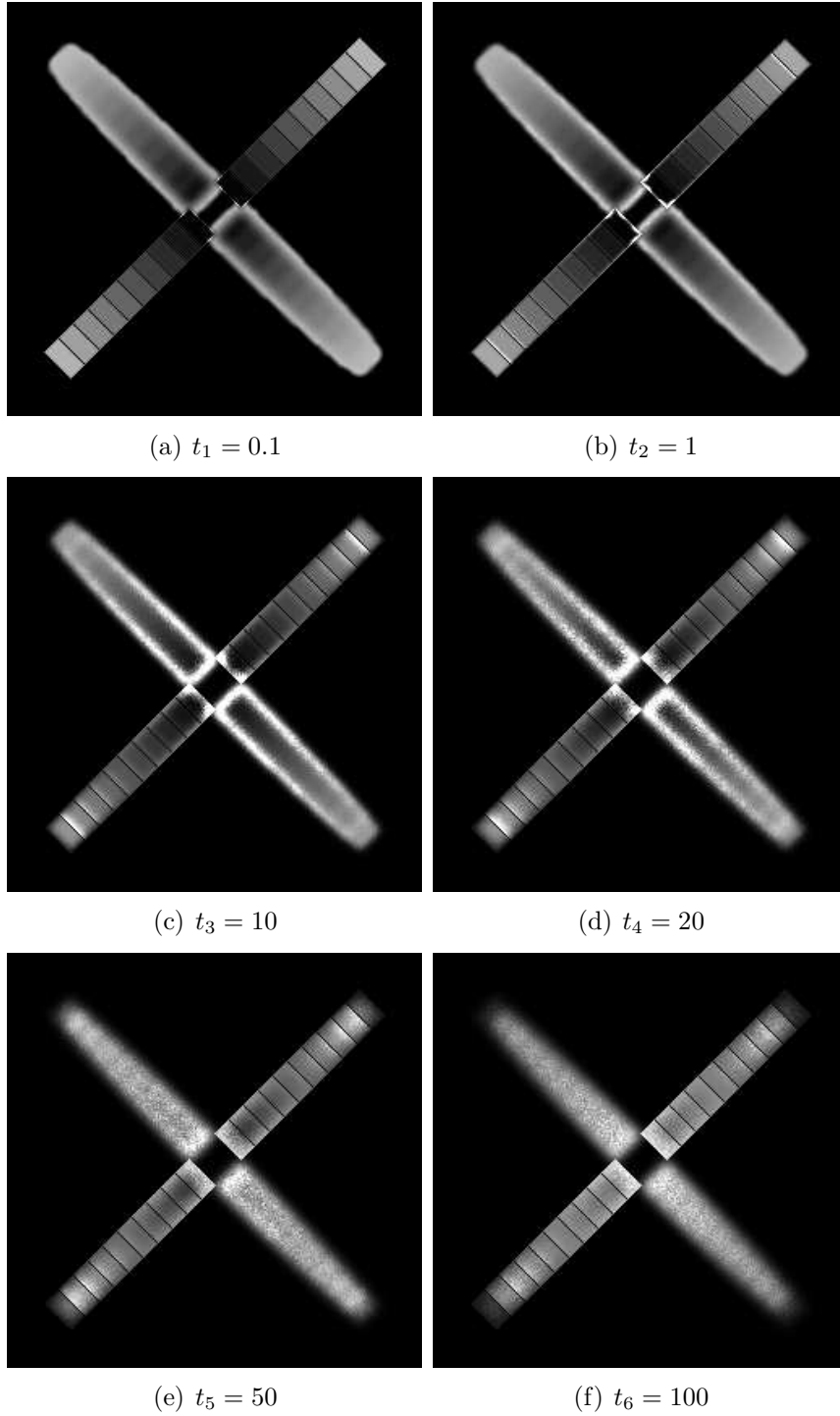


Figure 4.15. Image sequence according to Experiment 5/3. The start image is shown in Figure 4.12(c) and the stop image in Figure 4.1(b).

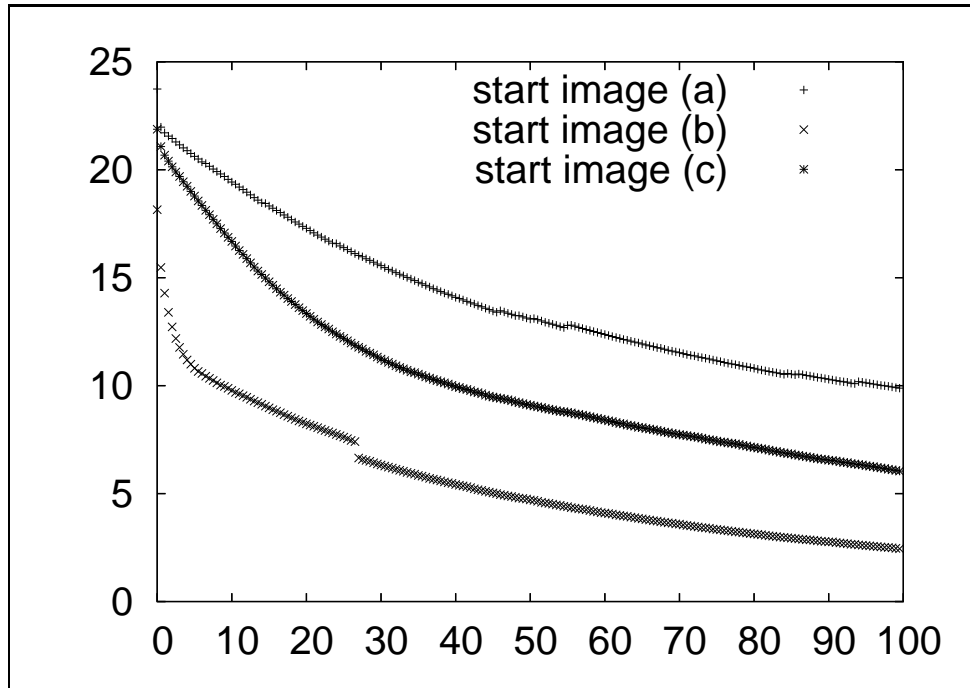


Figure 4.16. The diagram shows the behaviour of three \mathcal{L}^1 -distances ϵ_a between \mathbb{F}_t and \mathbb{F}_∞ in time (x -axis). The three functions \mathbb{F}_t result from Experiments 5/1-3. There we used the images shown in Figure 4.12 as start images and used the transformation algorithm with maximum scale in order to reconstruct the stop image shown in Figure 4.1(b). The upper line corresponds to Experiment 5/1, the middle to Experiment 5/3 and the lower to Experiment 5/2.

Actually we do not want to see transformed images \mathbb{I}_t only for generic start and stop images $\mathbb{I}_0, \mathbb{I}_\infty$. So for the last **Experiments 6/1-3** in this section we use the three images shown in Figure 4.17 as stop images \mathbb{I}_∞ . We compute $s = 1000$ steps with step size $\Delta t = 10$ to reach the transformation time $t = 10000$ and perform $k = 100$ simulation runs for the Monte Carlo approximation. The start image \mathbb{I}_0 is congruent 256 and has the same size as the corresponding stop image. The image sequences shown in Figures 4.18-4.21 result from the application of the transformation algorithm with average scale. Here we use the average scale value because we want to show more details in the transformed images. On the other hand we have to accept that some areas of \mathbb{I}_t look unnaturally bright. The \mathcal{L}^1 -distances between the images in the sequences \mathbb{I}_t and the image \mathbb{I}_∞ are shown in Figure 4.22.



Figure 4.17. Here we see two snakes, the interior of a personal computer and the Rhenania building Mannheim/Germany. The sizes of these images are 300×200 , 350×232 and 492×492 Pixel.

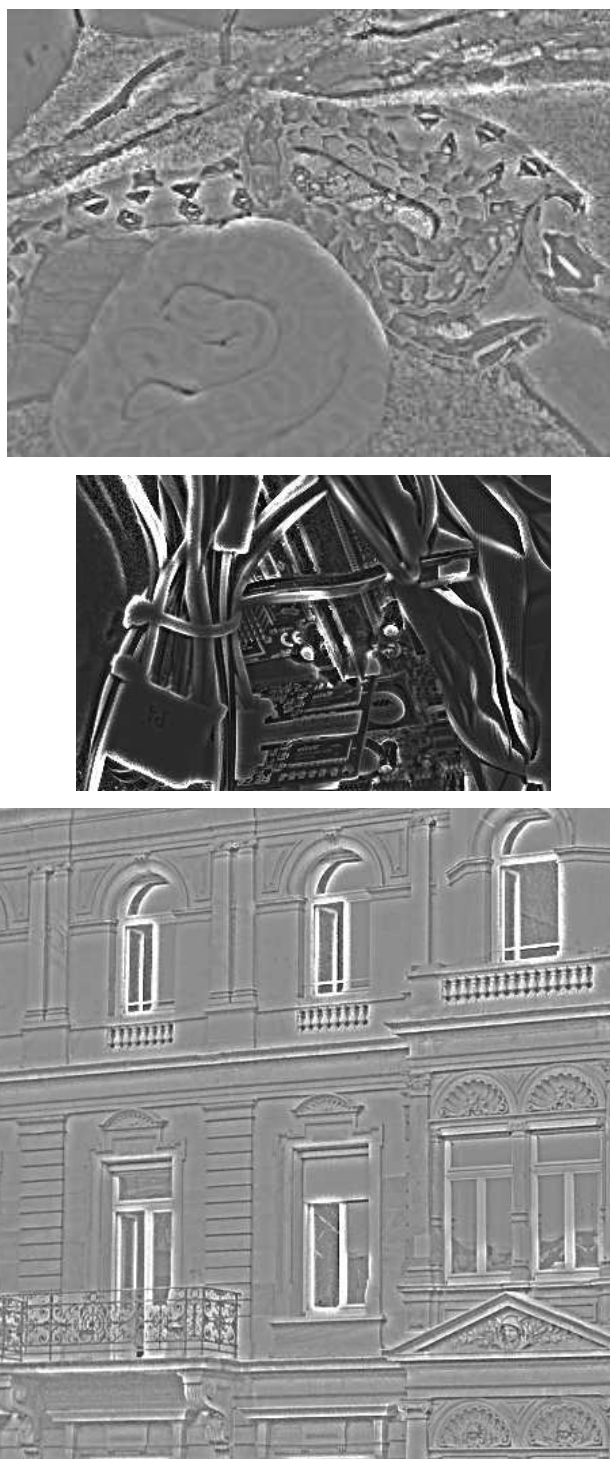


Figure 4.18. The transformed images according to Experiments 6/1-3 at transformation time $t_1 = 10$. The stop images are shown in Figure 4.17 and $\mathbb{F}_0 \equiv 256$.

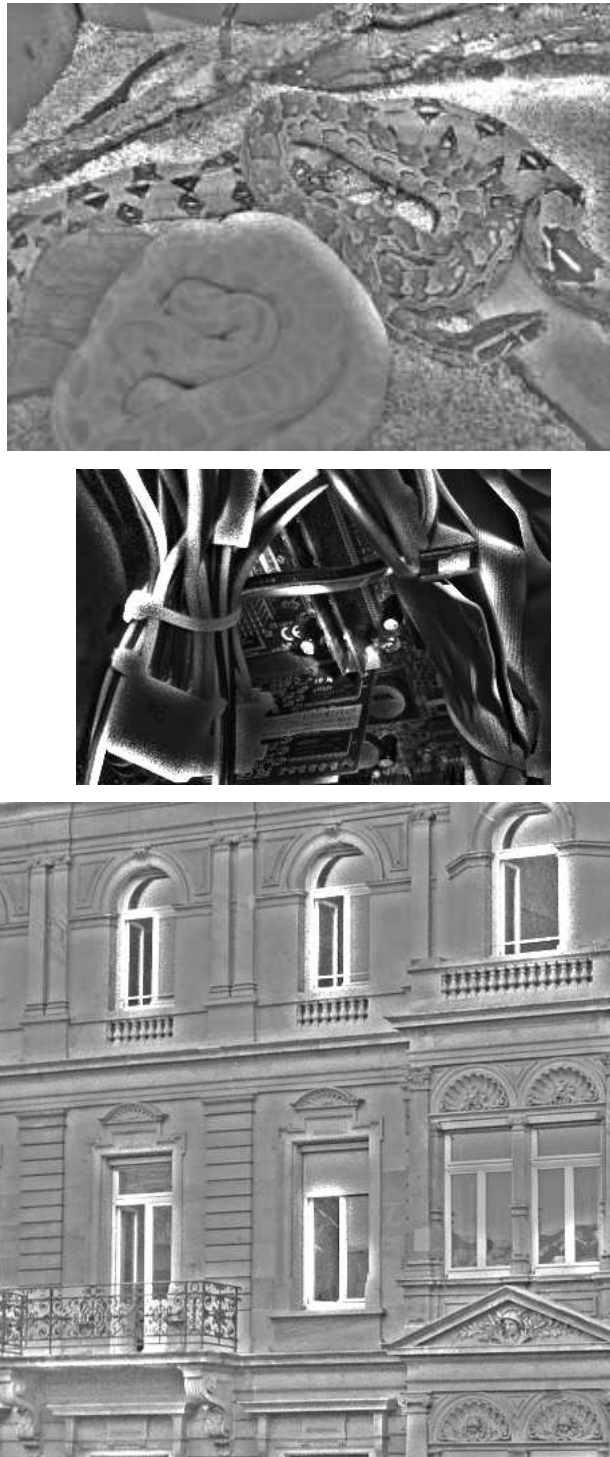


Figure 4.19. The transformed images according to Experiments 6/1-3 at transformation time $t_2 = 50$. The stop images are shown in Figure 4.17 and $\mathbb{F}_0 \equiv 256$.

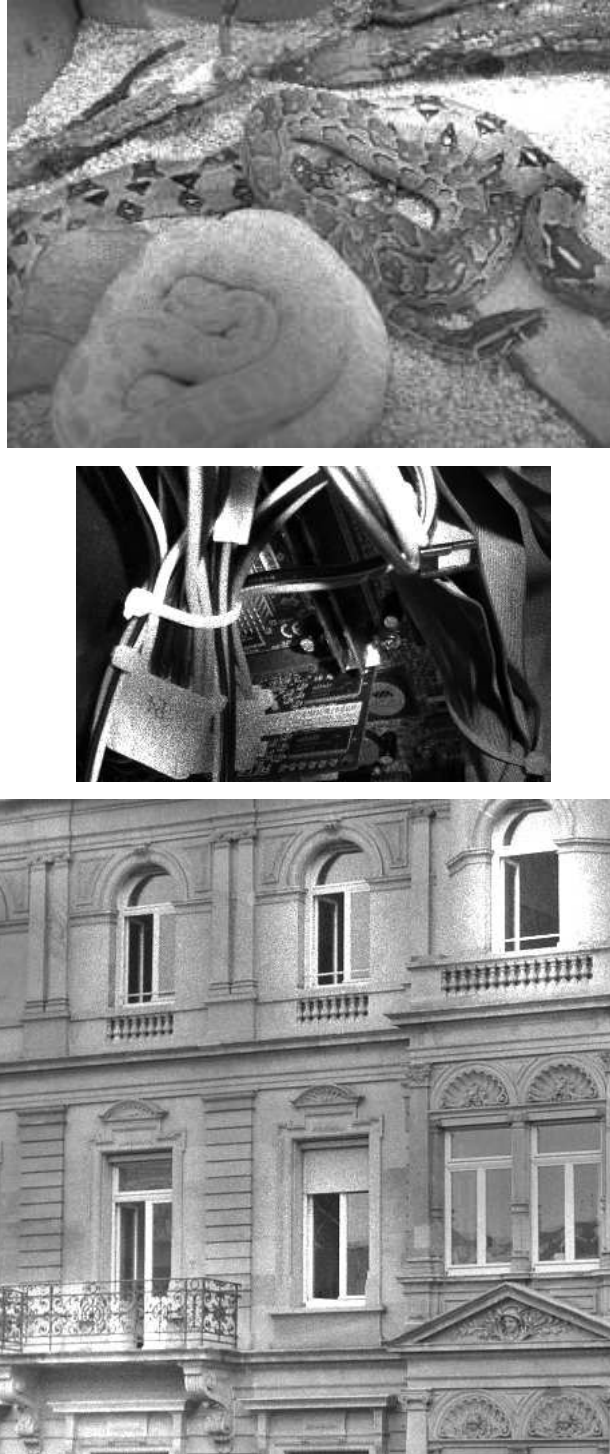


Figure 4.20. The transformed images according to Experiments 6/1-3 at transformation time $t_3 = 1000$. The stop images are shown in Figure 4.17 and $\mathbb{f}_0 \equiv 256$.

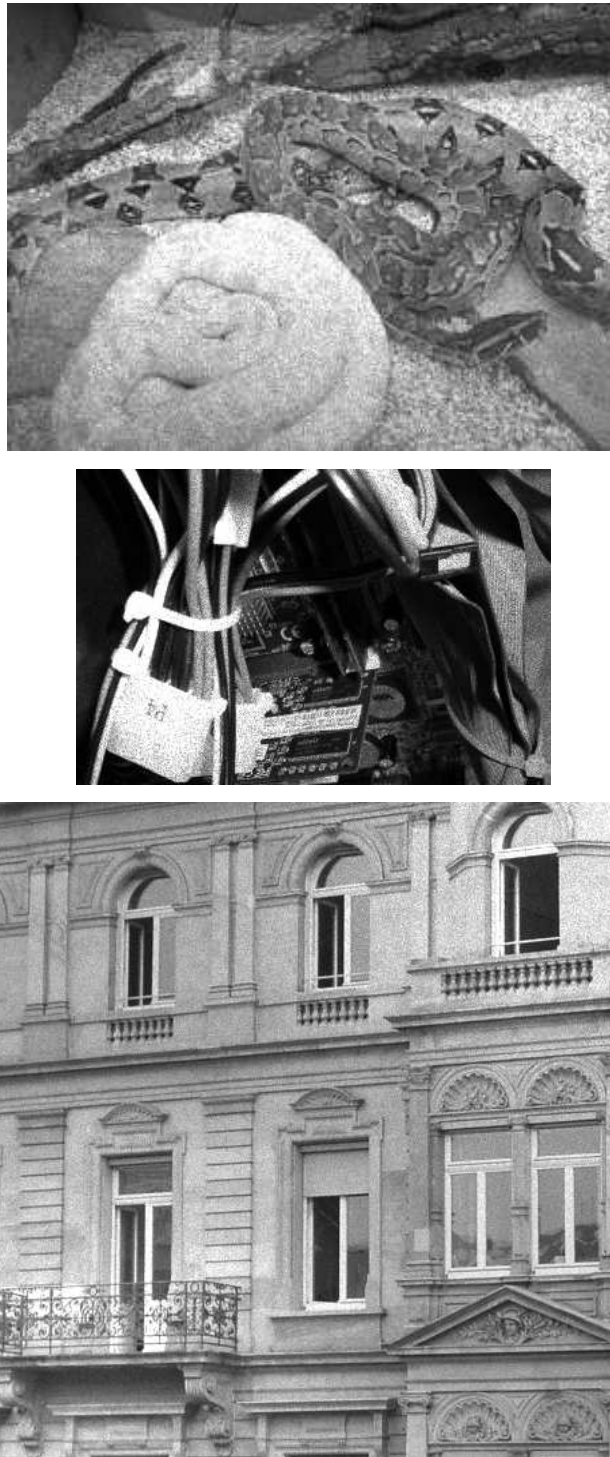


Figure 4.21. The transformed images according to Experiments 6/1-3 at transformation time $t_4 = 10000$. The stop images are shown in Figure 4.17 and $\mathbb{f}_0 \equiv 256$.

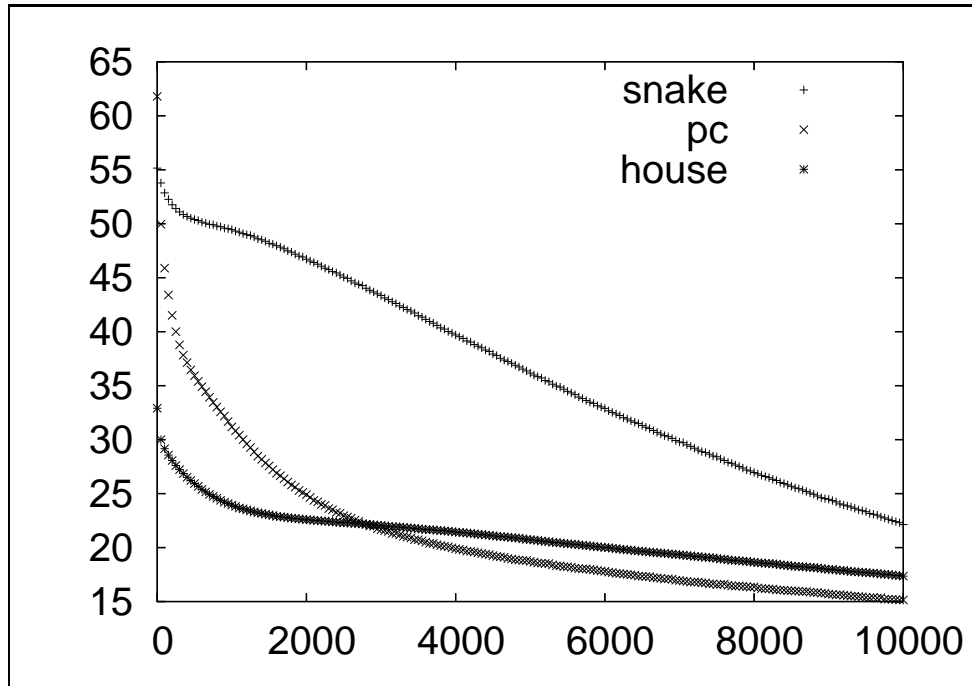


Figure 4.22. The diagram shows the behaviour of three \mathcal{L}^1 -distances between \mathbb{F}_t and \mathbb{F}_∞ in time (x -axis). The three function \mathbb{F}_t result from Experiments 6/1-3. There $\mathbb{F}_0 \equiv 256$ and we used the transformation algorithm with average scale in order to reconstruct the stop images shown in Figure 4.17. The upper line corresponds to Experiment 6/1. At time $t = 10000$ the error corresponding to Experiment 6/2 is less than the error corresponding to Experiment 6/3.

4.3 Reconstruction without spline interpolation

In this section we use the notation as before. Once again we consider the function

$$u(t, x, y) = \mathbb{E} \left[\frac{\tilde{\mathbb{F}}_0}{\tilde{\mathbb{F}}_\infty}(X_t^{(x,y)}) \right] \quad \text{for } (x, y) \in (0, x_n) \times (0, y_m), t \geq 0.$$

As we know, the diffusion coefficient σ of the reflected Itô diffusion X_t^x is equal to the negative 2-dimensional identity matrix $-I_2$. Hence the steps 3 to 8 of Algorithm 3.2.2 reduce to $X_{t+\Delta t}^x = X_t^x + b(X_t^x)\Delta t + \Delta B_i$ with

$$b(x, y) = -\frac{1}{\tilde{\mathbb{F}}_\infty(x, y)} \begin{pmatrix} \frac{\partial \tilde{\mathbb{F}}_\infty}{\partial x} \\ \frac{\partial \tilde{\mathbb{F}}_\infty}{\partial y} \end{pmatrix}(x, y) \quad \text{for } (x, y) \in \overline{D},$$

as mentioned before. We remind that $\tilde{\mathbb{F}}_\infty$ is a two times continuously differentiable spline function interpolating the discrete image values of the stop image \mathbb{F}_∞ . So we apply the approximation of the derivatives $\frac{\partial \tilde{\mathbb{F}}_\infty}{\partial x}, \frac{\partial \tilde{\mathbb{F}}_\infty}{\partial y}$ discussed in Section 3.4. We simply use the discrete derivative of the image \mathbb{F}_∞ to approximate the derivative of the interpolating spline function $\tilde{\mathbb{F}}_\infty$ at the corresponding pixel. To be precise, considering the pixel (i, j) , we approximate $\frac{\partial \tilde{\mathbb{F}}_\infty}{\partial x}$ for every $(x, y) \in [i - 1/2, i + 1/2) \times [j - 1/2, j + 1/2)$ by $1/2(\mathbb{F}_\infty(i + 1, j) - \mathbb{F}_\infty(i - 1, j))$ and analogously for the derivative in the y -direction. Note that there is no need for a different definition of the derivative for pixels lying on the boundary because of our image enlargement mechanism (see page 80), but we have to extend the definition of the derivative for (x, y) being in the closed square if either $i = m$ or $j = n$ (that is if (x, y) is at the upper or right border of \overline{D}). Using this approximation we save the time needed for the computation of the derivative of the spline function. We emphasise this because the values of $\frac{\partial \tilde{\mathbb{F}}_\infty}{\partial x}, \frac{\partial \tilde{\mathbb{F}}_\infty}{\partial y}$ have to be computed each time we evaluate $X_{t+\Delta t}^x = X_t^x + b(X_t^x)\Delta t + \Delta B_i$. If we denote by $s = t(\Delta t)^{-1}$ (assumed to be in \mathbb{N}) the number of steps we compute for the approximation of the reflected Itô diffusion $X_{t,\Delta t}^x$, we save $mnks$ times the computation of the derivatives $\frac{\partial \tilde{\mathbb{F}}_\infty}{\partial x}, \frac{\partial \tilde{\mathbb{F}}_\infty}{\partial y}$ – which is a lot (e.g. about $6.6 \cdot 10^{12}$ computation steps

for Experiment 4/3). By further inspection of the transformation algorithm we see that the spline function $\tilde{\mathbb{F}}_\infty$ now is just needed for the computation of $\tilde{\mathbb{F}}_0 \tilde{\mathbb{F}}_\infty^{-1}$, according to Step 3 in Algorithm 3.2.1. There $\tilde{\mathbb{F}}_0$ is also a two times continuously differentiable spline function interpolating the discrete image values of the start image \mathbb{F}_0 . So if we approximate $\tilde{\mathbb{F}}_0 \tilde{\mathbb{F}}_\infty^{-1}$ without using splines we avoid spline interpolation at all. For this purpose we follow the same strategy as in the case of the derivative. We simply approximate $\tilde{\mathbb{F}}_0(x, y) \tilde{\mathbb{F}}_\infty(x, y)^{-1}$ by $\mathbb{F}_0(i, j) \mathbb{F}_\infty(i, j)^{-1}$ for every $(x, y) \in [i - 1/2, i + 1/2) \times [j - 1/2, j + 1/2)$ and extend this definition if (x, y) is at the upper or right border of \overline{D} as before. The resulting algorithm using the approximations of the derivatives and the function values described as above is called *fast transformation algorithm*.

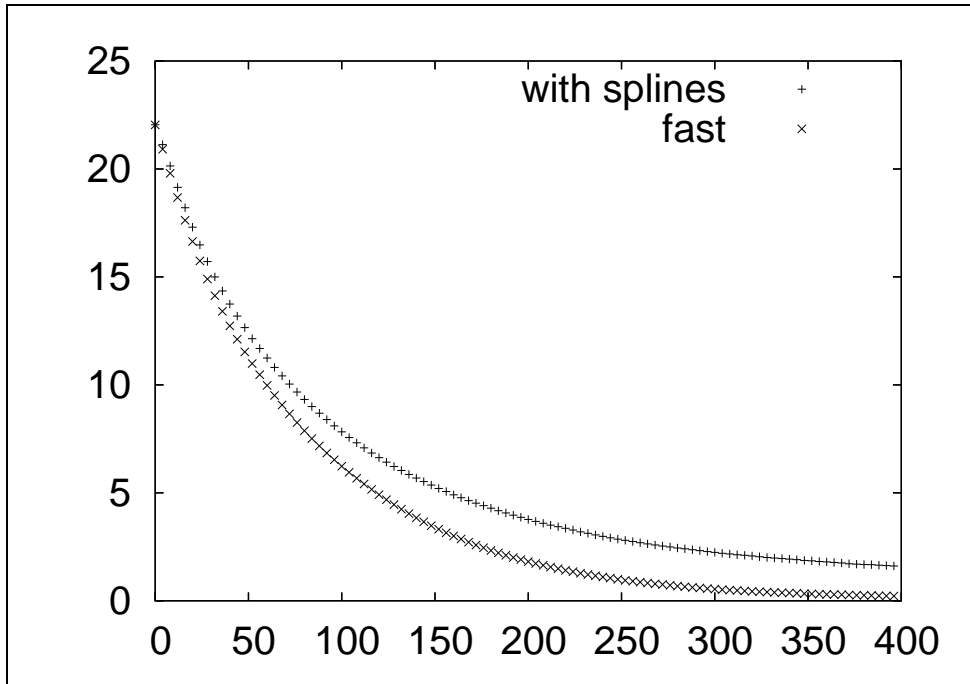


Figure 4.23. The diagram shows the behaviour of two \mathcal{L}^1 -distances in time. The error values ϵ_a are taken from the first experiment of this chapter (Experiment 1/1) where we used spline interpolation and from the application of the fast version of the transformation algorithm 4.0.1, using approximated function values (Experiment 7). For the plot we used one out of four values. The error resulting from the fast transformation is always less than the error resulting from the original transformation algorithm.

In order to show the difference between the transformation algorithm using spline interpolated functions $\tilde{\mathbb{F}}_0, \tilde{\mathbb{F}}_\infty$ and the usage of the fast transformation algorithm in **Experiment 7** we repeat the first experiment of this chapter (Experiment 1/1). As before we apply the transformation Algorithm 4.0.1 (now in the fast version) to the image pair $\mathbb{F}_0, \mathbb{F}_\infty$, as shown in Figure 4.1. We do not show the resulting image sequence because there are no interesting differences to the image sequence shown in Figure 4.2. The computation time has been reduced from 1 hour 38 minutes (Experiment 1/1 with spline interpolated functions) to 19 minutes (Experiment 7 with fast transformation). This means the fast algorithm is about 5 times faster than the original algorithm and the difference in their results is very small. The resulting error ϵ_a^f between \mathbb{F}_∞ and \mathbb{F}_t is shown in Figure 4.23. Additionally the error ϵ_a from Experiment 1/1 is shown to compare both functions. As we can see, the error ϵ_a^f is smaller and decreases faster than ϵ_a . A theoretical investigation of this behaviour seems interesting but here we leave this question open. Instead we go ahead to apply the transformation algorithm (in the fast version) to an existing problem in image processing.

The last example in this section uses the edge enhancing effect of the transformation algorithm. For this purpose in **Experiment 8** we choose $\mathbb{F}_0 \equiv 157$ and \mathbb{F}_∞ as the upper image in Figure 4.24. There we can see a fingerprint in a very bad quality. Some areas are nearly black and the ridges are not properly separated, whereas in other areas the ridges are missing at all. Usually fingerprint images are used to determine the *minutiae* – features as ridge endings, ridge bifurcation, ridge islands and so on. Therefore a good separation of the ridges is desired. In order to obtain such an image providing good ridge separation we apply the transformation algorithm with average scale performing $k = 50$ Monte Carlo simulation with step size $\Delta t = 0.1$ to the upper image in Figure 4.24. Note that we have chosen $\mathbb{F}_0 \equiv 157$, which is the average value of \mathbb{F}_∞ . The lower image in Figure 4.24 is the transformed image at transformation time $t = 10$. In order to highlight some interesting effects we have magnified three areas shown in Figure 4.25. The experiment took an overall time of 19 minutes.

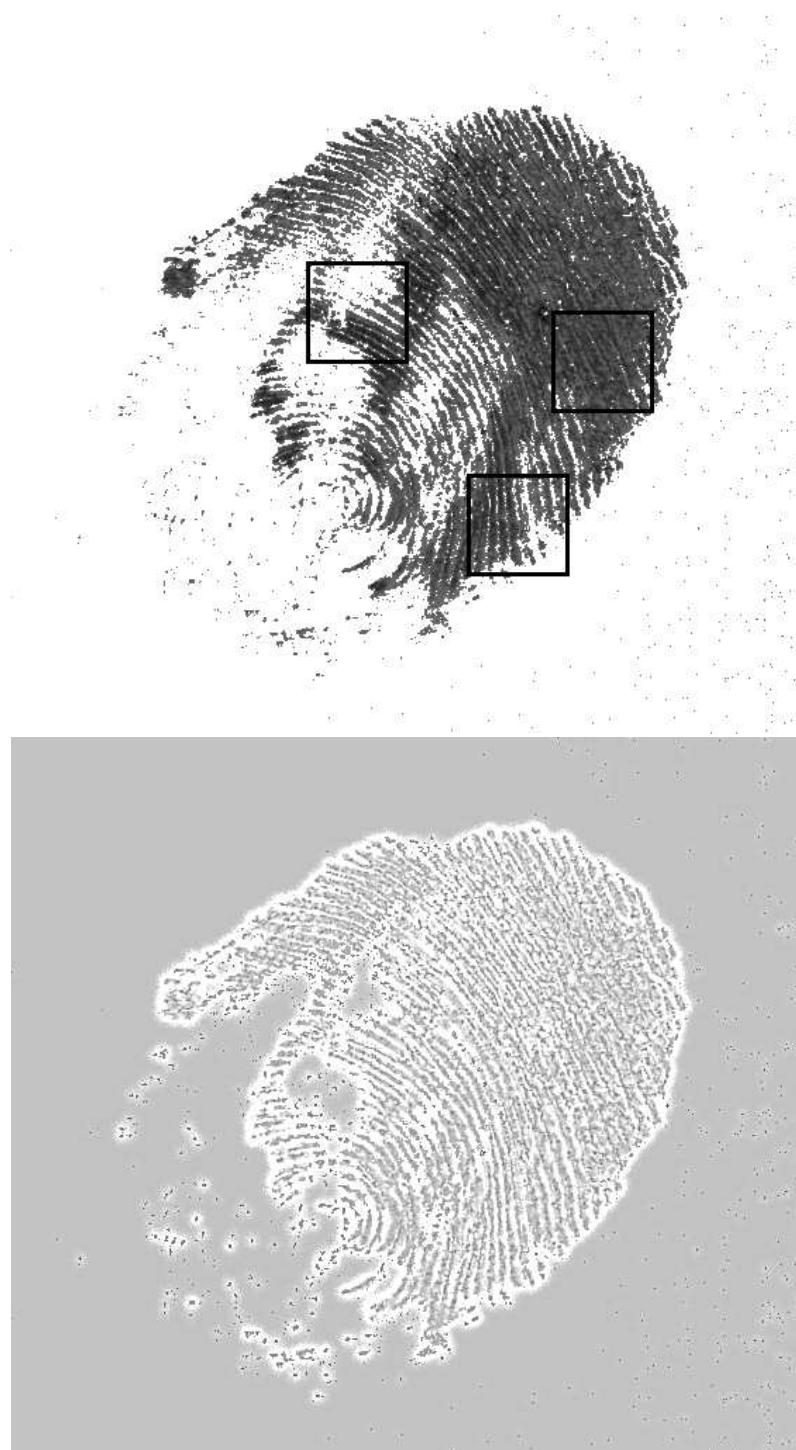


Figure 4.24. The upper image shows a fingerprint in bad quality. A magnification of the three highlighted areas is shown in Figure 4.25. The lower image is an early ($t=10$) reconstruction of the image above.

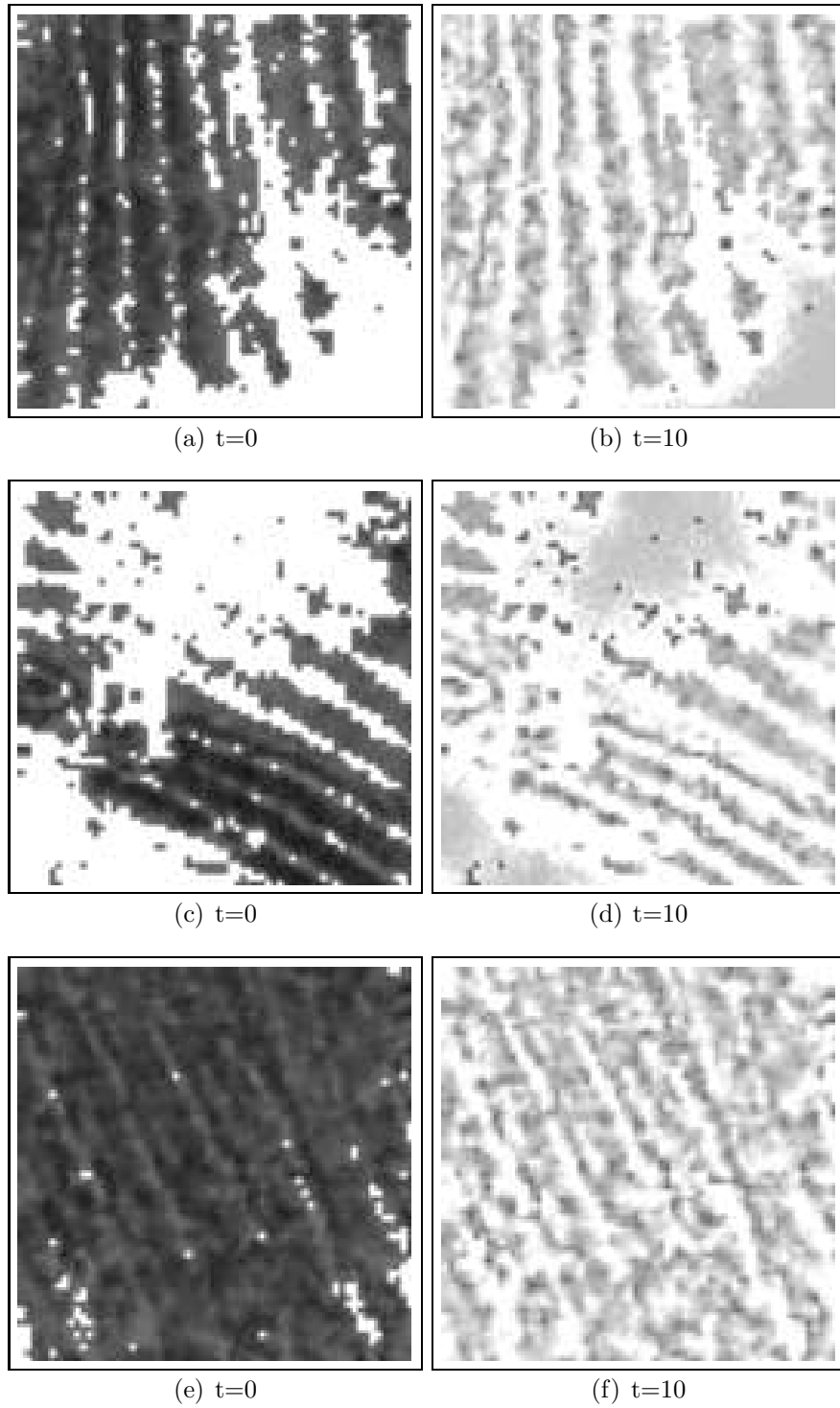


Figure 4.25. The figure shows three magnified parts of the images shown in Figure 4.24.

4.4 Image smoothing

After we have validated the principle function of the transformation algorithm, we turn to the application to a well known problem of image processing. We are interested in a basic problem called *image smoothing* (e.g. see [65]). There, by definition, the smoothness of an image depends on the absolute values of the gradients. So smoothing images means to decrease the absolute value of the gradients (and preserve the sign). De facto there exist image functions f and g where neither f is smoother than g nor g is smoother than f . However, we are not going to prove statements about the smoothness of \mathbb{F}_t . Instead we perform some transformation experiments to illustrate image smoothing with Algorithm 4.0.1. For this purpose in **Experiment 9** we repeat Experiment 1/1 from Section 4.2 and transpose the role of $\mathbb{F}_0, \mathbb{F}_\infty$ shown in Figure 4.1. Actually we invert the constant image (i.e. in this experiment we use $\mathbb{F}_\infty \equiv 256$) as we are instructed in Step 1 of Algorithm 4.0.1. Recall that we do this because we want to apply the transformation algorithm with maximum scale and for $\mathbb{F}_\infty \equiv 1$ it would follow $\mathbb{F}_t \leq 1$. We choose $\Delta t = 0.1$ and perform $k = 100$ Monte Carlo simulations to produced the image sequence shown in Figure 4.26. (The computation performed on a Intel Celeron D 366, 2.8 GHz takes 14 minutes 33 seconds to reach the transformation time $t = 20$.)

Remark. From $\mathbb{F}_\infty \equiv c$ follows $\tilde{\mathbb{F}}_\infty \equiv c$. But then the discrete derivative of \mathbb{F}_∞ used in the fast version of the transformation algorithm vanishes and the gradient of the corresponding spline interpolation $\nabla \tilde{\mathbb{F}}_\infty$ is also zero. Hence the approximated Itô diffusion used in all versions of the transformation algorithm is actually the approximation of a Brownian motion. If we denote the 2-dimensional Gaussian of variance σ^2 by ϕ_σ (as in Eqn. 3.10) it is well known (cp. e.g. [33, 56]) that for every $f \in C^0(\mathbb{R}^2)$ a solution of

$$\frac{\partial u}{\partial t} = \Delta u, \quad u_{t=0} = f \quad (4.6)$$

is given by the convolution $\phi_{\sqrt{2t}} * f$ for all $t > 0$. Actually, in the case $\mathbb{F}_\infty \equiv c$ we solve a Cauchy problem similar to 4.6 so we have a relation of \mathbb{F}_t at time $\frac{\sigma^2}{2}$ and smoothing by convolution with a Gaussian of variance σ^2 . The main difference of the Cauchy problem we solve and 4.6 is that we deal with functions defined

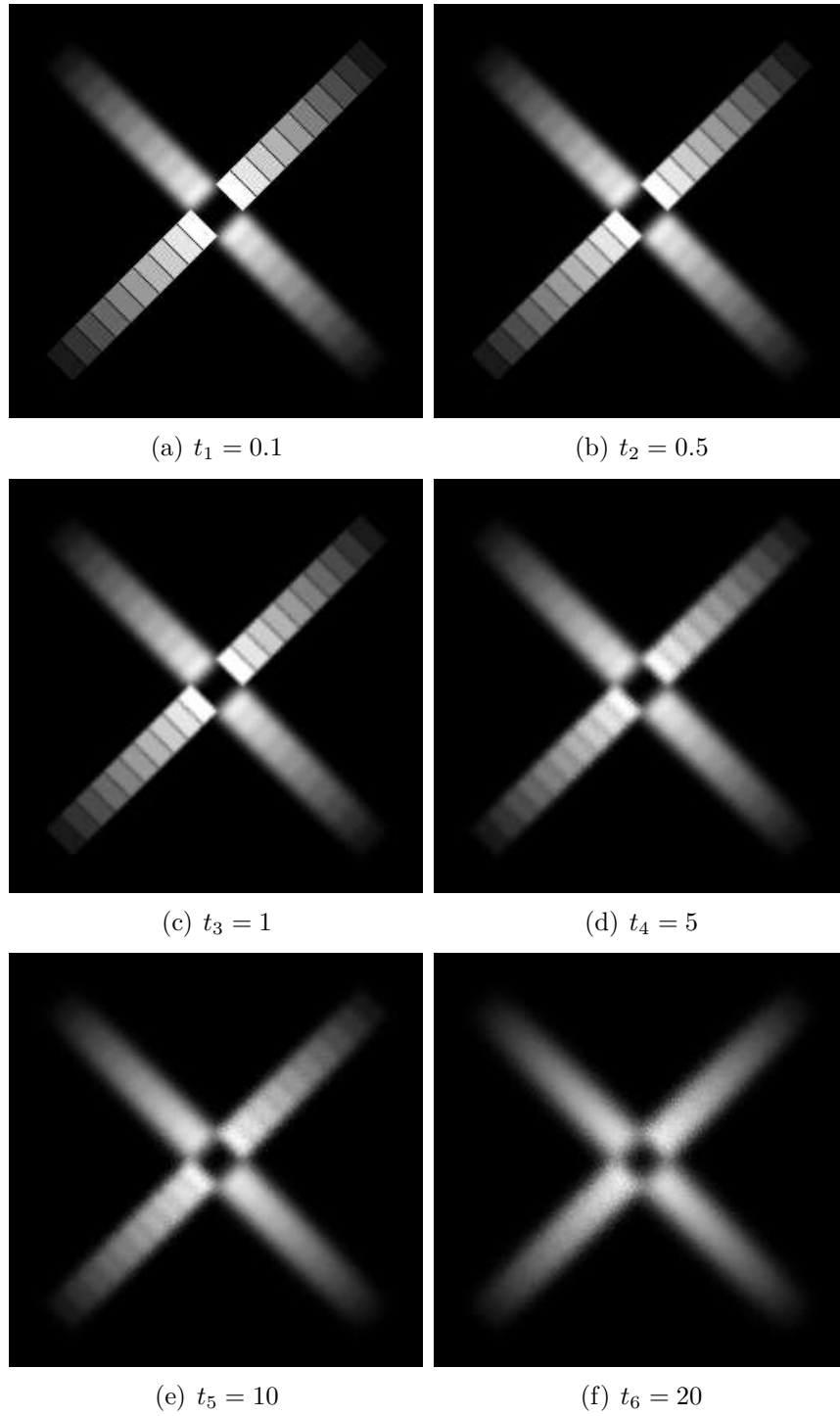


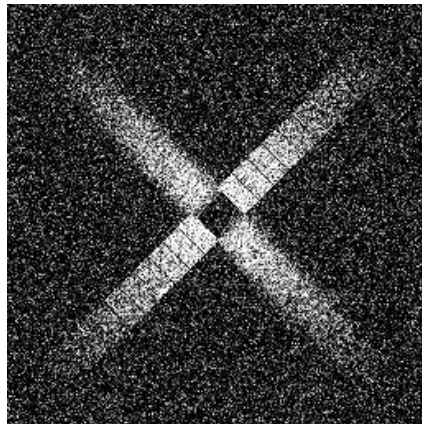
Figure 4.26. The sequence shows the results from images smoothing according to Experiment 9. The start image \mathbb{I}_0 is shown in Figure 4.1(b) and the stop image is $\mathbb{I}_\infty \equiv 256$. The step size is $\Delta t = 0.1$ and the number of Monte Carlo simulations is $k = 100$.

only on a subset D of \mathbb{R}^2 which fulfil a Neumann boundary condition. But we can extend $\tilde{\mathbb{I}}_0 c^{-1}$ easily to a two times continuously differentiable (periodic) function f defined on \mathbb{R}^2 . For this purpose we first mirror $\tilde{\mathbb{I}}_0 c^{-1}$ at the x -axis and then at the y -axis to obtain a two times continuously differentiable function defined on $(-x_n, x_n) \times (-y_n, y_n)$. This extended function (and its derivatives) fulfil a periodic boundary condition. So from a straight forward extension we obtain f as a two times continuously differentiable function on \mathbb{R}^2 . Furthermore, if $(B_t^x | t \geq 0)$ is a Brownian motion on \mathbb{R}^2 starting in $x \in D$ it is easy to show that in the case $\tilde{\mathbb{I}}_\infty = c$ we have

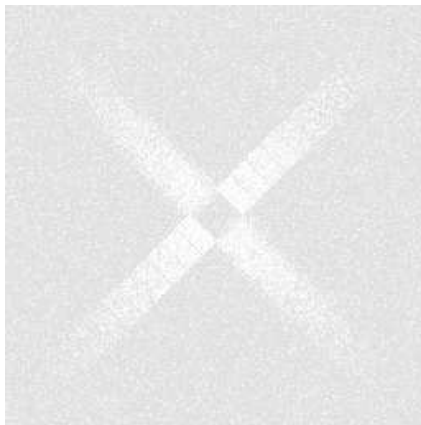
$$\mathbb{E} \left[\frac{\mathbb{I}_0}{\mathbb{I}_\infty}(X_t^x) \right] = \mathbb{E}[f(B_t^x)].$$

From this argument we get a rigorous connection to image smoothing by convolution with a Gaussian in the case $\mathbb{I}_\infty = \text{const.}$

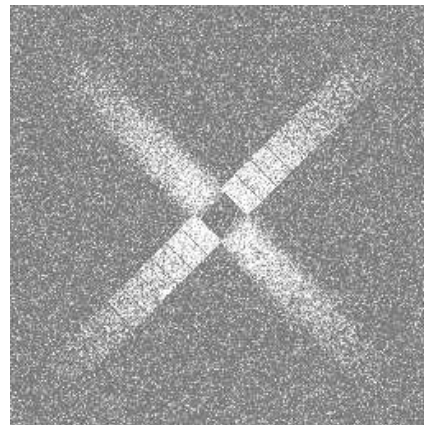
Now we corrupt the start image from Experiment 9 with 70 % noise using the **gimp** software package. The result (as shown in Figure 4.27(a)) is used as start image \mathbb{I}_0 in **Experiment 10/1**. Further we choose the stop image $\mathbb{I}_\infty \equiv 256$ and the step size $\Delta t = 0.1$. Then we use the transformation algorithm with maximum scale performing $k = 100$ Monte Carlo simulations to produce the image sequences shown in Figure 4.28. As we can see, we have to accept the smoothing of edges if we want to suppress the noise. This is because the transformation algorithm reconstructs the stop image for $t \rightarrow \infty$ and \mathbb{I}_∞ contains no edges which could remain. However, we can choose \mathbb{I}_∞ as a brighter version of the start image. Two versions are shown in Figure 4.27. In **Experiments 10/2-3** we set the transformation parameters $\Delta t = 0.1$ and $k = 100$ as in Experiment 10/1 and apply the transformation algorithm with maximum scale to the start image \mathbb{I}_0 shown in Figure 4.27(a) to reconstruct \mathbb{I}_∞ shown in Figure 4.27(b) (Experiment 10/2). For Experiment 10/3 we choose \mathbb{I}_∞ as shown in Figure 4.27(c). The resulting images \mathbb{I}_t at transformation times $t = 0.1, 0.5, 1, 5, 10, 20$ from both experiments are shown in Figures 4.29, 4.30. So we can compare them to the images from Experiment 10/1. We can see that \mathbb{I}_∞ chosen as shown in Figure 4.27(c) preserves more of the edges than \mathbb{I}_∞ chosen as shown in Figure 4.27(b). So the question arises what happens if



(a) Start image No 10/1-3



(b) Stop image No 10/2



(c) Stop image No 10/3

Figure 4.27. The upper image shows the image from Figure 4.1(b) where 70% of all pixels have been corrupted with uniform noise. It is the start image in Experiments 10/1-3. The lower images are simply brighter versions of the start image (i.e. rescaled to $[226, 256]$ respectively $[126, 256]$).

we set $\mathbb{F}_\infty = \mathbb{F}_0$. But in this case we have $\mathbb{F}_t = \mathbb{F}_0$ for all $t \geq 0$. In other words, \mathbb{F}_t is constant in time and this is not an interesting case because we have no image processing effects during the transformation.

Now one may ask for the behaviour of \mathbb{F}_t if $\mathbb{F}_0|_{\tilde{D}} = \mathbb{F}_\infty|_{\tilde{D}}$ where \tilde{D} is a subset of D_{disc} . For this in **Experiment 11** we choose the start image \mathbb{F}_0 as shown in Figure 4.31(a). In order to smooth the upper half of the image and leave the lower half unchanged we choose the stop image \mathbb{F}_∞ shown in Figure 4.31(f). Further we choose $\Delta t = 1$ and $k = 100$. Then we use the transformation algorithm with maximum scale to produce the images shown in Figures 4.31(b)-4.31(e). As we can see, the part of \mathbb{F}_t where $\mathbb{F}_0 = \mathbb{F}_\infty$ remains constant during the transformation. This means that in this experiment the transformation algorithm changes only those pixels for which \mathbb{F}_0 and \mathbb{F}_∞ differ. Roughly speaking, this is an automatic pixel selection.

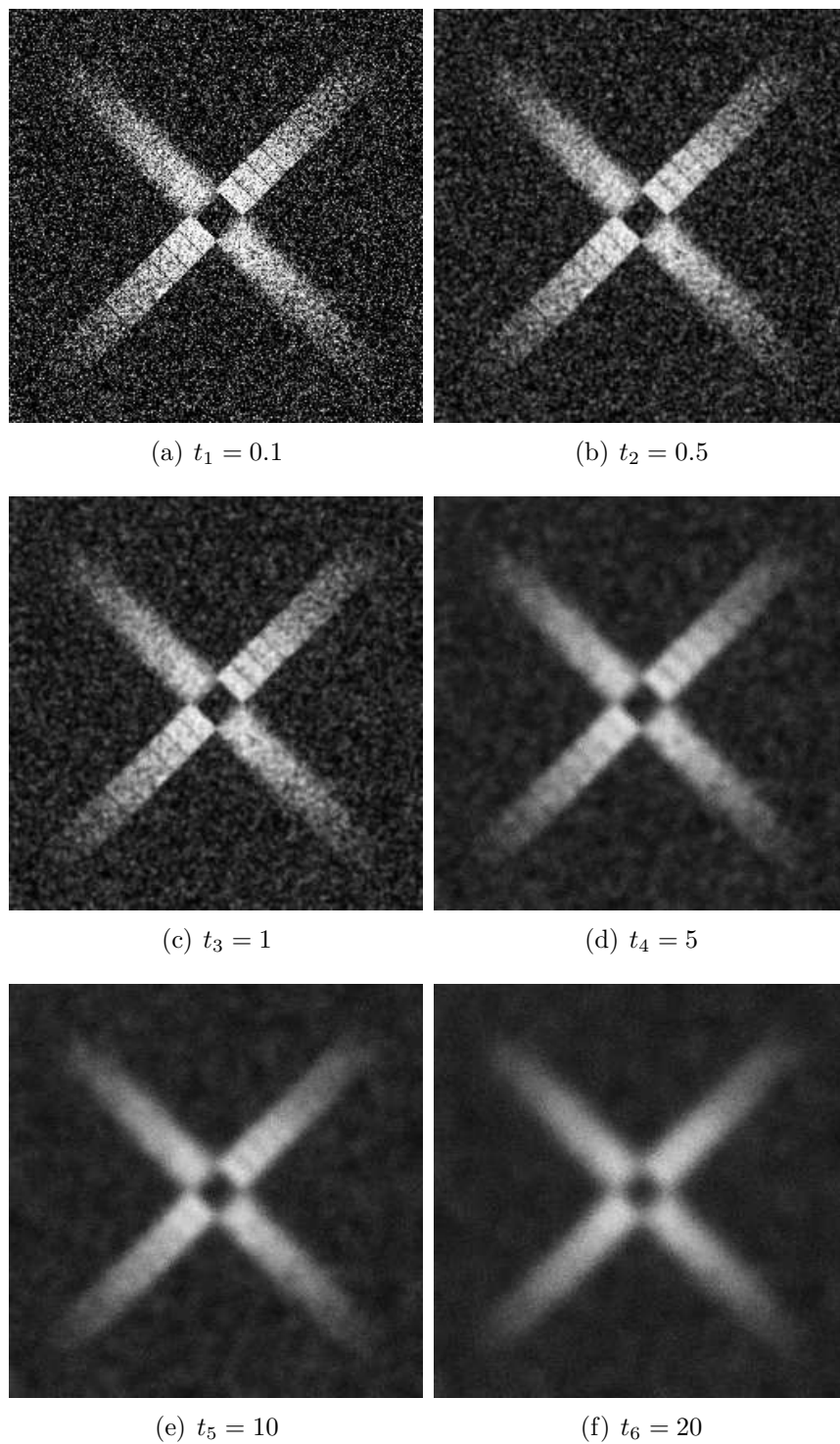


Figure 4.28. Image sequence corresponding to experiment No 10/1. The stop image is $\mathbb{f}_\infty \equiv 256$.

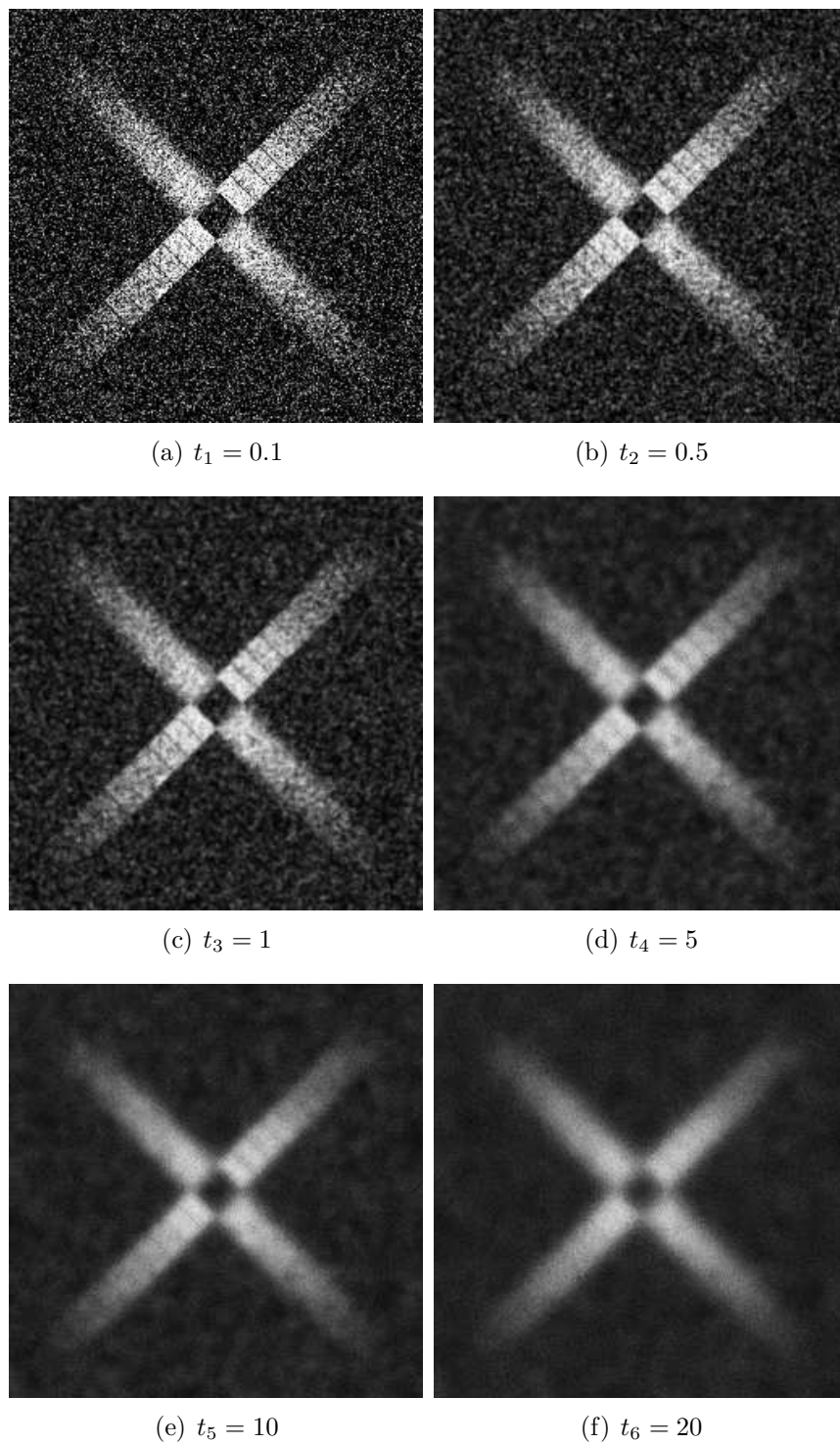


Figure 4.29. Image sequence corresponding to experiments No 10/2. The stop image is shown in Figure 4.27(b).

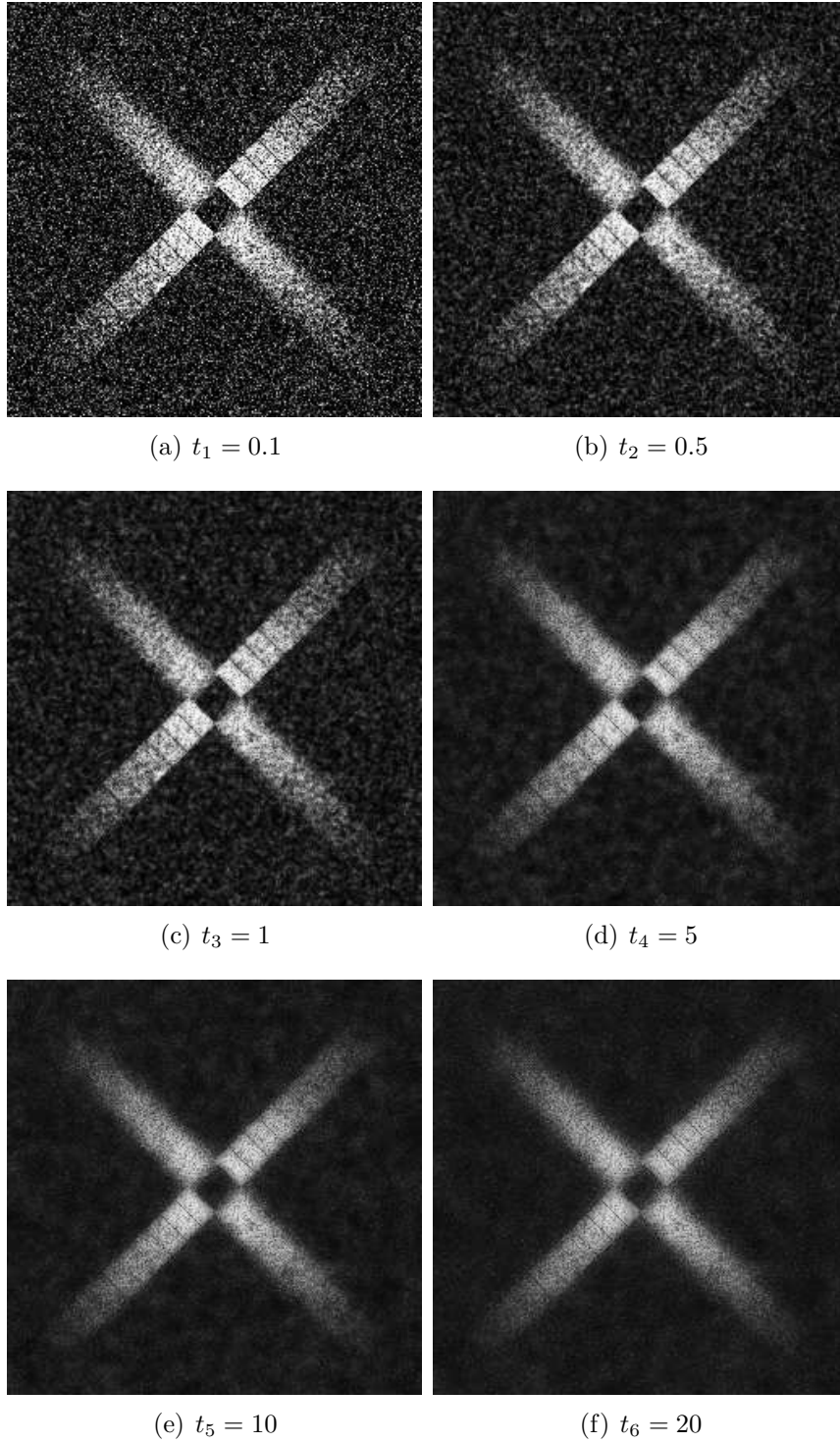


Figure 4.30. Image sequence corresponding to experiments No 10/3. The stop image is shown in Figure 4.27(c).

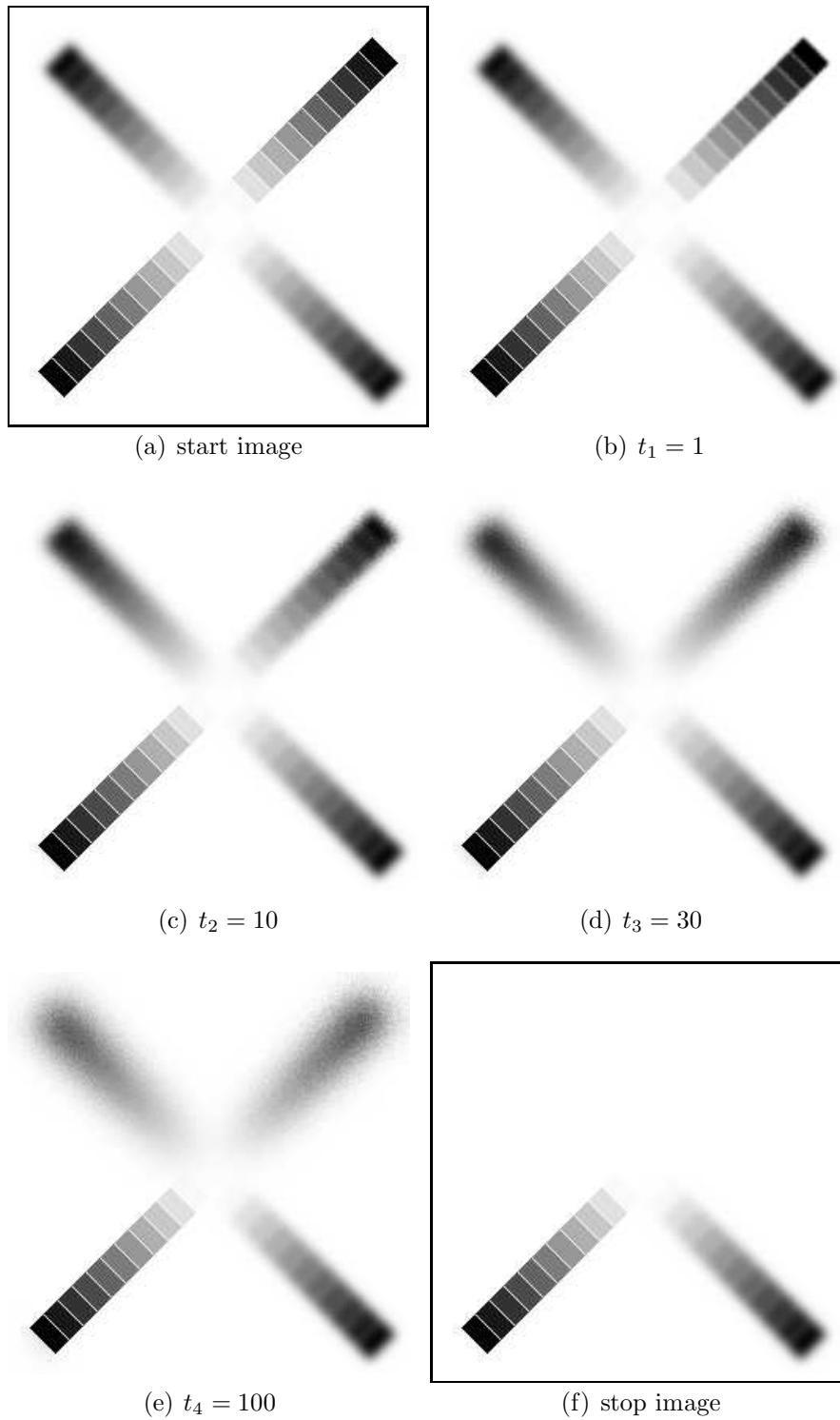


Figure 4.31. Partial image smoothing using the transformation algorithm with maximum scale ($\Delta t = 1$, $k = 100$).

As in Section 4.2, we are interested in the behaviour of \mathbb{I}_t for images showing natural objects. Therefore, in **Experiments 12/1-3**, we consider the images shown in Figure 4.17 as start images \mathbb{I}_0 . In each experiment the stop image is $\mathbb{I}_\infty \equiv 256$ and its size is equal to the size of the corresponding start image. We use the transformation algorithm with maximum scale to produce the image sequences shown in Figures 4.32-4.35. The transformation algorithm was set up with step size $\Delta t = 1$ and $k = 100$ Monte Carlo simulations. As we expect, the images are equably smoothed during the transformation.

Now we want to preserve some details of the images during the transformation. For this reason, in **Experiments 13/1-3**, we take the start images as in Experiments 12/1-3 but we choose different stop images (in order to take advantage of our method compared with smoothing by convolution with a Gaussian). The stop images for this experiments (shown in Figure 4.36) were generated using the despeckle algorithm from the `gimp` software package. The internal parameters of the despeckle algorithm were set up to recursive processing with mask size 3 and black/white threshold 30/225. Figures 4.37-4.40 show the image sequences we obtained by application of the transformation algorithm with average scale. The transformation parameters were set up to $\Delta t = 0.1$ and $k = 100$. As we can see, the resulting images are smooth but they contain more details than the images resulting from Experiments 12/1-3 (as intended).



Figure 4.32. The transformed images according to Experiments 12/1-3 at time $t_1 = 1$. The Start images are shown in Figure 4.17, whereas the stop image is congruent 256.



Figure 4.33. The transformed images according to Experiments 12/1-3 at time $t_2 = 10$. The Start images are shown in Figure 4.17, whereas the stop image is congruent 256.



Figure 4.34. The transformed images according to Experiments 12/1-3 at time $t_3 = 50$. The Start images are shown in Figure 4.17, whereas the stop image is congruent 256.

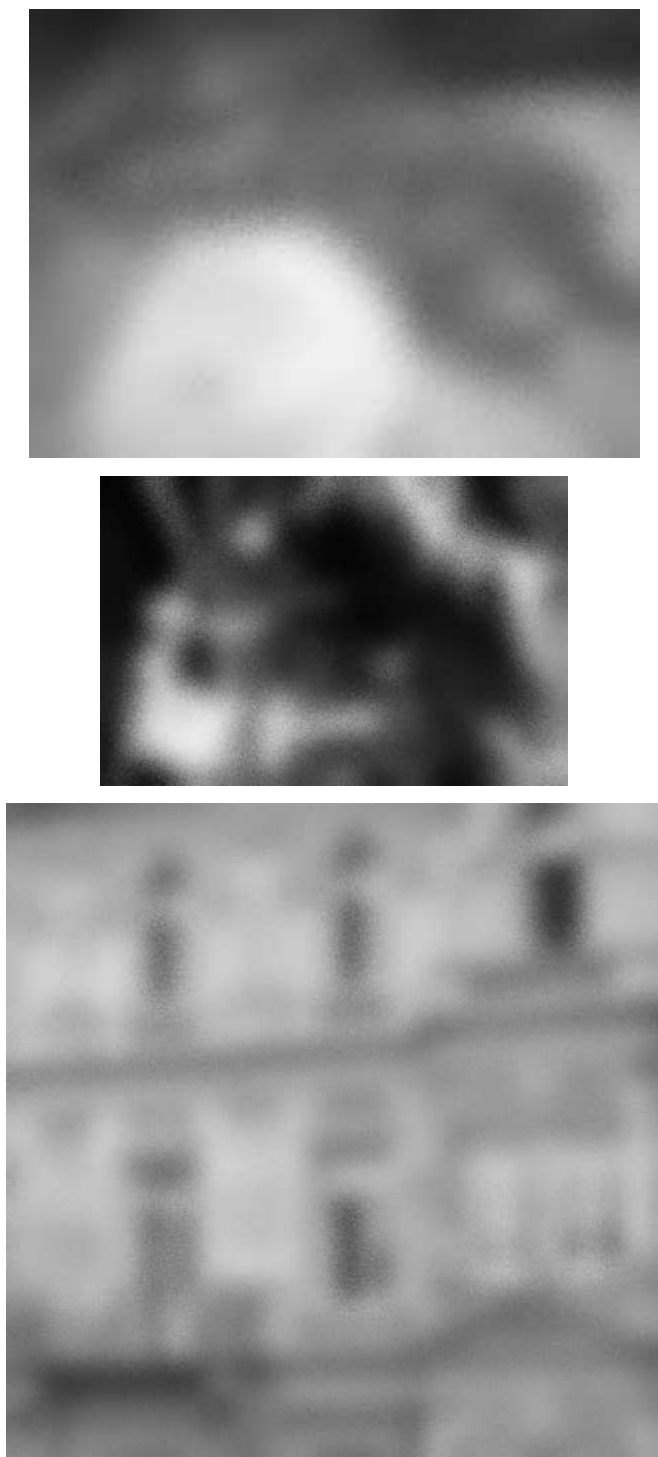


Figure 4.35. The transformed images according to Experiments 12/1-3 at time $t_4 = 100$. The Start images are shown in Figure 4.17, whereas the stop image is congruent 256.

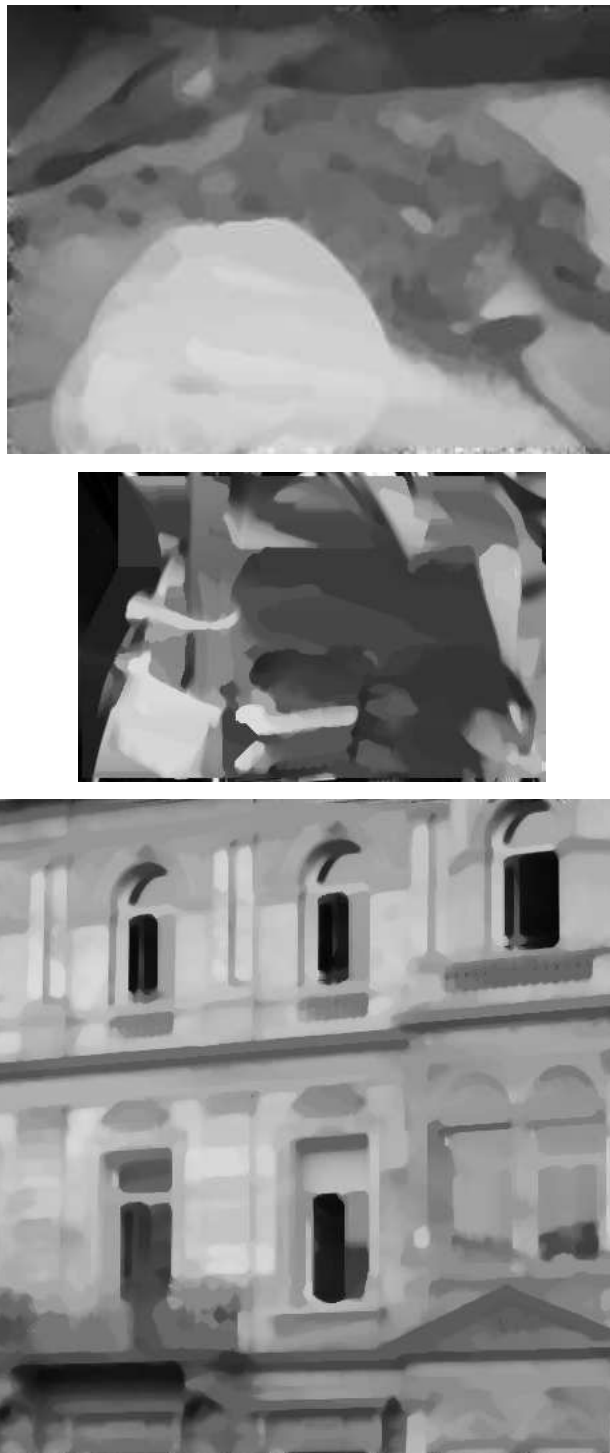


Figure 4.36. The stop images for Experiments 13/1-3. They were generated from the images shown in Figure 4.17 using a despeckle algorithm.



Figure 4.37. The transformed images according to Experiments 13/1-3 at time $t_1 = 0.1$. The start images are shown in Figure 4.17, whereas the stop images are shown in Figure 4.36.



Figure 4.38. The transformed images according to Experiments 13/1-3 at time $t_2 = 1$. The start images are shown in Figure 4.17, whereas the stop images are shown in Figure 4.36.



Figure 4.39. The transformed images according to Experiments 13/1-3 at time $t_3 = 5$. The start images are shown in Figure 4.17, whereas the stop images are shown in Figure 4.36.



Figure 4.40. The transformed images according to Experiments 13/1-3 at time $t_4 = 10$. The start images are shown in Figure 4.17, whereas the stop images are shown in Figure 4.36.

Now we make a connection to existing results. So in **Experiment 14/1** we consider the test image shown in Figure 4.41(a) of size 128×128 . It consists of a triangle and a rectangle and has frequently been used in literature (cp. e.g. [6, 82]). In order to give an impression of the de-noising effect of the transformation algorithm we corrupted 70% of all pixels of the test image using the `gimp` software package. The result, as shown in Figure 4.41(b), is used as the start image \mathbb{F}_0 . Now we apply the fast transformation algorithm with average scale to \mathbb{F}_0 using step size $\Delta t = 10$ and perform $k = 100$ Monte Carlo simulations to reconstruct $\mathbb{F}_\infty \equiv 256$. The transformed image at times $t = 10, 100, 500, 1000$ is shown in Figure 4.42. As mentioned before, in the case $\mathbb{F}_\infty = \text{const}$ we do not expect better results than this provided by a convolution with a Gaussian. Instead, we only make use of the potential of our new method if we choose a stop image which is not constant. So in **Experiment 14/2** we proceed similar to Experiments 13/1-3 and generate a stop image shown in Figure 4.43(f), using the `despeckle` algorithm of the `gimp` software package. We set the internal parameters of the `despeckle` algorithm to non-recursive processing with mask size 4 and black/white threshold 0/255. Then we apply the fast transformation algorithm with average scale to the image shown in Figure 4.41(b). We have chosen $\Delta t = 0.1$ and $k = 100$ to generate the images shown in Figure 4.42(b)-(e). As we can see the noise in the stop image is reduced by the `despeckle` algorithm. For this we have to accept an unnaturally strait rectangle. If we look at the transformed images we can see that the noise is reduced as in the stop image (or even better) and the rectangle looks more like the rectangle shown in the start image.

4.5 Remark on colour images

In difference to gray-value images a colour image usually consists of three times more information than the same image seen in gray-values. This is true because for every gray-value we have a corresponding triple of values at the colour image side. Hence, we can decompose each colour image f into three one-channel images f_R , f_G and f_B and interpret each of them as gray-value image. (Here we have chosen the indices R, G, B because we assume that the colour

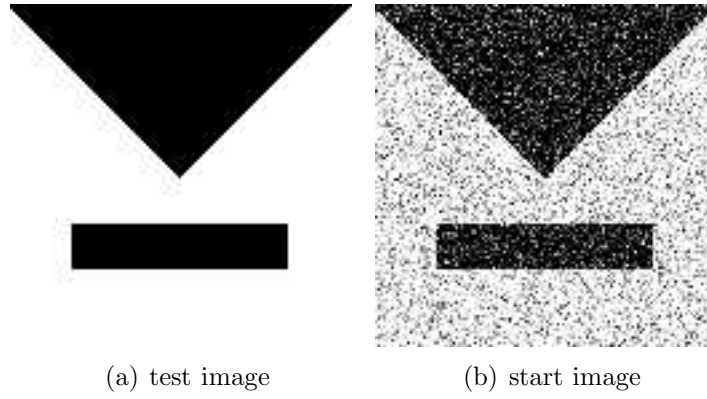


Figure 4.41. The test image has been corrupted with 70% uniform noise to obtain the start image.

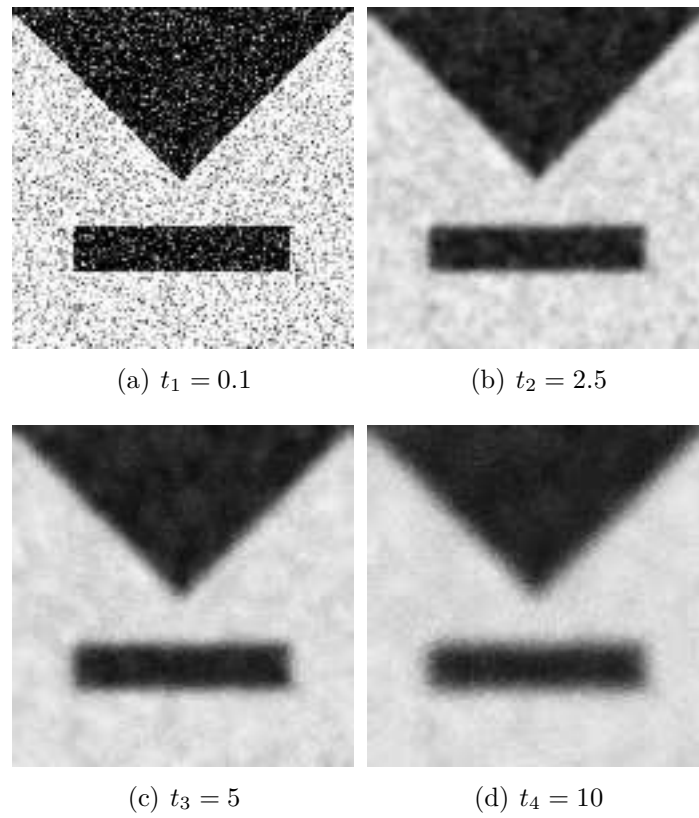


Figure 4.42. Reconstruction sequence illustrating the de-noising effect. The stop image is congruent 256. The transformation parameters are $\Delta t = 0.01$ and $k = 100$ (Experiment 14).

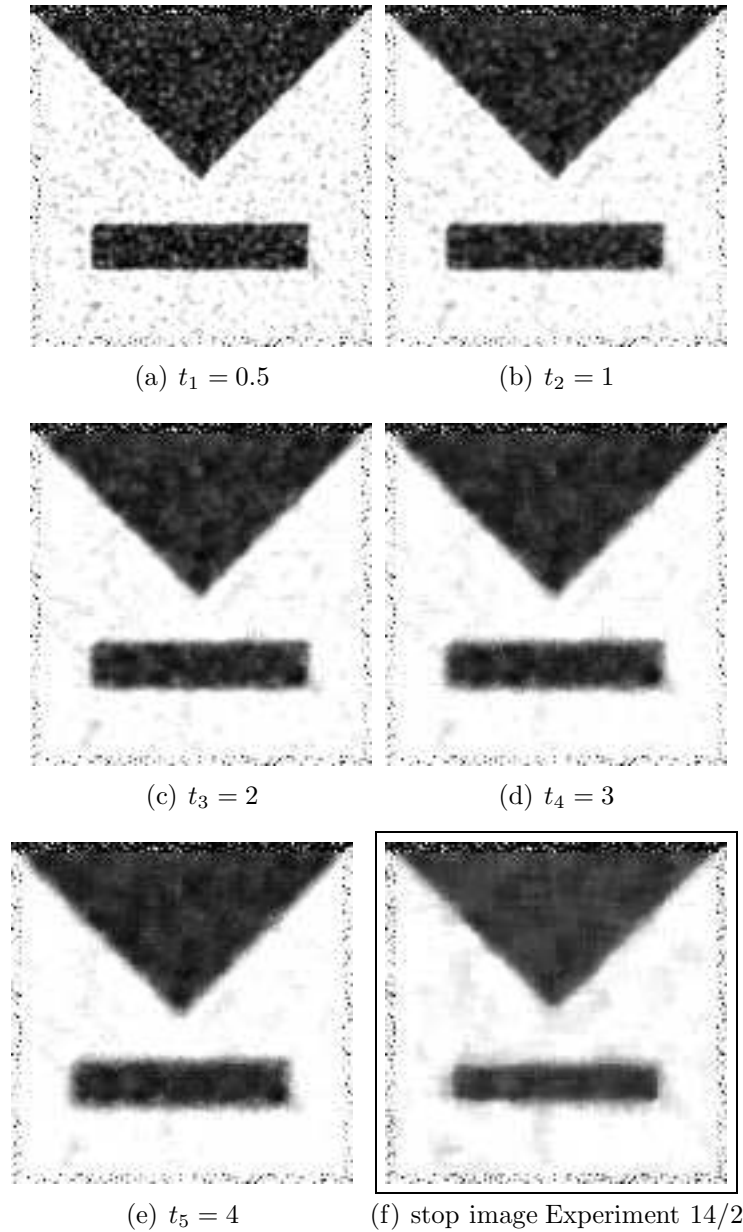


Figure 4.43. In Figures (a)-(e) the transformed images resulting from Experiment 14/2 are shown. The stop image shown in Figure (f) results from an application of a despeckle algorithm to the image shown in Figure 4.41(b).

images are given in the *RGB colour space*. For more information about that e.g. see [28].) After this we are able to apply any of the algorithms described in this work to these three images. Finally we recompose the three results in the obvious way to one colour image. Thus we can apply the algorithms introduced here to colour images without problems. Of course the same holds true for multi-channel images such as medical images.

Experiments							
No.	images			MC	Δt	using splines	scale value
	start	stop	size				
1/1	$\equiv 256$	Fig. 4.1(b)	256×256	50	1	yes	1
1/2	$\equiv 256$	Fig. 4.1(b)	256×256	50	1	yes	max
1/3	$\equiv 256$	Fig. 4.1(b)	256×256	50	1	yes	avr
2/1	$\equiv 256$	Fig. 4.1(b)	256×256	10	1	yes	1
2/2	$\equiv 256$	Fig. 4.1(b)	256×256	10	0.1	yes	1
2/3	$\equiv 256$	Fig. 4.1(b)	256×256	10	0.01	yes	1
3/1	$\equiv 256$	Fig. 4.1(b)	256×256	100	1	yes	1
3/2	$\equiv 256$	Fig. 4.1(b)	256×256	100	0.1	yes	1
3/3	$\equiv 256$	Fig. 4.1(b)	256×256	100	0.01	yes	1
4/1	$\equiv 256$	Fig. 4.1(b)	256×256	1000	1	yes	1
4/2	$\equiv 256$	Fig. 4.1(b)	256×256	1000	0.1	yes	1
4/3	$\equiv 256$	Fig. 4.1(b)	256×256	1000	0.01	yes	1
5/1	Fig. 4.12(a)	Fig. 4.1(b)	256×256	100	0.1	yes	max
5/2	Fig. 4.12(b)	Fig. 4.1(b)	256×256	100	0.1	yes	max
5/3	Fig. 4.12(c)	Fig. 4.1(b)	256×256	100	0.1	yes	max
6/1	$\equiv 256$	Fig. 4.17(a)	300×200	100	10	yes	avr
6/2	$\equiv 256$	Fig. 4.17(b)	350×232	100	10	yes	avr
6/3	$\equiv 256$	Fig. 4.17(c)	400×400	100	10	yes	avr
7	$\equiv 256$	Fig. 4.1(b)	256×256	50	1	no	1
8	$\equiv 256$	Fig. 4.24	564×511	50	0.1	no	avr
9	Fig. 4.1(b)	$\equiv 256$	256×256	100	0.1	no	max
10/1	Fig. 4.27(a)	$\equiv 256$	256×256	100	0.1	no	max
10/2	Fig. 4.27(a)	Fig. 4.27(b)	256×256	100	0.1	no	max
10/3	Fig. 4.27(a)	Fig. 4.27(c)	256×256	100	0.1	no	max
11	Fig. 4.31(a)	Fig. 4.31(f)	256×256	100	1	no	max
12/1	Fig. 4.17(a)	$\equiv 256$	300×200	100	1	no	max
12/2	Fig. 4.17(b)	$\equiv 256$	350×232	100	1	no	max
12/3	Fig. 4.17(c)	$\equiv 256$	400×400	100	1	no	max
13/1	Fig. 4.17(a)	Fig. 4.36(a)	300×200	100	0.1	no	avr
13/2	Fig. 4.17(b)	Fig. 4.36(b)	350×232	100	0.1	no	avr
13/3	Fig. 4.17(c)	Fig. 4.36(c)	400×400	100	0.1	no	avr
14/1	Fig. 4.41(a)	$\equiv 157$	256×256	100	0.01	no	avr
14/2	Fig. 4.41(a)	Fig. 4.43(f)	256×256	100	0.1	no	avr

Chapter 5

Results and Perspectives

In Chapter 1 we have introduced the basic idea of the *Image Reconstruction as Groundstate of Hamiltonian Operators* H in the Hilbert space $L^2(\mathbb{R}^d, \lambda^d)$. We considered this space because there the results we needed were already proven. So we could focus on introducing the basic idea of the reconstruction. For this we defined $H := -\frac{1}{2}\Delta + \frac{\Delta f_\infty}{2f_\infty}$ with domain $\mathcal{D}_H = \overline{C_2}(\mathbb{R}^d)$. The function $f_\infty \in \overline{C_2}(\mathbb{R}^d)$ was chosen strictly positive. Then we deduced the reconstruction property

$$f_t := \exp(-tH)f_0 \rightarrow cf_\infty \quad \text{for } f_0 \in \mathcal{D}_H, \quad (5.1)$$

where $c := (f_0, f_\infty)_{L^2(\mathbb{R}^d, \lambda^d)}$, under the condition

$$\frac{\Delta f_\infty}{2f_\infty}(x) \rightarrow \infty \quad \text{for } |x| \rightarrow \infty.$$

Finally we used a unitary map between $L^2(\mathbb{R}^d, \lambda^d)$ and $L^2(\mathbb{R}^d, f_\infty^2 \lambda^d)$ to reach the representation

$$f_t := \mathbb{E} \left[\frac{f_0}{f_\infty}(X_t) \right] f_\infty \quad \text{for } f_0 \in \mathcal{D}_H, \quad (5.2)$$

where we defined $(X_t|t \geq 0)$ as Itô diffusion on \mathbb{R}^d .

Then in Chapter 2 we repeated the argument of Chapter 1 but now we considered the space $L^2(D, \lambda^d)$ for $D \subset \mathbb{R}^d$ open, bounded and convex. In order to present the basic reconstruction idea in the space $L^2(D, \lambda^d)$ we had to prove several statements. But first of all we introduced strong Neumann boundary

conditions for D with possibly non-smooth boundary. Then we found that in $L^2(D, \lambda^d)$ the spectrum of the operator H , now defined for $f \in \overline{C_2}(D)$ with either strong Neumann 0 or Dirichlet 0 boundary conditions, is purely discrete. Moreover we found that the smallest eigenvalue possesses the eigenfunction f_∞ and has multiplicity one. These facts played the central role in the introduction of the basic idea of the reconstruction in Chapter 1 because from these two statements we derived the reconstruction property given in Equation 5.1. Then we represented the function f_t as in Equation 5.2. But in this case $(X_t|t \geq 0)$ has been defined as the solution of a Skorokhod problem. In order to prove Equation 5.2 we derived a version of the Feynman-Kac formula for solutions of Skorokhod problems. In the more general context of locally square integrable martingales this result is already known. Because of the absence of generality we were able to give a new, easy proof. Finally we showed that f_t converges in $L^2(D, \lambda^d)$ to cf_∞ for t to ∞ and that this convergence is actually point-wise.

We considered the space $L^2(D, \lambda^d)$ to prepare applications in image processing. There, $D \subset \mathbb{R}^2$ is a rectangle and the functions f are extensions of image functions (e.g. data provided by digital cameras). In Chapter 3 we gave a short resume of two existing mechanisms providing strictly positive $f \in \overline{C_2}(D)$ with either strong Neumann 0 or Dirichlet 0 boundary conditions starting from discrete data. Then we discussed approximations of function values of $f \in \overline{C_2}(D)$ and of its gradient. Moreover in Chapter 3 we formulated an algorithm which can be used to approximate $f_t(x)$ for $x \in D$. Therefore we used an existing discrete approximation for the solution X_t of a Skorokhod problem. In fact, we extended an existing approximation scheme to a scheme of higher order. Actually, the extension has no relevance for the special experiments we performed. So the extension is described for the mathematical (scientific) interest and can be seen as an add on to the main work.

Finally, in Chapter 4, we formulated an algorithm for image transformation providing a sequence of images $\mathbb{F}_0, \dots, \mathbb{F}_t$. There \mathbb{F}_0 is interpreted as image data corresponding to the extension f_0 . Moreover we know that the parameters of the transformation algorithm can be chosen such that \mathbb{F}_t converges for $t \rightarrow \infty$ to $c\mathbb{F}_\infty$, the rescaled image data corresponding to the rescaled image cf_∞ . So we obtained a mechanism for image transformation from \mathbb{F}_0 to

$c\mathbb{F}_\infty$ providing the state of transformation as image function \mathbb{F}_t corresponding to the extension f_t (as defined in Equation 5.1). In order to illustrate the behaviour of \mathbb{F}_t we have chosen different image pairs $\mathbb{F}_0, \mathbb{F}_\infty$ to perform some computer experiments. Then we discussed two possibilities to choose c different from $(f_0, f_\infty)_{L^2(D, \lambda^d)}$ as time dependant scale values $c(t), \tilde{c}(t)$ and we have formulated two versions of the transformation algorithm using these time dependent scale values. In contrast to the original transformation algorithm these two versions provide rescaled images $c(t)^{-1}\mathbb{F}_t$ and $\tilde{c}(t)^{-1}\mathbb{F}_t$ converging to \mathbb{F}_∞ . Moreover, the image at time $t = 0$ is equal to \mathbb{F}_t . Then we formulated a fast version of the transformation algorithm. The version is called fast because the extension of the discrete image functions $\mathbb{F}_0, \mathbb{F}_\infty$ to differentiable functions is avoided. Instead the fast transformation uses some approximations discussed before. So the computation time needed for experiments using the fast transformation algorithm is five times less than the computation time for experiments using the original version of the transformation algorithm. Of course we illustrated the behaviours of the image functions \mathbb{F}_t resulting from experiments with all the different versions of the transformation algorithm. Finally we gave some examples for an application of the transformation algorithm to some well known problems of image processing by the choice of appropriate image pairs $\mathbb{F}_0, \mathbb{F}_\infty$. So we noticed an edge enhancing effect of the transformation algorithm in the reconstruction experiments. There we set $\mathbb{F}_0 = \text{const}$ and \mathbb{F}_∞ was chosen as a given image. We applied this new method to an image showing a fingerprint in bad quality. The resulting image shows enhanced and more separated ridges. Hence the automatic detection of interesting features (minutiae) in the resulting image is favoured.

As often the case, somehow, image smoothing is the reverse of edge enhancement. So we have illustrated that the transformation algorithm can be used to smooth images. For this we have interchanged the roles of the images $\mathbb{F}_0, \mathbb{F}_\infty$. Precisely, for simple image smoothing we set $\mathbb{F}_\infty = \text{const}$ and take \mathbb{F}_0 as a given image. For this setup of the transformation algorithm (the special case $\mathbb{F}_\infty = \text{const}$) we made a theoretical connection to smoothing by convolution with a Gaussian and performed the corresponding experiments. After that we made some experiments where we generated \mathbb{F}_∞ from the given im-

age \mathbb{F}_0 . In these experiments \mathbb{F}_∞ is not constant. Hence the resulting images \mathbb{F}_t are different to images produced by convolution with a suitable Gaussian. That means we found a generalisation of smoothing images by convolution with a Gaussian. Of course we illustrated the advantages of our generalisation (advanced smoothing) by some experiments. We have shown how the transformation algorithm can be used to smooth parts of an image whereas other parts of the image are conserved. Further we illustrated smoothing with conservation of image details on some level. Finally we have performed two experiments establishing a connection to some existing results concerning image smoothing. Precisely, we made transformation experiments illustrating the de-noising effect of our method.

In all we provided a new image processing method founded on our theoretical results and illustrated some possible applications. This method is more than an ad-hoc strategy to transform images into a more pleasant look as we have seen from the connection to image smoothing by convolution with a Gaussian. Besides, this work can be seen as starting point for further theoretical investigations as well as further computer experiments. For this we give a collection of some interesting questions and ideas.

- In the original version of the transformation algorithm we start with two discrete image functions $\mathbb{F}_0, \mathbb{F}_\infty$. Then we interpolate these image functions to obtain differentiable functions f_0, f_∞ defined on a rectangle. After an application of the transformation algorithm we end with a discrete image function \mathbb{F}_t . So one may ask for a possibility to avoid the use of f_0, f_∞ . We have chosen approximations for f_0, f_∞ which are constant on a small square around the discrete function value and used derivatives which correspond to discrete derivatives. These approximations are not theoretically founded but the results of the experiments are unexpectedly good. We note that \mathbb{F}_t converges faster to \mathbb{F}_∞ if we use the fast transformation than if we use the transformation with f_0, f_∞ (and we have shorter computation time – these are two different things). So it seems worth to make a theoretical investigation of discrete operators. Then the counterpart of the Itô diffusion may be a Markoff chain. So we would end in a completely discrete theory.

- We obtained the representation 5.2 of the function f_t as solution of a Cauchy problem. Then for the approximative computation of f_t we have chosen a Monte Carlo approach. For this we must accept the dissatisfying computation times. So if we find an analytic expression for f_t we can avoid the computation of 5.2. Hence we can avoid the Monte Carlo simulation and save computation time. An interesting approach for this purpose is the representation of 5.2 as integral over a function of transition probabilities.
- In order to investigate the convergence speed of \mathbb{F}_t to \mathbb{F}_∞ it would be interesting to know the spectrum of the operator $H := -\frac{1}{2}\Delta + \frac{\Delta f_\infty}{2f_\infty}$. Precisely it would be interesting to know the second lowest eigenvalue of H . Then we have

$$\begin{aligned}
|\alpha_0 v_0(x) - \exp(-tH)f_0(x)| &\leq \left| \sum_{k \in \mathbb{N}} \exp(-t\lambda_k) \alpha_k v_k(x) \right| \\
&\leq \exp(-t\lambda_1) \left| \sum_{k \in \mathbb{N}} \alpha_k v_k \right| \\
&= \exp(-t\lambda_1) |(f_0, f_\infty) f_\infty(x) - f_0(x)|
\end{aligned}$$

for all $x \in D$. Here we used the notation of Section 3.5.1.

- For further characterisation of the behaviour of $\mathbb{F}_t(x)$ for $x \in \tilde{D} \subset D_{\text{disc}}$ one can apply the statements given in Chapter 2 to the operator \tilde{H} acting on the space $L^2(\tilde{D}, \lambda^d)$. Therefore \tilde{D} has to be convex. So if \tilde{D} is not convex we have to decompose \tilde{D} into disjoint convex subsets $\tilde{D}_1, \dots, \tilde{D}_n$. Then we can perform transformation experiments using each of the subsets \tilde{D}_i . Afterwards we recompose the transformed image on \tilde{D} from the transformed image parts on \tilde{D}_i . Using this method we actually compute the transformed image just for the $x \in \tilde{D}$ and save the computation time needed to get the values of the transformed image $\mathbb{F}_t(x)$ for $x \in D_{\text{disc}} \setminus \tilde{D}$. Additionally from an experimental point of view it would be interesting to perform experiments using an explicitly non-convex subset \tilde{D} .
- Our experiments can not be used to give a statistical verification of our

theoretical results. Instead the experiments just illustrate the behaviour of the transformed image \mathbb{F}_t for a few different image pairs $\mathbb{F}_0, \mathbb{F}_\infty$. Nevertheless, a statistical verification seems interesting. Moreover one could investigate:

- other scale values than $c(t), \tilde{c}(t)$
- the dependency of the transformed image \mathbb{F}_t on the transformation parameters $\Delta t, k$ for more than one image pair $\mathbb{F}_0, \mathbb{F}_\infty$ and nine different setups of transformation parameters
- the difference between the fast transformation and the transformation using splines applied to the problems of image smoothing, de-noising and edge enhancement
- the edge enhancing effect in detail
- more than two different possibilities (colour scale and despeckle algorithm) to generate stop images from a given start image.

Especially an investigation of the last point seems very interesting because the stop image has a big influence on the behaviour of \mathbb{F}_t . Moreover we have seen that if $\mathbb{F}_\infty = \text{const}$ we are in the case of smoothing with a Gaussian. So it is obvious that the big advantage of our new method is the possibility to choose different images $\mathbb{F}_\infty \neq \text{const}$.

- It seems interesting to investigate the applicability of the image transformation to other problems of image processing such as super resolution or image segmentation as well as face recognition.

Notation

In Chapter 1

\mathbb{N}, \mathbb{N}_0	$\{1, 2, 3, \dots\}, \mathbb{N} \cup \{0\}$
$\mathbb{R}, \mathbb{R}_{\geq 0}, \mathbb{R}_{>0}$	real Numbers, $[0, \infty), (0, \infty)$
(\mathbb{R}^d, x)	d -dimensional Euclidian vector space
$\frac{\partial}{\partial x}$	partial derivative corresponding to the variable x
$C^2(\mathbb{R}^d), C^2(D)$	two times continuous differentiable functions with values in \mathbb{R} defined on \mathbb{R}^d or some open subset D
$\overline{\mathbb{R}}^d$	$\mathbb{R}^d \cup \{\pm\infty\}$
$\text{supp}(f)$	support of $f : D \rightarrow \mathbb{R}$ is $\{x \in D f(x) \neq 0\}$
$\ker(f)$	null space of f is $\{x \in D f(x) = 0\}$
$C_0^2(\mathbb{R}^d), C_0^2(D)$	f in $C^2(\mathbb{R}^d)$ respectively $C^2(D)$ with compact support
$\Delta, \Delta(\cdot)$	Laplace operator
I_d	d -dimensional unit matrix
(Ω, \mathcal{A}, P)	probability space
$\mathcal{B}(\mathbb{R}^d)$	Borel σ -algebra of \mathbb{R}^d
λ, λ^d	Lebesgue measure on \mathbb{R}, \mathbb{R}^d or on subsets
$\mathbb{E}[X], \text{Var}(X)$	expectation, variance of the random variable X
$L^2(\mathbb{R}^d, \lambda^d)$	Hilbert space of classes of square integrable functions
$(f, g), \ f\ $	inner product and Norm for $f, g \in L^2(\mathbb{R}^d, \lambda^d)$
H, \mathcal{D}_H	Hamilton operator on $L^2(\mathbb{R}^d, \lambda^d)$, domain of H
$\text{ran}(\mathcal{D}_H)$	range of H is $\{Hf f \in \mathcal{D}_H\}$
v_n, λ_n	Eigenvector of H and corresponding Eigenvalue
$\sigma(H)$	spectrum of H , here the set of all λ_n
$(T_t t \geq 0)$	strongly continuous semigroup on \mathcal{D}_H

b, σ	drift, diffusion coefficients
$(X_t t \geq 0), X_t^x$	Itô diffusion on \mathbb{R}^d or subsets, starting in x
\mathcal{F}_t	filtration generated by X_t – is $\sigma(X_s s \leq t)$
$L^2(\mathbb{R}^d, f_\infty^2 \lambda^d)$	Hilbert space, integrability w.r.t. $f_\infty^2 \lambda$
$(f, g)_{f_\infty}, \ f\ _{f_\infty}$	inner product and Norm for $f, g \in L^2(\mathbb{R}^d, f_\infty^2 \lambda^d)$
L, \mathcal{D}_L	operator on $L^2(\mathbb{R}^d, f_\infty^2 \lambda^d)$, domain of L
$(\hat{T}_t t \geq 0)$	strongly continuous semigroup on \mathcal{D}_L

In Chapter 2

$\overline{D}, \partial D$	closure, boundary of $D \subset \mathbb{R}^d$ using Euclidian metric
$L_{\text{loc}}^2(\mathbb{R}^d, \lambda^d)$	measurable functions, locally square integrable
\mathcal{N}_x	normal vectors at the boundary point x
$\mathcal{B}(x, r)$	open ball with centre x and radius r
$\overline{C}_2(D)$	$f \in C^2(D)$ continuously extendable to \overline{D} ; first and second order derivatives are continuous too
\mathcal{C}^m	boundary class with m degrees of smoothness
A_N, D_{A_N}	operator on $L^2(D, \lambda^d)$ with Neumann 0 boundary condition and its domain
A_D, D_{A_D}	operator on $L^2(D, \lambda^d)$ with Dirichlet 0 boundary condition and its domain
A_F, D_{A_F}	Friedrichs' extension of the operator A , domain
$H_A, \ f\ _A$	energetic space of the operator A , energetic norm
$W_2^1, \ f\ _{W_2^1}$	Sobolev space, Sobolev norm
τ_D^x	exit time of $\mathcal{X} = (X_t t \geq 0)$ from the region D
$C([0, \infty), \mathbb{R}^d)$	continuous functions on $[0, \infty)$ with values in \mathbb{R}^d
$\mathcal{E}, P_{\mathcal{X}}$	σ -algebra on $C([0, \infty), \mathbb{R}^d)$, probability measure on \mathcal{E}
$\gamma_D(\omega)$	limit points of the trajectories $X_t^x(\omega)$
1_D	characteristic function of the set D
$\mathbb{R}_{\geq 0}^d$	all elements of \mathbb{R}^d with first coordinate nonnegative
A^c	complement of $A = \Omega \setminus A$ for $A \in \Omega$
$(\hat{X}_t t \geq 0)$	Itô diffusion on D

In Chapter 3

$p_n(t)$	time-step function is $\max\{\frac{k}{n} k \in \mathbb{N}_0, \frac{k}{n} \leq t\}$
$B_t^{p_n}$	discretisation of the Brownian motion B_t
$f(t-)$	limit of $f(s)$ for s increasing to t
$(\overline{X}_t^n, \varphi_t^n)$	projection scheme approximation to (X_t, φ_t)
$X \sim \mathcal{N}(\mu, \sigma)$	X is a normal distributed random variable with expectation μ and standard deviation σ
$\lfloor x \rfloor$	floor function (largest integer $z \in \mathbb{Z}$ with $z \leq x$)
\mathbb{f}	discrete image function
$\hat{\mathbb{f}}, \tilde{\mathbb{f}}$	piecewise constant version, smooth version of \mathbb{f}
W_0	square function is one on a square of size one
$C^k(D)$	up to order k continuously differentiable functions
$C_0^k(D)$	$f \in C^k(D)$ with compact support
$\overline{C}_k(D)$	$f \in C^k(D)$ continuously extendable to \overline{D} ; derivatives up to order k continuous extendable too
Π_m	polynomials of order m
$S_{m,n}$	spline space of degree m with $n - 1$ inner nodes

Abbreviations

a.e.	almost every
a.s.	almost surely
CCD	Charged Coupled Device
cp.	compare
iff	if and only if
inf	infimum
ONB	ortho normal basis
resp.	respectively
sup	supremum
w.r.t.	with respect to

Appendix A

Friedrichs' Extension of Semi-Bounded Operators

Given a semi-bounded symmetric operator A we will define an extension of A which is self-adjoint. There may exist more than one possibility to do this and of course there may exist different extensions for the same operator A which are all self-adjoint. We will just use the way introduced by K. O. Friedrichs ([25]) called the *Friedrichs' extension* similar to the presentation given in [78]. In addition we use this appendix to repeat some common definitions.

Definition A.1. An operator A defined on a Hilbert space $(H, (.,.))$ with domain \mathcal{D}_A is called *semi-bounded (below)* iff there is a constant $c \in \mathbb{R}$ such that $\forall x \in \mathcal{D}_A$ we have $(Ax, x) \geq c \cdot \|x\|^2$. We call the operator A *symmetric* iff $\forall x, y \in \mathcal{D}_A : (Ax, y) = (x, Ay)$.

It is clear that iff A is semi-bounded below then $-A$ is semi-bounded above and so it is sufficient just to talk about one kind of semi-boundedness. Hence we suppress the supplement 'below' in the following.

Definition A.2. An operator B with domain \mathcal{D}_B is called *extension* of the operator A iff $\mathcal{D}_A \subset \mathcal{D}_B$ and $\forall x \in \mathcal{D}_A$ we have $Ax = Bx$.

In the following we assume the domain \mathcal{D}_A of the operator A is dense in the Hilbert space H where A acts on. Moreover we consider the operator A as linear.

Definition A.3. The *adjoint operator* A^* is defined by

$$A^*y := y^* \text{ for all } y \in \mathcal{D}_{A^*}$$

with domain

$$\mathcal{D}_{A^*} := \{y \in H \mid \exists y^* \in H : \forall x \in \mathcal{D}_A : (Ax, y) = (x, y^*)\}.$$

The operator A is called *self-adjoint* iff $A = A^*$.

Obviously the Domain \mathcal{D}_{A_F} of the extension A_F we are looking for must be a subset of \mathcal{D}_{A^*} . On the other hand it must be a superset of \mathcal{D}_A . So we first construct this superset as closure of \mathcal{D}_A in the following norm.

Definition A.4. For every semi-bounded operator A with $(Ax, x) \geq c \cdot \|x\|^2$ and every $e \in \mathbb{R}$ with $e + c > 0$ we define an inner product by

$$(x, y)_e := (Ax, y) + e \cdot (x, y) \quad \forall x, y \in \mathcal{D}_A$$

and consequently we have

$$\|x\|_e := \sqrt{(x, x)_e}$$

as the *energetic norm* on \mathcal{D}_A . The closure of \mathcal{D}_A in this norm is denoted by

$$H_e := \{x \in H \mid \exists \text{ Cauchy sequence in } (\mathcal{D}_A, \|\cdot\|_e) \text{ converging to } x\}$$

and is called the *energetic space* of A .

Remark. Actually one can prove $H_e = H_{\tilde{e}}$ and equivalence of the norms $\|\cdot\|_e$ and $\|\cdot\|_{\tilde{e}}$ if $\tilde{e} \in \mathbb{R}$ with $\tilde{e} + c > 0$ (see [78] theorem IV.17.10). Cause we do not distinguish between equivalent norms the definition above is justified and we use H_A , $(x, y)_A$ and $\|x\|_A$ as notation. Moreover $(H_A, (\cdot, \cdot)_A)$ is a Hilbert space (see [78]).

Now we give the main statement of this appendix.

Theorem A.5. *In the notation above the operator*

$$\begin{aligned} A_F x &:= A^* x \quad \forall x \in \mathcal{D}_{A_F} \\ \mathcal{D}_{A_F} &:= \mathcal{D}_{A^*} \cap H_A \end{aligned}$$

is a self-adjoint extension of A called Friedrichs' extension. Further it is $(A_F x, x) \geq c \cdot \|x\|^2$ with the same constant c as for the operator A .

A proof is given in [78] Theorem IV.17.11 so we do not repeat it here. Finally we give some common definitions leading to the *Sobolev space* W_m^p introduced in the articles [74, 75]. We start with a preliminary definition.

Definition A.6. For $d \in \mathbb{N}$ we consider the non-negative integers $\alpha_1, \dots, \alpha_d$. Then we call the d -tuple $\alpha = (\alpha_1, \dots, \alpha_d)$ a *multi-index* and define for every $x = (x_1, \dots, x_d)$ the term $x^\alpha := x_1^{\alpha_1} \dots x_d^{\alpha_d}$. Further we take $|\alpha| = \alpha_1 + \dots + \alpha_d$.

Definition A.7. Let D denote an open subset of \mathbb{R}^d . We say a series of functions $(f_n | n \in \mathbb{N})$ converges in $C^\infty(D)$ to f and write $f_i \xrightarrow{D} f$ iff:

- a) It exists a compact set $K \subset D$ such that for all $i \in \mathbb{N}$ the support of f_i is a subset of K .
- b) For every multi-index α the series $D^\alpha f_i$ converges uniformly to $D^\alpha f$.

Here we used the notation

$$D^\alpha f := \frac{\partial^{|\alpha|} f}{\partial x_1^{\alpha_1} \dots \partial x_d^{\alpha_d}} \quad \text{for } |\alpha| \geq 1$$

as the usual partial derivatives and $D^0 f = f$. Now we are ready to define the space of distributions as follows.

Definition A.8. A (*real valued*) *distribution* φ is a continuous, linear map from $C^\infty(D)$ to \mathbb{R} . So for every $r_1, r_2 \in \mathbb{R}$ and $f_1, f_2 \in C^\infty(D)$ we have $\varphi(r_1 f_1 + r_2 f_2) = \varphi(r_1 f_1) + \varphi(r_2 f_2)$ and for every series $(f_i | i \in \mathbb{N})$ of functions in $C^\infty(D)$ with $f_i \xrightarrow{D} f$ for some $f \in C^\infty(D)$ the series $\varphi(f_i)$ converges in \mathbb{R} to $\varphi(f)$. The space of all distributions is denoted by $D'(D)$. A derivative is defined by $D^\alpha \varphi(f) := (-1)^{|\alpha|} \varphi(D^\alpha f)$ for all $f \in C^\infty(D)$.

174 Appendix A. Friedrichs' Extension of Semi-Bounded Operators

In fact now we have to verify the properties of a derivative (linearity and continuity) and possibly remark that the definition above is equal to the usual derivative if $\varphi \in C^\infty(D)$. For all this we refer one more time to the existing literature as mentioned before and proceed to give the last definition.

Definition A.9. For every $m \in \mathbb{N}_0$, $0 \leq p \leq \infty$ and $f \in C^\infty(D)$ we define

$$\|f\|_{W_m^p} := \left(\sum_{0 \leq |\alpha| \leq m} (\|D^\alpha f\|_p)^p \right)^{\frac{1}{p}}$$

as a norm on $L^p(D, \lambda)$ where $\|f\|_p := (\int |f|^p d\lambda)^{\frac{1}{p}}$ is the usual L^p norm. Then

$$W_m^p(D) := \{f \in L^p(D, \lambda) | \forall 0 \leq |\alpha| \leq m : D^\alpha f \in L^p(D, \lambda)\}$$

equipped with the norm $\|f\|_{W_m^p}$ is called Sobolev space.

Appendix B

Skorokhod's Problem

In 1961 Anatolii Vladimirovich Skorokhod published about diffusion processes at the positive half-line with reflection at 0 (see [71]). Afterwards many other authors entered this subject [51, 50, 54, 81]. Here we will give a short introduction to the formulation of the problem in order to get use of the notation. Following we link this notation to the one used by Tanaka [77], Watanabe [81] and many others. In 1978 Tanaka gave a more general result concerning arbitrary bounded convex subsets of \mathbb{R}^d which will be useful for us. Similar results proven different were given by Lions and Sznitman [46] and Saisho [66].

Let $(X_t|t \in \mathbb{R}_+)$ denote an Itô diffusion on the half-line according to the stochastic differential equation

$$dX_t = \sigma(t, X_t)dB_t + b(t, X_t)dt \quad (\text{B.1})$$

$$X_0 > 0$$

where $(B_t|t \in \mathbb{R}_+)$ is an 1-dimensional Brownian motion. As we can see, Equation B.1 determines the behaviour of the process only for strictly positive values so the question arises what happens if $X_t = 0$. Skorokhod added a boundary term to Equation B.1 which, now written in integral notation, changes to

$$X_t = X_0 + \int_0^t \sigma(s, X_s) dB_s + \int_0^t b(s, X_s) ds + \int_0^t c(s) 1_0(X_s) ds \quad (\text{B.2})$$

where c is strictly positive. If c is finite, the process will take some time to leave the boundary and we observe delayed reflection. In order to construct instantaneous reflection Skorokhod has chosen a different representation that avoids infinite values.

Definition B.1. Let $(X_t|t \in \mathbb{R}_+)$ be an Itô diffusion. A strictly positive function $\varphi : \mathbb{R}_+ \rightarrow \mathbb{R}$ is called *reflection function* for X_t iff φ is a.s. continuous and monotone increasing. Moreover φ has to be constant iff $X_t \neq 0$ (i.e. there is $\epsilon > 0$ such that $\varphi(t + \epsilon) - \varphi(\max\{t - \epsilon, 0\}) = 0$).

Now by use of this definition we give the original formulation of Skorokhod's problem.

Skorokhod's Problem. Let $\sigma : \mathbb{R}_+ \times \mathbb{R}_+ \rightarrow \mathbb{R}$ and $b : \mathbb{R}_+ \times \mathbb{R}_+ \rightarrow \mathbb{R}$ denote continuous functions satisfying a Lipschitz condition in the second variable. So we can find a constant K such that $\forall t \in \mathbb{R}_+ : \forall x, y \in \mathbb{R}_+$ we have

$$|\sigma(t, x) - \sigma(t, y)| \leq K \cdot |x - y| \quad \text{and} \quad |b(t, x) - b(t, y)| \leq K \cdot |x - y|.$$

Then finding a solution $(X_t, \varphi(t)|t \in \mathbb{R}_+)$ of the stochastic differential equation

$$X_t = X_0 + \int_0^t \sigma(s, X_s) dB_s + \int_0^t b(s, X_s) ds + \varphi(t) \quad (\text{B.3})$$

where φ is a reflection function of the positive stochastic process X_t with $\varphi(0) = 0$ is called *Skorokhod's Problem*.

Contrary to our expectation the problem above is not ambiguous. There exists just one function φ at all we can solve Equation B.3 for. We do not go into detail here because, as mentioned before, this was introductory to the topic. We switch now to the case of higher dimension and arbitrary bounded convex region following the argument first given in [77]. There the counterpart of the reflection function is an *associated* function introduced in an deterministic setting.

Definition B.2. By $C_r(\mathbb{R}_+, \overline{D})$ we denote the space of all \overline{D} -valued right continuous functions on \mathbb{R}_+ with left limits. Then the function $\varphi \in C_r(\mathbb{R}_+, \mathbb{R}^d)$

with coefficients φ_i is called associated with $X \in C_r(\mathbb{R}_+, \overline{D})$ iff the following four statements hold true:

a) $\forall i = 1, \dots, d: \forall t \in \mathbb{R}_{>0} : \exists M > 0 :$

$$[\varphi_i](t) = \sup \sum_{k=1} |\varphi_i(t_k) - \varphi_i(t_{k-1})| < M$$

where we take the supremum over all $0 = t_0 < t_1 < \dots < t_n = t$ which are partitions of $[0, t]$. ($[\varphi_i](t)$ is called *variation* of φ_i on $[0, t]$.)

b) $\varphi(0) = 0$.

c) The set $\{t \in \mathbb{R}_+ | X(t) \in D\}$ has $[\varphi]$ -measure 0.

d) If we express φ as

$$\varphi(t) = \int_0^t \eta(s) d[\varphi](s)$$

with a ($[\varphi]$ -a.s. uniquely determined) unit vector valued function $\eta(t)$.

Then for $[\varphi]$ -almost all $t \in \mathbb{R}_+$ the vector $\eta(t)$ is a normal at $X(t)$.

The last condition is guaranteed if:

d') For every function $f \in C(\mathbb{R}_+, \overline{D})$ we have $\int_D (f(t) - X(t)) \cdot \varphi(dt) \geq 0$.

No we will explain an easy example (given in [77]) to clarify the definition.

Example. In this example we consider ∂D as smooth and denote the unique inward normal at $x \in \partial D$ by $\eta(x)$. If we define

$$\varphi(t) := \int_0^t 1_{\partial D}(X(s)) \eta(X(s)) dp(s) \quad (\text{B.4})$$

for some non-decreasing function $p \in D(\mathbb{R}_+, \mathbb{R}_+)$ with $p(0) = 0$ and bounded variation then φ is an associated function of X .

We note that the variation $[\varphi](\cdot)$ of the function φ determines a measure on $\{[0, t] | t > 0\}$ and so by the *Extension Theorem of Caratheodory* determines a measure on the Borel σ -algebra $\mathcal{B}([0, \infty))$ ¹. Now we verify conditions a)-d) of Definition B.2.

¹Further information can be found in [11, 31, 34, 64, 80, 85, 86]. Many texts in probability theory include information about the formulation of the *Lebesgue-Stieltjes integrals* with respect to right-continuous functions. We refer to [52, 63, 70].

ad a) The components of the composition $\eta \circ X$ are continuous functions. Hence $1_{\partial D}(X(s))\eta(X(s))$ is Borel measurable whenever we have $\{t \in \mathbb{R}_+ | X(t) \in \partial D\} \in \mathcal{B}([0, \infty))$. But this is true because X is in $C_r(\mathbb{R}_+, \overline{D})$ which implies measurability. So we found out that φ is of bounded variation as integral over an integrable function. (Actually it is absolutely continuous and a.e. differentiable as a function of the upper bound [63].)

ad b) $\varphi(0) = 0$

ad c) We have $X \in C_r(\mathbb{R}_+, \overline{D})$ so for every $t_0 \in \{t \in \mathbb{R}_+ | X(t) \in D\}$ exists $\epsilon > 0$ such that $[t_0, t_0 + \epsilon) \subset \{t \in \mathbb{R}_+ | X(t) \in D\}$. But for every $[t_0, t_1) \subset \{t \in \mathbb{R}_+ | X(t) \in D\}$ we have

$$\begin{aligned} [\varphi]((t_0, t_1)) &= |\varphi(t_1) - \varphi(t_0)| \\ &= \int_{t_0}^{t_1} 0 \cdot \eta(X(s)) dp(s) \\ &= 0. \end{aligned}$$

It follows $[\varphi](\{t \in \mathbb{R}_+ | X(t) \in D\}) = 0$.

ad d) For $t_0 \in \mathbb{R}_+$ with $X(t_0) \in \partial D$ the derivative of φ is a.s. given by $\eta(X(t_0))[p](t_0)$ which is the inward normal at $X(t_0)$.

Now we change to a stochastic viewpoint where the role of the right-continuous functions is played by the sample-paths of suitable stochastic processes and repeat the results given in [77, 81]. As usual by (Ω, \mathcal{F}, P) we denote a probability space and by $(\mathcal{F}_t | t \geq 0)$ an increasing family of sub- σ -algebras of \mathcal{F} with $\mathcal{F}_t = \bigcap_{\epsilon > 0} \mathcal{F}_{t+\epsilon}$. It is assumed that \mathcal{F} and each \mathcal{F}_t contains all P -negligible sets. Moreover $B_t = (B_t^1, \dots, B_t^k)$ is an \mathcal{F}_t -adapted k -dimensional Brownian motion with $B_0 = 0$.

Skorokhod's Problem. Let $\sigma : \mathbb{R}_+ \times \overline{D} \rightarrow \mathbb{R}^d \times \mathbb{R}^k$ and $b : \mathbb{R}_+ \times \overline{D} \rightarrow \mathbb{R}^d$ denote Borel measurable functions of (t, x) . We assume that they are Lipschitz continuous and fulfil a linear growth condition. The Skorokhod Problem

corresponding to the stochastic differential equation

$$dX_t = \sigma(t, X_t)dB_t + b(t, X_t)dt + d\varphi_t$$

with $X_0 = x \in \overline{D}$ is to find a pair of \mathcal{F}_t -adapted processes (X_t, φ_t) where almost all paths of φ_t are associated to those of the \overline{D} -valued process X_t .

Theorem B.3 ([77] Theorem 4.1). *If D is a bounded and convex region and $x \in \overline{D}$ the solution of Skorokhod's Problem is path-wise unique.*

Remark B.4 ([81] Remark 3). If the boundary of D is smooth such that “the construction can be localised and therefore reduced to the case of the half-space” the infinitesimal generator of the process X_t is an extension of

$$Af := \sum_{i,j=1}^d a^{i,j} \frac{\partial^2 f}{\partial x_i \partial x_j} + \sum_{i=1}^d b^i \frac{\partial f}{\partial x_i}$$

with domain

$$\mathcal{D}_A := \left\{ f \in C_0^2(\mathbb{R}_+^d) \mid \left. \frac{\partial f}{\partial \eta} \right|_{\partial D} = 0 \right\}$$

where $2a^{ij} = \sum_{k=1}^d \sigma^{ik} \sigma^{kj}$ and η is the inward normal at $x \in \partial D$.

Appendix C

Multidimensional Stochastic Taylor Expansion

According to the deterministic Taylor expansion we will construct a stochastic counterpart following the argumentation of [15] (the one dimensional case is also treated in [55, 39]). During the construction we will have different possibilities how to proceed, so there exist many different stochastic Taylor expansions. In fact that means the term Stochastic Taylor expansion is not well defined if we understand it as a function rather it is a class of functions. Nevertheless we will not go into detail, just talk about one function out of this class.

So as usual by (Ω, \mathcal{A}, P) we denote a probability space and consider the m -dimensional Brownian motion $B_t := (B_t^1, \dots, B_t^m) \in \mathbb{R}^m$ for $t \in \mathbb{R}_{\geq 0}$ which is adapted to the filtration $\mathcal{F} := (\mathcal{F}_t = (\mathcal{F}_1, \dots, \mathcal{F}_m) | t \geq 0)$. There the i -th component $\mathcal{F}_t^i := \sigma(B_s^i | s \leq t)$ is the sigma algebra generated by the history of the i -th component of B_s up to time t . In order to assign some properties to the coefficients of the involved SDE we define as follows.

Definition C.1. For every $d, m \in \mathbb{N}$ and $T \in \mathbb{R}_{>0}$ by $\mathcal{W}_{\mathcal{H}}^{d \times m}(T)$ we denote the set of functions $f : [0, \infty) \times \Omega \rightarrow \mathbb{R}$ with

- a) f is $\mathcal{B} \times \mathcal{F}$ measurable, where $\mathcal{B} := \sigma([0, \infty))$,
- b) there exists an increasing family \mathcal{H} of σ -algebras \mathcal{H}_t ; $t \geq 0$ such that B_t is a martingale with respect to \mathcal{H}_t and f_t is \mathcal{H}_t adapted,

c)

$$P\left(\int_0^T f(s, \omega)^2 ds < \infty\right) = 1.$$

Now we put

$$\mathcal{W}_{\mathcal{H}}^{d \times m} := \cup_{T \geq 0} \mathcal{W}_{\mathcal{H}}^{d \times m}(T).$$

Definition C.2. Let $v(t, \omega) = (v_{i,j}(t, \omega)) \in \mathcal{W}_{\mathcal{H}}^{d \times m}$ be such that for every $i \in \{1, \dots, d\}$ and $j \in \{1, \dots, m\}$ we have

$$P\left(\int_0^T v_{i,j}(s, \omega)^2 ds < \infty \text{ for all } t \geq 0\right) = 1.$$

Further let $u_i(t, \omega)$ denote \mathcal{H}_t -adapted functions with

$$P\left(\int_0^T |u_{i,j}(s, \omega)| ds < \infty \text{ for all } t \geq 0\right) = 1 \text{ for } i = 1, \dots, d.$$

Then a process $X_t = (X_t^1, \dots, X_t^d)$ satisfying the stochastic differential equation

$$\begin{cases} dX_t^1(\omega) = b_1(X_t(\omega))dt + \sum_{j=1}^m \sigma_{1,j}(X_t(\omega))dB_t^j(\omega) \\ \vdots \\ dX_t^d(\omega) = b_d(X_t(\omega))dt + \sum_{j=1}^m \sigma_{d,j}(X_t(\omega))dB_t^j(\omega) \end{cases} \quad (\text{C.1})$$

with $X_0 = x$ is called *d-dimensional Itô diffusion*. If we define the matrix

$$\sigma(t, \omega) := (\sigma(X_t(\omega))_{i,j})_{\substack{1 \leq i \leq m \\ 1 \leq j \leq d}}$$

and the vectors

$$b(t, \omega) := \begin{pmatrix} b_1(X_t(\omega)) \\ \vdots \\ b_d(X_t(\omega)) \end{pmatrix}, \quad dB_t := \begin{pmatrix} dB_t^1 \\ \vdots \\ dB_t^m \end{pmatrix}$$

then we rewrite Equation C.1 in matrix notation as

$$dX_t(\omega) = b(t, \omega)dt + \sigma(t, \omega)dB_t(\omega). \quad (\text{C.2})$$

Now we are prepared to state the well known multi dimensional Itô formula. For simplicity we restrict our self to scalar valued functions. As a matter of fact it holds also true for vector valued functions which can be seen easily by application of the following theorem to each component.

Theorem C.3. *Let $g(t, x) : [0, \infty) \times \mathbb{R}^n \rightarrow \mathbb{R}$ denote a continuous differentiable function with respect to the variable t . Additionally we assume g to be two times continuous differentiable with respect to x . Further let $(X_t|t \geq 0)$ denote an d -dimensional Itô diffusion satisfying Equation C.2, then the process $Y_t(\omega) := g(t, X_t(\omega))$ is an 1-dimensional Itô process satisfying*

$$\begin{aligned} dY_t = & \frac{\partial g}{\partial t}(t, X_t)dt + \frac{1}{2} \sum_{i_1, i_2=1}^d \sum_{j=1}^m \sigma_{i_1, j} \sigma_{i_2, j}(t, X_t) \frac{\partial^2 g}{\partial x_{i_1} \partial x_{i_2}}(t, X_t)dt \\ & \sum_{i=1}^d b_i(t, X_t) \frac{\partial g}{\partial x_i}(t, X_t)dt + \sum_{i=1}^d \sum_{j=1}^m \sigma_{i, j}(t, X_t) \frac{\partial g}{\partial x_i} dB_t^j \end{aligned} \quad (\text{C.3})$$

for every $t \geq 0$.

A proof can be found at different places i.e. [39, 27, 48] and of course the statement is formulated for a more general class of processes long ago (cp. [42]). Furthermore the argumentation to prove the statement of Theorem C.3 is similar to that one we used to prove Theorem 2.6.1 so we skip it here. Instead let us define

$$L^0 := \frac{\partial}{\partial t} + \sum_{i=1}^d b_i \frac{\partial}{\partial x_i} + \sum_{i_1, i_2=1}^d \sum_{j=1}^m \sigma_{i_1, j} \sigma_{i_2, j} \frac{\partial^2}{\partial x_{i_1} \partial x_{i_2}}$$

and $L := (L^1, \dots, L^m)$ with

$$L^j := \sum_{i=1}^d \sigma_{i, j} \frac{\partial}{\partial x_i}$$

which allows us to rewrite Equation C.3 as

$$g(t, X_t(\omega)) = g(0, x_0(\omega)) + \int_0^t L^0 g(s, X_s(\omega)) ds + \int_0^t Lg(s, X_s(\omega)) dB_s$$

So we return to the question of an equivalent to the Taylor expansion in our

stochastic context an apply the Itô formula to the functions b_i and $\sigma_{i,j}$. This shows

$$\begin{aligned}
dX_t^i(\omega) = & \left(b_i(0, x_0(\omega)) + \int_0^t L^0 b_i(s, X_s(\omega)) ds \right) dt \\
& + \left(\sum_{k=1}^m \int_0^t L^k b_i(s, X_s(\omega)) dB_s^k \right) dt \\
& + \sum_{j=1}^m \left(\sigma_{i,j}(0, x_0(\omega)) + \int_0^t L^0 \sigma_{i,j}(s, X_s(\omega)) ds \right) dB_t^j \\
& + \sum_{j=1}^m \left(\sum_{k=1}^m \int_0^t L^k \sigma_{i,j}(s, X_s(\omega)) dB_s^k \right) dB_t^j
\end{aligned}$$

for $i = 1, \dots, d$. As mentioned at the beginning of this section we will have different options to proceed. We decide to apply formula C.3 to the terms $L^k \sigma_{i,j}$ and obtain

$$\begin{aligned}
dX_t^i(\omega) = & \left(b_i(0, x_0(\omega)) + \int_0^t L^0 b_i(s, X_s(\omega)) ds \right) dt \\
& + \left(\sum_{k=1}^m \int_0^t L^k b_i(s, X_s(\omega)) dB_s^k \right) dt \\
& + \sum_{j=1}^m \left(\sigma_{i,j}(0, x_0(\omega)) + \int_0^t L^0 \sigma_{i,j}(s, X_s(\omega)) ds \right) dB_t^j \\
& + \sum_{j=1}^m \left(\sum_{k=1}^m \int_0^t \left\{ \begin{aligned} & L^k \sigma_{i,j}(0, x_0(\omega)) \\ & + \int_0^s L^0 L^k \sigma_{i,j}(r, X_r(\omega)) dr \\ & + \sum_{l=1}^m \int_0^s L^l L^k \sigma_{i,j}(r, X_r(\omega)) dB_r^l \end{aligned} \right\} dB_s^k \right) dB_t^j
\end{aligned} \tag{C.4}$$

once more for $i = 1, \dots, n$. This procedure can be continued up to any desired approximation order. It is obvious that the result depends on the choice of the term we apply the Itô formula to.

Bibliography

- [1] R.A. Adams and J.F. Fournier. *Sobolev Spaces*. Academic Press, second edition, 2003.
- [2] S. Agmon. *Lectures on Elliptic Boundary Value Problems*, volume 2 of *Mathematical Studies*. Van Nostrand, 1965.
- [3] W. Allegretto. On the Equivalence of Two Types of Oscillation for Elliptic Operators. *Pacific Journal of Mathematics*, 55:319–328, 1974.
- [4] W. Allegretto. Spectral Estimates on Oscillation of Singular Differential Operators. *Proceedings of the American Mathematical Society*, 73:51, 1979.
- [5] W. Allegretto. Positive Solutions and Spectral Properties of Second order Elliptic Operators. *Pacific Journal of Mathematics*, 92:15–25, 1981.
- [6] L. Alvarez and P.L. Lions. Image Selective Smoothing and Edge Detection by Nonlinear Diffusion. *II, SIAM Journal of Numerical Analysis*, 29:845–866, 1992.
- [7] R.F. Anderson and S. Orey. Small Random Perturbations of Dynamical Systems with Reflecting Boundary. *Nagoya Mathematical Journal*, 60:189–216, 1976.
- [8] S.V. Anulova and V.A. Liptser. Diffusional Approximation for Processes with the Normal Reflection. *Theory of Probability and Applications*, 35:411–423, 1988.
- [9] T.M. Apostol. *Mathematical Analysis*. Massachusetts-London, 1957.

-
- [10] H. Bauer. *Wahrscheinlichkeitstheorie und Grundzüge der Maßtheorie*. De Gruyter Lehrbuch, third edition, 1978.
 - [11] N.H. Bingham, C.M. Goldie, and J.L. Teugels. *Regular Variation*. Encyclopedia of Mathematics and its Applications. Cambridge University Press, 1987.
 - [12] P. Blanchard and E. Brüning. *Distributionen und Hilbertraumoperatoren*. Mathematische Methoden der Physik. Springer, 1993.
 - [13] R.J. Chitashvili and N.L. Lazrieva. Strong Solutions of Differential Equations with Boundary Conditions. *Stochastics*, 5:225–309, 1981.
 - [14] H.L. Cycon, R.G. Froese, W. Kirsch, and B. Simon. *Schrödinger Operators*. Springer, 1987.
 - [15] S. Cyganowski, P.E. Kloeden, and J. Ombach. *From Elementary Probability to Stochastic Differential Equations with MAPLE*. Springer, 1999.
 - [16] E.B. Davies. *One Parameter Semigroups*. Academic Press, 1980.
 - [17] C. de Boer. *A Practical Guide to Splines*, volume 27 of *Applied Mathematical Sciences*. Springer, revised edition, 2001.
 - [18] T. Deck. *Der Itô-Kalkül - Einführung und Anwendungen*. Springer, 2006.
 - [19] R.M. Dudley, H. Kunita, and F. Ledrappier. *Lecture Notes in Mathematics 1097*. Springer, 1982.
 - [20] P. Dupuis and H. Ishii. SDEs with Oblique Reflections on Nonsmooth Domains. *Ann. Prob.*, 21:554–580, 1993.
 - [21] H. Federer. *Geometric Measure Theory*. Number 153 in Grundlehren der mathematischen Wissenschaften in Einzeldarstellung. Springer, 1969.
 - [22] G.S. Fishman. *Monte Carlo*. Springer, 1965.
 - [23] O. Forster. *Analysis I-III*. Number 31 in Grundkurs Mathematik. Vieweg Studium, fifth edition, 1985.

-
- [24] M. Freidlin. *Functional Integration and Partial Differential Equations*. Number 109 in Annals of Mathematics Studies. Princeton University Press, 1985.
 - [25] K.O. Friedrichs. The Identity of Weak and Strong Extensions of Differential Operators. *Transactions of American Mathematical Society*, 55:132–152, 1944.
 - [26] I.I. Gichman and A.W. Skorochod. *Stochastische Differentialgleichungen*. Mathematische Lehrbücher und Monographien. Akkademie-Verlag Berlin, 1971.
 - [27] I.I. Gihman and A.V. Skorohod. *The Theory of Stochastic Processes I–III*. Number 232 in Grundlehren der Mathematischen Wissenschaften. Springer, 1979.
 - [28] R.C. Gonzalez and R.E. Woods. *Digital Image Processing*. Prentice-Hall, second edition, 2002.
 - [29] W. Hackenbroch and A. Thalmaier. *Stochastische Analysis*. Teubner Stuttgart, 1994.
 - [30] H. Hadwiger. *Vorlesung über Inhalt, Oberfläche und Isoperimetrie*. Number 93 in Die Grundlehren der mathematischen Wissenschaften in Einzeldarstellung. Springer, 1957.
 - [31] P.R. Halmos. *Measure Theory*. Van Nostrand, 1950.
 - [32] J.M. Hammersley and D. Handscomb. *Monte Carlo Methods*. Methuen, 1964.
 - [33] G. Hellwig. *Partial Differential Equations*. Teubner, second edition, 1977.
 - [34] H. Heuser. *Lehrbuch der Analysis*, volume 1. Teubner Stuttgart, tenth edition, 1993.
 - [35] G.C. Holst. *CCD Arrays, Cameras and Displays*. JCD Publishing, second edition, 1998.

-
- [36] G.C. Holst. *Sampling, Aliasing, and Data Fidelity for Electronic Imaging Systems, Communications, and Data Acquisition*. JCD Publishing, 1998.
 - [37] B. Jähne. *Digital Image Processing*. Springer, fifth edition, 2002.
 - [38] T. Kato. *Perturbation Theory for Linear Operators*. Springer, 1980.
 - [39] P.E. Kloeden and E. Platen. *Numerical Solution of Stochastic Differential Equations*. Springer, 1999.
 - [40] H. König. Ein einfacher Beweis des Integralsatzes von Gauß. *Jahresbericht der Deutschen Mathematiker Vereinigung*, 66:119–138, 1964.
 - [41] K. Krickenberg. Über den Gaußschen und Stokesschen Integralsatz. *Mathematische Nachrichten*, 10:261–314, 1953.
 - [42] H. Kunita and S. Watanabe. On Square Integrable Martingales. *Nagoya Mathematical Journal*, 30:209–245, 1967.
 - [43] O.A. Ladyzhenskaya. *The Boundary Value Problems of Mathematical Physics*. Number 49 in Applied Mathematical Sciences. Springer, 1985. orig. pub. Moscow 1973.
 - [44] O.A. Ladyzhenskaya and N.N. Ural'tseva. *Linear and Quasilinear Elliptic Equations*. Number 46 in Mathematics in Science and Engineering. Academic Press, 1968. orig. pub. Moscow 1964.
 - [45] R. Lasser. *Introduction to Fourier Series*. Dekker, 1996.
 - [46] P.L. Lions and A.S. Sznitman. Stochastic Differential Equations with Reflecting Boundary Conditions. *Communications on Pure and Applied Mathematics*, 37:511–537, 1984.
 - [47] J.D. Lipson. *Elements of Algebra and Algebraic Computing*. Addison Wesley, 1981.
 - [48] R.S. Liptser and A.N. Shirayev. *Statistics of Random Processes I-III*. Number 5 in Applications of Mathematics. Springer, 1977.

- [49] G.G. Lorentz. Beweis des Gaußschen Integralsatzes. *Mathematische Zeitschrift*, 51:61–81, 1947.
- [50] H.P. McKean. A. Skorokhod's Stochastic Integral Equation for a Reflecting Barrier Diffusion. *Journal of Mathematics Kyoto University*, 3:86–88, 1963.
- [51] H.P. McKean. *Stochastic Integrals*. Academic Press, 1969.
- [52] P.A. Meyer. *Probability and Potentials*. Blaisdell, 1966.
- [53] W. Moss and J. Piepenbrink. Positive Solutions of Elliptic Equations. *Pacific Journal of Mathematics*, 75:219–226, 1978.
- [54] N. Ikeda and S. Watanabe. *Stochastic Differential Equations and Diffusion Processes*. North-Holland, 1989.
- [55] B. Øksendal. *Stochastic Differential Equations*. Springer, fifth edition, 1998.
- [56] I.G. Petrowski. *Vorlesungen über partielle Differentialgleichungen*. Teubner Leipzig, 1955.
- [57] R. Pettersen. Approximations for Stochastic Differential Equations with Reflecting Convex Boundaries. *Stochastic Processes and Applications*, 59:295–308, 1995.
- [58] J. Piepenbrink. Nonoscillatory Elliptic Equations. *Journal of Differential Equations*, 15:541–550, 1974.
- [59] J. Piepenbrink. A Conjecture of Glazman. *Journal of Differential Equations*, 24:173–177, 1977.
- [60] W.K. Pratt. *Digital Image Processing*. Wiley-Interscience, second edition, 1991.
- [61] M. Reed and B. Simon. *Analysis of Operators*. Academic Press, 1978.
- [62] M. Reed and B. Simon. *Functional Analysis*. Academic Press, revised and enlarged edition, 1980.

- [63] H.L. Royden. *Real Analysis*. Macmillan, second edition, 1968.
- [64] W. Rudin. *Real and Complex Analysis*. MacGraw-Hill series in higher mathematics. MacGraw-Hill, international student edition, 1970.
- [65] J.C. Russ. *The Image Processing Handbook*. Springer, third edition, 1998.
- [66] Y. Saisho. Stochastic Differential Equations for Multidimensional Domain with Reflecting Boundary. *Probability Theory and Related Fields*, 74:455–477, 1987.
- [67] I.J. Schoenberg. Contributions to the Problem of Approximation of Equidistant Data by Analytic Functions. *Quarterly of Applied Mathematics*, 4, 1945.
- [68] H. Schubert. *Topologie*. B.G. Teubner, third edition, 1971.
- [69] C.E. Shannon. The Mathematical Theory of Communication. Technical Report 27, Bell System Technical Journal, 1948.
- [70] A.N. Shiriyayev. *Probability*. Graduate Texts in Mathematics. Springer, 1984.
- [71] A.V. Skorokhod. Stochastic Equations for Diffusions in a Bounded Region. *Probability Theory and Applications*, 6:264–274, 1961.
- [72] L. Słomiński. On Approximations of Solutions of Multidimensional SDE's with Reflecting Boundary Condition. *Stochastic Processes and their Applications*, 50:197–219, 1993.
- [73] L. Słomiński. Euler's Approximations of Solutions of SDE's with Reflecting Boundary. *Stochastic Processes and their Applications*, 94:317–337, 1999.
- [74] S.L. Sobolev. On a Theorem of Functional Analysis. *Mathematics Sbornik*, 46:471–496, 1938.
- [75] S.L. Sobolev. Application of [Functional Analysis in Mathematical Physics. *American Mathematical Society, Math. Mono.*, 7, 1963. orig. pub. Leningrad 1950.

-
- [76] S.L. Sobolev. *Einige Anwendungen der Funktionalanalysis auf Gleichungen der mathematischen Physik*. Akademie-Verlag, 1964.
 - [77] H. Tanaka. Stochastic Differential Equations with Reflecting Boundary Condition in Convex Regions. *Hiroshima Mathematical Journal*, 9:163–177, 1979.
 - [78] H. Triebel. *Höhere Analysis*. Verlag Harri Deutsch, 1980.
 - [79] H. von Weizsäcker and G. Winkler. *Stochastic Integrals*. Advanced Lectures in Mathematics. Vieweg, 1990.
 - [80] W. Walter. *Analysis II*. Grundwissen Mathematik 4. Springer, 1990.
 - [81] S. Watanabe. On Stochastic Differential Equations for Multidimensional Diffusion with Boundary Condition. *J. Math. Kyoto Univ.*, 2(11):545–551, 1971.
 - [82] J. Weickert. *Anisotropic Diffusion in Image Processing*. Teubner, 1998.
 - [83] J. Weidmann. *Grundlagen*, volume 1 of *Lineare Operatoren in Hilberträumen*. Teubner, 2000.
 - [84] A.D. Wentzel. *A Course in the Theory of Stochastic Processes*. McGraw-Hill, 1981.
 - [85] A.C. Zaanen. *Integration*. Wiley, 1967.
 - [86] W.P. Ziemer. *Weakly Differentiable Functions*. Number 120 in Graduate Texts in Mathematics. Springer, 1989.

Zusammenfassung

Diese Arbeit beschreibt die mathematischen Grundlagen für ein neues Verfahren, welches zur Lösung von verschiedenen Problemen der Bildverarbeitung verwendet werden kann und gibt Beispiele zur Anwendung auf das Problem der Hervorhebung von Kanten, der Bildglättung und der Rauschreduktion. Die Grundidee des in dieser Arbeit entwickelten Verfahrens basiert auf der Tatsache, dass der zu einem Hamilton-Operator $H := -\frac{1}{2}\Delta + V$ gebildete Operator $\exp(-tH)$ jede Funktion $f_0 : \mathbb{R}^2 \rightarrow \mathbb{R}$ aus dem Definitionsbereich von H (unter gewissen Bedingungen) für t gegen Unendlich bis auf eine Konstante auf den Grundzustand von H abbildet. Für eine vorgegebene Funktion $f_\infty : \mathbb{R}^2 \rightarrow \mathbb{R}_{>0}$ setzen wir $V := \frac{\Delta f_\infty}{2f_\infty}$ und haben damit H so arrangiert, dass sein Grundzustand die vorgegebene Funktion f_∞ ist. Es resultiert also für jedes $t \geq 0$ eine Funktion $f(t) := \exp(-tH)f_0$ (entsprechend einem transformierten Bild zur Zeit t), die zur Zeit $t = 0$ mit einer vorgegebenen Funktion f_0 übereinstimmt und für t gegen Unendlich punktweise gegen ein Vielfaches der Funktion f_∞ konvergiert. Darüber hinaus genügt die Funktion $f(t)$ der Diffusionsgleichung

$$\frac{df}{dt} = \frac{1}{2}\Delta f - Vf.$$

Somit erhalten wir einen Transformationsalgorithmus der von f_0 und f_∞ (sowie von der später verwendeten Diskretisierungsgröße Δt) abhängt und uns erlaubt, den Fortgang der Transformation anhand der Funktion f_t zu beobachten. Zum Abschluss der Arbeit zeigen wir dann, dass wir aus diesem Transformationsalgorithmus durch die Wahl verschiedener Parameter f_0, f_∞ Algorithmen gewinnen, die sich zur Anwendung auf die oben genannten Probleme der Bildverarbeitung eignen. Die Anwendung unseres Verfahrens auf weitere Probleme der Bildverarbeitung (z.B. Bildvergrößerung, Bildrestauration, Gesichtserkennung) ist ebenfalls denkbar, wird hier aber nicht diskutiert.

Um die prinzipielle Idee des Transformationsalgorithmus im Rahmen der L^2 -Theorie genauer zu erläutern betrachten wir zu Beginn der Arbeit (in Kapitel 1) Funktionen $f_0, f_\infty \in L^2(\mathbb{R}^d, \lambda^d)$. Wir wählen $f_\infty > 0$ so, dass für $|x| \rightarrow \infty$ das Potential $V(x)$ unbeschränkt wächst. In diesem Fall können wir ein Ergebnis aus [61] auf den Operator H anwenden. Wir erhalten daraus, dass der Hamilton-Operator H halbbeschränkt ist und ein rein diskretes Spektrum von Eigenwerten hat. Die zugehörigen Eigenfunktionen bilden eine Orthonormalbasis des Raumes $L^2(\mathbb{R}^d, \lambda^d)$ und der Eigenraum zum Eigenwert 0 ist eindimensional (d.h. der Grundzustand ist eindeutig). Dann definieren und diskutieren wir die Darstellung $f(t) = \exp(-tH)f_0$, mit deren Hilfe wir auch die Konvergenz von $f(t)$ gegen f_∞ (bis auf eine Konstante) nachweisen. Anschließend stellen wir die Funktion $f(t)$ mit Hilfe einer Brownschen Bewegung $(B_t^x | t \geq 0)$, die in $x \in \mathbb{R}^d$ startet, als

$$f(t)(x) = \mathbb{E} \left[\exp \left(- \int_0^t V(B_s^x) ds \right) f_0(B_t^x) \right], \quad \text{für } t \geq 0 \quad (\text{Z.1})$$

dar, weil sich der Erwartungswert approximativ durch eine Monte-Carlo Simulation berechnen lässt und wir diesen Ansatz weiter verfolgen wollen. Die Identifikation von $\exp(-tH)f_0(x)$ und Z.1 geschieht dabei über das Cauchy-Problem

$$\frac{du}{dt} = \frac{1}{2} \Delta u - Vu$$

mit der Startbedingung $u(0) = f_0$. Da der Exponentialterm in Gleichung Z.1 bei einer Monte-Carlo Approximation große Werte annehmen kann, die bei Computersimulationen zu Problemen führen können, wollen wir diesen Term vermeiden. Dazu benutzen wir die unitäre Abbildung $f \mapsto f \cdot (f_\infty)^{-1}$ zwischen $L^2(\mathbb{R}^d, \lambda^d)$ und $L^2(\mathbb{R}^d, f_\infty^2 \lambda^d)$. Gemäß dem kommutativen Diagramm

$$\begin{array}{ccc} L^2(\mathbb{R}^d, \lambda^d) & \xleftarrow{\cdot f_\infty} & L^2(\mathbb{R}^d, f_\infty^2 \lambda^d) \\ \downarrow H & & \downarrow L \\ L^2(\mathbb{R}^d, \lambda^d) & \xrightarrow{\cdot (f_\infty)^{-1}} & L^2(\mathbb{R}^d, f_\infty^2 \lambda^d) \end{array}$$

führt dies zu dem Operator $L = -\frac{1}{2}\Delta - (\nabla \ln f_\infty)\nabla$ und dem Cauchy-Problem

$$\frac{d\tilde{u}}{dt} = -L\tilde{u}$$

mit der Startbedingung

$$\tilde{u}(0) = \frac{f_0}{f_\infty}.$$

Mit dessen Hilfe erhalten wir wie zuvor die gewünschte Identifikation

$$\exp(-tL)\frac{f_0}{f_\infty}(x) = \mathbb{E}\left[\frac{f_0}{f_\infty}(X_t^x)\right], \quad \text{für } x \in \mathbb{R}^d, t \geq 0. \quad (\text{Z.2})$$

Hier ist $(X_t^x|t \geq 0)$ eine d -dimensionale Itô-Diffusion mit Diffusionskoeffizient $\sigma = -I_d$ und Drift $b = -\nabla \ln f_\infty$.

Nun müssten wir für jedes $x \in \mathbb{R}^d$ die rechte Seite von Z.2 berechnen um die Funktion $f(t)$ zu erhalten. Tatsächlich würde es sogar genügen die rechte Seite von Z.2 für alle x im Träger D der Funktion $f(t)$ zu berechnen, denn außerhalb des Trägers ist die Funktion kongruent 0 und die Funktionswerte sind somit bekannt. Hat $f(t)$ einen beschränkten Träger D , was im Fall einer Anwendung auf Probleme der Bildverarbeitung immer gewährleistet ist, so könnten wir den Erwartungswert in Gleichung Z.2 durch eine Monte-Carlo Simulation approximativ berechnen. Wir wollen die vorgegebenen Bilddaten allerdings nicht zu Funktionen auf \mathbb{R}^d fortsetzen, die außerhalb eines beschränkten Gebietes kongruent 0 sind, denn wir wollen Funktionen f_∞ betrachten, die strikt positiv sind. Also erzeugen wir aus den diskreten Bilddaten mittels Splineinterpolation Funktionen, die nicht auf \mathbb{R}^d , sondern einer Teilmenge D des \mathbb{R}^2 (einem Rechteck) definiert sind. Außerdem arrangieren wir die Splineinterpolation so, dass die resultierenden (glatten) Funktionen Dirichlet- oder Neumann-Randbedingungen (in beiden Fällen mit den Konstanten 0) erfüllen. So betrachten wir also im folgenden solche Funktionen $f_0, f_\infty : D \rightarrow \mathbb{R}$ mit Dirichlet- oder Neumann-Null-Randbedingung, die zusätzlich noch zweimal stetig differenzierbar sind und nehmen f_∞ als strikt positiv an.

Die Tatsache, dass es sich bei D um ein Rechteck, also um ein nur stückweise glatt berandetes Gebiet handelt, macht hier die Reformulierung von Aussagen notwendig, die für den Fall von glatt berandeten Gebieten bereits bekannt sind.

Beispielsweise haben wir den Begriff der Neumann-Randbedingung zu ersetzen, da in den Punkten des Randes von D in denen ∂D nicht glatt ist, keine eindeutige Normale existiert. So erfüllt die Funktion f_∞ die starke Neumann-Null-Randbedingung, falls die Ableitung auf dem Rand (außerhalb der Eckpunkte) in Richtung der Normalen Null ist, was der üblichen Neumann-Null-Randbedingung entspricht. Wir fordern dann aber zusätzlich, dass die Randa-bleitung in den Eckpunkten in allen Richtungen $\nu \in \mathcal{N}_x$ verschwindet, wobei wir \mathcal{N}_x als eine Menge von Normalen im Randpunkt x definieren. Im nächsten Schritt verallgemeinern wir dann D zu einer konvexen, beschränkten Teilmenge des \mathbb{R}^d . Wir stellen unsere theoretischen Betrachtungen also in einen allgemeineren Rahmen, als es für die später diskutierten Anwendungen erforderlich wäre.

Wie zuvor wählen wir f_∞ strikt positiv und beweisen, dass der Operator $H = -\frac{1}{2}\Delta + \frac{\Delta f_\infty}{2f_\infty}$, definiert auf $\overline{C_2(D)}$, mit Dirichlet- oder Neumann-Null-Randbedingungen auch ein Operator mit rein diskretem Spektrum ist. Wir zeigen weiter, dass 0 der kleinste Eigenwert von H ist und dass der zugehörige Eigenraum Dimension eins hat. Zusammen mit bereits vorhandenen Ergebnissen über Lösungen von Differentialgleichungen zweiter Ordnung führt dies zur punktweisen Konvergenz der Funktion $f(t) = \exp(-tH)f_0$ gegen f_∞ . Wir betrachten dabei den Fall eines glatt berandeten Gebietes und den allgemeineren Fall des konvexen Gebietes weitestgehend getrennt. In beiden Fällen benutzen wir wie zuvor ein Cauchy-Problem, um $f(t)$ wie in Gleichung Z.1 als Erwartungswert darzustellen. Wieder behandeln wir zuerst den Fall eines glatten Randes und geben Lösungen des Cauchy-Problems in der Form Z.1 an, wobei wir die Brownsche Bewegung im Fall einer Neumann-Null-Randbedingung durch eine (am Rand von D) reflektierte Brownsche Bewegung ersetzen. Für den Dirichlet-Fall benutzen wir eine Brownsche Bewegung, die am Rand von D gestoppt wird. Gleiches gilt für die transformierte Darstellung wie in Gleichung Z.2, die wir ebenfalls durch ein Cauchy-Problem identifizieren. Dort sind entsprechend eine reflektierte bzw. eine gestoppte Itô-Diffusion zu verwenden.

Aus [66] wissen wir, dass die reflektierten Itô-Diffusionen Lösungen von Skorokhod-Problemen sind. Wir benutzen diese Tatsache, um die explizite Konstruktion einer reflektierten Itô-Diffusion an einem nicht notwendig glat-

ten Rand zu vermeiden. Dafür beweisen wir eine Version der Itô-Formel für Lösungen von Skorokhod-Problemen, mit deren Hilfe wir dann die Identifikation für die reflektierte Itô-Diffusion (wie in Gleichung Z.2) herleiten. Um nun Terme des Typs $f(t)(x) = \mathbb{E}[(f_0 f_\infty^{-1})(X_t^x)]$ für eine reflektierte Itô-Diffusion mittels Computer näherungsweise berechnen zu können, geben wir die Approximationen für X_t^x aus [72, 73] an. Wir erweitern diese, um Entsprechungen für bereits existierende Approximationsschemata an Itô-Diffusionen in \mathbb{R}^d zu finden¹. In Abschnitt 3.2 geben wir dann einen Algorithmus zur Approximation von $\mathbb{E}[(f_0 f_\infty^{-1})(X_t^x)]$ an und diskutieren sowohl stückweise konstante Approximationen der Funktionen f_0, f_∞ und des Driftkoeffizienten $b = -\nabla \ln f_\infty$ als auch auftretende Approximationsfehler.

Der letztlich resultierende Algorithmus zur Bildtransformation entsprechend dem zeitdiskreten Verhalten von $f(t)$ wird zum Abschluss der Arbeit (in Kapitel 4) anhand einiger Computerexperimente vorgeführt und diskutiert. Dabei illustrieren wir zuerst die prinzipielle Funktionsweise des Transformationsalgorithmus anhand verschiedener Beispiele. Schon in diesen Experimenten zeigt sich deutlich, dass in den transformierten Bildern Kanten hervorgehoben sind. Wir beschreiben dann eine Version des Transformationsalgorithmus, dessen Laufzeit um den Faktor 5 geringer ist und dessen Ergebnisse visuell kaum von den Ergebnissen des ursprünglichen Transformationsalgorithmus zu unterscheiden sind. Diese Version des Transformationsalgorithmus benutzen wir anschließend um anhand eines Fingerabdruckes zu zeigen, wie sich die kantenhervorhebende Wirkung unserer Methode vorteilhaft einsetzen lässt. Anschließend führen wir den abgeleiteten Algorithmus zur Bildglättung exemplarisch vor. Wir zeigen den Zusammenhang zur Bildglättung durch Faltung mit Gauss-Funktionen und illustrieren auch die Unterschiede gegenüber unserer Methode. Den Abschluss der Experimente bildet eine exemplarische Anwendung unserer Methode auf das Problem der Rauschreduktion. Insgesamt entsprechen die Ergebnisse der Experimente unseren auf Grund der theoretischen Erkenntnisse entstandenen Erwartungen und zeigen die Anwendbarkeit der von uns entwickelten Methode auf die betrachteten Probleme der Bildverarbeitung.

¹Die Erweiterungen der Approximationsschemata stellen eine Ergänzung der eigentlichen Arbeit dar. Sie werden nicht zur Formulierung des Transformationsalgorithmus benötigt.

Lebenslauf

Name

Alexander Dejon

Geboren am 16. Februar 1972 in Simmern/Hunsrück

Bildungsgang

1978–1984 Grundschule und Gymnasium in Simmern/Hunsrück

1984–1988 Gesamtschule Kastellaun (qual. Sek. I)

1988–1991 BASF AG Ludwigshafen/a.Rh.
Ausbildung zum Chemielaborant (IHK Abschluß)

1991 Knoll AG Ludwigshafen/a.Rh. (BASF Pharma)

1991–1994 Mannheim Kolleg am Karl-Friedrich-Gymnasium (Abitur)

1995 Universität Mannheim

Zivildienst

1995–1996 DRK Rettungssanitäter in Ludwigshafen/a.Rh.

Studium

1996–2002 Dipl.-Mathematik an der Universität Mannheim,
Nebenfach Wirtschaftsinformatik

Beruf

seit 2002 Universität Mannheim, Lehrstuhl Mathematik V
Wissenschaftlicher Mitarbeiter